

Decoding Cortical Motor Goal Representations in a 3D Real-World Environment

Dissertation for the award of the degree
Doctor rerum naturalium

submitted by

Michael Berger

from Herne

Faculty of Biology
Georg-August-Universität Göttingen
Doctoral program *Systems Neuroscience*
of the Georg-August University School of Science (GAUSS)

Göttingen, 2018

Thesis Committee

Prof. Dr. Alexander Gail (Supervisor)

Sensorimotor Group, Cognitive Neuroscience Laboratory, German Primate Center, Göttingen

Prof. Dr. Hansjörg Scherberger

Neurobiology Laboratory, German Primate Center, Göttingen

Prof. Dr. Fred Wolf

Research Group Theoretical Neurophysics, Max Planck Institute for Dynamics and Self-Organization, Göttingen

Members of the Examination Board

Referee: Prof. Dr. Alexander Gail (Supervisor)

Sensorimotor Group, Cognitive Neuroscience Laboratory, German Primate Center, Göttingen

Co-referee: Prof. Dr. Hansjörg Scherberger

Neurobiology Laboratory, German Primate Center, Göttingen

Further members of the Examination Board

Prof. Dr. Fred Wolf

Research Group Theoretical Neurophysics, Max Planck Institute for Dynamics and Self-Organization, Göttingen

Prof. Dr. Julia Fischer

Cognitive Ethology Laboratory, German Primate Center, Göttingen

Prof. Dr. Tobias Moser

Institute for Auditory Neuroscience & InnerEarLab University Medical Center Göttingen, Göttingen

Prof. Dr. Tim Gollisch

Department of Ophthalmology, School of Medicine, Göttingen

Date of oral examination: 26.10.2017

For Caro

Acknowledgements

First, I want to thank Alexander Gail for giving me the opportunity to work on this exciting project and to pursue my graduate studies. His guiding advice was always helpful, yet, he provided me enough freedom to shape this project in my own way. I am very thankful for that freedom especially given the complexity (and expenses) involved. I also want to thank Stefan Treue who guided together with Alexander Gail the ‘WeCo’ projects providing me the chance to get involved in animal welfare and animal research communication beyond neuroscience. In this context, I am grateful for the collaboration with Antonino Calapai with whom I could realize those projects. I would like to thank my advisory committee members Fred Wolf and for useful advices and feedback over the past years. Furthermore, I thank Julia Fischer, Tobias Moser and Tim Gollisch for kindly agreeing to evaluate my work.

The projects in this thesis would have never been realized without the help of many people. My deepest thank to Sina Plümer for preventing the lab to fall into chaos, and also for training and taking care of Lukas. I am grateful to Leonore Burchardt for the help with monkey training and training me on monkey training. I would like to thank Janine Kuntze for taking care of the friendliest of all monkeys. Also, I like to express my gratitude to Luisa Klotz and Dirk Prüße for further technical assistance and the animal caretakers (Janine, Carina, Max, Debbie and Andrea). I very much appreciated the help from Klaus Heisig regarding all sorts of mechanical constructions. There was a lot to build and to rebuild whenever the monkeys decided. And when the tools in our lab were not sufficient anymore, I am thankful for the help of Marvin Kulp for large constructs and Peer Strogies for very small constructs. Furthermore, I like to thank Ralf Brockhausen for taking care that the data is at the same spot as the day before, Beatrix Glaser for making all the administrative work so easy, Matthis Drolet and Katharina Menz for further IT support and Holger Sennhenn-Reulen for consulting in statistics. I am very grateful to Pierre Morel and Enrico Ferrea for making the life in the office so enjoyable and for all the scientific discussion. And also Valeska Stephan, Philipp Ulbrich, Benedict Wild, Cliodhna Quigley and all other lab members and former lab members who made the place and the time so excellent. In addition, I’m thankful to Julia Nowak, Attila Trunk, Naubahar Agha, Philipp, Benedict, Pierre and Enrico for the valuable feedback to my thesis.

I would like to express my gratitude to the students who contributed to this work. Peter Neumann, Maximilian Stecker and Annika Hinze carried out the psychophysics project and invested hours and hours in data collection. Baltasar Rüchardt was extremely helpful in implementing the

motion capture system. Pinar Yurt, Laura Molina, Christin Schwarz and again Baltasar and Peter were very dedicated in assisting the data collection for the ‘WeCo’ projects.

Finally, I would like to thank all people beyond the lab who supported and accompanied during the last years. Many thanks to my friends from Göttingen, from my time during undergraduate studies and during school. And of course, thank you, my family, for always supporting and believing in me.

Table of contents

I	General introduction	1
1	General introduction	3
1.1	Neural encoding of near and far space	4
1.2	The fronto-parietal reach network in the macaque brain	7
1.3	From constraint towards freely moving non-human primates	12
1.4	Aim of the project	14
II	Original manuscripts	17
2	Peri-hand space beyond reach	21
3	The Reach Cage	49
4	Neural encoding of far-located reach goals	75
5	A cage-based training system for neuroscience research	107
6	Standardized automated training	119
III	General discussion	133
7	General discussion	135
7.1	Conclusion	139
	References	141

Part I

General introduction

Chapter 1

General introduction

Primates can accurately reach to and grasp even small objects in a large and complex environment. While moving our hand to a desired position in a remarkably precise manner is intuitive for us, it involves highly complex computations performed by our brain. Computations underlying an intentional hand movement towards an object involve a spatial representation of the body, the hand and the object. To build up such representations, the brain needs to process a multitude of sensory information, such as visual and proprioceptive signals. Each modality enters the neuronal system in its own way dependent on how the sensory receptors are arranged. For instance, we obtain information about the external world by the visual system while proprioception provides information about the state of muscles and joints. When we want to relocate our hand to a certain point in the environment, the brain needs to compare that information to identify the direction from the hand to the reach goal and ultimately generate motor commands for the muscles. Substantial portions of the brain are involved in the process of transforming sensory information allowing the integration of information from different modalities (Cohen & Andersen, 2002; Colby, 1998; Crawford et al., 2011; Rizzolatti & Luppino, 2001). Such processes are not restricted to the immediate reachable space. When we see an object that is located far away, we can decide to go towards the object and reach for it. To understand the neural underpinnings of movement planning and execution, it is important to study movements beyond the reachable space. However, it is difficult to study neurophysiological signals in humans or non-human primates when whole-body movements are involved due to the sensitivity of neural recording equipment or lack of appropriate experimental environments.

The work described in this thesis is motivated by the question of how we encode reach targets that are located far away from the body. In this introduction, I provide a brief overview of research suggesting that spatial encoding in the primate brain depends on whether the space is close or distant to the body. This research triggered the question if the cortical circuitry in the primate brain, known for encoding reach goals near the body, is also responsible for encoding reach goals far from the body. Thus, I continue with a description of this network of brain areas, the fronto-parietal reach network. To approach this research question with experiments involving

non-human primates, an experimental environment is needed that allows whole-body movements of the animal. Therefore, I describe the requirements for experimental setups suitable for sensorimotor research when working with non-human primates, and its implications for animal welfare. Additionally, I will review recent advances in wireless neural recording technology that allow for electrophysiological recordings in physically unconstrained non-human primates.

1.1 Neural encoding of near and far space

Previous experiments about goal-directed reaching mainly focused on the space in close proximity to the body, and therefore within reach distance. One aim of this thesis is to extend the current research about movement planning and execution beyond the reachable space. There is evidence that neural processes might be categorically different between the space near and far from the body.

Patients with unilateral lesions in the middle cerebral artery territory can suffer from a visual neglect for which they have deficits in attending the contralesional side of the visual space relative to an object or to the own body (Li & Malhotra, 2015). A typical experiment to identify unilateral spatial neglect is the line bisection task in which patients are asked to mark the middle of a horizontal line. Patients will considerably misjudge the middle in the opposite direction of the side which is affected by the neglect. For example, a patient with a lesion on the left hemisphere would show a right-sided neglect. That means, the patient can not properly attend to the right part of the line and mark the middle too far to the left. Halligan and Marshall reported a patient with lesions in the right parietal cortex, temporal cortex and some subcortical structures (cerebral peduncle, pons and internal capsule) after a stroke that revealed a left-sided visual neglect in the line bisection task (Halligan & Marshall, 1991). However, when performing the task with a laser pointer at a distance of 2.44m, the patient performed significantly better. This indicates that the brain lesion impacted neural circuitry responsible for spatial attention in near but not far space. Another patient with lesions in the right temporal and occipital cortex showed a left-sided visual neglect at a distance of 3.5m but not for tasks on a desk in front of (Vuilleumier et al., 1998). This suggests that different brain areas encode the space near or far from the body. Yet, another study reported a patient with a near-space specific left-sided visual neglect resulting from a widespread lesion in the right hemisphere affecting frontal, temporal, parietal and occipital cortex and subcortical structures (basal ganglia and insula) (Berti & Frassinetti, 2000). While the patient performed the line bisection task with a laser pointer at 1m distance with little displacement error, the error was higher when performing the task at 0.5m distance. However, when using a stick in contrast to a laser pointer, the error was high at the far distance as well. This suggests, that this “near space” does not represent a defined distance from the body but rather reflects the space we can interact with which enlarges when using a tool such as a stick. Since lesions resulting from a stroke involve multiple areas, it is difficult to identify

the brain areas involved in far or near space processing. One study used repetitive transcranial magnetic stimulation on different cortical areas in the right hemisphere of healthy humans to induce far-space specific visual neglect (Bjoertomt et al., 2002). The researchers could induce a near-space visual neglect when stimulating the posterior parietal cortex and a far-space visual neglect when stimulating the ventral occipital lobe suggesting a dorsal-ventral segregation for near and far space processing. And again, another group showed that near-space neglect induced by repetitive transcranial magnetic stimulation can extend to far-space when using a tool (Giglia et al., 2015).

Further evidence that the space near the body is differently processed than the space far away comes from early electrophysiological studies with non-human primates. They found in the ventral premotor cortex (Fogassi et al., 1996; Graziano & Gross, 1994; Rizzolatti et al., 1981) and intraparietal sulcus (Graziano & Gross, 1994) neurons with tactile and visual receptive fields for which the visual receptive fields are anchored around their tactile receptive field on a part of the body. Those receptive fields cover a space anchored to the body that does not exceed the reachable space. This space is termed peripersonal space (Rizzolatti et al., 1981). Similar to the neglect studies, researchers could show that tool-use extends the receptive field of such neurons covering the enlarged space the monkey is now able to interact with (Iriki et al., 1996; Maravita & Iriki, 2004). The tool can be seen as a functional part of the body and in this respect the peripersonal space is considered to reflect a representation of the own body (Blanke et al., 2015; Maravita & Iriki, 2004). This view is supported by the rubber-hand illusion experiment which was originally studied with humans (Botvinick & Cohen, 1998). A fake arm is placed on top of the subject's occluded arm. When the fake arm and the occluded real arm received tactile stimulation simultaneously, the subjects reported that they felt the touch on the rubber arm as if it was their real arm. An experiment with monkeys showed that neurons in area 5 of the parietal cortex encode the visual location of a fake but realistic looking arm (Graziano et al., 2000). The researchers also tested a few neurons which did not respond to the fake arm in an experiment like the human study. And indeed, after simultaneous tactile stimulation most of the neurons responded to the location of the fake arm. The hand, body, real hand or fake hand do not relate to a single peripersonal space. Rather is the peripersonal space body-part specific. At least three different peripersonal spaces are known relative to respective body parts (Figure 1.1A): the peri-hand, peri-trunk and peri-head space (Blanke et al., 2015; Cléry et al., 2015).

Given that the peripersonal space is originally defined by the extent of multimodal receptive fields, the interaction of different sensory modalities (crossmodal interaction) within the peripersonal space should be higher than outside of. One way to test this in healthy subjects is by asking participants to discriminate a stimulus, often tactile, as fast as possible in one of two locations while ignoring a second stimulus, often visual (Spence et al., 2004b). Participants react faster if the visual distractor is congruent, i.e. at the location of the tactile stimulation, than if it is incongruent, i.e. at the other location. This is called the crossmodal congruency effect (CCE). In relation to the peri-hand space, tactile stimuli are delivered on index finger or thumb, and

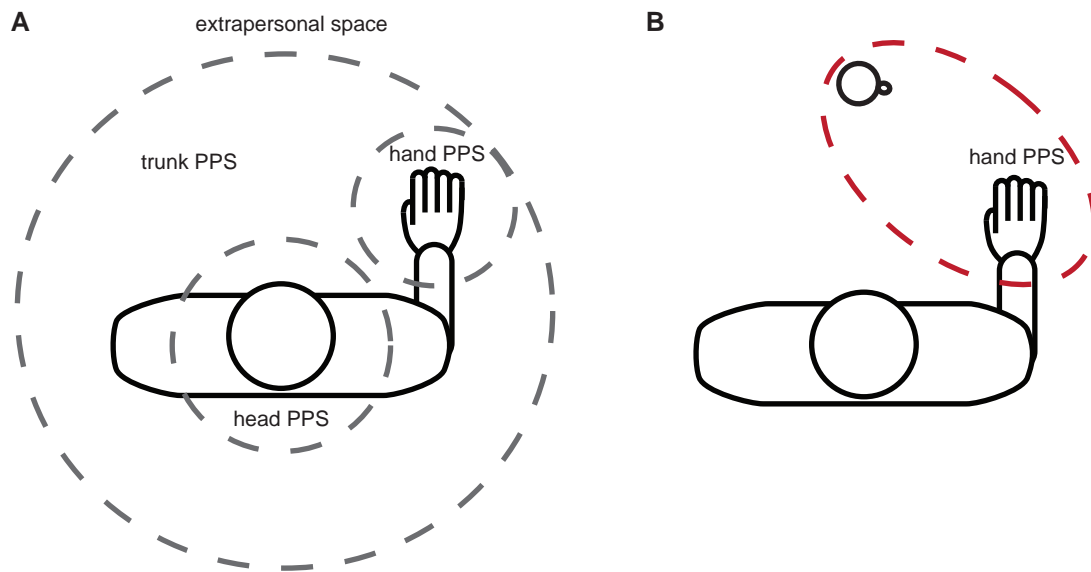


Figure 1.1: Peripersonal space. A) The peripersonal space covers our immediate surrounding. At least three different body-part centered peripersonal spaces exist: hand (peri-hand space), head (per-head space) and trunk (peri-trunk space). The space beyond the peripersonal space is called extrapersonal space. B) The peripersonal space can change with goal-directed reaching. When reaching to an object, the peri-hand space (red) expands to the object with onset of the movement.

when the distractors are placed further away from the hand, the crossmodal interaction decreases (Spence et al., 2004a). Usually, tactile stimuli are applied to both hands but the visual distractor is only placed at one hand. The hand without distractor serves as a baseline. This way it was shown that the CCE “follows” the hand when crossing arms (Spence et al., 2004a). This is in accordance with the electrophysiological results of bimodal hand centered receptive fields in the macaque brain. Further similarities were found when the CCE was tested on a tool (Holmes, 2012; Maravita et al., 2002) or a rubber hand (Maravita et al., 2003; Pavani et al., 2000). This suggests that the crossmodal congruency effect is a valid indicator for the extent of the peri-hand space.

Apart from the view that the peripersonal space reflects a representation of our body, there is a second (not opposing) view. Since the peripersonal space is constrained to the reachable space but extends with tool use, it is considered to be related to the encoding of interactions with objects in our environment (Brozzoli et al., 2011; Rizzolatti et al., 1997). However, very little is known about how the peripersonal space is modulated during goal-directed reaching. One study investigated the CCE during goal-directed reaching and grasping, and found an increase with onset of the hand movement (Brozzoli et al., 2010, 2009). According to their interpretation, the peri-hand space expands towards the reach goal (Figure 1.1B) (Brozzoli et al., 2014).

Those results and the fact that tool use extends the peripersonal space suggest that the peripersonal space reflects the space which we can interact with. That the brain contains such a representation is supported by electrophysiological studies investigating mirror neurons in the monkey ventral premotor cortex PMv (Bonini et al., 2014; Caggiano et al., 2009). Mirror

neurons respond to a specific goal-directed action if the monkey observed or performed this action. The two studies could show that mirror neurons respond differently whether the monkey can interact with the observed action or not, i.e. whether the action was far away or separated by a transparent barrier.

In conclusion, neurological, electrophysiological and behavioral observations suggest a categorical different encoding in the fronto-parietal network of a “near” and a “far” space. This differentiation does not simply reflect a metric distance but rather the possibility to act. It is not known, however, how these results would change when the reach goal is placed outside of the reachable space. If an object is not in the immediate reach but can be reached after walking to it, is this object in the near or far space?

1.2 The fronto-parietal reach network in the macaque brain

In the previous section we reviewed literature providing evidence that spatial encoding in the cortex of human and non-human primates can differ between the space near the body or far away. When considering goal-directed behavior, this leads to the question if far-located motor goals are encoded by the same cortical areas that also encode near-located motor goals. For far-located motor goals, it is necessary to walk towards the target to be able to reach them. That means that this walk-and-reach behavior involves a goal-directed whole-body movement. While studying the cortical involvement in goal-directed whole-body movements is an interesting topic on its own, it is beyond the scope of this thesis. Instead, the question addressed here is: Are the same cortical mechanisms responsible for spatial encoding of motor goals within reach also responsible for encoding motor goals beyond reach? To study single cell activity underlying goal-directed reaching, macaque monkeys are used as a model organism. Here, I will review the literature about spatial encoding of reach goals in the macaque cerebral cortex.

In primates, voluntary goal-directed reach movements are mostly guided by visual input. The brain integrates visual information with other sensory information to establish a spatial representation of the body as well as the external world. Visual processing in the cortex can be divided from the primary visual area V1 into two pathways, the ventral and dorsal pathway (Goodale & Milner, 1992; Mishkin & Ungerleider, 1982; Sakagami et al., 2006). According to this hypothesis, the ventral (“what”) pathway is responsible to identify objects in the visual scene, while the dorsal (“where”) pathway encodes the spatial representation of the scene, such as motor goals or body parts. Motor control networks for visually-guided reaching are part of the dorsal stream as they need to integrate the location of the end-effector (e.g. hand, eyes, whole-body or a tool) and the motor goal to generate an appropriate movement towards the goal.

The motor cortex is the cortical output to the spinal cord for movement signals and consists of premotor cortices, supplementary motor areas and the primary motor cortex (M1) (Dum & Strick, 2002). The link between visual and motor areas is the posterior parietal cortex (PPC), which

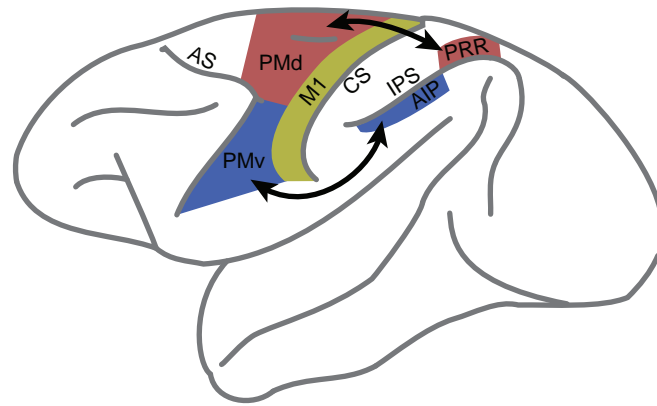


Figure 1.2: Fronto-parietal networks. Motor cortex and posterior parietal cortex are main contributors to the control of voluntary goal-directed movements. Different subnetworks are identified dependent on the movement type. Two networks are depicted here (1) Reaching: posterior reach region (PRR, in red) - dorsal premotor cortex (PMd, in red) - arm area M1 (in yellow); (2) Grasping: anterior intraparietal area (AIP, in blue) - ventral premotor cortex (PMv, in blue) - hand area M1 (in yellow). Premotor cortices are located directly anterior to M1 and are highly reciprocally connected with their respective counterparts in the posterior parietal cortex. Further abbreviations, AS: arcuate sulcus; CS: central sulcus; IPS: intraparietal sulcus.

receives input from different sensory areas and is heavily interconnected with premotor cortices in the motor cortex (Andersen et al., 1990; Colby & Duhamel, 1991; Felleman & Van Essen, 1991; Pandya & Kuypers, 1969; Wise et al., 1997). The PPC and the premotor cortices together with M1 form fronto-parietal networks (Figure 1.2) involved in processing visually-guided voluntary movements (Andersen & Cui, 2009; Colby & Goldberg, 1999; Kurata, 1991; Snyder et al., 1997). Different subsystems are responsible for different movement types, such as eye movements (lateral intraparietal area LIP, frontal eye field FEF), grasping (anterior intraparietal area AIP, ventral premotor cortex PMv and hand area M1), reaching (parietal reach region PRR, dorsal premotor cortex PMd and arm area M1) and defensive movements (ventral intraparietal area VIP and polysensory zone in the precentral gyrus PZ) (see reviews Graziano & Cooke, 2006; Johnson et al., 1996; Rizzolatti & Luppino, 2001; Snyder et al., 2000). Recent studies criticized this strict separation by showing that reaching and grasping is equally encoded in arm/hand area M1 (Rouse & Schieber, 2016), and PMd/PMv (Takahashi et al., 2017). However, these subnetworks are best studied for their proposed type of movement. Here, I will focus on the fronto-parietal reach network (PRR-PMd-M1).

Posterior parietal reach region: PRR encompasses more than one area in the PPC medial and posterior to LIP, such as the medial intraparietal area (MIP) and the dorsal part of the parieto-occipital area (PO), medial dorsal parietal area (MDP) and V6a (Snyder et al., 2000). Based on multiple anatomical and physiological studies those areas are considered to be a node in the network that controls reaching (Caminiti et al., 1996). But more modern studies of PRR usually focused on MIP (Andersen & Cui, 2009). Classically, the PPC was linked to selective spatial attention (Colby & Goldberg, 1999). However, Andersen and colleagues showed that PRR

neurons are selective for arm movements while LIP neurons are selective for eye movements to the same location (Andersen & Buneo, 2002; Snyder et al., 1997, 2000). They concluded that PPC activity is rather related to intention than attention. This view is also supported by a study showing that electrical stimulation of the PPC in humans does not trigger movements but the desire to move (Desmurget et al., 2009). Even imagined reach goals could be decoded from the PPC in a tetraplegic patient (Aflalo et al., 2015). Thus, PRR, although close to visual areas, is involved in planning reach movements.

Dorsal premotor cortex: PMd receives its input from the dorsal pathway via strong reciprocal connections from PRR (Johnson et al., 1996; Kurata, 1991; Marconi et al., 2001; Pandya & Kuypers, 1969; Wise et al., 1997). Additionally, PMd receives input from the ventral pathway via the prefrontal cortex, which is known for higher order cognitive control (Miller & Cohen, 2001). PMd is highly involved in the preparation of reach movements (Crammond & Kalaska, 1994, 2000; Wise & Mauritz, 1985) and plays a role in the initiation of the movement (Kaufman et al., 2016; Mirabella et al., 2011). Inactivation of PMd results in errors of learned reach sequences but not purely visually-guided reaches suggesting that PMd activity reflects internally generated movement plans (Ohbayashi et al., 2016).

Primary motor cortex: M1 is caudal to PMd and has no clear border. Instead, the physiological differences change continuously from PMd to M1 (Johnson et al., 1996). Classically, M1 was considered the most low level output of the cerebral cortex to the muscles, since early studies involving electrical stimulation could elicit single muscle movements (Fulton, 1938). Later studies revealed that stimulation not only in premotor cortices but also in M1 can elicit more complex movements (Graziano, 2006). Additionally, not only M1 but also the premotor cortices project to the spinal cord (Dum & Strick, 2002). This led to the view that premotor cortices and the primary motor cortex are not necessarily on a different hierarchical level. Nonetheless, M1 is considered to be more involved in motor execution than motor planning as neurons show only little activity in the planning phase compared to premotor and parietal areas (Crammond & Kalaska, 2000; Georgopoulos et al., 1982; Kalaska & Crammond, 1992). M1 encodes intrinsic motor parameters such as force control (Evarts, 1969, 1968), but also kinematic parameters such as the velocity vector of the hand (Georgopoulos et al., 1986). This velocity vector was successfully decoded from extracellular activity recorded in monkeys and humans to control robotic arms (Collinger et al., 2013; Velliste et al., 2008; Wodlinger et al., 2014).

The question of interest for this thesis is: How does the fronto-parietal reach network encode the spatial location of the hand or the reach goal during motor planning and execution? Researchers investigated spatial encoding using variants of the center-out reach task (Figure 1.3A). The task requires to move the end-effector on the middle of a screen after a “go”-signal to an indicated location (target) in the periphery. Dependent on which type of movement is of interest the end-effector can be for instance a hand, a computer cursor or the eye. In the latter case, the “end-effector position” would be the visual fixation point. To study the neural correlates of movement planning, the planning phase needs to be separated from the execution phase. To do

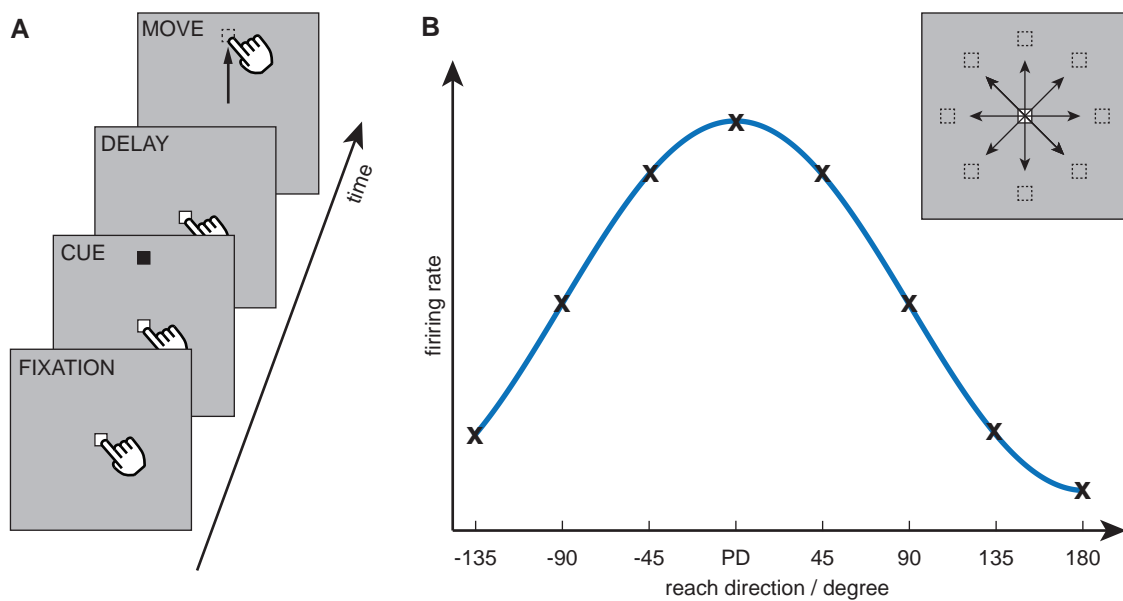


Figure 1.3: Directional tuning in an instructed delay center-out reach task. A) Task timeline of the task, FIXATION: Holding the hand on a fixation point in the middle; CUE: A cue in the periphery appears indicating the future reach target; DELAY: Waiting for a “go”-signal, for example the disappearance of the fixation point. If the target cue is not present anymore during this phase, the position needs to be memorized (memory-guided reach); MOVE: Moving as fast as possible to the target location. B) Firing rate of a hypothetical neuron dependent on the movement direction. The relationship can be modeled with a cosine function with a maximum in one direction (preferred direction, PD) and a minimum 180 degrees opposite. Neurons with such a directional tuning were observed in varying amounts in all areas of the fronto parietal reach network during CUE, DELAY and MOVE.

so, an instructed delay is integrated into the center-out reach task (Crammond & Kalaska, 2000). After receiving the cue indicating the target location the movement needs to be withheld until the appearance of the go-signal (Figure 1.3A). Then, the movement must be executed as fast as possible. The time when the go-signal occurs is randomized requiring to prepare the movement with appearance of the target cue. If the target cue is removed briefly after presentation, the subject must remember the target location during the delay phase and neural activity can not be attributed to pure sensory input.

By varying the location of the start and/or end position, spatial encoding regarding the used end-effector can be tested. In the classical center-out reach task, depicted in figure 1.3A, the targets are placed on a circle around the fixation point. This configuration allows to investigate movement direction and to test the correlation with neural activity. The relationship of single cell activity with reach direction was first studied in M1 showing a clear correlation (Georgopoulos et al., 1982). The directional modulation follows a cosine tuning (Figure 1.3B), which means that the cell is most active for a certain direction (preferred direction) but decreases its activity the more the movement direction diverges from the preferred direction with a minimum at the opposite direction. While early studies focused on reaching in a two-dimensional plane as depicted in Figure 1.3, the cosine tuning model holds true for reaches in three dimensional space

(Caminiti et al., 1990; Schwartz et al., 1988). Based on this theoretical framework, Schwartz and colleagues developed an algorithm to decode time-varying velocity vectors from neural recordings in M1 (Schwartz et al., 2001) to enable either monkeys (Velliste et al., 2008) or a tetraplegic patient (Collinger et al., 2013; Wodlinger et al., 2014) to perform a reaching task with a robotic arm directly controlled by the neural activity.

Directional tuning was also shown in PMd but the cosine tuning model explains M1 activity better than PMd activity (Crammond & Kalaska, 1996). Using an instructed delay task, researchers could investigate directional tuning during movement planning (Crammond & Kalaska, 2000). They showed that cells in PMd and M1 are tuned for reach direction during movement planning, but stronger in PMd than in M1. Directional tuned cells were found also in PRR during movement execution (Kalaska et al., 1983) and movement planning (Crammond & Kalaska, 1989). However, those studies did not take modulation relative to eye movements into account. While M1 activity could be explained well by the directional tuning model, the model performs worse for PMd and PRR. Modulation due to eye position/movements could be one explanation. This was investigated for reach planning by a series of studies using a variant of the center-out reach task for which the position of the visual fixation was part of the task as well as the position of the hand (Andersen & Buneo, 2002; Batista et al., 1999; Pesaran et al., 2006). Like in the classical center-out paradigm, the monkeys had to perform a delayed reach task from one location to another location on a screen. At the same time during a full iteration of the task, the monkeys had to maintain visual fixation of a defined point on the screen. The initial hand position as well as the visual fixation position was varied to test whether the location of the reach goal was encoded relative to the initial hand position (hand centered reference frame) or relative to the visual fixation point (eye centered reference frame) or relative to both. The researchers found that activity in PRR for reaches to the same target was mainly dependent on the position of the visual fixation point and less on the initial hand position. Thus, PRR encodes the target location predominantly in an eye-centered reference frame. Activity in PMd varies with eye, target and hand position. Different cells were found to encode the target position in an eye-centered reference frame, hand-centered reference frame, the relative position of eye and hand or a combination of those reference frames.

Most studies investigated spatial encoding of reach movements in a two-dimensional plane on a screen in front of the monkey. However, when considering walk-and-reach movements towards far-located motor goals, it is necessary to take the third axis into account indicating the distance to the body. Otherwise, studying spatial encoding of reach movements in depth follows the same logic as employed by studies using a computer screen at a fix depth. Monkeys are trained on a reach task with instructed delay while maintaining visual fixation on an instructed position. Target, initial hand and eye position are varied but this time at different depths. Depth encoding of different posterior parietal areas was investigated using this paradigm (see review Ferraina et al., 2009). One study investigated PRR during movement planning by varying the visual fixation and target position in depth (Bhattacharyya et al., 2009). They showed that PRR

encodes the target position relative to the visual fixation point, i.e. in an eye-centered reference frame as expected from previous studies using a screen at a fix depth. Additionally, the signal was modulated dependent on the absolute depth of the visual fixation. That means, combining the information about the visual fixation depth with the relative target position allows to infer the distance of the reach target relative to the body.

1.3 From constraint towards freely moving non-human primates

Sensorimotor neuroscience aims to understand planning and control of natural movements in the real world. However, experiments are performed in artificial environments specifically designed to answer a certain research question. To study the underlying neural mechanisms of a certain behavior, for instance straight reaches to different directions, researchers design experimental environments to isolate the behavior of interest. This bears the challenge to infer from experimental results to natural behavior for which no artificial behavioral constraints are applied. However, such isolation of a behavior is necessary to find the neural signals that correlate with the behavior of interest. For instance, if the gaze always follows an arm movement, do the recorded signal relate to the arm or eye movement? In a conventional experiment, researchers provide a clearly defined set of sensory inputs on which the subject is asked to perform a measurable action. Then they can analyze how the defined sensory input results in the measured behavior and draw conclusions of how the brain performs such tasks. To obtain further knowledge about computations performed by the brain, neuronal activity can be measured, for example by means of extracellular recordings in monkeys. In the end, researchers build models to interpret their observed correlation of sensory input, neural activity and behavior. However, for clear interpretations we need a sufficient knowledge about all three.

It is not the scope of this thesis to discuss the challenge to obtain appropriate neural signals, but it is equally important to understand the sensory input and the behavioral output generated by the brain (Krakauer et al., 2017). As a result, the sensory input, and alongside the experimental environment, is reduced to a necessary minimum without additional, potentially confounding, stimulations. The behavior is controlled by applying highly specific behavioral tasks, but also by means of physical restraints such as chin-rests, head fixation or arm fixation. For electrophysiological experiments with non-human primates, the monkeys are typically seated in a primate chair with only one hand having access to a manipulandum or touchscreen (Figure 1.4A). The chair imposes a fixed distance and orientation to a screen in an otherwise darkened room. Experiments in such environments lead to results clear enough to draw conclusions but bear the risk that we only witness a part of the picture too small for an appropriate interpretation. The other extreme would be to let the monkey freely perform in an enriched environment (Figure 1.4B) without any instructions while monitoring behavior and environment with modern

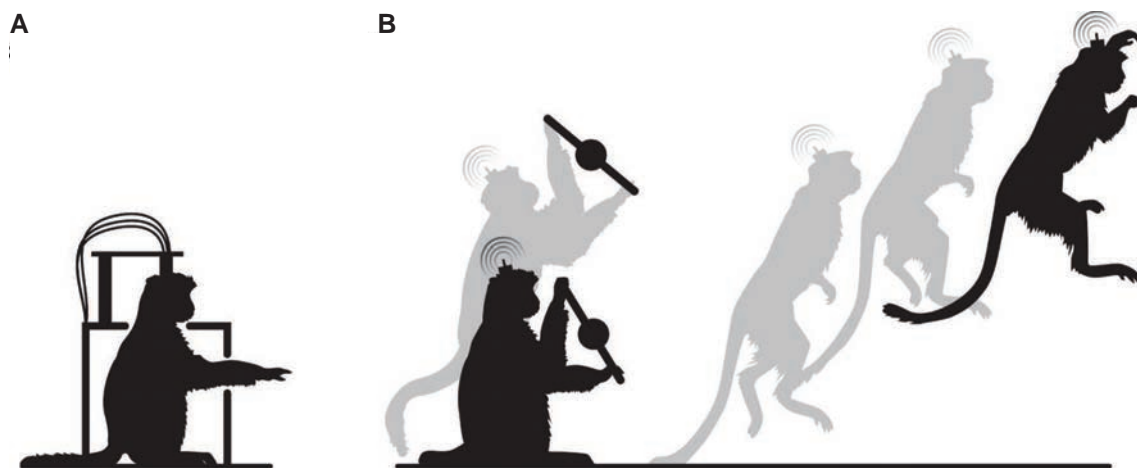


Figure 1.4: Chair seated vs freely moving monkey. A) Conventional monkey electrophysiological setup. The animal is seated in a primate chair in a fixed distance to a screen and a manipulandum or touchpanel. Often the head is fixed to the chair, partly as a requirement due to the tethered neural recording equipment. B) With wireless technology, electrophysiological recordings are possible outside a conventional monkey chair. More complex behavior involving interaction with an enriched environment and whole-body movements can be studied. Modified from (D Foster et al., 2014) (CC-BY 3.0)

techniques such as motion capture (Ballesta et al., 2014; Nakamura et al., 2016). However, while a clear identification of complex behavior is anything but easy, and while neural recordings of freely moving primates is another challenge, we would not necessarily be able to interpret the data even if all technical issues were solved. First, it is possible to perform multiple movements at the same time. Without a clearly defined and known structure in the behavior it is difficult to identify which neuronal process relate to which behavior. For instance, the planning of a movement would likely occur during the execution of the preceding movement imposing a challenge to understand what neuronal processes relate to the executed or planned movement. Second, for a statistical analysis it is necessary to obtain repetitions of the investigated behavior, otherwise it is difficult to distinguish a meaningful neural signal from noise. For those two reasons, the research described later in this thesis expands the highly constraint experimental environments (to study reach movements), to a less constraining environment (to study walk-and-reach movements) while keeping the necessary control of behavioral and environmental parameters.

When working with monkeys or animals in general, a constraining environment raises animal welfare concerns. While monkeys are a seldom used model, they are a necessity for invasive studies in sensorimotor neuroscience due to their human-like ability to reach and grasp and their ability to solve complex cognitive tasks. Such tasks require intensive training by means of positive reinforcement training. During training or experiments, the monkeys are seated in a primate chair and divided from their social group. It is necessary to increase the incentive to engage with the task by applying a caloric or fluid control schedule, i.e. the monkeys obtain their daily food or fluid as a reward for successfully interacting with the behavioral task (Prescott et al., 2010). Several research groups interested in behavioral and cognitive research implemented

devices for training and cognitive testing of monkeys within their home environment for which monkeys perform hundreds of trials daily with ad lib access to fluid and food (Andrews & Rosenblum, 1994; Bennett et al., 2016; Fagot & Bonté, 2010; Gazes et al., 2013; Kangas & Bergman, 2012; Richardson et al., 1990; Washburn et al., 1989; Washburn & Rumbaugh, 1992). The training approach presented by those studies differs in several respects to training chair-seated monkeys in sensorimotor neuroscience: 1) The monkeys can be exposed to the device for a longer period allowing them to choose their working regime in their own pace; 2) The monkeys can freely move in the cage sometimes even exposed to an enriched environment; 3) Often, the animals are in sight with their social group or even the whole group has access to such a device. Thus, a cage-based experimental setting has the potential to increase animal welfare relative to the conventional chair-based setting. Depending on the research question, it might not be beneficial to have a setup for which the animal is free to move or has access to its social group. However, it might still be possible, at least partly, to train the animals in a cage-based setting. Alternatively, such a setting could be used for preliminary tests to identify how individual animals cope with planned experiments. Such testing could be used to select animals for specific research projects.

In addition to the challenges of monitoring behavior and environment, neural recording techniques impose further constraints on movement. For instance, electroencephalography (EEG) easily picks up muscle activity which is stronger than brain activity, and even small movements in a scanner for magnetic resonance imaging (MRI) result in signal loss. In this thesis, I will focus on intracortical extracellular activity of individual neurons. This activity can be recorded from a microelectrode inside the brain. Conventionally, an electrode is inserted during the experiment through an opening in the skull by means of a micro-drive temporarily attached to the skull (Mountcastle et al., 1975). It allows searching for new neurons every session but requires head fixation, since the micro-drive would not withstand head movements. A more modern development are floating microelectrode arrays (Maynard et al., 1997; Musallam et al., 2007). Multiple electrodes are chronically implanted in the cortex only connected with a thin flexible cable to the electrical connector on the skull. While a readjustment of the electrode depth or position is not possible, it allows recording from many cells at the same time. And being fixed on the brain and not the skull, it is not susceptible to head movements.

However, monkeys are flexible animals that can easily reach the top of their head and climb on various structures. Even with floating microelectrode arrays, tethered neural recordings in a freely moving monkey are not possible or only under constraining circumstances (Ludvig et al., 2004; Sun et al., 2006). Recent technological advances led to wireless electrophysiological recordings in monkeys, and consequently, recording during unrestraint behavior (Agha et al., 2013; Fan et al., 2011; Fernandez-Leon et al., 2015; Grohrock et al., 1997; Jürgens & Hage, 2006; Miranda et al., 2010; Schwarz et al., 2014; Yin et al., 2014). A few studies already used such technology for studying freely moving monkeys in the context of locomotion (Capogrosso et al., 2016; D Foster et al., 2014), vocalization (Hage & Jurgens, 2006; Roy & Wang, 2012),

sleeping (Yin et al., 2014) or brain-machine interfaces (Rajangam et al., 2016; Schwarz et al., 2014). Reach movements were not studied except of very preliminary data of basic behavior simply to illustrate the potential of wireless neural recording technology (Fernandez-Leon et al., 2015; Gilja et al., 2010; Schwarz et al., 2014). No study involving freely moving monkeys investigated reaching in a clearly structured task, such as a walk-and-reach task.

1.4 Aim of the project

While there is a vast amount of literature about goal-directed reaching and there is evidence that spatial processing is different for the spaces close or distant to the body, there is no research about planning a movement to acquire a target beyond reach. This thesis is motivated by the question if the fronto-parietal reach network in the macaque monkey also encodes the position of motor goals which are located far from the body for which a walk-and-reach movement is necessary. This was not studied before mainly because an experimental environment was missing that allows for electrophysiological experiments in physically unconstrained non-human primates. The work described here focuses on removing physical constraints from current experimental environments in sensorimotor neuroscience. This approach will be evaluated under two aspects: 1) Can an environment without physical constraints effectively be used to benefit animal welfare in a conventional sensorimotor neuroscience setting with monkeys? 2) Without physical constraints, is it possible to obtain results known from highly constraining experiments with monkeys sitting in a primate chair? Since this work focuses on spatial encoding of reach goals, the last question can be formulated more specifically: Is it possible to study the spatial encoding of near-located reach targets in the fronto-parietal reach network in an environment without physical constraints? Once such an environment is established and proven to be useful for studying goal-directed reaching, the work extends the current knowledge to walk-and-reach movements towards far-located targets. The thesis encompasses five original manuscripts describing studies conducted in collaboration with other researchers. The individual contributions for each manuscript are disclosed after the introduction.

Chapter 2 describes the human psychophysics study *Remapping of peri-hand space beyond reach by walk-and-reach movements*. We investigated if crossmodal interference increases when starting a goal-directed movement towards a target outside the reach. As described in section 1.1, the crossmodal congruency effect relates to the peripersonal space and increases with onset of a goal-directed reaching movement (Brozzoli et al., 2010, 2009). We built a setup that allowed us to study the crossmodal congruency effect like the setup of Brozzoli and colleagues but incorporated walk-and-reach movements. We found a similar increase for the onset of walk-and-reach movements as in normal reach movements to near targets suggesting that the peri-hand space expands to movement goals independent of the distance to the body.

Based on this behavioral similarity, we further investigated whether the fronto-parietal reach network encodes the reach goal location for targets out of reach like reachable targets. At first, we had to develop a new experiment environment, as described in chapter 3 *The Reach Cage – an experimental environment for wireless neural recordings during structured behavior of physically unconstrained monkeys*. The “Reach Cage” allowed us to study motor preparation and execution of reach and walk-and-reach movements in monkeys. We show that the Reach Cage is suitable to examine goal-directed behavior of physically unconstrained rhesus monkeys in a structured goal-directed reach task. By using modern wireless neural recording technology, we could record electrophysiological data from all three brain areas of the fronto-parietal reach network (PRR, PMd and M1) in one monkey. The analysis of this data is presented in chapter 4 *Neural encoding of far-located reach goals in motor, premotor, and parietal cortex in a physically unconstrained monkey performing a walk-and-reach task*. We validate that the results for near-located motor goal encoding of reach movements resemble the results obtained from conventional experiments with monkeys seated in a primate chair. Furthermore, we could examine motor goal encoding of far-located targets for which walk-and-reach movements are necessary. Our results suggest that the fronto-parietal reach network shows little involvement in planning and execution of whole-body movements. Especially activity in PMd and PRR is mainly related to the arm movement little affected by whole-body movement and posture.

Since a cage-based setup seems to be an alternative to conventional chair-based setups for training non-human primates to at least some behavioral tasks used in sensorimotor neuroscience, we designed a training approach usable inside the monkey’s home environment without the need for constant supervision. As described in the chapter 5 *A cage-based training, cognitive testing and enrichment system optimized for rhesus monkeys in neuroscience research*, we developed a touchscreen based training device that can be attached to compartments inside a monkey facility to train rhesus monkeys on various cognitive and sensorimotor tasks. Using this device, we trained eight rhesus monkeys towards a memory guided reach task, as described in chapter 6 *Standardized automated training of rhesus monkeys for neuroscience research in their housing environment*. The training was solely guided by an autonomous algorithm. While the rigid nature of our training algorithm is mostly not optimized for training speed, we argue that the comparison of training progress can be a useful tool for selecting animals that cope better with a cognitive neuroscience research environment.

Part II

Original manuscripts

Peri-hand space expands beyond reach in the context of walk-and-reach movements

Michael Berger, Peter Neumann, Alexander Gail

MB, PN and AG designed the study; MB supervised data collection; MB analyzed the data; MB prepared all figures; MB and AG interpreted the data; MB and AG wrote the manuscript; all authors reviewed the manuscript.

The Reach Cage environment for wireless neural recordings during structured goal-directed behavior of unrestrained monkeys

Michael Berger, Alexander Gail

MB and AG designed the experiment; MB collected the data; MB analyzed the data; MB and AG interpreted the data; MB wrote the manuscript; AG edited the manuscript.

(preprint published on *bioRxiv* - Berger & Gail (2018))

Neural encoding of far-located reach goals in motor, premotor, and parietal cortex in a physically unconstrained monkey performing a walk-and-reach task

Michael Berger, Alexander Gail

MB and AG designed the experiment; MB collected the data; MB analyzed the data; MB and AG interpreted the data; MB wrote the manuscript; AG edited the manuscript.

A cage-based training, cognitive testing and enrichment system optimized for rhesus macaques in neuroscience research

Antonino Calapai, Michael Berger, Michael Niessing, Klaus Heisig, Ralf Brockhausen, Stefan Treue, Alexander Gail

AC and MB are shared first authors. ST and AG are shared last authors. MB, AC, MN, ST and AG designed the experiment; MB and AC collected the data; KH built the device; RB wrote the software; AC analyzed the data; MB, AC, ST, and AG interpreted the data; MB and AC wrote the manuscript; ST and AG edited the manuscript.

(published in *Journal of Neurophysiology* - Berger et al. (2017))

Standardized automated training of rhesus monkeys for neuroscience research in their housing environment

Michael Berger, Antonino Calapai, Valeska Stephan, Michael Niessing, Leonore Burchardt Alexander Gail, Stefan Treue

MB and AC are shared first authors. AG and ST are shared last authors. MB, AC, VS, MN, LB, AG, and ST conceived and designed research; MB, AC, VS, MN, and LB performed experiments; MB analyzed data; MB, AC, VS, MN, AG, and ST interpreted results of experiments; MB prepared figures; MB and AC drafted manuscript; AG and ST edited and revised manuscript; MB, AC, VS, MN, LB, AG, and ST approved final version of manuscript.

(published in *Behavior Research Methods* - Calapai et al. (2017))

Chapter 2

Peri-hand space expands beyond reach in the context of walk-and-reach movements

2.1 Abstract

Multisensory integration can be demonstrated by crossmodal interference, like the crossmodal congruency effect (CCE), and is typically limited in spatial range. The so defined peripersonal space (PPS) is centered on the relevant body part, e.g. the hand, but can spatially expand to encompass tools or reach targets during goal-directed behavior. Previous studies considered expansion of the PPS towards goals within immediate or tool-mediated reach, but not the translocation of the body as during walking. Here, we used the CCE to test if PPS can also expand further to include far located walk-and-reach targets accessible only by translocation of the body. Also, we tested for orientation specificity of the hand-centered reference frame asking if the CCE inverts with inversion of the hand orientation during reach. We show a high CCE with onset of the movement not only towards reach targets but also walk-and-reach targets. When subjects have to change hand orientation, the CCE decreases, if not vanishes, and does neither fully reflect start nor endpoint hand orientation. We conclude that the PPS can expand to the action space beyond immediate or tool-mediated reaching distance, but is not purely hand-centered with respect to orientation.

2.2 Introduction

To physically interact with our environment, our brain integrates multisensory information to build a representation of the location of our body, limbs and targets. When reaching for an object, the brain needs to know the position of the object, the reaching hand and the trunk to turn or even walk towards the object before reach. Electrophysiological studies in non-human primates showed that interconnected areas in the premotor and parietal cortex (fronto-parietal network) compute the hand, body and object position to plan and control hand and arm movements

(Andersen & Cui, 2009; Caggiano et al., 2009; Caminiti et al., 2017, 2015; Graziano & Cooke, 2006; Rizzolatti & Luppino, 2001; Rizzolatti et al., 1998). Corresponding to the multisensory nature of the problem, studies found visuo-tactile neurons with body-centered visual receptive fields covering the immediate space around the body in premotor cortex (Fogassi et al., 1996; Graziano & Gross, 1994; Rizzolatti et al., 1981b) and posterior parietal area 7b (Graziano & Gross, 1994). The space around the body covered by those receptive fields was termed peripersonal space (PPS). The PPS was proposed to represent an action space and as such is linked to the fronto-parietal circuitry controlling hand and arm movements (Cléry et al., 2015b; Rizzolatti et al., 1997). The PPS can expand around tools (Iriki et al., 1996; Maravita & Iriki, 2004), around a video image of the own hand (Iriki et al., 2001), and around a fake and virtual arm (Graziano et al., 2000; Shokur et al., 2013). Expansion of the PPS, as defined by visuo-tactile receptive fields, beyond immediate or tool-mediated reach, to our knowledge, was not tested. Specifically, it is unknown how the PPS changes with goal-directed behavior when full body movements such as walking are involved. It is unclear if the action space, to which the PPS is linked, relates only to immediate actions such as reaching to an object, or also encompasses more complex actions such as walk-and-reach movements to a goal located further away.

The PPS is not unique to non-human primates and the concept has been linked to human neuropsychological and behavioral phenomena. Evidence from several lines of research suggests that also the human brain contains a representation of the space immediately surrounding the body. Studies with patients suffering from visuo-spatial neglect showed that such a neglect can be restricted to a space close (Halligan & Marshall, 1991) or distant (Vuilleumier et al., 1998) to the body. Such neglect-like symptoms constrained to one space were also induced in healthy subjects by applying transcranial magnetic stimulation on the posterior parietal cortex (Bjoertomt et al., 2002; Mahayana et al., 2014). In line with the expansion of visuo-tactile receptive fields around tools in monkeys (Iriki et al., 1996; Maravita & Iriki, 2004), a neglect near the body can also expand away from the body when using a tool (Berti & Frassinetti, 2000; Giglia et al., 2015). Based on fMRI studies, the human fronto-parietal network, like in monkeys, is considered to be a main contributor in processing the PPS and coordinating goal directed movements (Barany et al., 2014; Brozzoli et al., 2012; Cléry et al., 2015a; Makin et al., 2007).

At least three body-part specific PPS have been described, surrounding the hand (peri-hand), trunk (peri-trunk) and head (peri-head) (Blanke et al., 2015; Cléry et al., 2015b; Farnè et al., 2016; Serino et al., 2015). To examine the extent of PPS in healthy human subjects, researchers investigate effects of multimodal integration related to the specific body part. The crossmodal congruency task proved to be efficient in measuring the peri-hand space (Spence et al., 2004b). The crossmodal congruency effect (CCE) is the difference in reaction time, or error rate, of speeded tactile discriminations with spatially congruent versus incongruent distractors (Shore et al., 2006). The CCE is spatially restricted and strongest for the space immediately around the hand (Spence et al., 2004a). This space can expand with tool use (Holmes, 2012; Maravita et al., 2002a), fake arms (Pavani et al., 2000), and the mirror-image of the own hand (Maravita

et al., 2002b). However, the hand-centeredness of the CCE was only tested with respect to hand displacement but not hand-orientation. It is unclear if the centering of the peri-hand space on the hand is only with respect to its location or whether rotating the hand also has an effect on the CCE.

Modification of the extent of the PPS dependent on interactions with the environment bears the question: How does goal-directed behavior modulate the PPS? Two studies used the CCE to investigate the change in peri-hand space while subjects grasped (Brozzoli et al., 2009) or pointed to (Brozzoli et al., 2010) a small cylinder with index finger and thumb. They found that peri-hand space expands with movement onset towards the hand target (Brozzoli et al., 2014). It is unclear, however, if such expansion is restricted to the immediate reachable space or if the PPS can also expand to far located targets when performing a walk-and-reach movement to the target.

Here we asked if goal directed walk-and-reach behavior can lead to an expansion of the peri-hand space, measured by the CCE, beyond the immediate reach. Furthermore, we tested if the CCE reference frame follows with hand rotation. In healthy human subjects, we measured the CCE before, at and after onset of goal-directed reach or walk-and-reach movements with and without rotating the hand during the movement. We report that the CCE increases for walk-and-reach movements already during movement onset just the same as for simple reaches. Additionally, we show that the hand rotation during the movement leads to a strong decrease, if not disappearance, of the CCE. Nonetheless, even after several hundred trials of practice with inverted hand orientation, the baseline CCE without the reaching task is not altered compared to practice without inverted hand orientation.

2.3 Results

To investigate crossmodal interference during goal-directed reach and walk-and-reach movements, we measured reaction times (RT) in a vibro-tactile discrimination task and quantified the CCE during different phases of the movements from 59 subjects (figure 2.1).

Average reaction times for the walk-and-reach cross-modal congruency (CC) task are shown in figure 2.2. During normal hand orientation, discrimination in *congruent* trials was reliably faster than in *incongruent* trials for both near and far targets. This CCE became stronger during movement onset and conduction. To quantify our results, first, we calculated a linear mixed effect model (LME) for RTs with interacting fixed effects of DISTANCE (*near, far*), CONGRUENCY (*congruent, incongruent*), TIMING (*static, onset, move*) and ORIENTATION (*normal, inverse*) and a non-interacting fixed effect of PARTICIPATION ("0" first time, "1" second time, etc.; see methods). The ANOVA table (Table 2.2) based on the LME indicated a significant main effect of CONGRUENCY on RTs [$F(1,702) = 22.97, p < 0.001$]. Furthermore, CONGRUENCY significantly interacted with ORIENTATION [$F(1,702) = 34.7, p < 0.001$] and with ORIENTATION X TIMING [$F(2,702) = 3.67, p = 0.026$]. This means, as expected, the

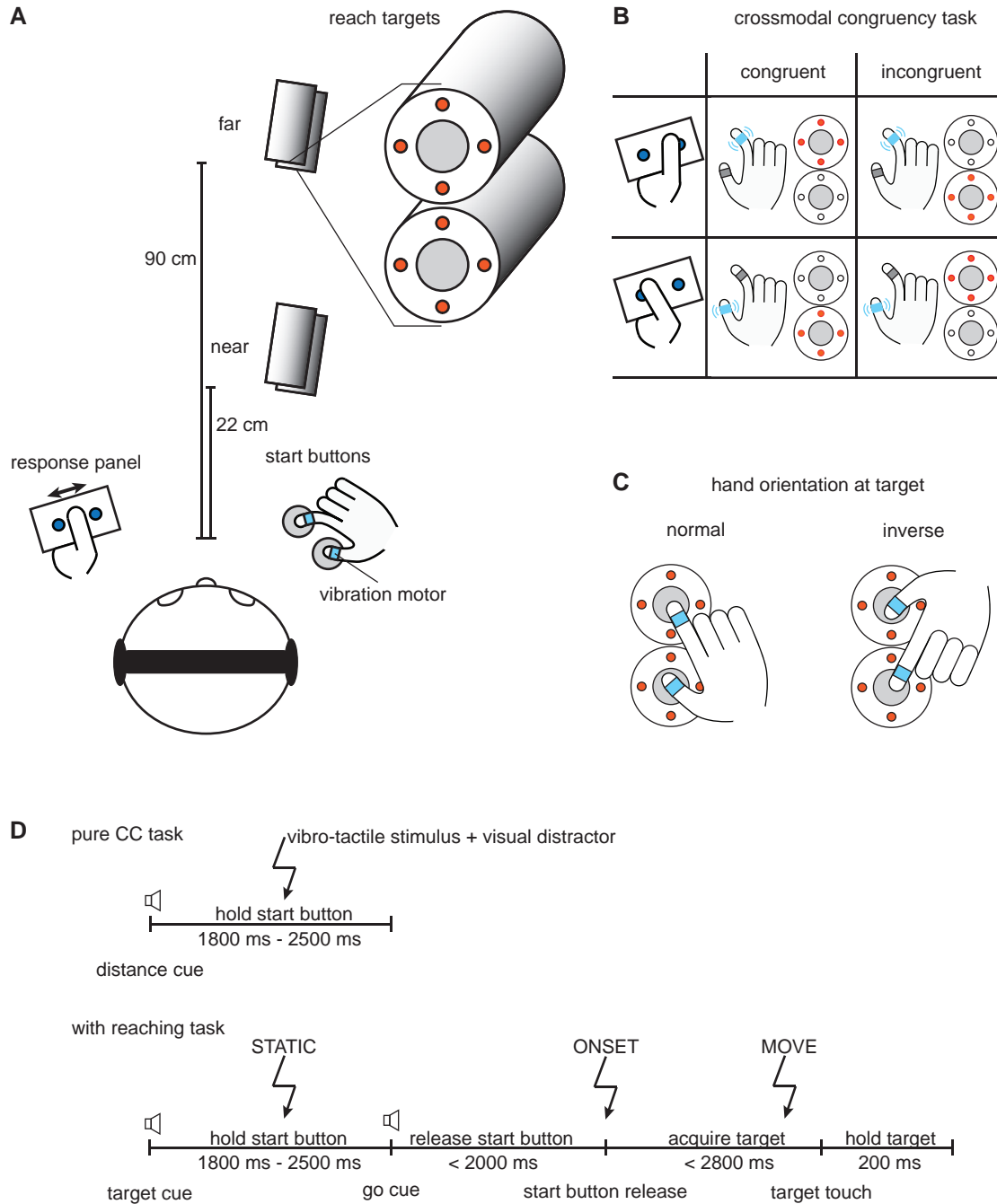


Figure 2.1: Setup and dual task. A) The subject stands inside the setup wearing headphones, holding the response panel with two push buttons (dark blue) in the left hand, and touching two touch sensors (grey) with right index finger and thumb. Vibration motors are attached to the right index finger and thumb (light blue). Near and far targets are in front of the subject each containing two touch sensors and four LEDs (red) around each touch sensor.

Figure 2.1: (continued) B) In the cross-modal congruency (CC) task, the subject is asked to discriminate whether vibro-tactile stimulation was applied to the index finger or thumb by pressing the correct button on the response panel with the thumb of the left hand. A visual distractor is presented on one of the two touch sensors of the reach target simultaneously and spatially congruent or incongruent to the vibro-tactile stimulation. C) In parallel, the subject has to perform a walk-and-reach task reaching both touch sensors of the instructed near or far target either with the index finger on the top and the thumb on the bottom sensor (*normal*) or the other way around (*inverse*). D) Task timeline. The subject needs to hold the start buttons and an auditory cue signals which target is going to be the reach target. For the pure CC task, only the speeded response to the visuo-tactile stimulus pair (flash symbol) is required. The auditory cue signals on which distance (*near* or *far*) the visual distractors are going to be presented in each trial. For the walk-and-reach CC task, upon the second appearance of the auditory cue (go cue), the subject needs to reach to the cued target. The visuo-tactile stimulation can be before (*static*), at (*onset*) or after (*move*) the subject's hand releases the start button. (Figure drawn by MB)

CCE (main effect of CONGRUENCY on RT) is present, and its strength depends on the task conditions. This is the case for ORIENTATION and TIMING but not DISTANCE as evident by the (lack of) interactions. While DISTANCE had no main effect on tactile discrimination RTs in the walk-and-reach CC task with normal hand orientation, we found a significant interaction with ORIENTATION [$F(1,739) = 11.39, p < 0.001$]. Detailed ANOVA tables can be found in the supplementary material.

Congruency did not have an effect on the performance of the reaching task itself, i.e. start button release time (RT_{reach}) and movement time (MT_{reach}) did not depend on congruency (figure 2.5, tables 2.3, 2.4).

To test how crossmodal interaction is influenced by the behavioral task, we computed the CCE, rather than raw RTs, for each subject and condition and used a LME to test the dependency of the CCE on DISTANCE, TIMING and ORIENTATION as interacting fixed effects, PARTICIPATION as non-interacting effect, and SUBJECTS as random intercept. Average values and their standard errors for each condition are shown in figure 2.3. Violin plots depicting the distribution of the data are shown in the supplementary material (figure 2.6). Regarding hand orientation, one hypothesis predicts that the CCE should be invariant to hand orientation, while an alternative hypothesis predicts that the CCE should be inverted in sign (i.e. "rotate" with the hand). To distinguish the latter case from less specific effects of hand orientation on the CCE in the context of LME modelling (both cases would lead to a significant main or interaction effect of the factor ORIENTATION), we calculated the CCE model twice: first, with the congruency pairing of fingers and distractors as defined in figure 2.1; second, with inverted finger-to-distractor pairing. If CCE inverts in sign with hand orientation without being affected in strength then the latter model should show no effect of ORIENTATION. In both models, we found a significant main effect of ORIENTATION on CCE [$F(1,375) = 131.5, p < 0.001$ / $F(1,354) = 125.95, p < 0.001$] and an interaction effect for TIMING and ORIENTATION [$F(2,323) = 14.59, p < 0.001$ / $F(2,321) = 3.11, p = 0.046$] (Table 2.5/2.6). We found no effect of DISTANCE on CCE, neither a main effect [$F(1,249) = 0.17, p = 0.68$ / $F(1,352) = 2.2, p = 0.14$] nor an interaction effect with

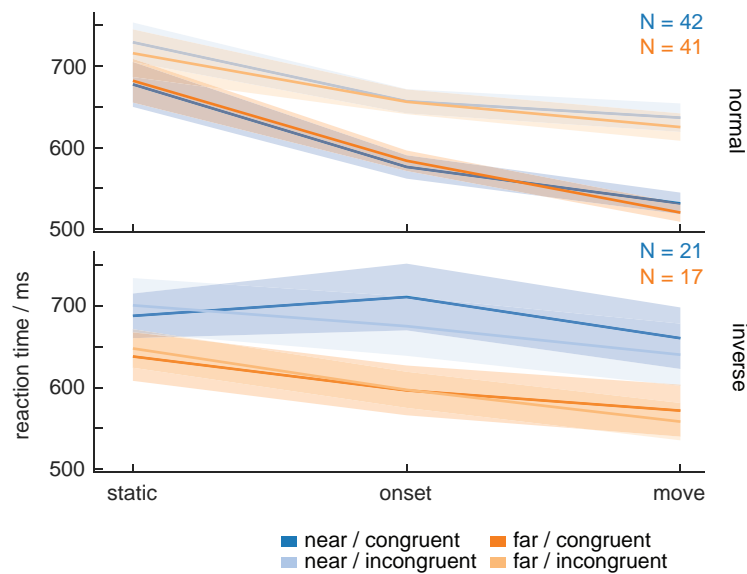


Figure 2.2: Average RT for tactile discrimination in the walk-and-reach CC task as function of stimulus timing and hand orientation. Discrimination RT decreases with progression of the reach movement. The crossmodal congruency effect (CCE) exists for normal hand orientation (top) as *incongruent* (light) reaction times are slower than *congruent* (dark). Solid lines indicate the mean, transparent areas the s.e.m.

TIMING [F(2,323) = 1.03, $p = 0.36$ / F(2,321) = 0.9, $p = 0.41$], ORIENTATION [F(1,370) = 2.36, $p = 0.13$ / F(1,360) = 0.32, $p = 0.57$] or both [F(2,323) = 0.67, $p = 0.51$ / F(2,321) = 1.39, $p = 0.25$]. This means that there is no indication that the CCE differs between direct reach and walk-and-reach movements, and that inversion of hand orientation does influence CCE but does not simply invert it.

We performed post-hoc multiple comparison tests based on simplified models of the CCE without the fixed effects DISTANCE and PARTICIPATION (normal finger-to-distractor pairing, Table 2.7; inverted finger-to-distractor pairing, Table 2.8) to better describe the effect of hand orientation on CCE. For normal hand orientation and normal finger-to-distractor pairing, the CCE increases from *static* (LME estimate: 45 ms) to *onset* (LME estimate: 78 ms; difference: 34 ms, $p = 0.004$) and further from *onset* to *move* (LME estimate: 106 ms; difference: 28 ms, $p = 0.024$). We did not find any significant effect between stimulation times for inverted hand orientation in either model. In both models (normal/inverted), we found a decrease in CCE when the hand was inverted during reaching at *static* (LME estimate: 9/-16 ms; difference 36/64 ms, $p = 0.036$ / <0.001), *onset* (LME estimate: -22/15 ms, difference: 100/67 ms, $p < 0.001$) and *move* (LME estimate: -20/12 ms; difference: 126/97 ms, $p < 0.001$). This shows that a change in hand orientation during the movement affects the CCE but not in a way that would be consistent with an inversion of the hand reference frame. None of the CCEs with inverted hand orientation are significantly different from zero.

The subjects performed the pure CC task without reaching at the beginning of the session. At this point, subjects had not yet performed any reaches towards the distractor-bearing targets and

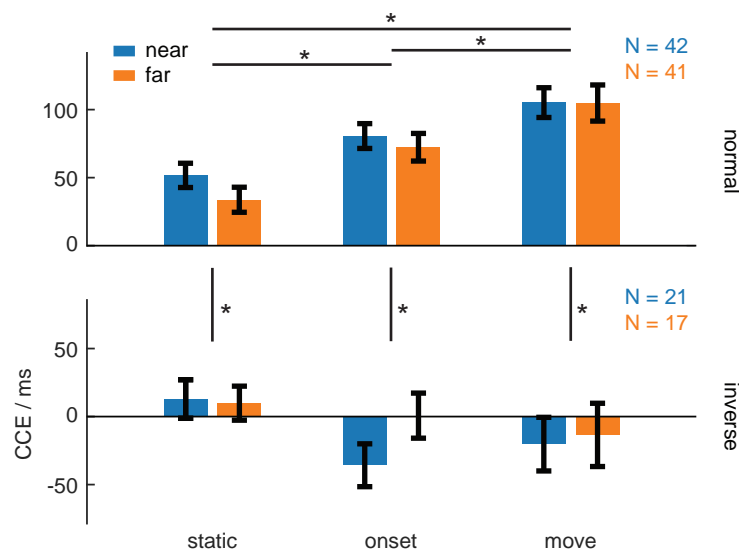


Figure 2.3: The crossmodal congruency effect (CCE) in the walk-and-reach CC task. For normal hand orientation (top) the CCE increases with stimulation at the time of movement onset (*onset*) and during movement execution (*move*), compared to the static condition. This is the case, both, for direct reaches (*near*) and walk-and-reach movements (*far*). The CCE decreases for all conditions when the hand orientation is inverted during movement (here: finger-to-distractor pairing the same as for normal reaches). No significant differences in the CCE between *near* and *far* were found. Bars indicate the mean, black error bars the s.e.m. Asterisks depict significant differences ($p < 0.05$) for post-hoc multiple comparisons not including distance (*near*, *far*) as a factor.

were not instructed on the reaching task either. Still, we could already measure a CCE (figure 2.4, blue). This suggests that a finger-to-distractor pairing was already established (index finger – top and thumb – bottom). We wanted to know whether the hand orientation, experienced during the walk-and-reach CC task, would change this pairing. If so, practicing reaching movements with consistently inverted hand orientation should counteract the finger-to-distractor pairing and decrease the CCE in the pure CC task. To test this, subjects performed the pure CC task again at the end of the session after performing the walk-and-reach CC task. One group performed the walk-and-reach task only with normal hand orientation, while the other subjects performed the walk-and-reach task in two blocks, first with normal hand orientation and second with inverted hand orientation. We calculated a LME with the fixed factor ORIENTATION defining whether or not inverted hand orientation was part of the preceding walk-and-reach task of the same session and factor SUBJECT as random intercepts. The CCE was smaller in the second pure CC task compared to the first, both, when *inverse* walk-and-reach trials (green) and when only *normal* walk-and-reach trials (red) were performed in-between, with no significant difference ($t(82) = 0.03$, $p = 0.98$). This suggests that reaching practice does not affect the CCE in the non-reaching context in a hand-orientation specific manner.

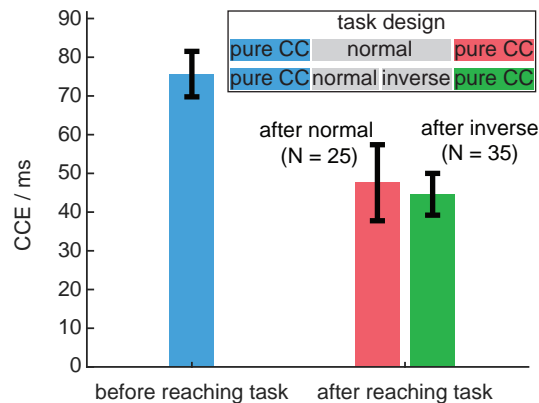


Figure 2.4: CCE of the pure CC task performed before (blue) and after (red, green) the walk-and-reach CC task (see inset). The CCE decreases with practice, but this decrease is not specific to the hand-orientation during practice: There is no significant difference in later CCE if the preceding reaching involved *inverse* walk-and-reach trials (red) or not (green). Bars indicate the mean, black error bars the s.e.m.

2.4 Discussion

Previous studies have shown that the interference between tactile information on the hand and task-irrelevant visual information on an object increases from the time of movement onset when reaching with the hand towards the object (Brozzoli et al., 2010, 2009). Our results confirm this change in the crossmodal congruency effect (CCE) with reaching. In addition, when we compared the CCE in direct reaches to walk-and-reach movements to a target far from the body, we found no difference in CCE between near and far target reaches. To test for the spatial reference frame of congruency in the CCE, subjects inverted their hand during the movement so that thumb and index finger touched the target at the location where in the normal task the respective incongruent distracting light was presented. In the inverted hand condition the CCE decreased, if not vanished, for all timing conditions, but did not invert the congruency pairing between stimulated fingers and distractor light. A decrease in CCE based on practice between before and after the reaching task was independent of the different hand orientations. We conclude that the peripersonal space (PPS), as mapped with the CCE, expands to reach targets beyond the immediate reaching radius during goal-directed walk-and-reach movements.

Reach vs. walk-and-reach movements

The goal of our study was to test if a visual distractor would affect tactile stimulus discrimination even when being located on a reach target that is so far away that subjects first have to walk up to the target before reaching it. We could not find any significant differences between reach and walk-and-reach movements in the CCE. As described in previous studies (Brozzoli et al., 2010, 2009), we found a CCE already during movement planning (*static*), and also in the reference condition without any reach movement involved, i.e. in a non-reaching context (pure CC task). The fact that the CCE increases with onset of the movement above the level seen before the onset

of the movement, can be taken as indication that the peri-hand space expands with onset of a reaching movement towards the reach target (Brozzoli et al., 2014). Based on this interpretation and given that we could not find a difference between reach and walk-and-reach movements, the peri-hand space even extends towards reach goals out of reach and is, as such, independent of a relocation of the body.

Usually the PPS, and correspondingly the CCE, is discussed in context of the reachable space as defined by the space in front of the subject within the immediate reach of the hand (Brozzoli et al., 2014; Farnè et al., 2016; Van der Stoep et al., 2015). This emphasis comes from early studies in non-human primates that show two categories of visuo-tactile neurons, one with visual receptive fields close to the skin and the other with visual receptive fields further away but within reaching distance (Rizzolatti et al., 1981a,b). However, in those studies, as well as most other studies in the context of reaching with humans or non-human primates, animals or humans are sitting without having the option to move beyond the reachable space. Body movements towards a target located further away were not considered. Our results suggest that PPS is defined by the space within we can interact with our environment considering all types of body movements, including walk-and-reach behavior. CCE effects restricted to the reachable space in this sense would reflect the restricted operational space resulting from restrained experimental conditions that do not allow the participant to interact with the space beyond the immediate reach. This view is in line with studies about tool use that show that the PPS can expand beyond the immediate reach (Berti & Frassinetti, 2000; Giglia et al., 2015; Holmes, 2012; Iriki et al., 1996; Maravita & Iriki, 2004; Maravita et al., 2002a) and a reach study showing that mirror neurons respond differently when the observed action is blocked by a transparent barrier while still being within arm's length physical distance (Caggiano et al., 2009). Our behavioral findings add to the converging evidence from multiple lines of research that operational distance rather than physical distance determines the PPS and that this operational distance can be rather far reaching.

Hand orientation during reaching behavior

The PPS can be centered on different body parts, as suggested by bimodal receptive fields in non-human primates (Fogassi et al., 1996; Rizzolatti et al., 1981b), fMRI studies in humans (Brozzoli et al., 2012; Makin et al., 2007), and also spatial properties of behavioral multimodal integration (Serino et al., 2015; Spence et al., 2004a). Frames of reference are defined not only by their center-of-origin, but also their orientation and scaling of the dimensions. Since previous studies focused only on the distance of the body part, mostly hand, from a stimulus or object, conclusions are restricted to the center-of-origin of the reference frame. It is not clear from such data how orientation relative to the target object influences the PPS. For example, a hand-centered frame of reference in the strictest sense would predict that the thumb becomes congruent to the top light and the index finger congruent to the bottom when inverting the hand. Here, we showed a strong decrease, if not disappearance, of the CCE for all stages (*static, onset, move*)

during the walk-and-reach task when the subject inverted their hand during the reach (figure 2.3). This means, CCE was neither invariant to hand orientation, nor did it simply invert with hand orientation. In other words, hand orientation does not affect the CCE in a strictly hand-centered fashion which would be determined by the positions of the fingers on the target after completion of the reach.

Our study is not the only one that found incomplete inversion of the CCE with hand orientation. A recent study tested the effect on hand orientation on CCE during the reach to a bottle displayed on a computer screen (Belardinelli et al., 2018). Similar to our results, hand orientation affected the CCE before and after movement onset. In contrast to our results, some but not all conditions revealed a significant inverted CCE. One explanation for the stronger hand-orientation effect could be that different visual stimuli (bottle upright and bottle upside-down) were used which could have induced a stronger affordance for the different hand orientation. Still, and like in our results, an inversion of the congruency in the finger-to-distractor pairing following hand rotation cannot fully explain the findings in this previous study.

What could be possible explanations for the asymmetry in the CCE with hand orientation? Staying within the concept of hand-centered reference frames, one could argue that hand inversion was incomplete due to the task design, since we did not test different hand orientations at the start of the movement. This is also true for the study of Belardinelli and colleagues. Our motivation for this arrangement was to quantify possible dynamics of reference frame changes during reach planning and conduction, which we did not observe. Starting and conducting the reach with vertical hand orientations matched to the final hand position could have led to fully anti-symmetric task design with CCE inversion. If this is true, our lack of a CCE for trials with inverted hand orientation could be a consequence of the start and end position of the hand contributing to the CCE in opposing manner.

Alternatively, and independent of the reference frame concept, one could argue that the inverted configuration is less common. Even before any practice or instruction of the reaching task (pure CC task), we measured a positive CCE with distractor lights placed on the vertically oriented near and far targets and with the hand in a horizontal starting position. This suggests that ‘index finger above thumb’ represents a canonical orientation which is more ergonomic due to the anatomy of the arm and hand, and thereby is also over-trained during lifetime. Studies with a fake arm model showed that it is possible to embody the fake arm and build a PPS around it in relatively short time and even when the fake arm is detached from the body, but not when it is rotated to be in an unnatural position (Blanke et al., 2015; Botvinick & Cohen, 1998; Graziano et al., 2000; Maravita et al., 2003; Pavani et al., 2000). While embodiment is a result of congruent multimodal stimulation and the present study does not deal with the question of embodiment, the results suggest that multisensory integration might be restricted to plausible body configurations. If the CCE for normal as opposed to inverted hand is an effect of learning/exposure to common postures, it should be possible to also unlearn this association at least partly. Yet, several hundred reaches with inverted hand orientation did not have a significantly different effect on the end-

of-session CCE than with non-inverted hand orientation. If more practice over multiple days, weeks or months would change this, is unclear. However, the same mechanism that prevents to embody an anatomically unrealistically placed arm could be responsible for reducing crossmodal interaction for an unnatural reach.

Conclusion

The CCE increases with goal-directed reaching behavior even before the hand gets closer to the object suggesting a remapping of the PPS to reach goals (Belardinelli et al., 2018; Brozzoli et al., 2010, 2009). We showed that this holds true even for walk-and-reach movements to reach goals located beyond immediate reach. Furthermore, we tested whether the finger-to-distractor congruency pairing explains CCE effects. When inverting the hand, and thus the finger-to-distractor pairing, during the movement, the CCE decreases but does not simply invert according to the new pairing. We conclude that during planning and execution of goal-directed walk-and-reach movements the PPS expands to the action space independent of whether the movement goal is within immediate reach or not. The hand-related CCE does not only reflect a hand-centered reference frame but changes non-uniformly when the hand is rotated.

2.5 Methods

Subjects

Fifty-nine healthy, right handed (self-reported) subjects with normal or corrected-to-normal vision participated in the study (36 f, 23 m; 25 +/- 4 [s.d.] years; 6 have not reported their age). Participants were instructed prior to the experiments and gave their informed consent to take part in this study. Participants received a performance-independent hourly monetary compensation. Experiments were in accordance with institutional guidelines for experiments with humans, adhered to the principles of the Declaration of Helsinki, and were approved by the ethics committee of the Georg-Elias-Mueller-Institute for Psychology, University of Göttingen.

Experimental setup

Experiments took place in a quiet and dimly lit room. Small vibration motors (3.3 volts DC; Vibration Motor 11.6×4.6×4.8 mm, Pololu, Las Vegas, Nevada) were taped to the subjects' right index finger and thumb. Strength of the motor was set to maximum to ensure that the vibro-tactile stimulation was above the detection threshold for all subjects. We were only interested in reaction time related crossmodal congruency effects and not effects related to detection error. In the left hand, subjects held a custom-built response panel with two push buttons (GQ 19H-N, Conrad, Hirschau, Germany) arranged in a way that the left thumb could conveniently rest between and easily touch either button upon request. During the experiment, subjects wore headphones (AKG K-182,

Harman Deutschland GmbH, Garching, Germany) and listened to Brown noise (generated with "myNoise" and available on <https://mynoise.net/NoiseMachines/whiteNoiseGenerator.php>). Volume of the noise was adjusted for each subject individually that it felt comfortable and that they could not self-reportedly hear the sound originated from the vibration motors. Auditory cues were also delivered by the headphones.

A total of six (three pairs) capacitive touch sensors (EC3016NPAPL, Carlo Gavazzi, Steinhäusen, Switzerland) were mounted at three distances (*start*: 0 cm, *near*: 22 cm, *far*: 90 cm) in front of the subjects (figure 1 A). Touch sensors were offset to the right just far enough that they would not block subjects' straight ahead walking movements. At trial start, subjects stood in front of a pair of two touch sensors serving as start 'buttons'. The two sensors were mounted at approximately hip level with touch surfaces facing upward at 8 cm horizontal distance center-to-center. They could be comfortably reached with a relaxed right arm and used as resting position for the right index finger and thumb. The other two sensor pairs served as reach targets in front of the subjects at two different depths (horizontal start button-to-target distance – *near*: 22 cm; *far*: 90 cm) with vertically oriented touch surfaces facing the subject at 7.5 cm inter-digit separation. Subjects could comfortably reach to the near target without moving their shoulder or body. Subjects had to make a step forward to conveniently reach the far target. Since we are interested in crossmodal interference beyond the immediate reach, any distance that requires body relocation was sufficient for the *far* condition. Although participants needed to perform only one step, we call this the behavior walk-and-reach. The height of the targets was individually adjusted to eye level for each subject. Four synchronized RGB LEDs (WS2812B, Worldsemi Co., Daling Village, China) were located around each touch sensor for delivering the visual distractor cue.

The vibration motors, sensors and LEDs were controlled by a custom-built microcontroller-based interface which in turn was controlled by two custom-written C++ software packages, MoRoCo and MaCaQuE (Berger & Gail, 2018) (MaCaQuE software and schematics available on GitHub: <https://github.com/sensorimotorgroupdpz/MaCaQuE>), operated on a Mac Mini (Apple Inc., Cupertino, California).

Experimental task

To measure the crossmodal congruency effect (CCE), subjects needed to make a discrimination response on the response panel in their left hand to a 50 ms vibration on their right hand (figure 2.1 B). More specifically, they were asked to press the button to the left of their left thumb if they felt a vibration on their right thumb, and press the button to the right of their left thumb if they felt a vibration on their right index finger (tactile discrimination task). Subjects were asked to perform the discrimination task as fast as possible and the first response was registered as long as the next trial did not start yet. At the same time, the subjects were instructed to look at the

near or far target at which a task-irrelevant red light as visual distractor was presented for 50 ms, simultaneously to the vibration, either by the LEDs around the upper or the lower touch sensor.

In the visuo-tactile reference condition (pure CC), subjects performed two blocks of trials in a version of the crossmodal congruency (CC) task without movement context. Subjects conducted the tactile discrimination in combination with visual distractors on the "target" object while holding their right thumb and index finger on the start button, but without conducting a reach (figure 2.1 D). The subjects were asked to focus on the relevant target which was instructed by an auditory cue in the beginning of each trial. Target (near/far) and distractor location (top/bottom) were randomly interleaved. One block of the pure CC task was conducted in the beginning, one at the end of each experimental session.

The walk-and-reach CC task, the main part of the experiment, was conducted between the two blocks of the pure CC task. It consisted of an instructed-delay reach and walk-and-reach task to the cued targets which the subjects needed to perform simultaneously with the tactile discrimination task. The task contained the following stages after initiating a trial by touching the start buttons: 1) A high or low auditory cue was delivered on the headphones to indicate the near or the far target (DISTANCE); 2) Subjects had to remain still and keep the start buttons touched for another 1800 ms to 2500 ms; 3) When the same sound appeared for the second time (go cue), the subjects had to release the start button within a 2000 ms time window and reach to the cued target within a 2800 ms time window; 4) When the subjects touched the cued target with both fingers for at least 200 ms, the trial was counted as correct as signaled by a high-pitched tone. If the subjects during any stage did not perform the task correctly, the trial was counted as failed, which was signaled by a low buzzer tone. Auditory target cues and auditory feedback stimuli on reach performance were all easily distinguishable, as confirmed by oral report of the subjects. The subjects need to perform the tactile discrimination task in parallel. The vibro-tactile stimulation with visual distractor was delivered once per trial at different time points either during the delay, with onset of the movement or during the movement (see factor TIMING). Subjects did not receive any feedback about whether they performed the tactile discrimination task correctly or not. Within a block of trials, all conditions (= combinations of categorical task parameters relevant for this block; see list below) of the combined tactile discrimination and delayed walk-and-reach task were randomized. Regarding the parameter of the walk-and-reach task, conditions with a lower success rate appeared more often to obtain an equal number of trials for which the walk-and-reach task was performed correctly. This was not the case regarding the CC task performance: The performance of the tactile discrimination had no influence on the randomization. The duration of the instructed delay was drawn from a homogeneous distribution between minimum and maximum delay (see above), independent of the other parameters. If tactile stimulation was delivered within the instructed delay period, durations before and after the stimulation were drawn from homogeneous distributions between 1200 ms (before) / 550 ms (after) and 1550 ms (before) / 900 ms (after).

Factor CONGRUENCY: In accordance with the setup of Brozzoli and colleagues (Brozzoli et al., 2010, 2009), and considering that for a reach to the target one would naturally place the index finger on the higher sensor and the thumb on the lower, we defined the congruency of visual distractor and tactile stimulus as follows, *congruent*: upper four LEDs – index finger or lower four LEDs – thumb; *incongruent*: upper four LEDs – thumb or lower four LEDs – index finger. When the hand was inverted during the reaching phase (see below), we tested the CCE under two congruency definitions 1) the same as for normal reaches and 2) with an inverted definition (*congruent*: upper four LEDs – thumb or lower four LEDs – index finger; *incongruent*: upper four LEDs – index finger or lower four LEDs – thumb)

Factor DISTANCE: In the walk-and-reach CC task, at the beginning of each trial, an auditory cue (low or high frequency tone; 235 ms) indicated which target (*near*: reach, or *far*: walk-and-reach) subjects had to reach and at which place the distractor would be displayed. If DISTANCE was not randomized in a block, we kept the respective auditory cue to signal the start of the trial. The subjects were supposed to keep ocular fixation on a point in the middle between the two touch sensors of the cued target.

Factor ORIENTATION: The walk-and-reach CC task was performed under two different hand orientations, *normal*: touching the top sensor with the index finger and the bottom sensor with the thumb, and *inverse*: touching the top sensor with the thumb and the bottom with the index finger (figure 1 C). *Normal* and *inverse* reaches were performed in blocks of 120 correct trials ([*congruent, incongruent*] x [*static, onset, move*] x 20 trials) per each of the two conditions ([*near, far*]). Thus, subject knew the hand orientation condition from the beginning of each trial.

Factor TIMING: The goal was to measure the CCE at different time points of a goal-directed reach and walk-and-reach movement. The visuo-tactile stimulus pair, to which the subjects had to respond as fast as possible, appeared once per trial at three different timing conditions: either 550 ms to 900 ms before the go cue for the reach movement (*static*), at movement onset (*onset*), or during the movement, i.e. 200 ms (*near*) or 450 ms (*far*) after movement onset (*move*). Movement onset was registered on-line by the release of the start buttons and triggered the *onset* visuo-tactile stimulus with less than 10 ms delay. The time for the stimulation onset in the *move* condition was chosen to be just before target acquisition based on the fastest movement time in a pilot experiment (not shown). For the data presented in this study, this time point corresponded to approximately 24% (*near*) and 38% (*far*) of all movement time and was earlier than the fastest movement time (*near* 266 ms, *far* 481 ms). The inter-trial interval, i.e. the time from trial completion until the new trial could be triggered by the subject, for all tasks was 2 seconds. The next trial started, indicated by the first auditory cue, once the start buttons were touched after the inter-trial interval. A subject's manual response to the tactile stimulation was accepted as long as it was within the same trial including inter-trial interval, thus, at least up to 2 seconds after the vibration.

In summary, a complete set of all possible experimental conditions comprised in total 480 trials for the walk-and-reach task ([*congruent, incongruent*] x [*near, far*] x [*normal, inverse*] x

[*static, onset, move*] x 20 trials), 160 trials for the two pure CC task (2 x [*congruent, incongruent*] x [*near, far*] x 20 trials). This number of trials would have been too demanding for the subjects to run in a single session. Therefore, we recorded the data in three different experimental sessions. For all sessions the factors CONGRUENCY and TIMING were fully randomized. The permutations of the factors DISTANCE and ORIENTATION were distributed over separate blocks, i.e. per each block and session one combination of the two factors was used and, hence, the four possible combinations resulted in four separate blocks distributed over two sessions (see table 1). In the 3rd experimental session the factor DISTANCE was randomized within a block, while ORIENTATION was always *normal*. The sessions and blocks (within a session) are described here in the order in which they were recorded:

<i>session</i>	<i>CC before</i>	<i>walk-and-reach 1</i>	<i>walk-and-reach 2</i>	<i>CC after</i>
<i>near-normal-inverse:</i>	pure CC task - near	normal – near	inverse – near	pure CC task - near
<i>far-normal-inverse:</i>	pure CC task - far	normal – far	inverse – far	pure CC task - far
<i>near-far-normal:</i>	pure CC task	normal		pure CC task

Table 2.1: Blocks for each experimental session of the walk-and-reach CC task in original temporal order.

A pause was introduced between each block of a session. Subjects were allowed to practice before each block as long as they needed to feel confident with the task of the upcoming block.

Exclusion criteria

Each subject's dataset had to fulfill three criteria to be considered for data analysis:

1) Subjects needed to perform at least 20 trials for each condition in which both, the reach task and the crossmodal congruency task, were performed correctly. We aimed for 30 trials per conditions, but we stopped the walk-and-reach blocks earlier for some subjects to keep a whole experimental session within 1.5 hours. We chose to include only subjects with a minimum of 20 trials per condition but then included all correctly performed trials of these subjects in the analysis.

2) Subjects should not be biased towards one vibration motor to avoid that they use a strategy that favors a motor no matter what stimulation condition which might diminish the CCE. To test for such bias, we pooled across all conditions and blocks. As quantification, we defined a modulation index, $\frac{\mu(RT_{indexfinger}) - \mu(RT_{thumb})}{\sigma(RT_{indexfinger}) + \sigma(RT_{thumb})}$ for which μ is the mean and σ the standard deviation. Subjects with a modulation index exceeding the average modulation index across subjects by two standard deviations were excluded.

3) We witnessed that RT for *static* was unreasonably higher than for all other condition in some subjects. We expected that RT could be higher for *static* than for *onset* or *move* due to tactile suppression (Juravle & Spence, 2015). However, for a few subjects the difference was so high that we suspect subjects to have waited purposefully or accidentally for the go cue before responding to the tactile stimulus. As a precaution, we excluded those subjects. To identify those subjects, we calculated a modulation index, again $\frac{\mu(RT_{condition1}) - \mu(RT_{condition2})}{\sigma(RT_{condition1}) + \sigma(RT_{condition2})}$. We excluded

subjects with a modulation index exceeding the average modulation index across subjects by four standard deviations.

Based on the three criteria, we excluded 4 subjects for *near-normal-inverse*, 2 subjects for *far-normal-inverse* and 2 subjects for *near-far-normal*. Remaining numbers of recorded subjects were, *near-normal-inverse*: 21 (15 f, 6 m, 24 +/- 3 [s.d.] years); *far-normal-inverse*: 17 (11 f, 6 m, 25 +/- 3 [s.d.] years); *near-far-normal*: 25 (17 f, 8 m, 26 +/- 4 [s.d.] years). For each session, subjects performed all conditions, except of one subject in *near-far-normal* for whom there was a technical failure during the last block (pure CC task). Only few subjects performed more than one session: 4 in *near-normal-inverse* and *near-far-normal*; 3 in *near-normal-inverse* and *far-normal-inverse*; 1 in *near-far-normal* and *far-normal-inverse*. For data analysis, we pooled over all sessions and included the information about subject participation in the statistical model (see below).

Tactile discrimination and reach performance analyses

We measured the reaction time as time between visuo-tactile stimulus and left-hand button press in the tactile discrimination task (RT), the time between go cue and start button release in the reach task (RTreach). We also measured movement time during the reach (MTreach) as time between start button release and target acquisition. We excluded 9% of all walk-and-reach trials for which the walk-and-reach task was not performed correctly and 9% of all trials for which no response to the discrimination task was given. We computed each subject's averages of the three measures separately for each condition. We quantified the CCE based on the difference of the mean reaction times as $RT(\textit{incongruent}) - RT(\textit{congruent})$.

All data processing was performed using MATLAB (MathWorks Inc., Natick, Massachusetts) and R (R-Foundation, Vienna, Austria). For visualization we used the data visualization toolbox *gramm* (Morel, 2018). For statistical analysis, we used linear mixed effect models (LME) using the function 'lmer' with maximum log-likelihood estimation from the 'lmerTest' library in R. Based on the LME, we generated analyses of variance (ANOVA) tables with Satterthwaite approximation for degrees of freedom using the function 'anova' from the 'lmerTest' library. Our interpretation if an effect is significant or not is based on those ANOVA tables. For post-hoc multiple comparisons, we perform a generalized linear hypothesis test (function 'glht' from the library 'multcomp') on the respective model and extracted adjusted p-values based on a single multivariate test statistic extracted from the model. This method is described in detail in (Hothorn et al., 2008).

We computed LMEs for the observations y of subjects' RT, MTreach, RTreach and CCE, respectively. As fixed effects, we used CONGRUENCY (*congruent*, *incongruent*), ORIENTATION (*normal*, *inverse*), TIMING (*static*, *onset*, *move*) and DISTANCE (*near*, *far*). Since the subjects' performance and the CCE could be influenced by practice (Gill et al., 2017; Spence et al., 2004b), we also added PARTICIPATION as fixed effect, which is 0 when participated for the first time, 1 for the second time etc. Subjects were used as random intercepts. The model in

Wilkinson notation:

$$y \sim \text{ORIENTATION} * \text{TIMING} * \text{DISTANCE} * \text{CONGRUENCY} + \text{PARTICIPATION} + (1 | \text{SUBJECT})$$

for which y is either RT, RTreach or MTreach. First, we tested whether the CCE was present in our data by testing if CONGRUENCY has an effect on RT. Furthermore, we tested if DISTANCE has an effect on RT. We also tested whether CONGRUENCY has an effect on RTreach or MTreach to see if the CCE influences the reach and walk-and-reach behavior.

After we validated the presence of the CCE, we were mainly interested in effects on the CCE. Accordingly, we computed a LME for CCE:

$$\text{CCE} \sim -1 + \text{ORIENTATION} * \text{TIMING} * \text{DISTANCE} + \text{PARTICIPATION} + (1 | \text{SUBJECT})$$

As we found no effect for DISTANCE and PARTICIPATION, we computed a simplified model without DISTANCE and PARTICIPATION. Finally, we performed a post-hoc multiple comparisons test comparing all three stimulation times within normal hand orientation and inverted hand orientation, comparing hand orientations within all three stimulation times and comparing all three stimulation times with inverted hand orientation against the zero intercept resulting in twelve comparisons. To test for hand orientation specificity of the CCE, we repeated this analysis of the CCE but inverted the congruency pairing of finger to distractor for the trials with inverted hand orientation.

To test whether the training effect on the CCE is different when performing the reach task with a normal or inverted hand orientation, we tested the effect of the preceding hand orientation on the CCE of the pure CC task after the reaching task. We calculated a LME with ORIENTATION of the preceding block as fixed effect (*normal* for *near-far-normal* and *inverse* for the other two experimental sessions *near-normal-inverse* and *far-normal-inverse*) and SUBJECT as random intercept.

2.6 Acknowledgements

We thank Annika Hinze and Maximilian Stecker for help with data collection, Philip Ulbrich and Elisabeth Lindner for constructive feedback, Klaus Heisig for technical support and Holger Sennhenn-Reulen for help with data analysis.

This work was supported by the German Research Foundation (DFG RU-1847, grant GA1475-C1) and the European Commission in the context of the Plan4Act consortium (EC-H2020-FETPROACT-16 732266 WP1)

2.7 Competing interests

The authors declare no competing interests.

2.8 Authors contribution

MB, PN and AG designed the study; MB supervised data collection; MB analyzed the data; MB prepared all figures; MB and AG interpreted the data; MB and AG wrote the manuscript; all authors reviewed the manuscript.

References

- Andersen, R. A. and Cui, H. (2009). Intention, action planning, and decision making in parietal-frontal circuits. *Neuron*, 63(5):568–583.
- Barany, D. A., Della-Maggiore, V., Viswanathan, S., Cieslak, M., and Grafton, S. T. (2014). Feature interactions enable decoding of sensorimotor transformations for goal-directed movement. *Journal of Neuroscience*, 34(20):6860–6873.
- Belardinelli, A., Lohmann, J., Farnè, A., and Butz, M. V. (2018). Mental space maps into the future. *Cognition*, 176:65–73.
- Berger, M. and Gail, A. (2018). The reach cage environment for wireless neural recordings during structured goal-directed behavior of unrestrained monkeys. *bioRxiv*.
- Berti, A. and Frassinetti, F. (2000). When far becomes near: Remapping of space by tool use. *Journal of Cognitive Neuroscience*, 12(3):415–420.
- Bjoertomt, O., Cowey, A., and Walsh, V. (2002). Spatial neglect in near and far space investigated by repetitive transcranial magnetic stimulation. *Brain*, 125(9):2012–2022.
- Blanke, O., Slater, M., and Serino, A. (2015). Behavioral, neural, and computational principles of bodily self-consciousness. *Neuron*, 88(1):145–166.
- Botvinick, M. and Cohen, J. (1998). Rubber hands "feel" touch that eyes see. *Nature*, 391(6669):756.
- Brozzoli, C., Cardinali, L., Pavani, F., and Farnè, A. (2010). Action-specific remapping of peripersonal space. *Neuropsychologia*, 48(3):796–802.
- Brozzoli, C., Ehrsson, H. H., and Farnè, A. (2014). Multisensory representation of the space near the hand: from perception to action and interindividual interactions. *The Neuroscientist: a review journal bringing neurobiology, neurology and psychiatry*, 20(2):122–35.

- Brozzoli, C., Gentile, G., and Ehrsson, H. H. (2012). That's near my hand! parietal and premotor coding of hand-centered space contributes to localization and self-attribution of the hand. *Journal of Neuroscience*, 32(42):14573–14582.
- Brozzoli, C., Pavani, F., Urquizar, C., Cardinali, L., and Farnè, A. (2009). Grasping actions remap peripersonal space. *Neuroreport*, 20(10):913–917.
- Caggiano, V., Fogassi, L., Rizzolatti, G., Thier, P., and Casile, A. (2009). Mirror neurons differentially encode the peripersonal and extrapersonal space of monkeys. *Science*, 324(5925):403–406.
- Caminiti, R., Borra, E., Visco-Comandini, F., Battaglia-Mayer, A., Averbeck, B. B., and Luppino, G. (2017). Computational architecture of the parieto-frontal network underlying cognitive-motor control in monkeys. *eNeuro*, 4(1):ENEURO.0306–16.2017.
- Caminiti, R., Innocenti, G. M., and Battaglia-Mayer, A. (2015). Organization and evolution of parieto-frontal processing streams in macaque monkeys and humans. *Neuroscience and Biobehavioral Reviews*, 56:73–96.
- Cléry, J., Guipponi, O., Odouard, S., Wardak, C., and Ben Hamed, S. (2015a). Impact prediction by looming visual stimuli enhances tactile detection. *Journal of Neuroscience*, 35(10):4179–4189.
- Cléry, J., Guipponi, O., Wardak, C., and Ben Hamed, S. (2015b). Neuronal bases of peripersonal and extrapersonal spaces, their plasticity and their dynamics: Knowns and unknowns. *Neuropsychologia*, 70:313–326.
- Farnè, A., Serino, A., van der Stoep, N., Spence, C., and Di Luca, M. (2016). Depth: the forgotten dimension. *Multisensory Research*, 29(6–7):1–32.
- Fogassi, L., Gallese, V., Fadiga, L., Luppino, G., Matelli, M., and Rizzolatti, G. (1996). Coding of peripersonal space in inferior premotor cortex (area f4). *Journal of neurophysiology*, 76(1):141–57.
- Giglia, G., Pia, L., Folegatti, A., Puma, A., Fierro, B., Cosentino, G., Berti, A., and Brighina, F. (2015). Far space remapping by tool use: A rtms study over the right posterior parietal cortex. *Brain Stimulation*, 8(4):795–800.
- Gill, S., Blustein, D., Wilson, A., and Sensinger, J. (2017). Crossmodal congruency effect scores decrease with repeat test exposure. *bioRxiv*, page 1–12.
- Graziano, M. S. A. and Cooke, D. F. (2006). Parieto-frontal interactions, personal space, and defensive behavior. *Neuropsychologia*, 44(13):2621–2635.

- Graziano, M. S. A., Cooke, D. F., and Taylor, C. S. R. (2000). Coding the location of the arm by sight. *Science*, 290(5497):1782–1786.
- Graziano, M. S. A. and Gross, C. G. (1994). The representation of extrapersonal space: A possible role for bimodal, visual-tactile neurons. *The cognitive neurosciences*, page 1021–1034.
- Halligan, P. W. and Marshall, J. C. (1991). Left neglect for near but not far space in man. *Nature*, 350(6318):498–500.
- Holmes, N. P. (2012). Does tool use extend peripersonal space? a review and re-analysis. *Experimental Brain Research*, 218(2):273–282.
- Hothorn, T., Bretz, F., and Westfall, P. (2008). Simultaneous inference in general parametric models. *Biometrical Journal*, 50(3):346–363.
- Iriki, A., Tanaka, M., and Iwamura, Y. (1996). Coding of modified body schema during tool use by macaque postcentral neurones. *NeuroReport*, 7(14):2325–2330.
- Iriki, A., Tanaka, M., Obayashi, S., and Iwamura, Y. (2001). Self-images in the video monitor coded by monkey intraparietal neurons. *Neuroscience Research*, 40(2):163–173.
- Juravle, G. and Spence, C. (2015). Speed of reaction to sensory stimulation is enhanced during movement. *Acta Psychologica*, 161:154–161.
- Mahayana, I. T., Liu, C.-L., Chang, C. F., Hung, D. L., Tzeng, O. J. L., Juan, C.-H., and Muggleton, N. G. (2014). Far-space neglect in conjunction but not feature search following transcranial magnetic stimulation over right posterior parietal cortex. *Journal of neurophysiology*, 111(4):705–14.
- Makin, T. R., Holmes, N. P., and Zohary, E. (2007). Is that near my hand? multisensory representation of peripersonal space in human intraparietal sulcus. *The Journal of neuroscience: the official journal of the Society for Neuroscience*, 27(4):731–40.
- Maravita, A. and Iriki, A. (2004). Tools for the body (schema). *Trends in Cognitive Sciences*, 8(2):79–86.
- Maravita, A., Spence, C., and Driver, J. (2003). Multisensory integration and the body schema: Close to hand and within reach. *Current Biology*, 13(13):R531–R539.
- Maravita, A., Spence, C., Kennett, S., and Driver, J. (2002a). Tool-use changes multimodal spatial interactions between vision and touch in normal humans. *Cognition*, 83(2).
- Maravita, A., Spence, C., Sergent, C., and Driver, J. (2002b). Seeing your own touched hands in a mirror modulates cross-modal interactions. *Psychol Sci*, 13(4):350–355.

- Morel, P. (2018). Gramm: grammar of graphics plotting in matlab. *Journal of Open Source Software*, 3(23):568.
- Pavani, F., Spence, C., and Driver, J. (2000). Visual capture of touch: Out-of-the-body experiences with rubber gloves. *Psychological Science*, 11(5):353–359.
- Rizzolatti, G., Fadiga, L., Fogassi, L., and Gallese, V. (1997). The space around us. *Science*, 277(5323):190–191.
- Rizzolatti, G. and Luppino, G. (2001). The cortical motor system. *Neuron*, 31(6):889–901.
- Rizzolatti, G., Luppino, G., and Matelli, M. (1998). The organization of the cortical motor system: New concepts. *Electroencephalography and Clinical Neurophysiology*, 106(4):283–296.
- Rizzolatti, G., Scandolara, C., Matelli, M., and Gentilucci, M. (1981a). Afferent properties of periarculate neurons in macaque monkeys. i. somatosensory responses. *Behavioural Brain Research*, 2(2):125–146.
- Rizzolatti, G., Scandolara, C., Matelli, M., and Gentilucci, M. (1981b). Afferent properties of periarculate neurons in macaque monkeys. ii. visual responses. *Behavioural Brain Research*, 2(2):147–163.
- Serino, A., Noel, J. P., Galli, G., Canzoneri, E., Marmaroli, P., Lissek, H., and Blanke, O. (2015). Body part-centered and full body-centered peripersonal space representations. *Scientific Reports*, 5(November):18603.
- Shokur, S., O’Doherty, J. E., Winans, J. A., Bleuler, H., Lebedev, M. A., and Nicolelis, M. A. L. (2013). Expanding the primate body schema in sensorimotor cortex by virtual touches of an avatar. *Proceedings of the National Academy of Sciences*, 110(37):15121–15126.
- Shore, D. I., Barnes, M. E., and Spence, C. (2006). Temporal aspects of the visuotactile congruency effect. *Neuroscience Letters*, 392(1–2):96–100.
- Spence, C., Pavani, F., and Driver, J. (2004a). Spatial constraints on visual-tactile cross-modal distractor congruency effects. *Cognitive, Affective and Behavioral Neuroscience*, 4(2):148–169.
- Spence, C., Pavani, F., Maravita, A., and Holmes, N. (2004b). Multisensory contributions to the 3-d representation of visuotactile peripersonal space in humans: Evidence from the crossmodal congruency task. *Journal of Physiology Paris*, 98(1–3 SPEC. ISS.):171–189.
- Van der Stoep, N., Nijboer, T. C. W., Van der Stigchel, S., and Spence, C. (2015). Multisensory interactions in the depth plane in front and rear space: A review. *Neuropsychologia*, 70:335–349.

- Vuilleumier, P., Valenza, N., Mayer, E., Reverdin, A., and Landis, T. (1998). Near and far visual space in unilateral neglect. *Annals of Neurology*, 43(3):406–410.

2.9 Supplementary figures

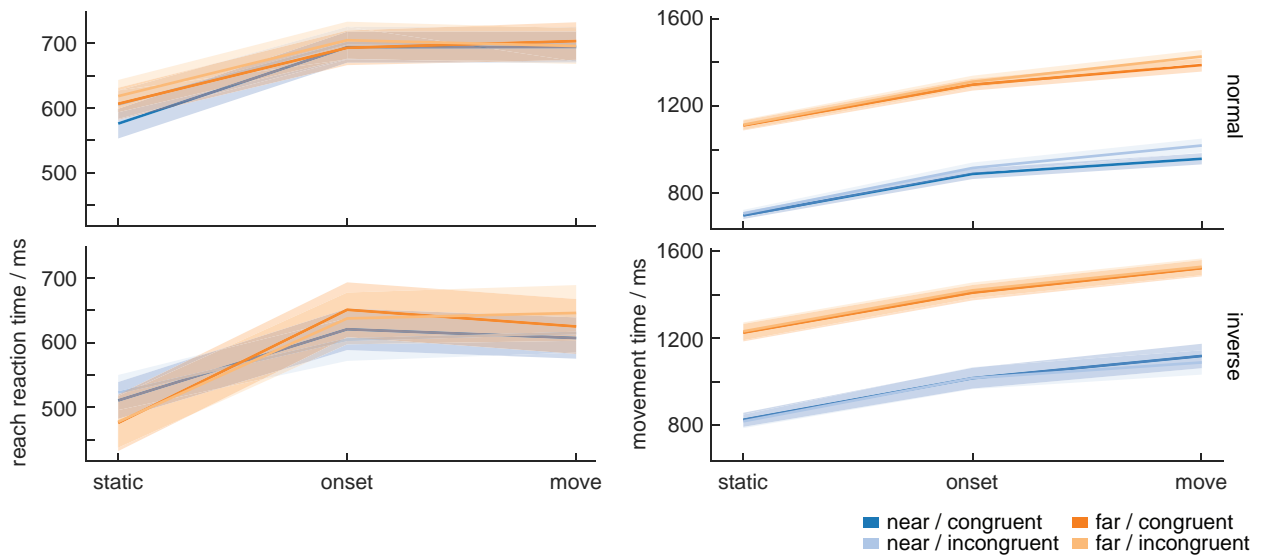


Figure 2.5: Average reach and walk-and-reach behavior. Left plots show the reaction times in the walk-and-reach task, i.e. the time between go-cue and movement onset. In the *static* condition, the crossmodal congruency task happened before the go cue allowing the subjects to fully concentrate on the reaching task. Right plots show the movement times of the walk-and-reach task, i.e. the time between movement onset and target touch. Naturally, walk-and-reach movements (*far*) take longer than just simple reaches. Solid lines indicate the mean, transparent areas s.e.m.

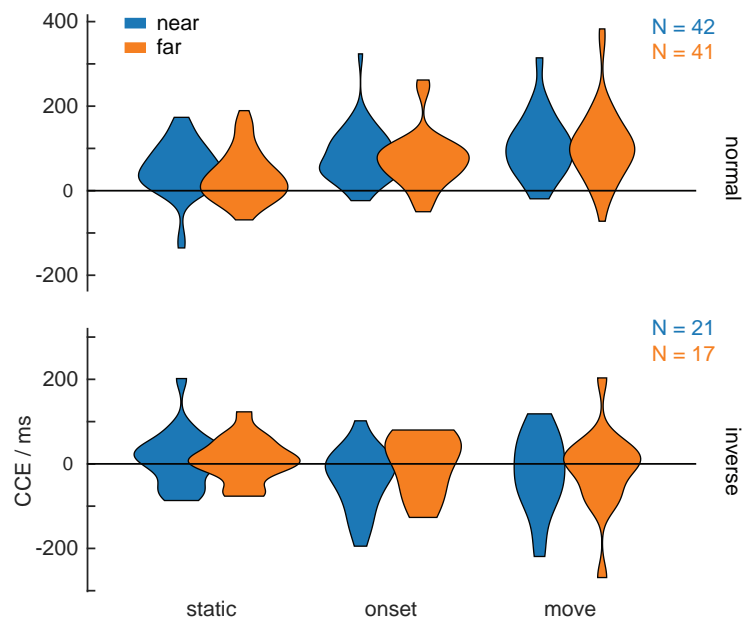


Figure 2.6: Violin plots showing the distribution of CCEs. It is the same data presented in figure 2.3.

2.10 Statistic tables

Analysis of Variance Tables of type III with Satterthwaite approximation for degrees of freedom
 Factors: time = TIMING; orient = ORIENTATION; dist = DISTANCE; congr = CONGRUENCY.

(Significant codes: 0 - '***' - 0.001 - '**' - 0.01 - '*' - 0.05 - '.' - 0.1 - ' ' - 1)

	<i>Sum Sq</i>	<i>Mean Sq</i>	<i>NumDF</i>	<i>DenDF</i>	<i>F.value</i>	<i>Pr(>F)</i>
condition	896113	448056	2	701.51	58.005	< 2.2e-16 ***
orient	138	138	1	726.03	0.018	0.8937178
dist	11143	11143	1	748.34	1.443	0.2301134
congr	177422	177422	1	701.51	22.969	2.011e-06 ***
participation	361	361	1	755.70	0.047	0.8288121
time:orient	128172	64086	2	701.51	8.296	0.0002747 ***
time:dist	13465	6732	2	701.51	0.872	0.4187475
orient:dist	88001	88001	1	738.65	11.393	0.0007759 ***
time:congr	8931	4466	2	701.51	0.578	0.5612224
orient:congr	268039	268039	1	701.51	34.700	5.968e-09 ***
dist:congr	207	207	1	701.51	0.027	0.8701524
time:orient:dist	18392	9196	2	701.51	1.190	0.304687
time:orient:congr	56598	28299	2	701.51	3.664	0.0261328*
time:dist:congr	3999	2000	2	701.51	0.259	0.7719902
orient:dist:congr	4870	4870	1	701.51	0.630	0.4274512
time:orient:dist:congr	2593	1297	2	701.51	0.168	0.845518

Table 2.2: ANOVA table for reaction time to vibro-tactile stimulation (Figure 2.2)

	<i>Sum Sq</i>	<i>Mean Sq</i>	<i>NumDF</i>	<i>DenDF</i>	<i>F.value</i>	<i>Pr(>F)</i>
time	1786371	893185	2	701.46	109.437	< 2e-16 ***
orient	603865	603865	1	716.94	73.988	< 2e-16 ***
dist	17228	17228	1	755.30	2.111	0.14668
congr	5148	5148	1	701.46	0.631	0.42737
participation	3050	3050	1	751.17	0.374	0.54117
time:orient	37769	18885	2	701.46	2.314	0.09964 .
time:dist	20796	10398	2	701.46	1.274	0.28036
orient:dist	14347	14347	1	727.36	1.758	0.18530
time:congr	7256	3628	2	701.46	0.445	0.64131
orient:congr	1980	1980	1	701.46	0.243	0.62248
dist:congr	379	379	1	701.46	0.046	0.82940
time:orient:dist	67393	33697	2	701.46	4.129	0.01650 *
time:orient:congr	11251	5626	2	701.46	0.689	0.50228
time:dist:congr	2430	1215	2	701.46	0.149	0.86169
orient:dist:congr	916	916	1	701.46	0.112	0.73777
time:orient:dist:congr	1321	660	2	701.46	0.081	0.92229

Table 2.3: ANOVA table for reaction time for the start button release (Figure 2.5 left)

	<i>Sum Sq</i>	<i>Mean Sq</i>	<i>NumDF</i>	<i>DenDF</i>	<i>F.value</i>	<i>Pr(>F)</i>
time	9140317	4570158	2	700.79	438.14	< 2e-16 ***
orient	1295071	1295071	1	717.74	124.16	< 2e-16 ***
dist	8771245	8771245	1	755.89	840.90	< 2e-16 ***
congr	21184	21184	1	700.79	2.03	0.15458
participation	15445	15445	1	752.83	1.48	0.22405
time:orient	930	465	2	700.79	0.04	0.95640
time:dist	10489	5245	2	700.79	0.50	0.60505
orient:dist	17932	17932	1	728.74	1.72	0.19022
time:congr	7313	3656	2	700.79	0.35	0.70443
orient:congr	30069	30069	1	700.79	2.88	0.08998
dist:congr	376	376	1	700.79	0.04	0.84948
time:orient:dist	335	168	2	700.79	0.02	0.98405
time:orient:congr	23418	11709	2	700.79	1.12	0.32604
time:dist:congr	521	260	2	700.79	0.02	0.97535
orient:dist:congr	10965	10965	1	700.79	1.05	0.30558
time:orient:dist:congr	2988	1494	2	700.79	0.14	0.86660

Table 2.4: ANOVA table for movement time in the reach task (Figure 2.5 right)

	<i>Sum Sq</i>	<i>Mean Sq</i>	<i>NumDF</i>	<i>DenDF</i>	<i>F.value</i>	<i>Pr(>F)</i>
time	17863	8931	3	323.02	2.302	0.1017
dist	651	651	1	249.21	0.168	0.6824
orient	510121	510121	1	375.02	131.505	< 2.2e-16 ***
participation	5890	5890	1	269.27	1.518	0.2189
time:dist	7999	3999	2	323.02	1.031	0.3578
time:orient	113197	56598	2	323.02	14.591	8.58e-07 ***
dist:orient	9146	9146	1	370.18	2.358	0.1255
time:dist:orient	5186	2593	2	323.02	0.668	0.5132

Table 2.5: ANOVA table for CCE (Figure 2.3/2.6)

	<i>Sum Sq</i>	<i>Mean Sq</i>	<i>NumDF</i>	<i>DenDF</i>	<i>F.value</i>	<i>Pr(>F)</i>
time	113197	8931	3	320.91	19.725	8.325e-09 ***
dist	6305	6305	1	351.50	2.197	0.1391
orient	361375	361375	1	353.58	125.945	< 2.2e-16 ***
participation	180	180	1	367.45	0.063	0.8021
time:dist	5186	2593	2	320.91	0.904	0.4061
time:orient	17863	8931	2	320.91	3.113	0.0458 *
dist:orient	908	908	1	360.12	0.317	0.5740
time:dist:orient	7999	3999	2	320.91	1.394	0.2496

Table 2.6: ANOVA table for CCE with inverted CCE definition for inverted hand orientation

	<i>Estimate</i>	<i>Std. Error</i>	<i>z value</i>	<i>Pr(> z)</i>
move,normal - move,inverse == 0	126.450	12.631	10.011	< 0.001 ***
onset,inverse - move,inverse == 0	-2.242	14.528	-0.154	1
static,inverse - move,inverse == 0	28.765	14.528	1.980	0.324
static,normal - move,normal == 0	-61.896	9.547	-6.483	< 0.001 ***
onset,normal - move,normal == 0	-28.354	9.547	-2.970	0.029 *
static,inverse - onset,inverse == 0	31.007	14.528	2.134	0.241
onset,normal - onset,inverse == 0	100.338	12.631	7.944	< 0.001 ***
static,normal - onset,normal == 0	-33.542	9.547	-3.513	0.005 **
static,normal - static,inverse == 0	35.789	12.631	2.833	0.044 *
static,inverse == 0	8.738	11.320	0.772	0.975
onset,inverse == 0	-22.269	11.320	-1.967	0.331
move,inverse == 0	-20.027	11.320	-1.769	0.456

Table 2.7: Post-hoc multiple comparison on $CCE \sim -1 + time * orient + (1|subject)$

	<i>Estimate</i>	<i>Std. Error</i>	<i>z value</i>	<i>Pr(> z)</i>
move,normal - move,inverse == 0	97.432	10.998	8.859	< 0.001 ***
onset,inverse - move,inverse == 0	2.242	12.504	0.179	1
static,inverse - move,inverse == 0	-28.765	12.504	-2.300	0.176
static,normal - move,normal == 0	-61.896	8.217	-7.533	< 0.001 ***
onset,normal - move,normal == 0	-28.354	8.217	-3.451	0.006 **
static,inverse - onset,inverse == 0	-31.007	12.504	-2.480	0.115
onset,normal - onset,inverse == 0	66.836	10.998	6.077	< 0.001 ***
static,normal - onset,normal == 0	-33.542	8.217	-4.082	< 0.001 ***
static,normal - static,inverse == 0	64.301	10.998	5.847	< 0.001 ***
static,inverse == 0	-16.493	11.079	-1.489	0.665
onset,inverse == 0	14.514	11.079	1.310	0.78
move,inverse == 0	12.273	11.079	1.108	0.884

Table 2.8: Post-hoc multiple comparison on $CCE \sim -1 + time * orient + (1|subject)$ with inverted CCE definition for inverted hand orientation

Chapter 3

The Reach Cage environment for wireless neural recordings during structured goal-directed behavior of unrestrained monkeys

The preprint of this manuscript was published on the 24. April 2018 in *bioRxiv*.

The Reach Cage environment for wireless neural recordings during structured goal-directed behavior of unrestrained monkeys

Michael Berger^{1,2}, Alexander Gail^{1,2,3,4}

1 Cognitive Neuroscience Laboratory, German Primate Center - Leibniz-Institute for Primate Research, Göttingen, Germany

2 Faculty of Biology and Psychology, University of Göttingen, Göttingen, Germany

3 Leibniz-ScienceCampus Primate Cognition, Göttingen, Germany

4 Bernstein Center for Computational Neuroscience, Göttingen, Germany

Abstract

Sensorimotor neuroscience with non-human primates usually mandates partial movement restraint to confine behavioral parameters and protect recording equipment. We present the Reach Cage and a versatile visuo-haptic interaction system (MaCaQuE) for investigating goal-directed whole-body movements of unrestrained monkeys. Two rhesus monkeys learned to conduct instructed reaches towards targets flexibly positioned in the cage. 3-D wrist movements were tracked in real time with video motion capture. We wirelessly recorded up to 128 broad-band neural signals at single unit resolution from three cortical sensorimotor areas. We demonstrate that repeated movements show small enough trial-to-trial variation to allow grouping of data for sufficient statistical power, and single neuron activity is selective for different reach movements. In conclusion, the Reach Cage in combination with wireless recordings allows correlating multi-channel neural dynamics with trained repetitive simpler movements, equivalent to conventional experiments, but also more complex goal-directed whole-body motor behaviors, like walk-and-reach movements.

Keywords: arm movements, wireless neurophysiology, motion capture, primate, motor, parietal, premotor

Introduction

Sensorimotor neuroscience investigates how the brain processes sensory information, develops an action plan based on this information and ultimately performs a corresponding action. For instance, the fronto-parietal reach network is integrating hand, gaze and target position to compute the movement direction from the hand to the target (Andersen & Cui, 2009; Batista, Buneo, Snyder, & Andersen, 1999; Buneo, Jarvis, Batista, & Andersen, 2002; Pesaran, Nelson, & Andersen, 2006). To understand the neuronal basis of such behavior, spatial parameters such as head position, gaze direction, and body and arm posture need to be monitored and correlated with detailed measures of neural activity at the single unit resolution (Kuang, Morel, & Gail, 2016). Especially in system neuroscience with nonhuman

Correspondence to Michael Berger

E-mail: mberger@dpz.eu

Address: Cognitive Neuroscience Laboratory, German Primate Center - Leibniz-Institute for Primate Research, Kellnerweg 4, 37077 Göttingen, Germany

primates, this led to highly specialized and controlled experimental setups with strongly constrained motor behavior. Typically, monkeys are seated in a primate chair and respond to sensory cues by operating a manipulandum or touchscreen while single unit activity is recorded using intra-cortical electrodes. Such studies led to numerous important insights into neural correlates of visually guided reaching movements, for instance force encoding (Cheney & Fetz, 1980) direction encoding (Georgopoulos, Schwartz, & Kettner, 1986), spatial reference frames of reach goal encoding (Batista et al., 1999; Buneo et al., 2002; Pesaran et al., 2006), context integration (Gail & Andersen, 2006; Westendorff, Klaes, & Gail, 2010), obstacle avoidance (Kaufman, Churchland, & Shenoy, 2013; Mulliken, Musallam, & Andersen, 2008), or decision making (Cisek, 2012; Klaes, Westendorff, Chakrabarti, & Gail, 2011). Because of the physical restraint, arm movements were restricted to the immediately reachable space and well-controlled planning and execution of goal-directed movements could not be investigated in monkeys in larger environments. For example, to date it was not possible to investigate naturalistic goal-directed movements that require the monkey to walk towards a target and thus to investigate how monkeys plan to acquire a reach goal beyond the immediately reachable space.

In conventional experiments, single unit activity is recorded either with chronically implanted multi-electrode arrays or depth-adjustable single electrodes. Signals are processed by a head-mounted instrumentation amplifier ('headstage') and routed to a data acquisition system via cables. Such tethered connections make it impossible to record from freely moving primates, at least in the case of larger species such as macaques. A few studies showed that tethered recording of freely moving monkeys can be possible with smaller species such as squirrel monkeys (Ludvig, Tang, Gohil, & Botero, 2004) or marmosets (Nummela, Jovanovic, Mothe, & Miller, 2017). Using wireless recording technology in combination with chronically implanted arrays, recent studies achieved recordings of single unit activity in nonhuman primates investigating vocalization (Hage & Jurgens, 2006; Roy & Wang, 2012), simple uninstructed behavior (Gilja, Chestek, Nuyujukian, Foster, & Shenoy, 2010; Schwarz et al., 2014), locomotion (Foster et al., 2014; Yin et al., 2014), chair-seated translocation (Rajangam et al., 2016), and sleep (Yin et al., 2014). An experimental environment for monkeys performing well-structured, goal-directed sensorimotor tasks without physical restraint, while at the same time registering behavioral and neural data, is missing to date (see review Händel & Schölvinc, 2017).

An important translational goal of sensorimotor neuroscience with non-human primates is the development of brain-machine interfaces based on intracortical extracellular recordings to aid patients with severe motor impairments such as tetraplegia. Intracortical signals can be decoded to control external devices, as demonstrated in non-human primates (e.g. Hauschild, Mulliken, Fineman, Loeb, & Andersen, 2012; Musallam, Corneil, Greger, Scherberger, & Andersen, 2004; Santhanam, Ryu, Yu, Afshar, & Shenoy, 2006; Serruya, Hatsopoulos, Paninski, Fellows, & Donoghue, 2002; Taylor, Tillery, & Schwartz, 2002; Velliste, Perel, Spalding, Whitford, & Schwartz, 2008; Wessberg et al., 2000), and suited to partially restore motor function in quadriplegic human patients (Aflalo et al., 2015; Bouton et al., 2016; Collinger et al., 2013; Gilja et al., 2015; Hochberg et al., 2012; Wodlinger et al., 2014). Due to their medical condition, those patients are not able to move their limbs and, as such, those experiments could not test whether decoding remains stable while the subject performs additional or task-irrelevant movements. Ultimately, the control of prostheses should be possible in larger workspaces for which also whole-body movements are required for instance for amputee patients that lost a limb but otherwise do not suffer from any other disease. Little is known about the stability of decoding performance when movements are performed in parallel such as walking. Wireless technology can be used to reduce the physical restraint from brain-machine-interface studies (Schwarz et al., 2014). This was demonstrated, for example, with a monkey moving through a room by controlling a wheeled platform that carried the primate-chair in which the monkey was sitting (Rajangam et al., 2016). While this is an important proof-of-principle towards BMI wheelchair control in paralyzed patients, it is not suited to investigate naturalistic goal-directed movements in freely moving monkeys. For reliable BMI applications, it is necessary to identify motor control parameters that are not disturbed when performing multiple movements at the same time. Thus, experimental paradigms are required that allow to test complex behavior consisting of various movement types.

Here, we present an experimental environment, the Reach Cage, which is equipped with a visuo-haptic interaction system (MaCaQuE) and allows investigating movement planning and goal-directed movements of freely moving rhesus monkeys while recording cortical single-unit activity. We trained monkeys to perform controlled visually-guided reach movements with instructed delay to targets within and beyond the immediately reachable space. Using video-based motion capture of a stained spot on the fur, we measured three-dimensional wrist trajectories during task performance in real-time. We used wireless recording technology to record from single units in three cortical areas (parietal reach region PRR, dorsal premotor cortex PMd, and primary motor cortex M1) from a monkey performing reach and walk-and-reach movements. We show that the Reach Cage is suitable for sensorimotor neuroscience with physically unrestrained rhesus monkeys providing a richer set of motor tasks. Still, behavior and its neural correlates can be well identified and analyzed like in conventional experiments due to the highly structured task and setting.

Results

We developed the Reach Cage to expand studies of visual guided reaching movements to larger workspaces and study movements of rhesus monkeys performing structured reach tasks while being physically unrestrained. We report on quantitative assessment of the animals' behavior in the Reach Cage, as a basis for any further neuroscientific analysis. The timing of the monkeys' reaching behavior can be precisely controlled and measured with the touch and release times of our touch-sensitive cage-mounted targets (1st section). Additionally, 3-D reach kinematics can be measured directly with the video-based motion capture system (2nd section). Finally, we will show that wireless neural recording is possible in the Reach Cage (3rd section) and report on proof-of-concept single-unit activity during such structured task performance (3rd and 4th section).

Real-time control of behavior in physical unrestrained rhesus monkeys in the Reach Cage

The core element of our newly developed Reach Cage (Figure 1) is the Macaque Cage Query Extension (MaCaQuE). Using this interaction device, we were able to train two fully unrestrained rhesus monkeys to conduct a behavioral task common to sensorimotor neuroscience in primates in a temporally well-structured fashion.

Both animals learned within a single first session that touching a target presented on a MaCaQuE Cue and Target box (MCT, Figure 1B) leads to a liquid reward. Due to the computer-controlled precise timing and dosage of reward (Figure 1C), like in conventional chair-based setups, we could employ MaCaQuE for positive reinforcement training (PRT) to teach both animals a visually-guided target acquisition task with instructed delay (see Materials and Methods). Unlike conventional setups, MaCaQuE allowed for target placement beyond the immediate reach of the monkeys (Figure 1D). Monkey K performed the final stretch-and-reach version of the task (Figure 2A/B left) with 77% correct trials on average (s.d. 23%, 17 sessions) with up to 382 correct trials per session (mean 140, s.d. 99). Monkey L performed the final walk-and-reach (Figure 2A/B right) version of the task with 43% correct trials (s.d. 12%, 22 sessions) performing up to 405 correct trials per session (mean 153, s.d. 109). Most errors of monkey L were due to premature release of the start buttons prior to the go cue, especially for far targets (see also start button release timing below, Figure 2C). Trials with properly timed movement initiation were 83% correct in monkey L.

While the animals were not physically restricted to a specific posture, the strict timing of the task encouraged them to optimize their behavior. Since the MaCaQuE system makes information about MCT touches and releases available with minimal delay (< 1 ms), it is possible to enforce an exact timing of the monkeys' movements when solving a reaching task in the Reach Cage. Figure 2C shows the distribution of button release times and movement times towards near and far targets for monkey K (17 session, 2377 correct trials) and monkey L (22 sessions, 3366 correct trials). The movement times to the far targets were longer than to near targets, since a whole-body translocation is required to approach far targets (monkey K: near 267 ms, far 502 ms, t-test $p < 0.001$; monkey L: near 322 ms, far 896 ms, t-test $p < 0.001$). Also the button release time in both monkeys were higher for far compared

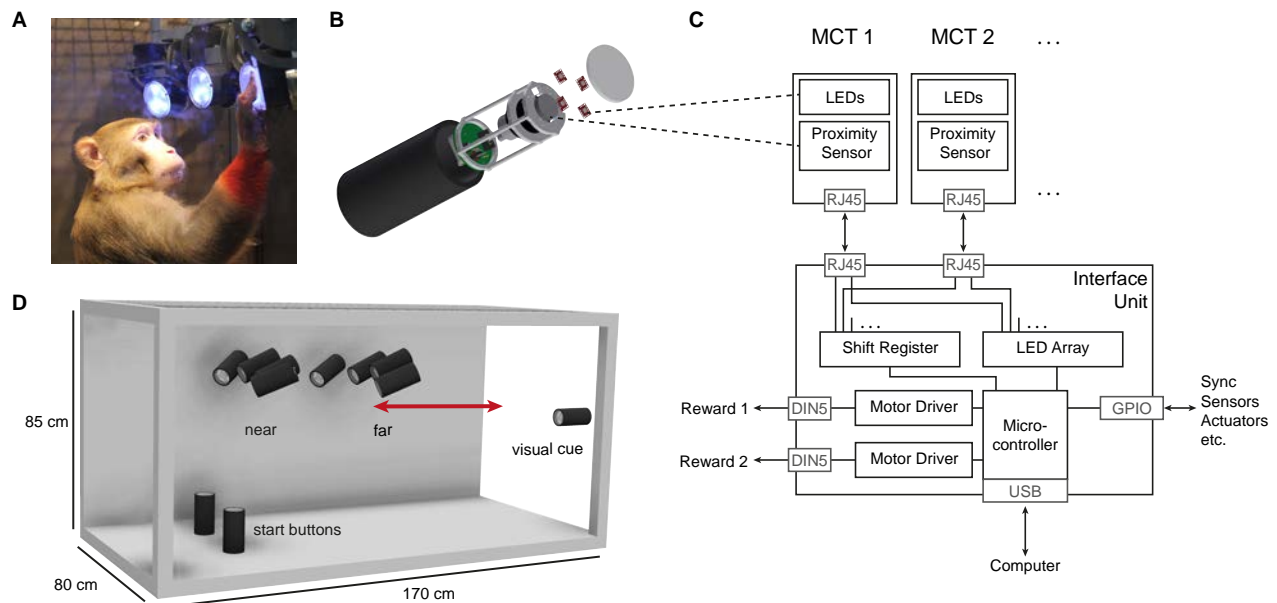


Figure 1: The Reach Cage setup. A) Monkey K touching one of the illuminated MCTs inside the Reach Cage. Red fur staining at the wrist was used for motion-capture. B) A MaCaQuE Cue and Target box (MCT) with proximity sensor to make the translucent front cover touch-sensitive and four RGB LEDs to illuminate it. C) Schematic of Macaque Cage Query Extension (MaCaQuE) showing the electronic components with the microcontroller interfacing between MCTs and an external computer for experimental control. D) Sketch of the Reach Cage with ten MCTs inside, two on the floor pointing upwards serving as a starting position for the monkey and two rows of four (near and far) pointing towards the starting position. Far MCTs were positioned such that monkey K could reach them from the starting position by stretching its body. For monkey L, the far MCTs were positioned to the back of the cage (red arrow) such that the animal needed to walk first. An eleventh MCT is positioned outside the cage for providing additional visual cues. The universal MCTs can be arranged flexibly to serve different purposes.

to near targets (monkey K: near 296 ms, far 414 ms, t-test $p < 0.001$; monkey L: near 511 ms far 652 ms, t-test $p < 0.001$). Button release time indicates the onset of the hand movement, not necessarily the whole body movement. Video analysis suggests that the monkeys started their body movements prior to the arm movements, thus, delaying the release of the start button in far reach trials. Standard deviations of movement time were higher for far than for near in monkey K (near 32 ms, far 56 ms; F-test $p < 0.001$) and - to a lesser extent - higher for near than for far in monkey L (near 110 ms, far 103 ms; F-test $p < 0.01$). The high coefficient of variation of button release time for monkey L (near 0.39, far 0.45) compared to monkey K (near 0.18, far 0.15) suggests that monkey L in contrast to monkey K was not yet reacting properly to the go cue. Monkey L later adopted proper response timing [data not shown].

The behavioral results as assessed with MaCaQuE via the proximity sensors of the MCTs demonstrate that the Reach Cage is suitable to train animals on goal-directed reaching tasks with target positions not being constrained by the immediately reachable space of the animal. The temporally and spatially well-structured task performance at the same time allows behavioral and neurophysiological analyses as applied in more conventional settings.

Movement kinematics of an unrestrained rhesus monkey performing a memory-guided reaching task in the Reach Cage

Since we do not impose physical restraint, the monkeys have more freedom to move than in conventional setups. We used motion capture to analyze the variability of the reach kinematics of monkey K performing the stretch-and-reach version of the task.

We measured 3-dimensional trajectories of monkey K's wrist. Permanent hair-dye on the fur of monkey K was sufficient for a reliable color tracking for around three months. Figure 2D shows the

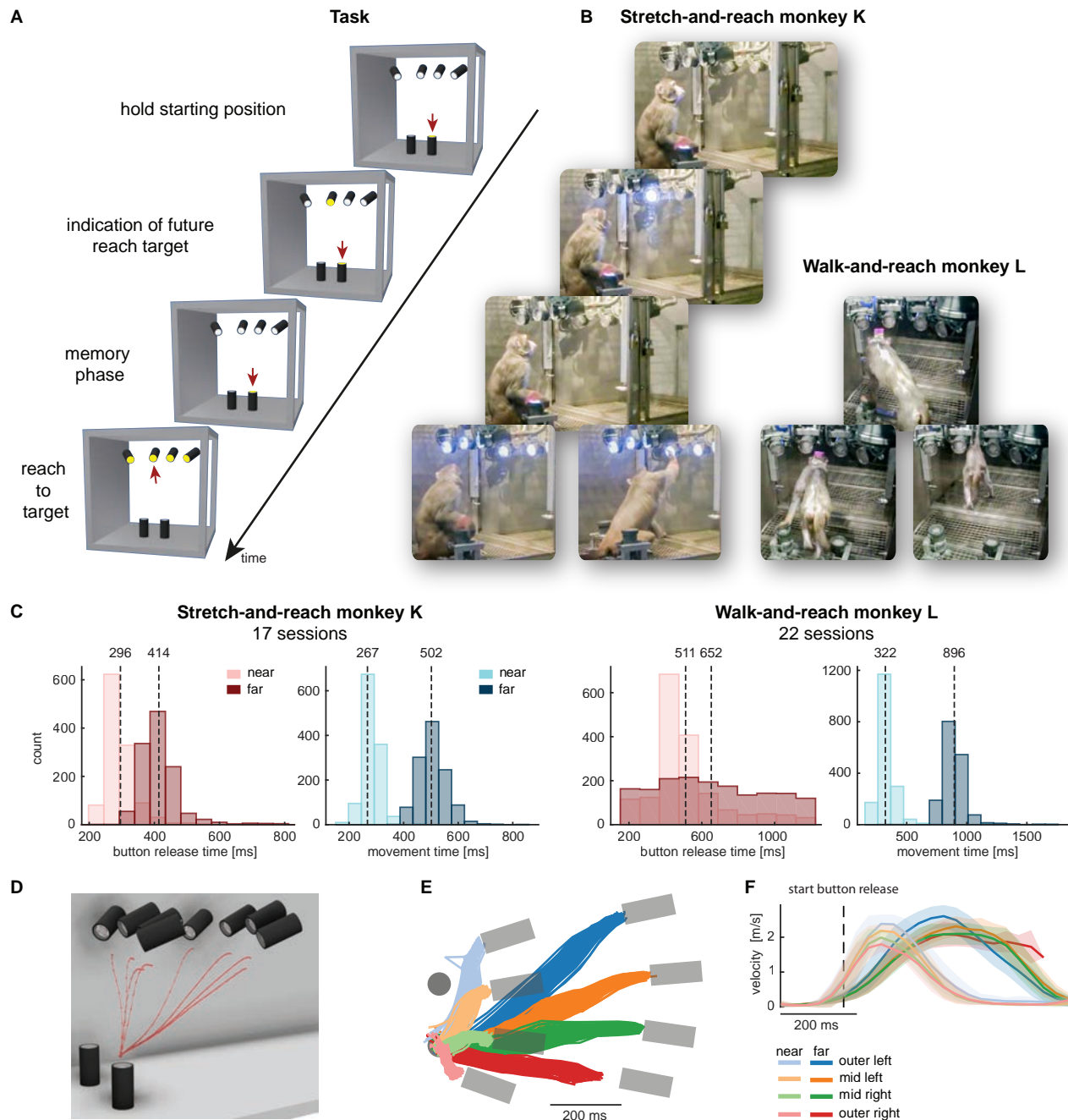


Figure 2: Structured behavior during task performance in unrestrained animals. A) Timeline of the stretch-and-reach version of the task (see Materials and Methods for differences to the walk-and-reach version). Yellow MCTs indicate illumination. Only near targets are shown to illustrate this example trial, in which the second left-most near target was indicated as target and had to be reached after an instructed delay in response to the go cue (transient illumination of all targets). B) An example trial to a far target for monkey K (stretch-and-reach, left) and monkey L (walk-and-reach, right). The frames of the surveillance video correspond to the time periods of the trial illustrated in A. C) Times between go cue and start button release (button release time), and between start button release and target acquisition (movement time) were distributed narrowly in most cases for reaching movements to near (bright) and far (dark) targets. Dashed lines and corresponding numbers indicate the average. D-F) Monkey K's wrist motion capture for reaches to the eight targets from 200 ms before start button release until 600 ms after start button release (stretch-and-reach task). Since the far outer right target was partly occluded for one of the cameras (see vertical metal frame in B), the part of the trajectories (red) closest to this target is missing, while all other trajectories were captured entirely. D) Average reach trajectories reconstructed in the 3-dimensional Reach Cage model. E) Top view of target (grey) positioning inside the cage with 2-dimensional reach trajectories. F) Average absolute velocities of wrist movement. Shaded area represents standard deviation.

reconstruction of the average 3-dimensional trajectories within the Reach Cage volume. Trial-by-trial individual trajectories indicate that the monkey performed relatively straight reaches with low spatial variability (Figure 2E). The speed profiles of the wrist movement (Figure 2F) show the typical bell shape of directed reaching movements and large overlap between different near and between different far targets indicating smooth continuous movements. To quantify the variability in the reach trajectories, we calculated for each target separately and at each time point the Euclidean distance between the single-trial trajectories and the trial-averaged trajectory. The highest observed trial-averaged Euclidean distance over the course of the trajectories was 65 mm (s.d. 40 mm). Since the monkeys were free to position their hand on the proximity sensors, the measured variability in wrist position was not zero during hold phases. In the 150 ms before start button release, the average Euclidean distance was 9 mm (s.d. 7 mm), after target acquisition it was 11 mm (s.d. 7 mm). As a reference, the transparent front plate of the targets has a diameter of 75 mm and the center-to-center distance between neighboring targets is around 130 mm (near) and 210 mm (far).

The kinematic analyses demonstrate that animal K not only complied with the spatial and temporal task requirements in terms of starting and endpoint acquisition but also adopted reliable repetitive behavior in terms of overall reach kinematics. We computed trial-averaged video streams for both animals which confirm that animal L adopted an equivalent behavior, evident from the fact that the overlaid videos for same-target trials slightly blur but do not wash out the animal image (see Rich Media File supplemental materials).

Multi-channel single cell activity can be recorded in the Reach Cage using wireless technology

A main goal of this study was to provide a proof-of-concept that the Reach Cage is an adequate setting for studying neural activity of monkeys during movement planning and execution of goal-directed behavior. We here provide this proof-of-concept with recordings from three different sensorimotor areas of animal L during the walk-and-reach task. Implant development and methodological details will be discussed below (Material and Methods).

We chronically implanted a total of 192 electrodes in primary motor cortex (M1), dorsal premotor cortex (PMd) and posterior parietal cortex of monkey L using six 32-channel floating microwire areas (FMA). We recorded broadband neural data while the monkey performed a visually-guided delayed walk-and-reach task (Figure 3). The animal moved through the cage with the wireless electronics and protective cap without apparent issues and performed the behavioral task as without electronics and cap.

We recorded 21 sessions from one array at a time using the 31-channel wireless headstage (number of session per array: 2 PRR-posterior; 7 PRR-anterior; 2 M1-medial; 4 M1-lateral; 4 PMd-posterior; 2 PMd-anterior). While implants were designed to also use a 127-channel wireless headstage, we here mostly report 31-channel recordings. 127-channel recordings were less stable than the 31-channel recordings, with more frequent data loss and higher likelihood of artifacts. When the signal was stable it was possible to isolate single and multi-unit waveforms (Figure 3A). For the purpose of the current study, simultaneous recordings of four FMA arrays are not relevant. Once antennas were oriented appropriately, we did not experience signal loss with the 31-channel headstage and could record broadband signals with receiving antennas either placed inside or outside the cage. The recording and transmission quality of the signal was high and the raw signals show clearly distinguishable spiking activity (Figure 3B). The activity of the example channel is clearly modulated by the task events as spiking as well as low-frequency components of the activity changes after go cue and start button release. This example signal trace shows a stable signal during the movement of the animal, as was the case for the other channels monitored online during the monkey's movements. If present, artifacts or signal loss resulted in strong signal modulation or high voltage peaks clearly exceeding neuronal signals and easily detectable by eye during the recording. We did experience such artifacts when the animal moved its head very close to metal, particularly when drinking from the reward bowl mounted on metal bars of the cage frame.

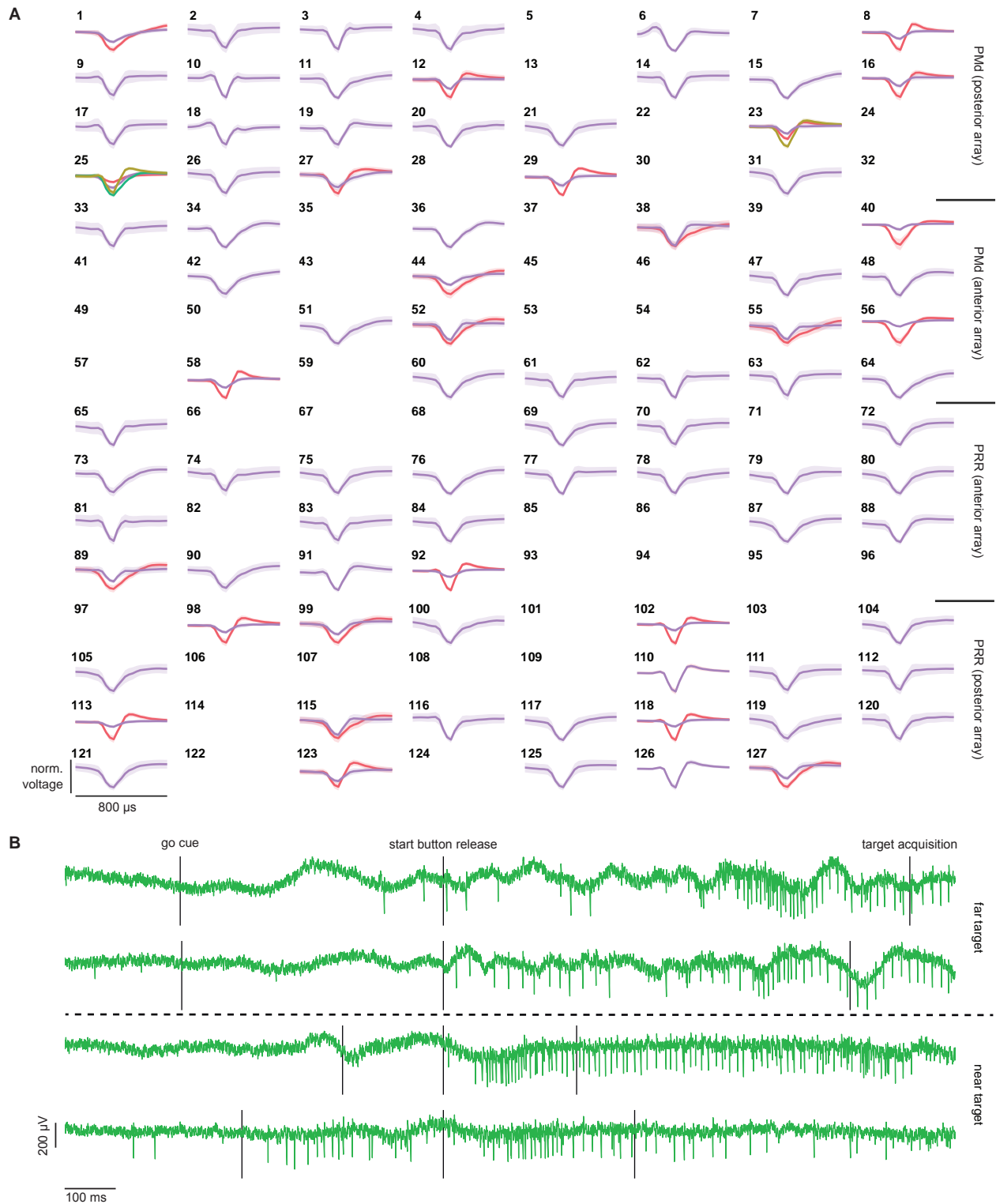


Figure 3: Wireless recording quality in the Reach Cage. A) Averaged waveforms from 127 channels (two PMd and two PRR FMA arrays) recorded wirelessly in parallel. Waveforms are normalized to the highest waveform per channel. Numbers indicate channel number. Light shaded area represents standard deviation. B) Raw broadband extracellular voltage from a single electrode of a 32-channel electrode array in area PMd of monkey L. Traces from four trials during the walk-and-reach task are shown. Black vertical lines indicate task events, first - go cue; second - start button release; third - target acquisition. Time axis is aligned to start button release. For the first two trials, the target was a far target and for the last two it was a near target. Neural spiking is clearly isolatable from the background noise of the signal during all phases of behavior.

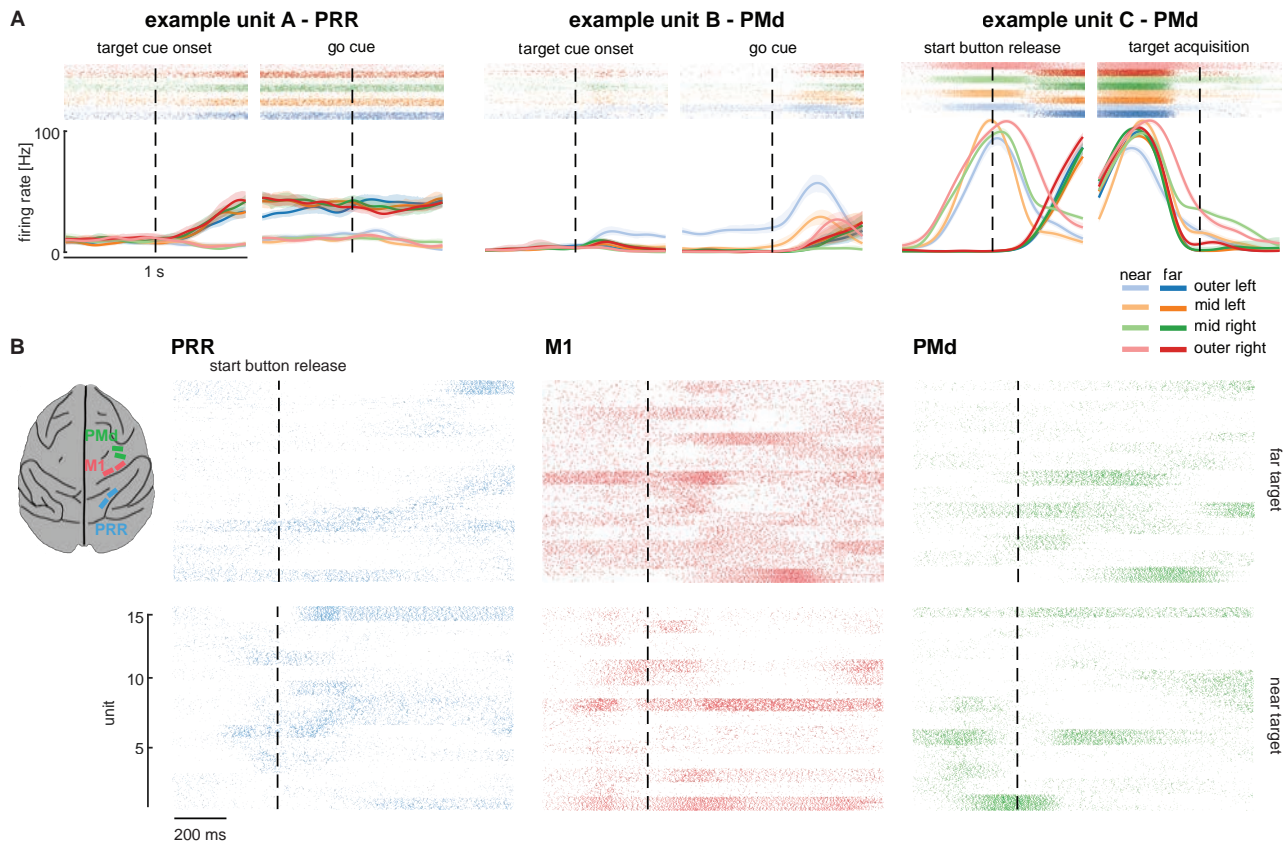


Figure 4: Extracellular single-unit recordings while monkey L performs a delayed walk-and-reach task in the Reach Cage. A) Example cells modulated to the task. Top plots are a raster plot, for which each spike is shown as one line, on top of the corresponding per target averaged spike densities. Time axes are aligned cue onset and go cue (cell A and B) or start button release and target acquisition (cell D). Shaded area represents the 95% bootstrap confidence interval. B). Raster plots of 15 units per area during trials towards the near mid left target (top) and the far mid left target (bottom). Time axis is aligned to start button release (dashed line). For each unit 31 - 49 trial repetitions are shown. Array placement is indicated on a brain sketch (left).

From the data of all neural recording sessions, we could isolate waveforms from the broadband data. The data obtained from the 31-channel recordings revealed clear and stable waveform cluster over the session durations, allowing us to isolate single and multi-unit activity from all arrays. We identified units in the 21 sessions. For the six arrays, we could isolate a maximum of the following number of units per session with an average firing rate above 1Hz: 14 (PRR-posterior); 19 (PRR-anterior); 31 (M1-medial); 20 (M1-lateral); 36 (PMd-posterior); 26 (PMd-anterior).

In summary, the Reach Cage proved to be suitable for addressing neuroscientific question based on single unit recordings. Broadband wireless neural signals showed excellent spike isolation and modulation of spike frequency correlated with behavioral events.

Reach Cage recordings allow novel sensorimotor neuroscientific studies

The precise behavioral control of the unrestraint animals in the Reach Cage together with the wireless recording opens opportunities for addressing new research questions. Activity patterns of single units while the animal performed the task indicate task-specific response modulations with high across-condition selectivity and within-condition trial-to-trial reliability (Figure 4).

During planning and execution of (walk-and-) reach movements, neural activity was modulated with respect to direction and distance of the targets. We quantified the neural modulation using a modulation index regarding target distance (distMI) and target direction for near (nearMI) and far (farMI) targets. Example A (Figure 4A) shows a unit from PRR with higher firing rate for far targets than for near targets during movement planning, i.e. after cue onset and prior to movement (after

target cue onset: Kruskal-Wallis $p < 0.001$, $\text{distMI} = 0.54$; before go cue: Kruskal-Wallis $p < 0.001$, $\text{distMI} = 0.55$). The activity of this unit does not differ between target directions after target cue onset (near: Kruskal-Wallis $p = 0.69$, $\text{nearMI} = 0.09$; far: Kruskal-Wallis $p = 0.07$, $\text{farMI} = 0.08$) and only weakly before the go cue (near: Kruskal-Wallis $p = 0.04$, $\text{nearMI} = 0.12$; far: Kruskal-Wallis $p < 0.01$, $\text{farMI} = 0.1$). Example B shows a unit from PMd the activity of which is clearly modulation for near targets (after target cue onset: Kruskal-Wallis $p < 0.001$, $\text{nearMI} = 0.75$; before go cue: Kruskal-Wallis $p < 0.001$, $\text{nearMI} = 0.96$) with a preference for the near outer left target. After the go cue, also the activity for the mid left target increase indicating that this unit is probably selective for leftward reaches. During the delay phase the activity for far targets is less strongly modulated (after target cue onset: Kruskal-Wallis $p = 0.03$, $\text{farMI} = 0.23$; before go cue: Kruskal-Wallis $p = 0.02$, $\text{farMI} = 0.58$). Example C shows a unit from PMd aligned to the movement phase. The unit has a strong peak of activity aligned with arm movement onset. For near targets the activity peaks with the start button release, which corresponds to the movement onset of the reaching (contralateral) arm. For far targets, the start button release does not correspond to the movement onset of the reaching arm but approximately to the onset of the whole-body movement, which includes limb movements for locomotion. There is little activity around start button release resulting in a strong difference in neural activity between near and far targets (before start button release: Kruskal-Wallis $p < 0.001$, $\text{distMI} = 0.99$). When aligning the data to the time of target acquisition, the period of the goal-directed arm movements for near and far targets mostly overlap. Correspondingly, the activity peaks for far and near target reaches are aligned resulting in a weaker near-far modulation (before target acquisition: Kruskal-Wallis $p < 0.001$, $\text{distMI} = 0.05$). Neural activity patterns in all three brain areas were modulated during walk-and-reach movements. In Figure 4C we show the activation of 15 units per each area during the period lasting from 1.5 seconds before until 1 second after the start button release. As example data, repeated movements to the near mid left (bottom) and far mid left target (top) are shown in the raster plots. During this time period of the trial almost all units were modulated, i.e. either excited or inhibited.

Taken together, we can record neural activity from a large number of recording sites spread over multiple sensorimotor areas while animals conduct structured cognitive sensorimotor tasks in the Reach Cage. The presented example data suggests that neural activity (1) differs between reach and walk-and-reach movements already during early movement planning (example unit A); (2) encodes near target location during movement planning (example unit B) similar to conventional settings; and (3) can be aligned to the contralateral arm movement independent of body movements (example unit C).

Discussion

We introduced the Reach Cage as novel experimental environment for sensorimotor neuroscience with physically unrestrained rhesus monkeys. As core interactive element, we developed MaCaQuE, a new experimental control system for sensorimotor tasks in cage environments. We trained two monkeys to conduct spatially and temporally structured reach tasks that required them to reach to targets near or far from them with a stretch-and-reach movement (monkey K) or a walk-and-reach movement (monkey L). With MaCaQuE, we could measure button release and movement times in response to visual cues with high temporal precision, which revealed, for example, faster hand movement initiation for near compared to far targets. Using motion capture, we additionally could track wrist trajectories for reach and stretch-and-reach movements of an unrestraint monkey (K) in the Reach Cage. Trajectories were consistent over trials and showed typical speed profiles as known from experiments with highly trained chair-seated monkeys. We could wirelessly record broadband neural signals of up to 127 channels from three brain areas (M1, PMd, PRR) of monkey (L) performing a walk-and-reach task. Like in more restricted conventional settings, neurons were clearly modulated by the task events and encoded information about the location of immediate reach targets. Beyond this, neurons revealed selective activity patterns when the monkey planned and conducted full-body movements. With our Reach Cage approach we provide a proof-of-concept for wireless neural recordings during structured behavior in unrestraint rhesus monkeys, significantly expanding the scope of sensorimotor systems neuroscience.

Neural recordings in unrestrained non-human primates

Only few studies demonstrated wireless recordings of neural single unit activity in physically unrestrained non-human primates so far. Those studies focused on locomotion (Capogrosso et al., 2016; Foster et al., 2014; Yin et al., 2014), vocalization (Hage & Jurgens, 2006; Roy & Wang, 2012), or showed proof-of-concept data of sleep (Yin et al., 2014) or basic uninstructed behavior (Fernandez-Leon et al., 2015; Gilja et al., 2010; Schwarz et al., 2014). One study used a wireless brain-machine-interface to let monkeys control a robotic wheelchair in which they sat (Rajangam et al., 2016). Other studies used tethered recordings to investigate primates freely exploring the environment while being attached to a pole (Sun et al., 2006), to a cable assembly (Ludvig et al., 2004) or seated in a chair they could move (Rolls, Robertson, & Georges-François, 1997). Alternatively, data logging can be used to store the recorded data on a head-mounted device (Jackson, Mavoori, & Fetz, 2007), with the limitation that the logging device is detached from any behavioral monitoring or task instruction system. In none of the mentioned wireless settings, precisely timed and spatially well-structured goal-directed behavior, or even movement planning, in unrestrained monkeys was investigated. This is what we achieved with the Reach Cage.

Structured behavior in the Reach Cage with MaCaQuE

With the Reach Cage, we aimed for maximal freedom of the animal to move and combined this with the conventional approach of a highly trained and structured task that (1) allows us to identify certain periods, such as movement preparation; (2) ensures that the animal focuses on the specific behavior due to the task demand and (3) provides repetition for a statistical analysis. With this combination, we were able to train the animals to conduct goal-directed walk-and-reach movements upon instruction, a behavior which cannot be studied in conventional chair-based settings.

The animals' movement behavior was only constrained by the task and the overall cage volume. Nonetheless, reach trajectories revealed fast straight movements with a typical bell shaped speed profile comparable to conventional setups (Georgopoulos, Kalaska, & Massey, 1981) and little trial-to-trial variability. Apparently, over the course of training, the animals had optimized their movement behavior and adopted consistent starting postures and stereotyped movement sequences. Video analyses additional to the wrist motion capture confirmed this notion. This spatio-temporal consistency of the behavior over many trials allows analytical approaches to both the behavioral and the neural data equivalent to conventional settings. Even without motion capture, we were able to use the interaction device MaCaQuE to monitor movement parameters such as the hand release time of the start button as response to the go signal and the movement time from the start button to the reach target. Both timing measures showed narrow distributions, further underlining the well-structured behavior induced by the task.

MaCaQuE can serve as a robust-cage-based equivalent to illuminated push-buttons (Batista et al., 1999; Buneo & Andersen, 2012) or a touch screen (Klaes et al., 2011; Westendorff et al., 2010) in conventional experiments, or as an alternative to wall-mounted touch screens in the housing environment (Berger et al., 2017; Calapai et al., 2017). Yet, the MaCaQuE system is more flexible. Targets and cues are vandalism-proof and can be placed at any position in large enclosures, allowing for 3-dimensional arrangements and an arbitrarily large workspace. If more explorative, less stereotyped behavior is of interest, the trial-repetitive nature of the current task can easily be replaced by alternative stimulus and reward protocols, e.g. for foraging tasks. In another study (not shown here), we used MaCaQuE with humans and expanded it to deliver vibro-tactile stimuli to the subjects' fingers and to receive additional input from push buttons in parallel to the reach target input and output. Similar to other systems for neuroscience experimentation and training (Libey & Fetz, 2017; Ponce, Genecin, Perez-Melara, & Livingstone, 2016; Teikari et al., 2012), we used low-cost off-the-shelf components with an easy-to-program microcontroller platform as a core.

While we could track the wrist's movement, reliable motion capture with monkeys provides a technical challenge. At least two cameras need to see a marker or body part to reconstruct a 3-

dimensional position. Occlusion by objects or the animal itself is usually an issue (Chen & Davis, 2000; Moeslund, Hilton, & Krüger, 2006). When using systems based on physical markers (active LEDs or passive reflectors), rhesus monkeys tend to rip off the markers attached to their body. An alternative are fluorescent or reflective markers directly painted to the skin of the animal (Courtine et al., 2005; Peikon, Fitzsimmons, Lebedev, & Nicolelis, 2009), which also require continuously repeated shaving, or markers that cannot be removed, such as collars (Ballesta, Reymond, Pozzobon, & Duhamel, 2014). A video-based marker-free system using skeleton models was recently reported (Nakamura et al., 2016), however, this or similar systems were not yet reported in a larger, more complex environment with monkeys. We used a commercially available system with only four VGA cameras tracking a permanently dyed part on the animal's fur and the colored cap of the head implant (data not shown). Since we knew the behavior of the animal due to the structured task, we could set up the cameras to record reach trajectories to near and far targets.

When some behavioral parameters could not be controlled, physical restraint is used in conventional setups. For instance only the animal's hand contralateral to the investigated brain hemisphere gets access to a touchscreen. Here, in the beginning, Monkey L triggered the targets with its tongue and not its hand. Also for a subsequent study not reported in this manuscript, we trained monkey K on a walk-and-reach version of the task but using its left and not right hand. In both cases, we could train the monkeys to perform the behavior we intended by manual PRT in combination with MaCaQuE. Once trained, the monkeys performed the intended behavior consistently without manual PRT. Monkey K performed the same behavioral task with its left hand with 78% correct trials on average (s.d. 2%, 2 sessions). During monkey K's first training, we used only one position for reward delivery. We varied the position by placing the reward bowl right, left and behind of the starting position of the behavioral task. For all three reward positions, monkey K turned its body towards the reward system when being in the start position during the task. Introducing a second reward system and randomly assigning the reward to one of the systems each trial made it impossible for the monkey to know the position of reward delivery. Since then, we did not see an apparent change in body posture during the task based on the reward position. Based on this experience, we conclude that even without full control of all behavioral parameter it is possible with proper setup configuration and short periods of manual training to consistently instruct the animal on the desired behavior without applying physical restraint. However, full-body motion capture or at least markers on and multiple-camera view of more than one extremity would be beneficial to automatically detect undesired and reinforce desired behavior.

The animals performed a reasonable amount of trials in the Reach Cage (around 200 - 300 correct trials per session), despite a clearly higher per-trial physical effort compared to conventional setups due to the full-body movements. As common in cognitive neuroscience research, we applied a fluid control regime (Prescott et al., 2010) to increase the incentive of the liquid rewards. One of the two monkeys (monkey L) performed tasks in conventional setups before (Morel et al., 2015) and showed a higher motivational level in the Reach Cage seen by an increase in number of trials performed despite a higher amount of reward per correct trial. While the Reach Cage is less suitable for neuroscience experiments that rely on an extraordinary degree of control over the sensory input, for instance vision research with precise gaze control, our results suggest that it is a suitable alternative for a certain range of motor and sensorimotor neuroscience studies which enables a much richer repertory of possible movements to be studied.

Motor-goal encoding in the Reach Cage

Previous studies provided evidence that it is possible to identify simple goal-directed behavior of a fully unrestrained monkey in single and multi-unit activity (Gilja et al., 2010; Schwarz et al., 2014). However, those studies only tested a short period of uninstructed behavior as a proof-of-concept. Here, single units of all three brain areas that we recorded from were clearly modulated by task events and target choice. Due to the trial structure of the trained behavior, conventional temporal alignment and trial-averaging approaches were sufficient already to reveal such target selectivity in different periods of the trial, as seen from the example neurons. We applied neither physical restraint on body posture

or movement, nor controlled gaze of the animal and visual input as strictly as in conventional setups, for which experiments often take place in a darkened room with only the controlled stimuli being visible. Therefore, it was not a priori clear if reach goal selectivity would be measurable in a way comparable with conventional experiments previously performed in our and other labs, particularly in posterior parietal cortex, where spatial frames of reference play a critical role (Batista et al., 1999; Bhattacharyya, Musallam, & Andersen, 2009; Klaes et al., 2011; Pesaran et al., 2006; Westendorff et al., 2010). Yet, animals were accustomed to the structure of the task and showed high consistency in their movement patterns. This is the likely reason why the observed neural responses in fronto-parietal cortices of monkey L during planning and execution of near-target reaches were highly reminiscent of data from comparable goal-directed reaching movements in chair-seated animals. But neuronal activity was also present during planning of reaches beyond immediate reach, i.e. for planned stretch-and-reach and walk-and-reach movements. A more detailed quantification of similarities and differences will need further experiments.

Another study used data-logging to simultaneously record single-unit activity from primary motor cortex and EMG activity from the contralateral wrist during free behavior (Jackson et al., 2007). The firing rate of most of the cells was correlated with muscle activity. Interestingly, during a center-out reach task with EMG cursor control in a conventional restraining setup, the muscle-neural activity correlation was only weakly related to the correlation seen during free behavior. It remains to be tested if neural activity related to a behavioral task without physical restraint, like in the Reach Cage, would be stronger correlated with activity related to uninstructed behavior.

Neural signal quality in the Reach Cage

We recorded mostly artifact-free broadband data during the behavioral task despite whole-body movements. This is true despite the cage edges and one side, as well as the top and bottom grid consisting of stainless steel. Artifacts were visible outside of the task in predictable circumstances, when the animal moved the head with the transmitter close to a metal part (e.g. when drinking from a reward bowl) or too close to an antenna. Due to the known structure of the behavioral task, we could predict roughly the animal's head movements and setup the antennas so that they provided clean signals during the behavior of interest. Although we focused on single unit data, the quality of the broadband signals suggests that LFP analysis is possible as well. Even outside the immediate workspace of our behavioral task, signal loss and artifacts were seldom. For free behavior, such as exploration of the environment, using as little metal as possible in the cage certainly would be beneficial. This was not the case for the 127-channel system for which the higher bandwidth makes the system more prone to artifacts and signal loss. We were not able to obtain stable recording over a whole experimental session. However, periods of data loss were short and the signal quality was otherwise similar to the 31-channel system suggesting that the 127-channel system would perform adequately in an environment optimized for RF-transmission. Apparently, the currently used metal cage including the MaCaQuE hardware interfered more strongly with the high-bandwidth wireless signal transmission. The cage could be optimized by systematically replacing metal parts with non-ferromagnetic materials.

Conclusion

Systems neuroscience can benefit from the possibility of quantifying free behavior and simultaneously recording brain activity, particularly but not only in sensorimotor research. Its technical realization is far from simple, though, especially with the complex movements primates are capable of. When using wireless technology, a desirable approach would be to let the monkey freely decide on their behavior to obtain neural correlates of most natural behavior (Gilja et al., 2010) while motion capture provides the related movement kinematics (Ballesta et al., 2014; Bansal, Truccolo, Vargas-Irwin, & Donoghue, 2012; Nakamura et al., 2016; Peikon et al., 2009). But even if full-body motion capture would be available, it will remain a major challenge to identify to what extent neural activity relates to sensory input, the currently performed movement or the planning of the next movement in free behavior. With the Reach Cage and the MaCaQuE system, we introduce a compromise, in which animals

are not physically restrained in their movements, but still conduct structured cognitive and sensorimotor tasks, easing analyses of behavior and wirelessly recorded neural activity from large-scale neural networks. Such combination will provide important insights into the neural basis of more complex behavior than previously available.

Materials and Methods

Animals

Two male rhesus monkeys (*Macaca mulatta* K age: 6 years; and L age: 15 years) were trained in the Reach Cage. Both animals were behaviorally trained with positive reinforcement learning to sit in a primate chair. Monkey K did not participate in any research study before but was trained on a goal-directed reaching task on a cage-based touchscreen device (Berger et al., 2017). Monkey L was experienced with goal-directed reaching on a touch screen and with a haptic manipulandum in a conventional chair-seated setting before entering the study (Morel et al., 2015). It was chronically implanted with a transcutaneous titanium head post, the base of which consisted of four legs custom-fit to the surface of the skull. The animal was trained to tolerate periods of head fixation, during which we mounted equipment for multi-channel wireless recordings. We implanted six 32-channel floating microelectrode arrays (Microprobes for Life Science, Gaithersburg, Maryland) with custom electrode lengths in three areas in the right hemisphere of cerebral cortex. Custom designed implants protected electrode connectors and recording equipment. The implant design and implantation procedures are described below.

Both animals were housed in social groups with one (monkey L) or two (monkey K) male conspecific in facilities of the German Primate Center. The facilities provide cage sizes exceeding the requirements by German and European regulations, access to an enriched environment including wooden structures and various toys (Calapai et al., 2017). All procedures have been approved by the responsible regional government office [Niedersächsisches Landesamt für Verbraucherschutz und Lebensmittelsicherheit (LAVES)] under permit numbers 3392 42502-04-13/1100 and comply with German Law and the European Directive 2010/63/EU regulating use of animals in research.

MaCaQuE

We developed the Macaque Cage Query Extension (MaCaQuE) to provide computer-controlled visual cues and reach targets at freely selectable individual positions in a monkey cage (Figure 1). MaCaQuE comprises a microcontroller-based interface, controlled via a standard PC, plus a variable number of MaCaQuE Cue and Target boxes (MCT). The MCT cylinder is made of PVC plastic and has a diameter of 75 mm and a length of 160 mm. At one end of the cylinder the MCTs contain a capacitive proximity sensor (EC3016NPAPL, Carlo Gavazzi, Steinhausen, Switzerland) and four RGB-LEDs (WS2812B, Worldsemi Co., Daling Village, China), both protected behind a clear polycarbonate cover. With the LEDs, light stimuli of different color (8-bit color resolution) and intensity can be presented to serve as visual cues (Figure 1B). The LEDs surround the proximity sensor which registers when the monkey touches the middle of the polycarbonate plate with at least one finger. This way the MCT acts as a reach target. LEDs, sensor plus a custom printed circuit board for the controlling electronics and connectors are mounted to a custom designed 3D-printed frame made out of PA2200 (Shapeways, New York City, New York). A robust and lockable RJ45 connector (etherCON, Neutrik AG, Schaan, Liechtenstein) connects the MCT to the interface unit from the opposite side of the cylinder via standard Ethernet cables mechanically protected inside flexible metal tubing. The RGB-LEDs require an 800 kHz digital data signal. For noise reduction, we transmit the signal with a differential line driver (SN75174N, SN74HCT245N, Texas Instruments Inc., Dallas, Texas) via twisted-pair cabling in the Ethernet cable to a differential bus transceiver (SN75176B, Texas Instruments Inc.) on the MCT. Ethernet cables are CAT 6, however, any other category would be suitable (CAT 1 up to 1 Mhz). This setting allowed us to use cables up to 15 m. Hence, there are no practical limits on the spatial separation between MCTs and from the interface for applications even in larger animal

enclosures. We did not test longer cables. Apart from the one twisted-pair for the data stream of the RGB-LEDs, the Ethernet cable transmits 12 V power from the interface unit and the digital touch signal from the proximity sensor to the interface unit. The proximity sensor is directly powered by the 12 V line. The LEDs receive 5 V power from a voltage regulator (L7805CV, STMicroelectronics, Geneva, Switzerland) that scales the 12 V signal accordingly. The PVC and polycarbonate enclosure of the MCT as well as the metal cable protection are built robustly enough to be placed inside a rhesus monkey cage. MaCaQuE incorporates up to two units to deliver precise fluid rewards (Calapai et al., 2017). Each unit consists of a fluid container and a peristaltic pump (OEM M025 DC, Verderflex, Castleford, UK). MOSFET-transistors (BUZ11, Fairchild Semiconductor, Sunnyvale, California) on the interface unit drive the pumps.

The MCTs and reward systems are controlled by the Arduino-compatible microcontroller (Teensy 3.x, PJRC, Sherwood, Oregon) placed on a custom printed circuit board inside the interface unit (Figure 1C). To operate a high number of MCTs the microcontroller communicates with the proximity sensor and LEDs using two serial data streams respectively. For the proximity sensor, we used shift registers (CD4021BE, Texas Instruments) that transform the parallel output from the MCTs to a single serial input to the microcontroller. The LEDs have an integrated control circuit to be connected in series. An additional printed circuit board connected to the main board contained 16 of the RGB-LEDs that receive the serial LED data stream from Microcontroller. We use this array of LEDs to convert the serial stream into parallel input to the MCTs by branching each input signals to the differential line drivers that transmit the signal to each MCT. To optimize the form factor of the interface unit we made a third custom printed circuit board that contains all connectors. In our current experiments, we assembled a circuit for connecting up to 16 MCTs but the MaCaQuE system would be easily expandable to a larger number. To set the transistors to drive the pumps of the reward systems, the 3.3V logic signal from the microcontroller is scaled up to 5V by a buffer (SN74HCT245N, Texas Instruments Inc., Dallas, Texas). Since MaCaQuE incorporates parts operating on 3.3V (microcontroller), 5V (LED array) and 12V (peristaltic pump and MCT), we used a standard PC-power supply (ENP-7025B, Jou Jye Computer GmbH, Grevenbroich, Germany) as power source. Additionally, twelve digital general-purpose-input-output (GPIO) pins are available on the interface, which were used to 1) send and receive synchronizing signals to other behavioral or neural recording hardware (strobe); 2) add a button to manually control reward units, and 3) add a switch to select which reward unit is addressed by the manual reward control. Further options like sending test signals or adding sensors or actuators are possible. Custom printed circuit boards are designed with EAGLE version 6 (Autodesk Inc., San Rafael, California).

We used Arduino-C to program the microcontroller firmware. MaCaQuE was accessed by a USB connection from a computer using either Windows or Mac OS. A custom-written C++ software package (MoRoCo) operated the behavioral task and interfaced with MaCaQuE via the microcontroller. We developed hardware testing software using Processing and C++.

Reach Cage

The Reach Cage is a cage-based training and testing environment for sensorimotor experiments with a physically unrestrained rhesus monkey (Figure 1A). Inner cage dimensions are 170 cm x 80 cm x 85 cm (W x D x H) with a metal mesh grid on top and bottom, a solid metal wall one long side (back) and clear polycarbonate walls on all other sides. The idea of the experiment was to implement a goal-directed reach task with instructed delay, equivalent to common conventional experiments, to compare neural responses during planning and execution of reaches towards targets at different positions in space.

We used MaCaQuE to provide ten visual cues and reach targets (MCTs) inside the cage. Two MCTs were positioned on the floor pointing upwards. Eight were placed 25 cm below the ceiling in two rows of four each, pointing toward the middle position between the two MCTs on the floor (Figure 1D). The floor MCTs provided the starting position for the behavioral task (start buttons). The monkey could comfortably rest its hands on the start buttons while sitting in between. The row of ceiling MCTs closer to the starting position was placed with a 10 cm horizontal distance and 60 cm vertical distance

to the starting position (near targets). We chose this configuration to provide a comfortable position for a rhesus monkey to reach from the starting positions to the near targets without the need to relocate its body. For monkey K, the second row of MCTs was positioned at 50 cm horizontal distance from the starting positions (far targets). In this setting, the animal needed to tilt and stretch its body in order to acquire one of the far targets (stretch-and-reach task; Figure 2B left). For monkey L, the far targets were placed at 100 cm horizontal distance from the start positions, requiring the animal to make steps towards the targets (walk-and-reach task; Figure 2B right). In this setting, an eleventh MCT was placed outside the cage in front of the monkey (when sitting in the starting position and facing the opposite wall) to provide an additional visual cue. For positive reinforcement training, MaCaQuE's reward systems can provide fluid reward through protected silicon and metal pipes into one of two small spoon-size stainless steel bowls mounted approx. 20 cm above the floor in the middle of either of the two long sides of the Reach Cage.

Behavioral task

Using the Reach Cage, we trained monkey K on a memory-guided stretch-and-reach task with instructed delay (Figure 3A). When the starting positions lit up, the monkey was required to touch the right start button and hold it (hand fixation). After 400 - 1000 ms, one randomly chosen reach target lit up for 600 ms indicating the future reach goal (cue). The animal had to remember the target position and wait for 400 - 2000 ms (memory period) until the lights of the starting positions turned off and concurrently lights of all targets turn on (go cue). The monkey then had a 600 ms time window starting 200 ms after the go cue to release its right hand from the right start button. We introduced the 200 ms delay to discourage the animal from anticipating the go cue and triggering a reach prematurely. After releasing the start button, the animal needed to reach to the remembered target within 1000 ms. Provided the animal kept touching for 300 ms, the trial counted as correct, indicated by a high pitch tone and reward. A lower tone indicated an incorrect trial. Reward was delivered by juice filled into one of two randomly assigned drinking bowls. We used unpredictable sides for reward delivery to prevent the animal from planning the movement to the reward before the end of the trial. We always used white light for visual cues during this task.

Monkey L performed a variant of the task, namely a walk-and-reach task with instructed delay. The variant of the task differed in four aspects from the task of monkey K. First, both starting positions had to be touched and held by the animal during fixation. Second, the target illumination remained during the instructed delay, i.e., the animal was not required to memorize the target position, but it still had to wait for the go cue before initiating the reach. Third, far targets were placed at 100 cm distance, which required the animal to walk-and-reach, and which also affected the timing of the task. Forth, the go cue was displayed on the outside-cage MCT (visual cue). This encouraged the animal to pay attention to this MCT during movement planning so that it did not miss the go cue which was unpredictable in time. The timeline of the walk-and-reach task was as follows: 1) the visual cue turned on (white) to indicate that a trial can be initialized; 2) both starting buttons had to be touched and held for 400 - 800 ms; 3) the future reach goal lit up (white) and stayed on; 4) after 1000 - 2200 ms the fixation stimulus turned from white to red ('go' signal); 5) at least one starting position had to be released within 1200 ms; 6) the target had to be acquired within 1800; 7) after 300 ms of holding the target the trial was correct and the animal received the reward and high-pitch acoustic feedback.

We did not impose the choice of hand on the monkeys in this study but let them freely pick their preferred hand. While monkey K reached to the targets with the right hand, monkey L used the left hand. Both animals consistently used their preferred hand and never switched.

Motion capture and analysis of behavior

The animals' behavior was analyzed in terms of accuracy (percent correct trials), timing (as registered by the proximity sensors), and wrist kinematics (video-based motion capture).

We analyzed start button release and movement times of both monkeys when they performed their respective task (monkey K: 17 sessions stretch-and-reach task; monkey L: 22 sessions walk-and-reach

task). Button release time is the time between the go cue and the release of one of the start buttons. Movement time is the time between the release of one of the start buttons and target acquisition. We analyzed the timing separately for each monkey and separately for all near and all far targets.

We recorded the wrist kinematics of monkey K in seven sessions. For this, we video-tracked the monkey K's right wrist position during the task with other behavioral and neural data. Using a video-based motion capture system (Cineplex Behavioral Research System, Plexon Inc., Dallas, Texas) we can measure the 3-dimensional positions of uniformly colored objects. With four Stingray F-033/C color cameras (Allied Vision Technologies GmbH, Stadtroda, Germany) objects can be tracked at a frame rate of up to 90 fps in VGA resolution. The system was calibrated with a checkerboard reference stimulus according to the Cineplex protocol using the built-in proprietary algorithm. Video processing and object tracking on camera and host PC takes less than 20 ms (camera shutter opening time not included). For synchronization with other data, the system sent a sync pulse every 90 frames to MaCaQuE.

We dyed the wrist of the animals' preferred arms with permanent red hair dye approved for human use (Preference Intensive Red, L'Oréal Paris). The stained fur provided a color object for tracking without the need for the animal to tolerate physical marker objects attached to the body or repeated shaving for visualizing markers on the skin.

To quantify reach trajectories of highly trained behavior, we analyzed five of those seven sessions of which the monkey performed more than 80% successful trials. Due to the attenuated illumination of the Reach Cage, we tracked arm movements from monkey K with 30 fps in the stretch-and-reach task. A total of 980 trials from 1486 successful trials in the seven sessions yielded at least five data points during the trial. Only those trials were included in the analysis. The trajectories were aligned to the button release time. This alignment time point is independent of the sampling time points of the Cineplex system. To quantify variability of the trajectories across trials as a function of time, we synchronized trajectories based on linear interpolation using the same sampling rate of 30Hz. We chose linear interpolation for simplicity since signal reconstruction according to sampling theory did not lead to different results. Further analyses were performed based on the linearly interpolated data. By illuminating all MCTs in different colors during a reference measurement, we were able to register the position of the touch sensitive surface of the MCTs in the same coordinate system as the recorded wrist positions. We oriented the coordinate system to be aligned with the cage. We calculated speed profiles as spatial derivative (difference of adjacent interpolated positions in time) in every trial.

Furthermore, we computed the average wrist trajectory for each target. To quantify the spatial variability of the reaching movement towards a certain target, we computed for each trajectory at each time point the 3-dimensional Euclidean distance to the average trajectory. Then, we averaged the Euclidean distances over all trajectories per target at each time point. From those averages, we calculated the maximum for each target. Additionally, to quantify the variability of a resting hand, we calculated for all targets the mean and standard deviation within the time windows 50 ms to 200 ms before start button release and after target acquisition.

The behavioral analyses were performed using Matlab (Mathworks Inc., Natick, Massachusetts) with the data visualization toolbox gramm (Morel, 2018). Additionally, we used Inventor (Autodesk Inc.) for visualizing the averaged 3-dimensional reach trajectories inside a model of the reach cage.

Implant system design

Wireless neural recordings from the cerebral cortex of rhesus monkeys during minimally restrained movements require protection of the electrode array connectors and the headstage electronics of the wireless transmitters. We designed a protective multi-component implant system to be mounted on the animal skull (Figure 5). The implant system and implantation technique was designed to fulfill the following criteria: 1) Electrode connectors need to be protected against dirt and moisture; 2) While the animal is not in the experiment, the implants need to be small and robust enough for the animal to live unsupervised with a social group in an enriched large housing environment; 3) During the experiment, the wireless headstage needs to be protected against manipulation by the animal and

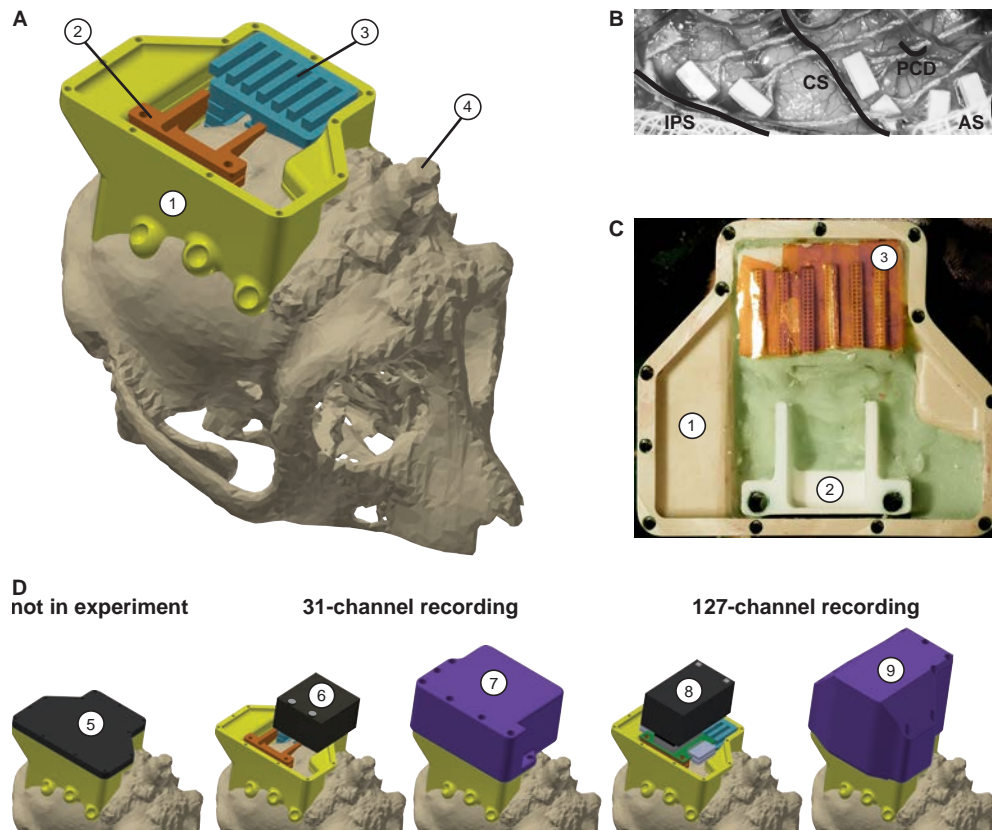


Figure 5: Implant system design. A) 3-dimensional computer models of the implants and electronics. The skull model of monkey L (beige) is extracted from a CT scan including the titanium implant for head fixation (4, headpost) which was already implanted before this study. Further implants are colored for illustrative purposes and do not necessarily represent the actual colors. B) Image of microelectrode array placement during the surgery. Anatomical landmarks descriptions: IPS - intraparietal sulcus; CS - central sulcus; PCD - postcentral dimple; AS - arcuate sulcus. C) Image of the implants on monkey L's head. D) Different configurations of wireless headstages and protection caps temporarily mounted on the implants. Numbers indicate: 1 - chamber; 2 - adapter board holder; 3 - array connector holder; 4 - headpost (from CT scan); 5 - flat protective cap; 6 - W32 headstage; 7 - protective cap for W32; 8 - W128 headstage; 9 - protective cap for W128.

potential physical impacts from bumping the head; 4) The head-mounted construction should be as lightweight as possible; 5) Placing of the electrode arrays and their connectors during the surgery needs to be possible without the risk of damaging electrodes, cables, or the brain; 6) Implant components in contact with organic tissue need to be biocompatible; 7) Temporary fixation of the animal's head in a primate chair needs to be possible for having access to implants and for wound margin cleaning; 8) Implants must not interfere with wireless signal transmission; 9) Optionally, the implant may serve as colored trackable object for the motion capture system.

We designed the implant system for two main configurations: first, a home configuration containing only permanently implanted components and being as small as possible when the animal is not in a recording session but in its group housing (Figure 5D, left); second, a recording configuration with removable electronic components being attached. This configuration should either fit the 31-channel headstage (Figure 5D, middle), or the 127-channel headstage (Figure 5D, right) of the wireless system (W32/W128, Triangle BioSystems International, Durham, North Carolina). The implant system consists of four custom-designed components: a skull-mounted outer encapsulation (chamber; no 1 in Figure 5A/C), a mounting base for holding a custom-designed printed circuit board (adapter board holder, no 2), a mounting grid to hold the connectors of the electrode arrays (connector holder, no 3), and a set of different-sized caps to contain (or not) the different wireless headstages (no 5-9). Dimensions of the wireless headstages are W32: 17.9 mm x 25 mm x 14.2 mm (W x D x H), 4.5g weight; W128: 28.7 mm x 34.3 mm x 14.2 mm (W x D x H), 10 g weight.

We designed the implants custom-fit to the skull of monkey L by using CT and MRI scans. Using 3D Slicer (Brigham and Women's Hospital Inc., Boston, Massachusetts), we generated a skull model out of the CT scan (Figure 5A) and a brain model out of the MRI scan (T1-weighted; data not shown). In the MRI data we identified the target areas for array implantation based on anatomical landmarks (intraparietal, central, and arcuate sulci; pre-central dimple), and defined Horsley-Clarke stereotactic coordinates for the craniotomy necessary for array implantation (Figure 5B). We used stereotactic coordinates extracted from the MRI scan to mark the planned craniotomy on the skull model from the CT scan. We then extracted the mesh information of the models and used Inventor (Autodesk Inc.) and CATIA (Dassault Systèmes, Vélizy-Villacoublay, France) to design virtual 3-dimensional models of the implant components which are specific to the skull geometry and planned craniotomy. Monkey L already had a titanium headpost implanted from previous experiments of which the geometry, including subdural legs, was visible in the CT (Figure 5A, no 4), and, therefore, could be incorporated in our implant design.

We built the chamber to surround the planned craniotomy and array connectors (Figure 5A/C, no 1). The chamber was milled out of polyether ether ketone (TECAPEEK, Ensinger GmbH, Nufringen, Germany) to be lightweight (14 grams; 60.3 mm max. length, 49.5 mm max. width, 31.2 mm max. height; wall thickness: 2 mm) and biocompatible. For maximal stability despite low diameter, stainless-steel M2 threads (Helicoil, Böllhoff, Bielefeld, Germany) were inserted in the wall for screwing different protective caps onto the chamber. The built-in eyelets at the outside bottom of the chamber wall allow mounting of the chamber to the skull using titanium bone screws (2.7 mm corticalis screws, 6-10 mm length depending on bone thickness, DePuy Synthes, Raynham, Massachusetts). Fluting of the lower half of the inner chamber walls let dental cement adhere to the chamber wall.

The subdural 32-channel floating microelectrode arrays (FMA, Microprobes for Life Science) are connected by a stranded gold wire to an extra-corporal 36-pin nano-strip connector (Omnetics Connector Corporation, Minneapolis, Minnesota). We constructed an array connector holder to hold up to six of the Omnetics connectors inside the chamber (Figure 5A/C, no 3). The connector holder was 3D-printed in a very lightweight but durable and RF-invisible material (PA2200 material, Shapeways). The holding grid of the array connector holder is designed such that it keeps the six connectors aligned in parallel with 2mm space between. The spacing allows to either: 1) connect six 32-channel Cereplex (Blackrock Microsystems LLC, Salt Lake City, Utah) headstages for tethered recording simultaneously on all connectors, 2) directly plug a 31-channel wireless system onto one of the array connectors, or 3) flexibly connect four out of six arrays with adaptor cables to an adaptor board, linking the arrays to a 127-channel wireless system. The total size of the array connector is 27 mm x 16.2 mm incorporating all six connectors. The bottom of the array connector holder fits the skull geometry with a cut-out to be placed above an anchor screw in the skull for fixation with bone cement (PALACOS, Heraeus Medical GmbH, Hanau, Germany). This is needed since the array connector is placed on the skull next to the craniotomy during insertion of the electrode arrays, i.e. before implantation of the surrounding chamber (see below). The medial side of the holding grid, pointing to the craniotomy, is open so that we can slide in the array connectors from the side during the surgery. On the lateral side small holes are used to inject dental cement with a syringe to embed and glue the connectors to the grid.

The 31-channel wireless headstage can be directly plugged into a single Omnetics nano-strip array connector. The 127-channel wireless headstage instead has Millmax strip connectors (MILLMAX MFG. CORP., Oyster Bay, New York) as input. A small adaptor board (electrical interface board, Triangle BioSystems International) builds the interface to receive up to four Omnetics nano-strip connectors from the implanted arrays via adaptor cables (Omnetics Connector Corporation). We constructed a small holder with two M3 Helicoils for permanent implantation to later screw-mount the adaptor board when needed during recording (Figure 5A/C, no 2). Fluting on the sides of the adaptor board holder helps embedding of the holder into dental cement. Like the array connector holder, the adaptor board holder was 3D-printed in PA2200.

Depending on the experiment and space needed, we used three different protective caps. While the animal was not in an experiment, a flat 4 mm machine-milled transparent polycarbonate cap with

rubber sealing protected the connectors against moisture, dirt and manipulations (Figure 5D, no 5). During experiments, we used two specifically designed protective caps for the two different wireless headstages. Both were 3D-printed in PA2200 in violet color for motion capture. Since the 31-channel wireless headstage is connected to the array connectors directly, it extends over the chamber walls when connected to one of the outermost connectors (Figure 5D, no 6). We designed the respective protective cap to cover this overlap (Figure 5D, no 7). The 127-channel wireless headstage (Figure 5D, no 8) with its adapter board is higher and overlaps the chamber on the side opposite to the connectors. We designed the respective cap accordingly (Figure 5D, no 9). Since the 3D-printed caps were only used during recording sessions, i.e. for less than 2h, without contact to other animals, and under human observation, we did not add extra sealing against moisture. However, by adding a rubber sealing, the internal electronics would be safe even for longer periods of time in a larger and enriched social-housing environment without human supervision.

Surgical Procedure

The intracortical electrode arrays and the permanent components of the chamber system were implanted in a single sterile surgery under deep gas anesthesia and analgesia via an IV catheter. Additionally, the animal was prophylactically treated with Phenytoin (5-10mg/kg) for seizure prevention, starting from one week before surgery and continuing until two weeks post-surgery (fading-in over 1 week), and with systemic antibiotics (Duphamox, 0.13 ml/kg, one day pre-surgery to one day post-surgery). During craniotomy, brain pressure was regulated with Mannitol (15.58 ml/kg; on demand). Analgesia was refreshed on a 5-h cycle continuously for four post-surgical days using Levomethadon (0.26 mg/kg), daily for 3 post-surgical days using Metacam (0.26 mg/ml) and for another four days (Rimadyl, 1.94 mg/kg) according to demand.

We implanted six FMAs in the right hemisphere of monkey L. Each FMA consists of 32 Parylene-coated Platinum/Iridium electrodes and four ground electrodes arranged in four rows of nine electrodes (covering an area of 1.8 mm x 4 mm) staggered in length row-wise. Two FMAs were placed in each of the three target areas: parietal reach region (PRR), dorsal premotor cortex (PMd) and arm-area of primary motor cortex (M1). PRR arrays were positioned along the medial wall of the intraparietal sulcus (IPS) starting about 7 mm millimeters away from the parieto-occipital sulcus (Figure 5B), with electrode lengths of 1.5 - 7.1 mm. M1 arrays were positioned along the frontal wall of the central sulcus, at a laterality between precentral dimple and arcuate spur, with electrode lengths of 1.5 - 7.1 mm. PMd arrays were positioned, between arcuate spur, precentral dimple and the M1 arrays, with electrode lengths of 1.9 - 4.5 mm.

Except for the steps related to our novel chamber system, the procedures for FMA implantation were equivalent to what was described in (Schaffelhofer, Agudelo-Toro, & Scherberger, 2015). The animal was placed in a stereotaxic instrument to stabilize the head and provide a Horsley-Clarke coordinate system. We removed skin and muscles from the top of the skull as much as needed based on our pre-surgical craniotomy planning. Before the craniotomy, we fixed the array connector holder to the skull with a bone screw serving as anchor and embedded in dental cement on the hemisphere opposite to the craniotomy. After removing the bone with a craniotome (DePuy Synthes) and opening the dura in a U-shaped flap for later re-suturing, we oriented and lowered the microelectrode arrays one-by-one using a manual micro-drive (Narishige International Limited, London, UK), which was mounted to the stereotaxic instrument on a ball-and-socket joint. Before insertion, the array connector was put into our array connector holder and fixed with a small amount of dental cement. During insertion, the array itself was held at its back plate by under-pressure in a rubber-coated tube connected to a vacuum pump which was attached to the microdrive. We slowly lowered the electrodes about 1 mm every 30 seconds until the back plate touched the dura mater. We let the array rest for four minutes before removing first the vacuum and then the tube.

After implanting all arrays, we arranged the cables for minimal strain and closed the dura with sutures between the cables. We placed Duraform (DePuy Synthes) on top, returned the leftover bone from the craniotomy and filled the gaps with bone replacement material (BoneSource, Stryker, Kala-

mazoo, Michigan). We sealed the craniotomy and covered the exposed bone surface over the full area of the later chamber with Super-Bond (Sun Medical Co Ltd, Moriyama, Japan). We secured the array cables at the entry point to the connectors and filled all cavities in the array connector holder with dental cement. We mounted the chamber with bone screws surrounding implants and craniotomy, positioned the adaptor board holder, and filled the inside of the chamber with dental cement (Figure 2C). Finally, we added the flat protective cap on the chamber.

Neural recordings

Neural recordings were conducted in monkey L during the delayed walk-and-reach task in the Reach Cage. The 31-channel wireless headstage (W32) recorded from a single array per session (Figure 5D, no 6), allowed headstage placement on any of the six array connectors. Alternatively, we used the 127-channel headstage (W128) recording from four arrays simultaneously (Figure 5D, no 8). The headstage amplifies the input voltage by a gain of 200 and transmits the analog signal with 3.05 GHz (W32) or 3.375 GHz (W128) transmission frequency to the receiver.

We used a 128-channel Cerebus system (Blackrock Microsystems LLC) for digitization and signal processing. The wireless receiver and an adapter, connected to the receivers output, reduce the overall gain to 1. The W32 system and W128 system have their own specific receiver, but we used the same Cerebus system for both wireless systems. 32-channel Cereplex headstages are connected to the adapter and digitize the signal with 30 kHz. MaCaQuE sends the trial number at the beginning of each trial to the parallel port of Cerebus system. We connected an additional shift register M74HC595 (STMicroelectronics) to the GPIO port of MaCaQuE for interfacing the Cerebus parallel port. The Cerebus system records the trial number along with a time stamp for offline data synchronization.

We performed the preprocessing of broadband data and the extraction of waveforms as previously described (Dann et al. 2016). First, the raw signal was high-pass filtered using a sliding window median with a window length of 91 samples (~3 ms). Then, we applied a 5000 Hz low-pass using a zero-phase second order Butterworth filter. To remove common noise, we transformed the signal in PCA space per array, removed principle components that represented common signals and transformed it back (Musial, Baker, Gerstein, King, & Keating, 2002). On the resulting signal, spikes were extracted by threshold crossing using a negative threshold defined by $-3.3725 \times \text{median}(|\text{signal}|)$. We sorted the extracted spikes manually using Offline Sorter V3 (Plexon Inc., Dallas, Texas). If single-unit isolation was not possible, we assigned the non-differentiable cluster as multi-unit, but otherwise treated the unit the same way in our analysis. The spike density function for the example units were computed by convolving spike trains per trial and per unit with a normalized Gaussian with standard deviation of 50 ms. The spike density function was sampled at 200 Hz.

We analyzed the firing rate of example units with respect to four different temporal alignments: target cue onset, go cue, start button release and target acquisition. To quantify neural activity during the delay period and the movement, we analyzed time windows of 500 ms either immediately before or after a respective alignment. Within those time windows we analyzed the modulation of firing rate relative to the position of the reach targets. The target setting provides a 2x4 design with factors distance (near, far) and direction (outer left, mid left, mid right, outer right). To show if firing rate is modulated with distance (considering all eight targets) or direction within a fixed distance (considering only four targets respectively), we calculated Kruskal-Wallis tests with a 5% alpha level. Additionally, we quantified the extent of modulation with a modulation index. The modulation index with respect to distance, near direction and far direction is reported as distMI, nearMI and farMI respectively. To calculate nMI and fMI we computed the average firing rate (fr) for each target. The modulation index is then defined for all near (nearMI) or all far (farMI) targets as $\frac{\max(fr) - \min(fr)}{\min(fr) + \max(fr)}$. For the distMI we averaged the firing rate across all near and all far targets and calculated the modulation index the same way. This is equivalent to $\frac{|fr_{near} - fr_{far}|}{fr_{near} + fr_{far}}$. Modulation indices range from 0 to 1 with 0 indicating no modulation and 1 maximum modulation.

Raw data and spike data processing was performed with Matlab and visualized using the toolbox gramm (Morel, 2018).

Acknowledgements

We thank Sina Plümer for help with data collection and technical support, Klaus Heisig and Marvin Kulp for help with mechanical constructions, Baltasar Röchardt for help with motion capture, Peer Strogies for help with implant design, Pierre Morel and Enrico Ferrea for helpful discussions, Leonore Burchardt for help with animal training and Janine Kuntze, Luisa Klotz and Dirk Prübe for technical support.

This work was supported by the German Research Foundation (DFG RU-1847, grant GA1475-C1 to A. Gail) and the European Commission in the context of the Plan4Act consortium (EC-H2020-FETPROACT-16 732266 WP1 to A. Gail).

Competing Interests

No competing interests declared

Rich Media Files

- **reach_cage_model.mp4** - 3-dimensional animation of the Reach Cage
- **stretch_and_reach_example.mp4** - Video of monkey K performing the stretch-and-reach task
- **motion_capture_example.mp4** - Wrist tracking of monkey K from all four cameras
- **averaged_reach_movements.mp4** - Trial-averaged video of monkey L for all reach movements towards near targets
- **averaged_walk-and-reach_movements.mp4** - Trial-averaged video of monkey L for all walk-and-reach movements towards near targets

References

- Aflalo, T., Kellis, S., Klaes, C., Lee, B., Shi, Y., Pejsa, K., ... Andersen, R. A. (2015). Decoding motor imagery from the posterior parietal cortex of a tetraplegic human. *Science*, *348*(6237), 906-910. doi: 10.1126/science.aaa5417
- Andersen, R. A., & Cui, H. (2009). Intention, action planning, and decision making in parietal-frontal circuits. *Neuron*, *63*(5), 568-583. doi: 10.1016/j.neuron.2009.08.028
- Ballesta, S., Reymond, G., Pozzobon, M., & Duhamel, J. R. (2014). A real-time 3d video tracking system for monitoring primate groups. *Journal of Neuroscience Methods*, *234*, 147-152. doi: 10.1016/j.jneumeth.2014.05.022
- Bansal, A. K., Truccolo, W., Vargas-Irwin, C. E., & Donoghue, J. P. (2012). Decoding 3d reach and grasp from hybrid signals in motor and premotor cortices: spikes, multiunit activity, and local field potentials. *Journal of Neurophysiology*, *107*(5), 1337-1355. doi: 10.1152/jn.00781.2011
- Batista, A. P., Buneo, C. A., Snyder, L. H., & Andersen, R. A. (1999). Reach plans in eye-centered coordinates. *Science*, *285*(5425), 257-260.
- Berger, M., Calapai, A., Stephan, V., Niessing, M., Burchardt, L., Gail, A., & Treue, S. (2017). Standardized automated training of rhesus monkeys for neuroscience research in their housing environment. *Journal of Neurophysiology*, *119*(3), 796-807. doi: 10.1152/jn.00614.2017
- Bhattacharyya, R., Musallam, S., & Andersen, R. A. (2009). Parietal reach region encodes reach depth using retinal disparity and vergence angle signals. *Journal of Neurophysiology*, *102*(2), 805-816. doi: 10.1152/jn.90359.2008
- Bouton, C. E., Shaikhouni, A., Annetta, N. V., Bockbrader, M. A., Friedenber, D. A., Nielson, D. M., ... Rezaei, A. R. (2016). Restoring cortical control of functional movement in a human with quadriplegia. *Nature*, *533*, 247-250. doi: 10.1038/nature17435
- Buneo, C. A., & Andersen, R. A. (2012). Integration of target and hand position signals in the posterior parietal cortex: effects of workspace and hand vision. *Journal of Neurophysiology*, *108*(1), 187-199. doi: 10.1152/jn.00137.2011
- Buneo, C. A., Jarvis, M. R., Batista, A. P., & Andersen, R. A. (2002). Direct visuomotor transformations for reaching. *Nature*, *416*(6881), 632-636. doi: 10.1038/416632a

- Calapai, A., Berger, M., Niessing, M., Heisig, K., Brockhausen, R., Treue, S., & Gail, A. (2017). A cage-based training, cognitive testing and enrichment system optimized for rhesus macaques in neuroscience research. *Behavior Research Methods*, *49*(1), 35-45. doi: 10.3758/s13428-016-0707-3
- Capogrosso, M., Milekovic, T., Borton, D., Wagner, F., Moraud, E. M., Mignardot, J. B., ... Courtine, G. (2016). A brain-spine interface alleviating gait deficits after spinal cord injury in primates. *Nature*, *539*(7628), 284-288. doi: 10.1038/nature20118
- Chen, X., & Davis, J. (2000). Camera placement considering occlusion for robust motion capture. *Computer Graphics Laboratory, Stanford University, Tech. Rep.* doi: 10.1.1.141.2999
- Cheney, P. D., & Fetz, E. E. (1980). Functional classes of primate corticomotoneuronal cells and their relation to active force. *Journal of neurophysiology*, *44*(4), 773-791. doi: 10.1152/jn.1980.44.4.773
- Cisek, P. (2012). Making decisions through a distributed consensus. *Current Opinion in Neurobiology*, *22*(6), 927-936. doi: 10.1016/j.conb.2012.05.007
- Collinger, J. L., Wodlinger, B., Downey, J. E., Wang, W., Tyler-Kabara, E. C., Weber, D. J., ... Schwartz, A. B. (2013). High-performance neuroprosthetic control by an individual with tetraplegia. *The Lancet*, *381*(9866), 557-564. doi: 10.1016/S0140-6736(12)61816-9
- Courtine, G., Roy, R. R., Hodgson, J., McKay, H., Raven, J., Zhong, H., ... Edgerton, V. R. (2005). Kinematic and emg determinants in quadrupedal locomotion of a non-human primate (rhesus). *Journal of Neurophysiology*, *93*(6), 3127-3145. doi: 10.1152/jn.01073.2004
- Fernandez-Leon, J. A., Parajuli, A., Franklin, R., Sorenson, M., Felleman, D. J., Hansen, B. J., ... Dragoi, V. (2015). A wireless transmission neural interface system for unconstrained non-human primates. *Journal of neural engineering*, *12*(5), 56005. doi: 10.1088/1741-2560/12/5/056005
- Foster, J. D., Nuyujukian, P., Freifeld, O., Gao, H., Walker, R., Ryu, S. I., ... Shenoy, K. V. (2014). A freely-moving monkey treadmill model. *Journal of Neural Engineering*, *11*(4), 46020. doi: 10.1088/1741-2560/11/4/046020
- Gail, A., & Andersen, R. A. (2006). Neural dynamics in monkey parietal reach region reflect context-specific sensorimotor transformations. *Journal of Neuroscience*, *26*(37), 9376-9384. doi: 10.1523/JNEUROSCI.1570-06.2006
- Georgopoulos, A. P., Kalaska, J. F., & Massey, J. T. (1981). Spatial trajectories and reaction times of aimed movements: effects of practice, uncertainty, and change in target location. *Journal of Neurophysiology*, *46*(4), 725-43.
- Georgopoulos, A. P., Schwartz, A. B., & Kettner, R. E. (1986). Neuronal population coding of movement direction. *Science*, *233*(4771), 1416-1419. doi: 10.1126/science.3749885
- Gilja, V., Chestek, C. A., Nuyujukian, P., Foster, J., & Shenoy, K. V. (2010). Autonomous head-mounted electrophysiology systems for freely behaving primates. *Current Opinion in Neurobiology*, *20*(5), 676-686. doi: 10.1016/j.conb.2010.06.007
- Gilja, V., Pandarinath, C., Blabe, C. H., Nuyujukian, P., Simeral, J. D., Sarma, A. A., ... Henderson, J. M. (2015). Clinical translation of a high-performance neural prosthesis. *Nature Medicine*, *21*(10), 1142-1145. doi: 10.1038/nm.3953
- Hage, S. R., & Jurgens, U. (2006). On the role of the pontine brainstem in vocal pattern generation: A telemetric single-unit recording study in the squirrel monkey. *Journal of Neuroscience*, *26*(26), 7105-7115. doi: 10.1523/JNEUROSCI.1024-06.2006
- Händel, B. F., & Schölvinc, M. L. (2017). The brain during free movement - what can we learn from the animal model. *Brain Research*. doi: 10.1016/j.brainres.2017.09.003
- Hauschild, M., Mulliken, G. H., Fineman, I., Loeb, G. E., & Andersen, R. A. (2012). Cognitive signals for brain-machine interfaces in posterior parietal cortex include continuous 3d trajectory commands. *Proceedings of the National Academy of Sciences*, *109*(42), 17075-17080. doi: 10.1073/pnas.1215092109
- Hochberg, L. R., Bacher, D., Jarosiewicz, B., Masse, N. Y., Simeral, J. D., Vogel, J., ... Donoghue, J. P. (2012). Reach and grasp by people with tetraplegia using a neurally controlled robotic arm. *Nature*, *485*(7398), 372-375. doi: 10.1038/nature11076
- Jackson, A., Mavoori, J., & Fetz, E. E. (2007). Correlations between the same motor cortex cells and arm muscles during a trained task, free behavior, and natural sleep in the macaque monkey. *Journal of Neurophysiology*, *97*(1), 360-374. doi: 10.1152/jn.00710.2006
- Kaufman, M. T., Churchland, M. M., & Shenoy, K. V. (2013). The roles of monkey m1 neuron classes in movement preparation and execution. *Journal of Neurophysiology*, *110*(4), 817-825. doi: 10.1152/jn.00892.2011
- Klaes, C., Westendorff, S., Chakrabarti, S., & Gail, A. (2011). Choosing goals, not rules: Deciding among rule-based action plans. *Neuron*, *70*(3), 536-548. doi: 10.1016/j.neuron.2011.02.053
- Kuang, S., Morel, P., & Gail, A. (2016). Planning movements in visual and physical space in monkey posterior parietal cortex. *Cerebral Cortex*, *26*(2), 731-747. doi: 10.1093/cercor/bhu312

- Libey, T., & Fetz, E. E. (2017). Open-source, low cost, free-behavior monitoring, and reward system for neuroscience research in non-human primates. *Frontiers in Neuroscience*, *11*(MAY), 265.
- Ludvig, N., Tang, H. M., Gohil, B. C., & Botero, J. M. (2004). Detecting location-specific neuronal firing rate increases in the hippocampus of freely-moving monkeys. *Brain Research*, *1014*(1-2), 97-109. doi: 10.1016/j.brainres.2004.03.071
- Moeslund, T. B., Hilton, A., & Krüger, V. (2006). A survey of advances in vision-based human motion capture and analysis. *Computer Vision and Image Understanding*, *104*(2-3), 90-126. doi: 10.1016/j.cviu.2006.08.002
- Morel, P. (2018). Gramm: grammar of graphics plotting in matlab. *Journal of Open Source Software*, *3*(23), 568. doi: 10.21105/joss.00568
- Morel, P., Ferrea, E., Taghizadeh-Sarshouri, B., Audí, J. M. C., Ruff, R., Hoffmann, K. P., ... Gail, A. (2015). Long-term decoding of movement force and direction with a wireless myoelectric implant. *Journal of Neural Engineering*, *13*(1), 16002. doi: 10.1088/1741-2560/13/1/016002
- Mulliken, G. H., Musallam, S., & Andersen, R. A. (2008). Forward estimation of movement state in posterior parietal cortex. *Proceedings of the National Academy of Sciences of the United States of America*, *105*(24), 8170-7. doi: 10.1073/pnas.0802602105
- Musallam, S., Corneil, B. D., Greger, B., Scherberger, H., & Andersen, R. A. (2004). Cognitive control signals for neural prosthetics. *Science*, *305*(5681), 258-262. doi: 10.1126/science.1097938
- Musial, P. G., Baker, S. N., Gerstein, G. L., King, E. A., & Keating, J. G. (2002). Signal-to-noise ratio improvement in multiple electrode recording. *Journal of Neuroscience Methods*, *115*(1), 29-43. doi: 10.1016/S0165-0270(01)00516-7
- Nakamura, T., Matsumoto, J., Nishimaru, H., Bretas, R. V., Takamura, Y., Hori, E., ... Nishijo, H. (2016). A markerless 3d computerized motion capture system incorporating a skeleton model for monkeys. *PLoS ONE*, *11*(11), e0166154. doi: 10.1371/journal.pone.0166154
- Nummela, S. U., Jovanovic, V., Mothe, L. d. l., & Miller, C. T. (2017). Social context-dependent activity in marmoset frontal cortex populations during natural conversations. *J. Neurosci*, *37*(29), 7036-7047. doi: 10.1523/JNEUROSCI.0702-17.2017
- Peikon, I. D., Fitzsimmons, N. A., Lebedev, M. A., & Nicolelis, M. A. L. (2009). Three-dimensional, automated, real-time video system for tracking limb motion in brain-machine interface studies. *Journal of Neuroscience Methods*, *180*(2), 224-233. doi: 10.1016/j.jneumeth.2009.03.010
- Pesaran, B., Nelson, M. J., & Andersen, R. A. (2006). Dorsal premotor neurons encode the relative position of the hand, eye, and goal during reach planning. *Neuron*, *51*(1), 125-134. doi: 10.1016/j.neuron.2006.05.025
- Ponce, C. R., Genecin, M. P., Perez-Melara, G., & Livingstone, M. S. (2016). Automated chair-training of rhesus macaques. *Journal of Neuroscience Methods*, *263*, 75-80. doi: 10.1016/j.jneumeth.2016.01.024
- Prescott, M. J., Brown, V. J., Flecknell, P. A., Gaffan, D., Garrod, K., Lemon, R. N., ... Whitfield, L. (2010). Refinement of the use of food and fluid control as motivational tools for macaques used in behavioural neuroscience research: Report of a working group of the nc3rs. *Journal of Neuroscience Methods*, *193*(2), 167-188. doi: 10.1016/j.jneumeth.2010.09.003
- Rajangam, S., Tseng, P. H., Yin, A., Lehew, G., Schwarz, D., Lebedev, M. A., & Nicolelis, M. A. (2016). Wireless cortical brain-machine interface for whole-body navigation in primates. *Scientific Reports*, *6*, 22170. doi: 10.1038/srep22170
- Rolls, E. T., Robertson, R. G., & Georges-François, P. (1997). Spatial view cells in the primate hippocampus. *European Journal of Neuroscience*, *9*(8), 1789-1794. doi: 10.1111/j.1460-9568.1997.tb01538.x
- Roy, S., & Wang, X. (2012). Wireless multi-channel single unit recording in freely moving and vocalizing primates. *Journal of Neuroscience Methods*, *203*(1), 28-40. doi: 10.1016/j.jneumeth.2011.09.004
- Santhanam, G., Ryu, S. I., Yu, B. M., Afshar, A., & Shenoy, K. V. (2006). A high-performance brain-computer interface. *Nature*, *442*(7099), 195-198. doi: 10.1038/nature04968
- Schaffelhofer, S., Agudelo-Toro, A., & Scherberger, H. (2015). Decoding a wide range of hand configurations from macaque motor, premotor, and parietal cortices. *Journal of Neuroscience*, *35*(3), 1068-1081. doi: 10.1523/JNEUROSCI.3594-14.2015
- Schwarz, D. A., Lebedev, M. A., Hanson, T. L., Dimitrov, D. F., Lehew, G., Meloy, J., ... Nicolelis, M. A. L. (2014). Chronic, wireless recordings of large-scale brain activity in freely moving rhesus monkeys. *Nature Methods*, *11*(6), 670-676. doi: 10.1038/nmeth.2936
- Serruya, M. D., Hatsopoulos, N. G., Paninski, L., Fellows, M. R., & Donoghue, J. P. (2002). Brain-machine interface: Instant neural control of a movement signal. *Nature*, *416*(6877), 141-142. doi: 10.1038/416141a
- Sun, N. L., Lei, Y. L., Kim, B. H., Ryou, J. W., Ma, Y. Y., & Wilson, F. A. (2006). Neurophysiological recordings in freely moving monkeys. *Methods*, *38*(3), 202-209. doi: 10.1016/j.ymeth.2005.09.018
- Taylor, D. M., Tillery, S. I. H., & Schwartz, A. B. (2002). Direct cortical control of 3d neuroprosthetic devices. *Science*, *296*(5574), 1829-1832.

- Teikari, P., Najjar, R. P., Malkki, H., Knoblauch, K., Dumortier, D., Gronfier, C., & Cooper, H. M. (2012). An inexpensive arduino-based led stimulator system for vision research. *Journal of Neuroscience Methods*, *211*(2), 227-236. doi: 10.1016/j.jneumeth.2012.09.012
- Velliste, M., Perel, S., Spalding, M. C., Whitford, A. S., & Schwartz, A. B. (2008). Cortical control of a prosthetic arm for self-feeding. *Nature*, *453*(7198), 1098-1101.
- Wessberg, J., Stambaugh, C. R., Kralik, J. D., Beck, P. D., M.Laubach, Chapin, J. K., ... Biggs, S. J. (2000). Real-time prediction of hand trajectory by ensembles of cortical neurons in primate. *Nature*, *408*(1), 361-365.
- Westendorff, S., Klaes, C., & Gail, A. (2010). The cortical timeline for deciding on reach motor goals. *Journal of Neuroscience*, *30*(15), 5426-5436. doi: 10.1523/JNEUROSCI.4628-09.2010
- Wodlinger, B., Downey, J. E., Tyler-Kabara, E. C., Schwartz, A. B., Boninger, M. L., & Collinger, J. L. (2014). Ten-dimensional anthropomorphic arm control in a human brain-machine interface: Difficulties, solutions, and limitations. *J Neural Eng*, *12*(1), 16011. doi: 10.1088/1741-2560/12/1/016011
- Yin, M., Borton, D. A., Komar, J., Agha, N., Lu, Y., Li, H., ... Nurmikko, A. V. (2014). Wireless neurosensor for full-spectrum electrophysiology recordings during free behavior. *Neuron*, *84*(6), 1170-1182. doi: 10.1016/j.neuron.2014.11.010

Chapter 4

Neural encoding of far-located reach goals in motor, premotor, and parietal cortex in a physically unconstrained monkey performing a walk-and-reach task

4.1 Abstract

Sensorimotor neuroscience with non-human primates is typically conducted in constraining environments which do not allow whole-body movements. Those studies provided insights into cortical control of goal-directed reaching movements in conjunction with eye movements and grasping. However, it is unknown how the brain encodes targets far from the body for which the monkey must make a walk-and-reach movement. With our recently developed cage-based experimental environment for rhesus monkeys, the Reach Cage, we investigated planning and execution of movements to targets within (near space) and beyond immediate reach (far space).

Here, we used a wireless neural recording system in combination with six chronically implanted 32-channel electrode arrays to record multi- and single-unit activity from three fronto-parietal sensorimotor areas while a monkey performed reach and walk-and-reach movements to two sets of four targets located in near and far space. We found that (1) neural activity is highly modulated by the spatial position of the near targets during the reach movement in all three brain areas and during movement planning in PRR and PMd resembling results from conventional experiments in constraining environments; (2) only PRR, if at all, encodes the spatial position of far-located reach-goals during movement planning; (3) neural activity differs strongly between reach and walk-and-reach movements early after the onset of the target cue in PMd, PRR and several hundred milliseconds later in M1; (4) the activity in PRR and PMd but not M1 was similar for goal-directed arm movements no matter if performed during walk-and-reach movements or

not. This suggests that body posture and whole-body movements have relatively little influence on PMd and PRR activity.

4.2 Introduction

In rhesus monkeys, the cortical control of reaching movements was extensively studied and revealed three interconnected areas of the cerebral cortex, namely the parietal reach region PRR, dorsal premotor cortex PMd and the arm area of the primary motor cortex M1, which provide main contributions to planning and control of voluntary goal-directed arm movements (Andersen & Cui, 2009; Johnson et al., 1996; Kalaska & Crammond, 1992; Rizzolatti et al., 2002; Snyder et al., 1997). This fronto-parietal reach network serves as a model to study not only motor control, but more generally goal-directed behavior, like rule-guidance (Gail & Andersen, 2006; Stoet & Snyder, 2004), decision making (Christopoulos et al., 2015; Cisek & Kalaska, 2005; Coallier et al., 2015; Klaes et al., 2011; Thura & Cisek, 2014) or reward encoding (Musallam et al., 2004; Pastor-Bernier & Cisek, 2011; Rajalingham et al., 2014). Since arm movements in the natural context are rarely conducted in isolation, they have been studied also in conjunction with eye movements (Batista et al., 1999; Cui & Andersen, 2007; Pesaran et al., 2006) and grasping movements (Hao et al., 2014; Rouse & Schieber, 2016; Schaffelhofer et al., 2015). Yet, it is unknown how the fronto-parietal reach network encodes reach goals that are outside immediate reach and that are embedded in more complex goal-directed whole-body movements, for example, to walk and then reach an object.

There are neuropsychological and neurophysiological findings suggesting that the space near the body is encoded differently than far space by fronto-parietal areas (see Farnè et al. (2016) for review). Visuospatial neglect can be restricted to the near or far space as shown by patients with parietal lesion (Halligan & Marshall, 1991; Vuilleumier et al., 1998) and transcranial magnetic stimulation over the parietal cortex (Bjoertomt et al., 2002). Micro-electrode recordings in premotor cortex and the posterior parietal cortex of non-human primates found bimodal neurons responding to visual and somatosensory stimulation with visual receptive fields being congruent with somatosensory receptive fields and thereby covering the space near the body, termed peripersonal space (Colby & Goldberg, 1999; Graziano et al., 1997; Rizzolatti et al., 1997, 1981). The extent of the peripersonal space can change depending on the context. Tool-use extends near space visuospatial neglect to far space (Berti & Frassinetti, 2000; Giglia et al., 2015). Similarly, visual receptive fields in bimodal neurons include the space around the tool (Iriki et al., 1996). Fake arms (“rubber hands”) can be perceived as part of the own body when applying multimodal stimulation, i.e. when inducing touch sensation on the actual arm and visual impressions of touch on the fake arm (Botvinick & Cohen, 1998). Neurons in primary motor cortex, primary somatosensory cortex and area 5 in the posterior parietal cortex respond to the visual presentation of a fake arm after congruent visuo-tactile stimulation of fake and real arm (Graziano et al., 2000;

Shokur et al., 2013). In addition to the research about multimodal integration, mirror neurons in the ventral premotor cortex respond differently to an observed action whether or not it is in reach (Bonini et al., 2014; Caggiano et al., 2009). Those neurons encode the possibility to interact with the observed action rather than depending on the mere geometrical distance from the body (Bonini et al., 2014). These findings indicate that encoding of bimodal sensory information and information about observed actions seems to be bound to one's own body boundaries, but also can be adapted in extent, if the space for interacting with the environment is reduced or expanded.

The neurophysiological findings which indicate that the separation of near (peripersonal) versus far space is related to the space in which we can act raise two questions. First, do perception- and behavior-based definitions of near versus far space depend merely on distance from the body, or - consistent with the physiology of multimodal receptive fields and mirror neurons - rather also on the possibility to interact with a target object? The latter is the case. Experiments on the crossmodal congruency effect (CCE), an interference of visual and somatosensory perception used to behaviorally map peripersonal space in healthy humans, showed that the behavioral peripersonal space extends towards reach-goals before they are touched (Brozzoli et al., 2010, 2009). This means that the behavioral peripersonal space can extend beyond the immediate body boundaries in the context of action planning. In a previous psychophysical study (chapter 2) we showed that this is even true for walk-and-reach movements in which the reach target is beyond reach from the current body position.

The fact that neurophysiological encoding of multisensory information and mirror-actions and the behavioral CCE both depend on reach-action space rather than body distance raise the second question. In how far does encoding of reach goal locations itself depend on distance from body or from immediate 'reachability'? Specifically, are reach goals which require a walk-and-reach movement to a far target, encoded equivalently to near reach goals in the fronto-parietal sensorimotor areas PRR and PMd? The expandability of multisensory and mirror-action encoding in the neighboring parietal and premotor areas towards tool-reachable targets and the expandability of the CCE towards walk-and-reach targets lets us predict that motor goal encoding should encompass also walk-and-reach targets in parietal and premotor cortex.

The neurophysiological properties in monkeys performing walk-and-reach movements were not studied before, partly because of two technical limitations. First, extracellular recording were performed by inserting a microwire in the cortex using a microdrive attached to a chamber on the skull of the monkey making it necessary to fixate the head (Mountcastle et al., 1975). When using chronically implanted microelectrode arrays floating on the brain, the electrodes are not prone to head movements anymore (Maynard et al., 1997; Musallam et al., 2007). However, tethered connections to the recording system still require restraint to prevent the animal from biting into or grabbing the cables. More recently, wireless recording equipment was developed finally allowing for neurophysiological recordings in freely moving monkeys (Gilja et al., 2010; Schwarz et al., 2014; Yin et al., 2014). The second limitation used to be the behavioral setup. For

a clear interpretation of the recorded neuronal data, sensorimotor neuroscience setups impose physical constraints to keep control over environmental parameters, such as sensory input. Monkeys are seated in a primate chair and exposed to a manipulandum, such as a joystick or a touch panel, in front of a limited workspace, often a screen. In the chapter 3, we presented a novel experimental environment for sensorimotor neuroscience with physically unconstrained monkeys, the Reach Cage. We showed that the Reach Cage allows for studying goal-directed walk-and-reach movements while having sufficient control or at least surveillance of the relevant behavioral parameters to interpret the behavior along with the neural data.

We trained one rhesus monkey to goal-directed reach and walk-and-reach movements with instructed delay to eight reach goals near and far from the animal in our newly developed Reach Cage. We used a wireless recoding system to record from multi and single-units in all three brain areas in the fronto-parietal reach network (PRR, PMd and arm area M1) with 64 chronically implanted electrodes in each area. By investigating the proportion of neurons modulated to reach target position and the overall difference in the activation pattern of the neuronal population we could show that the modulation to near space target position resembles results obtained from conventional experiments performed with monkeys seated in a primate-chair. However, we observed little modulation in activity between far targets during movement planning in PRR and no modulation in M1 and PMd indicating that, if at all, PRR is the only area in the fronto-parietal reach network which encodes target position beyond reach. Furthermore, we found differences in neural activity between reach and walk-and-reach movements very early in the planning phase in PMd and PRR and later in M1. Finally, we found that the neuronal population in PMd and PRR but not arm area M1 produces a similar activation pattern during the actual goal-directed arm movement for reach and walk-and-reach movements suggesting that PMd and PRR are specifically involved in arm movement control independent of whole-body movements or body posture.

4.3 Methods

Animal

One 15 year old male rhesus monkey (*Macaca mulatta*) participated in this study. Details about training, housing, implant design and implantation procedure are described in chapter 3. (monkey L).

All procedures have been approved by the responsible regional government office [Niedersächsisches Landesamt für Verbraucherschutz und Lebensmittelsicherheit (LAVES)] under permit number 3392 42502-04-13/1100 and comply with German Law and the European Directive 2010/63/EU.

Behavioral setup – the Reach Cage

The behavioral setup consists of metal cage with dimensions 170cm x 80cm x 85cm (W x D x H) (Reach Cage) experimentally controlled by the *MaCaQuE* system (Macaque Cage Query Extension) which we developed for this purpose (Figure 4.1A). We mounted ten MCT (*MaCaQue* cue and target boxes), with integrated proximity sensor and color-illuminable front plate inside the Reach Cage and one MCT outside (Figure 4.1B). The monkey can freely move around inside the Reach Cage (Figure 4.1C) to approach and touch any MCT and collect the fluid reward presented randomly on either side of the Reach Cage. Technical details on the Reach Cage, *MaCaQuE* and MCTs are described in chapter 3.

Two of the MCTs are placed on the floor pointing upwards (start buttons), and both have to be touched by the monkey to initiate a trial start. This configuration encourages a well-defined starting position of the animal within the Reach Cage, while not imposing any further constraints on its posture. The other eight MCTs inside the cage are mounted on the ceiling pointing to and well visible from the starting position (targets) and serve as reach goals during the behavioral task. A row of four of these targets is placed close to the starting position (near or ‘reach’) with a distance projected to the floor of the cage of approximately 10cm from the start buttons. We placed them comfortably within reach of the animal from the starting position. The second row of targets is placed to the back of the cage (far or ‘walk-and-reach’) for which the distance projected to the cage floor is approximately 100cm from the start buttons. To reach far targets from the starting position, the animal had to make at least one step towards them. The MCT outside the cage is placed in sights for the animal from the starting position for providing visual cues.

Two spoon-sized metal bowls are placed between the near and far targets symmetrically on the cage side walls. Each reward bowl is equipped with an automatic fluid dispenser. Whenever the animal finished a trial correctly, liquid reward is delivered to one of the two reward system automatically during the behavioral task by the controlling software. The side of reward is randomized to prevent spatial bias. All equipment inside the cage is durable and resistant to monkey behavior such as scratching, shaking or biting.

The controlling *MaCaQuE* hard- and software is based on a Teensy (PJRC, Sherwood, USA), an Arduino-like microcontroller platform and programmed using Arduino-C. *MaCaQuE* is responsible for addressing the MCTs and the peristaltic reward pumps (OEM M025 DC, Verderflex, Castleford, UK). The illumination of the MCT, registration of their touch, acoustic feedback to the animal and fluid reward as part of the behavioral task are achieved via *MaCaQuE* which itself is timed and controlled by a Mac Mini (Apple Inc., Cupertino, USA) using custom-written software in C++.

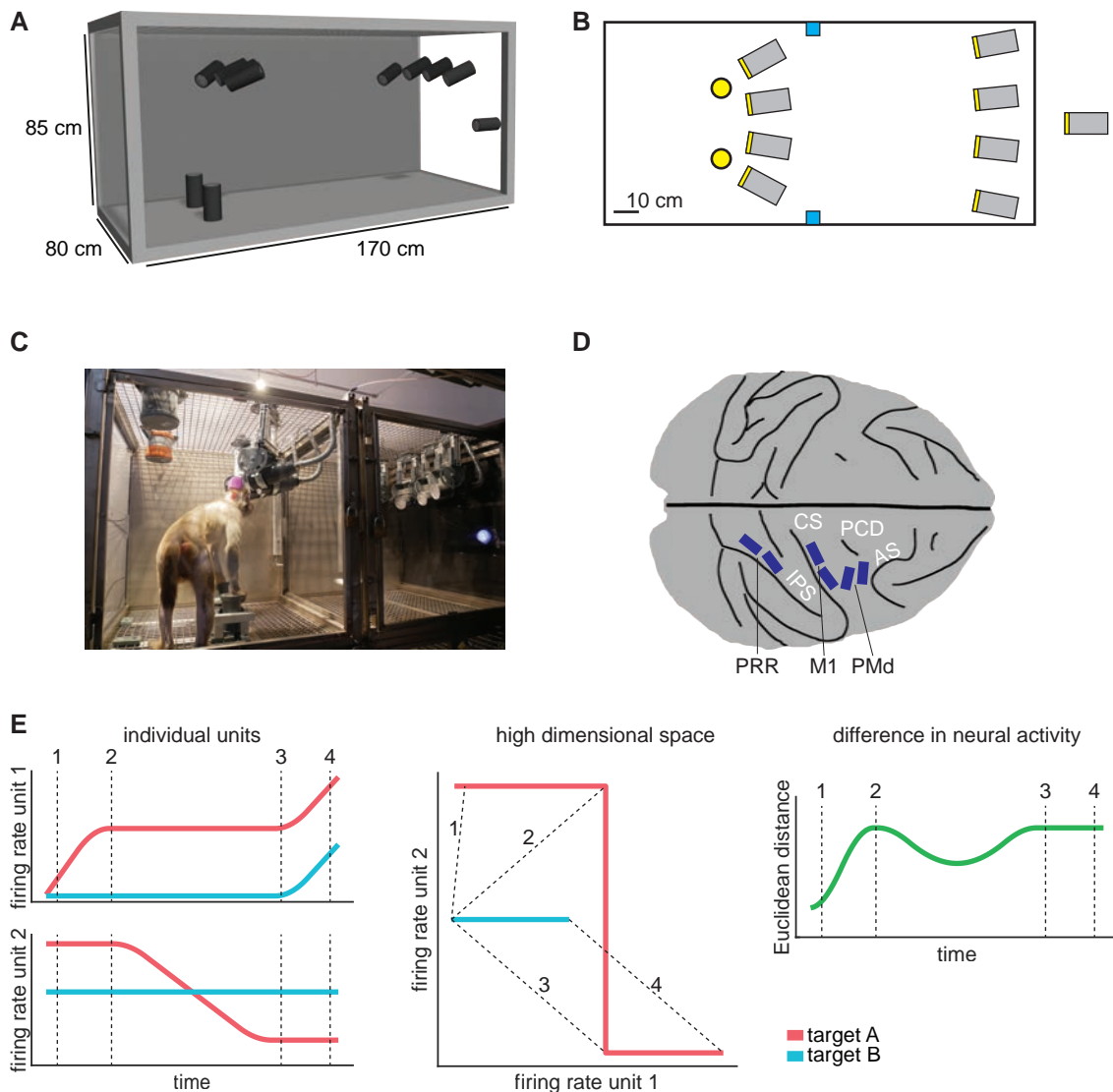


Figure 4.1: Methods. A) Virtual 3-dimensional model of the setup cage. Black cylinders depict the *MaCaQuE* cue and target boxes (MCT) with its touch sensitive illuminatable surface. B) Top-view sketch of the setup. MCTs are shown in grey with touch sensitive surface in yellow. The two yellow circles are two MCTs on the floor pointing upwards, the start buttons. The eight targets are placed on the ceiling pointing to the starting position. The eleventh MCT is placed outside the cage. Reward bowls are shown in blue. C) Image of the setup with monkey. D) Top-view sketch on the monkey's brain based on a 3-dimensional reconstruction from an MRI scan. The position of the six microelectrode arrays are shown in blue. Anatomical landmarks descriptions: IPS – intraparietal sulcus; CS – central sulcus; PCD – postcentral dimple; AS – arcuate sulcus. E) Cartoon of an example population of two units and their response behavior to two hypothetical targets A (red) and B (green). Left plots show the temporal evolution of the firing rate of the respective units. The middle plot illustrates the corresponding neural trajectory in the high dimensional (in this case 2-dimensional) space. The neural distance over time of the trajectories to target A and B are shown on the right. Four time points are marked in all plots (numbers 1 - 4).

Behavioral task

The monkey performed a delayed reach task from the start buttons to one of the eight targets in the cage (Figure 4.2A). When the MCT outside of the cage lightens up it signals the animal to initiate a trial. The timeline of a successful trial is as follows: 1) The animal initiates a trial by touching both start buttons (hand fixation acquisition); 2) The animal remains its hands on both start buttons for 400ms – 800ms (fixation hold); 3) One pseudo randomly assigned target lights up (target onset). The animal still needs to remain its hand on the start buttons for 1000ms – 2200ms; 4) The light outside the cage turns red signaling the animal to move (go cue). The animal releases at least one of its hands from the start buttons within 1200ms (movement onset). Movement onset is defined by the onset of the movement of one of the hands but does not reflect body movement onset; 5) The animal touches the illuminated target within 1800ms for far targets (target acquisition); 6) The animal remains its hand on the target for 300ms. If the animal performs all steps in succession correctly, the trial is counted as successful, a high-pitched tone appears and liquid reward is delivered to one randomly assigned reward bowl. If the animal performs one step incorrectly, the trial is aborted immediately, counted as an error and a low frequency tone appears.

Behavioral analysis

To analyze the behavior of the monkey during the reach task we used the Cineplex system (Plexon Inc., Dallas, USA) which contains four synchronized Stingray F-033/C color cameras (Allied Vision Technologies GmbH, Stadroda, Germany) with VGA resolution and 60 fps frame rate. We synchronized the camera setting with *MaCaQuE* events to extract video frames aligned to the periods and events of the task.

The Cineplex system can capture the 3D position of colored objects. In chapter 3 we provide a detailed description and present 3D wrist trajectories of a right-handed monkey performing a similar task but with far targets located closer to the starting position. Here, we were not able to capture wrist trajectories for far targets since workspace is larger and the monkey is left-handed. The long cage wall on the animals' left (during the behavioral task) is not transparent making tracking of the left side of the animal more difficult. To qualitatively assess the animal's behavior during the task we chose another approach. The cameras were stably mounted on a fix position that did not change between sessions. We averaged the videos frame-by-frame over trials to obtain a video showing the averaged behavior of the monkey. In detail, we extracted video segments from six sessions, around target onset (500ms before until 1500ms afterwards), go cue (500ms before until 1000ms afterwards) and movement onset (500ms before until 1000/1500ms (near/far) afterwards). For each session, we averaged the video segments over all successful trials for all eight targets individually, additionally, for all near targets together and all far targets together (supplementary material). Furthermore, we averaged corresponding average video

segments from each session to obtain an average across sessions. Based on these resulting video segments, we provide a qualitative description of the monkey's behavior during the task.

To understand the monkey's body orientation towards far targets over the course of the movement, for one session we compared the four average videos (one per target) of the camera facing the front of the animal while it moves towards each of the far targets. From each video, we manually defined frame-by-frame the average position of the monkey's right hand during the walk-and-reach movement. Based on the camera setting, we obtained the 2-dimensional hand trajectory relative to the far target positions. During the approximately first half of the walk-and-reach the hand moved from the start button to the floor of the cage. Knowing the cage dimensions and having the bottom cage grid as a reference, we estimated the location where the animal put its hand on the floor. From the lateral horizontal position of this landing point we then estimated the walking direction of the animal during walk-and-reach movements.

The average videos were generated and analyzed using Matlab (Mathworks Inc., Natick, USA).

Neural recording

We recorded from six 32-electrode floating microelectrode arrays (FMA; Microprobes for Life Science, Gaithersburg, USA) implanted in three areas of the right hemisphere: primary motor cortex (M1), dorsal premotor cortex (PMd) and parietal reach region (PRR) (Figure 4.1D). For neural recordings in the freely moving animal, we used a small lightweight wireless recording system (W32, Triangle BioSystems International, Durham, USA). A 31-channel wireless headstage recorded from a single array per session, with dimensions of 27mm x 30mm x 17mm (W x D x H) and 4.5g weight. An RF-transparent custom-designed cap, 52mm x 63mm x 29mm (W x D x H), allowed us to place the headstage on any of the six array connectors while preventing the animal to grab or accidentally hit the headstage against cage equipment. Chapter 3 provides a detailed description of the implants. Input voltage from the electrodes was amplified by a gain of 200x and transmitted as analog signal by frequency modulation with 3.05 GHz transmission frequency to the receiver. By picking up the signal on two redundant antennas, the system controls for potential artifacts introduced by the transmission.

We used a 128 channel Cerebus system (Blackrock) for digitization and signal processing. The W32 wireless receiver and its output adapter reduce the overall gain to 1x. A 32-channel Cereplex headstage is connected to an adapter and digitizes the signal at 30 kHz sampling rate and 16-bit resolution on each of the 31 channels.

We performed the preprocessing of broadband data and the extraction of waveforms as previously described (Dann et al., 2016). First, the raw signal was high-pass filtered using a sliding window median with a window length of 91 samples (~ 3 ms). Then, we applied a 5000Hz low-pass using a zero-phase second order Butterworth filter. To remove common noise, we transformed the signal in PCA space per array, removed principle components that

represented common signals and transformed it back (Musial et al., 2002). On the resulting signal, spikes were extracted by threshold crossing using a negative threshold defined by $-3.3725 \times \text{median}(|\text{signal}|)$. We sorted the extracted spikes manually using Offline Sorter V3 (Plexon Inc., Dallas, Texas). If single-unit isolation was not possible, we assigned the non-differentiable cluster as multi-unit but treated the unit the same way in our analysis.

Neural data analysis

The data is composed of six sessions in each of which one different electrode array was recorded. We analyzed the spike count and spike density for each trial in time windows $\pm 500\text{ms}$ around one of the four task events: 1) target onset; 2) go cue; 3) movement onset; 4) target acquisition. The spike density was estimated by convolving the spike trains of each single trial with a normalized Gaussian with standard deviation of 50ms. The spike density was sampled at 200Hz. Spike counts were used to analyze the functional dependency of individual neurons from the task parameters ('tuning'), average spike densities across same-condition trials were used to characterize populations responses in neural state space.

To test for significant modulation of individual unit responses as a function of reach target location we computed Kruskal-Wallis tests on the spike count distribution in each 500ms time window before and after a task event. We excluded the time window after target acquisition, since the reward is delivered already 300ms after target acquisition potentially inducing spatially modulated reward related signals. Reward related neural modulation is not the scope of this study. We tested if the spike count differs a) for target distance, by grouping all near and all far targets together; b) for target position only within in near, excluding far and c) for target position within far, excluding near. The result was Bonferroni corrected for repeated testing in the seven time windows. We excluded cells with an average firing rate during the task less or equal than 2Hz.

To identify common activity for each area per condition we computed the average spike density per unit per target. The population spike density per target and per area was computed by averaging the unit averaged spike density, excluding units with an average firing rate during the task less or equal than 2Hz. We tested for each time point if the average firing rate differs between near and far targets. To account for the multiple comparison problems across many time points we performed non-parametric permutations test based on t-statistics and a clustering algorithm to take into account that adjacent time points are not statistically independent (Maris & Oostenveld, 2007) and described in (Dann et al., 2016). In short, we calculate a t-test for near and far target spike density function to obtain the t-statistic and significance ($p < 0.05$) for each time point individually. Then we clustered adjacent time points for which the t-test was significant and t-statistic was positive or for which the t-test was significant and t-statistic was negative. For each cluster, we calculated the sum of the absolute t values as a single t-statistic for the whole cluster. To generate a test distribution, we performed the same test and clustering a

thousand times but with a randomly permuted correspondence to the ‘near’/‘far’ conditions. Our test distribution is the maximum cluster t-value of each permutation. The p-value for each cluster we want to test is the ratio of cluster t-values for the test distribution that are higher than the t-value of the tested cluster. If this p-value is below 0.05 we considered for all time points within this cluster that the average spike densities are significantly different between near and far targets. We performed this test for each time window and brain area independently and applied a Bonferroni correction for these 12 tests.

Further population analysis was performed considering the population of all neurons’ responses in one brain area as spanning a high dimensional space (neural state space). Figure 4.1E illustrates this approach with a ‘population’ of two hypothetical units). The left panels show the average spike density of the two units over time for two different conditions (green and red) or in our case two different targets. Four time points are illustrated by dashed lines. We describe the complete activation pattern by a point in a space where each dimension represents the firing rate of a certain unit. In our example, given that the population consists of two units, this would be a 2-dimensional space (middle plot). While the units change their activity over time, the state in the high dimensional space, representing the population activity, changes accordingly. The middle plot shows the trajectories that the population activity in the high dimensional space takes as time progresses. When there is no change in activity in the population, the state in the high dimensional space does not change, but if there is a strong fluctuation in activity, the state change will describe a long trajectory. In our example, the units react more to target one resulting in a long red line while there is only little change in unit 1 in the end resulting in a small green line. The four time points on the green and red line are connected by black lines, note that at points 1 - 3 the green population activity remains in the same state. Now, we can simply measure the difference in the population activity for targets A and B by computing the neural distance ND (Euclidean distance) on the averaged firing rates FR for each time point t:

$$ND_{AB}(t) = \sqrt{(FR_{unit1,targetA}(t) - FR_{unit1,targetB}(t))^2 + (FR_{unit2,targetA}(t) - FR_{unit2,targetB}(t))^2 + \dots}$$

Neural distance is a measure for the difference in activation pattern of a population between two experimental conditions. ND avoids two problems that come with computing the average level of activation across all neurons. First, population averages average out differences when one subset of the population is active for target A and a different subset for target B only. Second, the effect inhibition of activity (lower response level) in one neuron is not counteracting the effect of excitation in another neuron, i.e. both modulations add to neural distance.

When analyzed as function of time, not just statically, the high dimensional neural state space contains more information than just distance. For instance, if we compare time point 2, 3 and 4 in the hypothetical example (Figure 4.1E), we see that the activation of unit 1 increases for targets A and B, while for unit 2 it decreases for target A. Neural distance only provides the distance information and as such provides the same value for the three time points (right panel). Yet, in the state space (center panel) the evolution of the activity patterns for target A and B are

obviously different, seen by the direction of the two state space trajectories standing orthogonal to each other.

We analyzed the population activity of all three brain areas around the time of all four task events defined above. For each case, we calculated the ND between all possible combinations of target pairs. To estimate ND differences relative to the size of ‘noise’ fluctuations in ND (i.e. fluctuations not explained by neural modulation due to the experimentally controlled independent variable), we conducted a permutation test. For this, we randomly assigned a reach target to each trial. We re-calculated the average spike densities for each unit and each target (with the new trial-to-target assignment) and the resulting NDs. By repeating this procedure a 1000 times, we obtained a distribution of surrogate NDs. We computed the maximum as reference for our original ND of target pairs. To analyze the movement planning and execution phase in detail, we considered the four 500ms time windows after target onset, before go cue, after movement onset and before target acquisition. Within each window, we computed the average NDs relative to the surrogate ND with the highest value.

For the purpose of visualizing example trajectories, we computed a principle component analysis of the neural trajectories for each area and time window and plotted the first two principle components over time. ND measures and statistical analyses, in contrast, were based on the full neural state space (not the principle components).

4.4 Results

Behavior during movement goal acquisition

To study walk-and-reach behavior during movement planning and execution, we trained a monkey to perform a delayed reaching task in the Reach Cage (see Methods and chapter 3). Four targets were placed close to the starting position (near), so that the monkey could reach them without moving its body. Four other targets were placed further away (far) and required the monkey to make at least a step to reach them (Figure 4.2).

The movement of the monkey inside the reach cage was not physically constrained other than by the position of the start buttons and the target buttons. We monitored the animal’s behavior with four synchronized video cameras and extracted video segments from each successful trial around the four task events (see Methods) to analyze it. Apparently, the strict timing and fixed geometry of the task encouraged the monkey to optimize its behavior and to show rather stereotyped movement patterns in each trial and task condition. The repetitive and stereotyped nature of the motor behavior allowed us to average the video segments over all trials of the same task condition and to qualitatively analyze movement based on the average videos, in which one can still see a blurry but otherwise well localizable animal moving through the cage (see supplementary material S1 for videos).

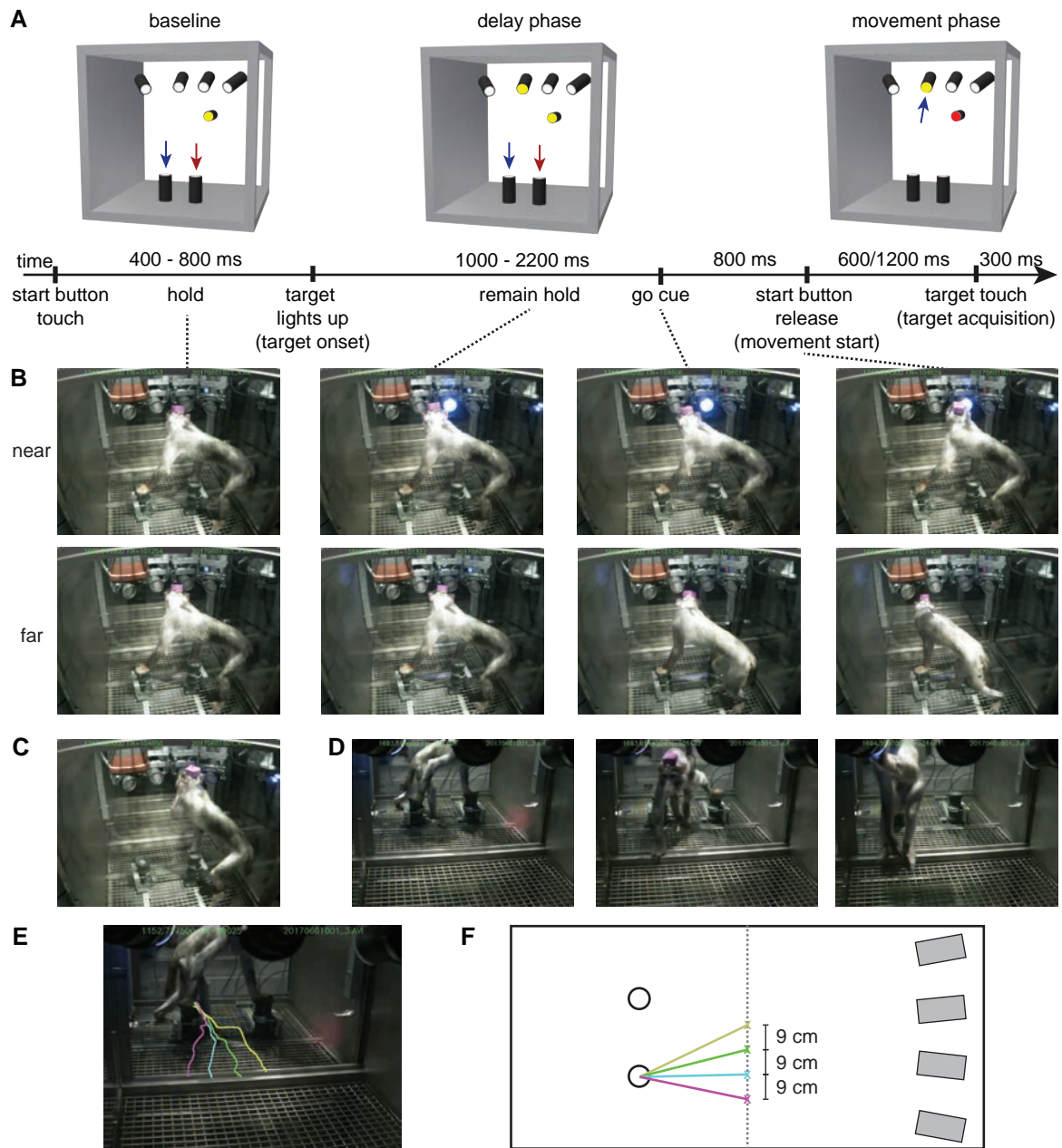


Figure 4.2: Monkey behavior during the task. Data is only from one session as an example. A) Timeline of the behavioral task. B) Single frames from one session. The frames are taken from the periods before target onset (baseline), during delay phase, at go cue and at movement onset. The monkey does not change its body posture when a near target is selected but puts its right leg in front before moving its hands once a far target is selected. C) Same example trial as in B near. The monkey touches the target. D) Same example trial as in B far. Movement period: left – at movement start (same frame but different camera as in the most right picture of B far); middle – during movement when the monkey puts its right hand on the floor for making a step towards the far target; right – at target acquisition. E) Trajectory of the averaged right hand position from the start button towards the cage floor for moving towards one of the four far targets. Background image is from one example trial. F) Top-view sketch of the setup showing the start buttons (circle) and far targets (grey rectangles) with the position where the animal places its right hand in the floor while moving to the respective far target. Dependent on which target is selected, the animal orients its body towards the target.

When the monkey initiated a trial, it stood behind the start buttons with the feet right of the buttons leaning on the buttons with both hands (Figure 4.2B upper). The head is above in the middle between the start buttons close to the near targets facing towards targets and visual cue. When a near target was indicated, the animal waited for the go cue and then lifted the left hand to reach to the indicated target while the right hand remained on the right start button (Figure 4.2C). The monkey looked towards the target leading to a slight change in posture, especially for the outer-right target given its body being standing on the right side. Otherwise, no strong change in posture is apparent before start button release.

For the far targets, the movement behavior is more complex (Figure 4.2B lower, D): 1) After a far target was cued, the animal put its right foot between the starting buttons to prepare the step; 2) After the go cue, the animal removed its right hand from the start button and started to walk by laying the right hand on the horizontal bar on the bottom of the cage half-distance towards the far targets and moving the left foot forward; 3) When the right hand is on the ground, the animal removed its left hand from the start button and moved it towards the target while continuing to move the left foot to the middle of the cage; 4) Once having a stance with the left foot, the monkey followed with the right foot and acquired the target with the left hand and followed with the right hand.

During walk-and-reach movements the monkey already oriented its body towards the respective target. To quantify this behavior, we analyzed the averaged video segments of the movement phase of one session (Figure 4.2E). In the video showing the front of the animal, we manually tracked the average position of the right hand towards the ground. The horizontal position of where the animal lays its right hand for the step forward clearly depended on the horizontal position of the far target (Figure 4.2E, F). The amount of horizontal spread matched the size one would expect for directly approaching each respective target (distance from the right (left in the image) side: $x_1 = 21\text{cm}$, $x_2 = 30\text{cm}$, $x_3 = 39\text{cm}$, $x_4 = 48\text{cm}$; uncertainty $\pm 2\text{cm}$). This means, rather than keeping the same walking movement for all far targets and only orienting the arm for the final reaching movement, as it is the case for acquiring the near targets, the monkey walked directly in the direction of the far targets. Consequently, the reach movement itself must have been quite similar for the four far targets.

Neural modulation of individual units

During the course of the task, at least four events can lead to a change in neural activation, 1) Target onset: The reach target lights up indicating the reach goal the monkey has to prepare for; 2) Go cue: The visual fixation cue turns red instructing the monkey to remove the hands from the start button; 3) Movement onset: The monkey removes one of its hands from a start button; 4) Target acquisition: the left hand of the monkey reaches the target. We were interested in how selectivity of neural activity depends on different near and far reach goals during different phases of a trial. Since we did not track full-body movement trial by trial, movement onset

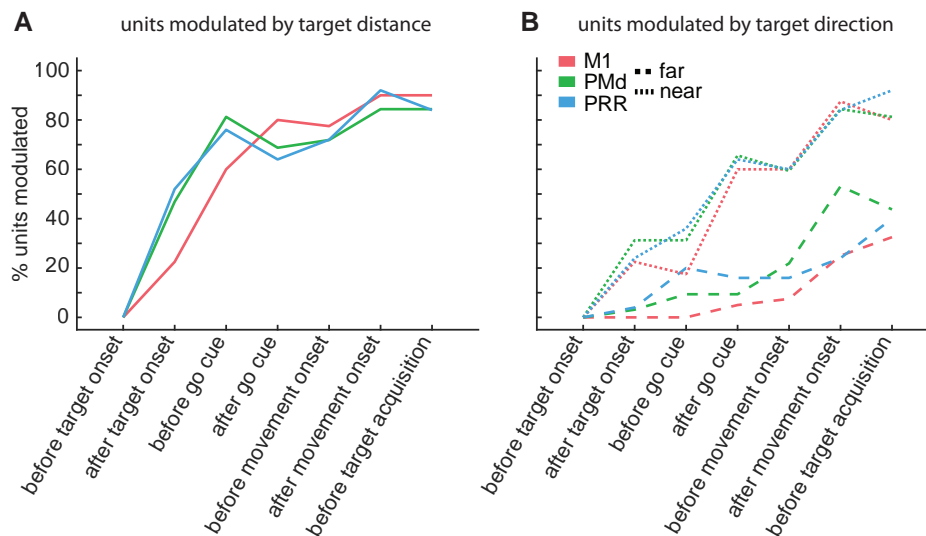


Figure 4.3: Modulation of individual units by target position. Analysis is based on the spike count distribution per target in 500ms time windows immediately before and after an event (target onset, go cue, movement start, target acquisition). Time window after target acquisition is not analyzed since it likely relates to behavior after the trial. Only units with average firing rate during the task greater than 2Hz were considered. A) Percentage of units per brain area modulated by near vs. far. B) Percentage of units per brain area modulated by target position only regarding near (small dashed) or far (long dashed) targets.

here corresponds to hand movement onset. For far targets the monkey already moved its right leg before onset of the arm movement (see above). But this should neither affect the planning activity prior to the go cue, nor the movement related activity prior to target acquisition, which was of particular interest.

We recorded multi and single units from primary motor cortex M1 ($N = 63$), premotor cortex PMd ($N = 63$) and parietal reach region PRR ($N = 41$) from one monkey using chronically implanted floating microelectrodes arrays and a wireless recording device. For the analysis of individual units, we only considered units with an average firing rate during the whole task above 2Hz (M1: 40, PMd: 35, PRR: 25). No unit is modulated by target direction or distance during baseline activity before target onset (Figure 4.3), indicating that the monkey was not biased towards a target or a certain set of targets. For all three brain areas, the activity differs between near and far targets already during the delay period (Figure 4.3A). For PMd and PRR 47% and 52% of the units respectively show such a difference after target onset and 81% and 76% before the go cue. During this period, only 23% (after target onset) and 60% (before go cue) of M1 units are distance modulated but the amount of unit's increases to around 80% as well just after the go cue. Target modulation for near targets is higher than for far targets during all time windows (except baseline) and for all areas (Figure 4.3B). PMd and PRR show a steady increase in number of units being modulated by near targets from target onset (31% PMd, 24% PRR) to target acquisition (81% PMd, 92% PRR). Units in M1 behave similarly except for the late delay period, where only 17.5% of the units are modulated by near target direction in contrast to 31% in PMd and 36% in PRR. For far targets, less than 25% of the units in all areas are

modulated before the movement. In M1, no unit is modulated before the go cue. In PRR 20% of the units are modulated during the late delay period before the go cue, in PMd 9%. During movement, the number of units modulated by far targets increases in M1 and PRR to 32.5% and 40%, respectively. PMd has the highest fraction of units modulated by far targets, with 53% just after movement onset (24% M1 and PRR) and 44% before target acquisition.

This means that most units in all three areas respond differently to reach and walk-and-reach movements during movement execution. This is also true during movement planning for PMd and PRR but less for M1. Furthermore, most units in all area are also modulated by near target position during movement execution. During reach planning PMd and PRR show a higher portion of modulated units than M1. Finally, modulation to far targets is weaker for all areas and time windows. Like for reach movements, highest number of modulated units is during movement execution. PMd shows a clearly higher modulation after the movement onset compared to PMd and M1. During planning of walk-and-reach movements, only PRR showed a notably portion of modulated units.

Population activity

So far, we considered each unit individually and not as part of a population. To gain a better understanding of the neural dynamics in the local network of an area, we consider the activity of all recorded units in this area at a given time as a point in a multidimensional neural state space in which the firing rate of each unit defines a dimension in this space (Figure 4.1E). We do not exclude any units for this analysis because passing of a significance threshold in individual neurons is not a prerequisite. Since we use non-normalized firing rates, the low firing units will contribute less to the population dynamics than high-firing neurons.

To get a first idea of the population dynamics in the walk-and-reach task, we visualized the time window of +/- 500ms around the time of the four events: target onset, go cue, movement onset and target acquisition (Figure 4.4).

With target onset, the monkey receives the information of which target will be the reach goal, and consequently, the neural activity separates between near and far targets in all areas. This is clearly visible in PRR and PMd but less apparent in M1. Around the go cue, near and far target trajectories are visibly separated for all three areas. For PMd and M1 the spread between near target trajectories looks larger than between far target trajectories also before the go cue. It suggests that PMd and M1 are more modulated for different reach movements than walk-and-reach movements during the delay phase. During movement, the pattern becomes more complex. In PMd the neural trajectories look similar between near and far targets but the curvature for far targets is less pronounced than for near targets. In M1 the variance of the population activity is mainly driven by the separation towards near targets producing very different looking neural trajectories for near and far targets. Interestingly while the shapes of the trajectories show clear differences between reach and walk-and-reach movements for all areas in

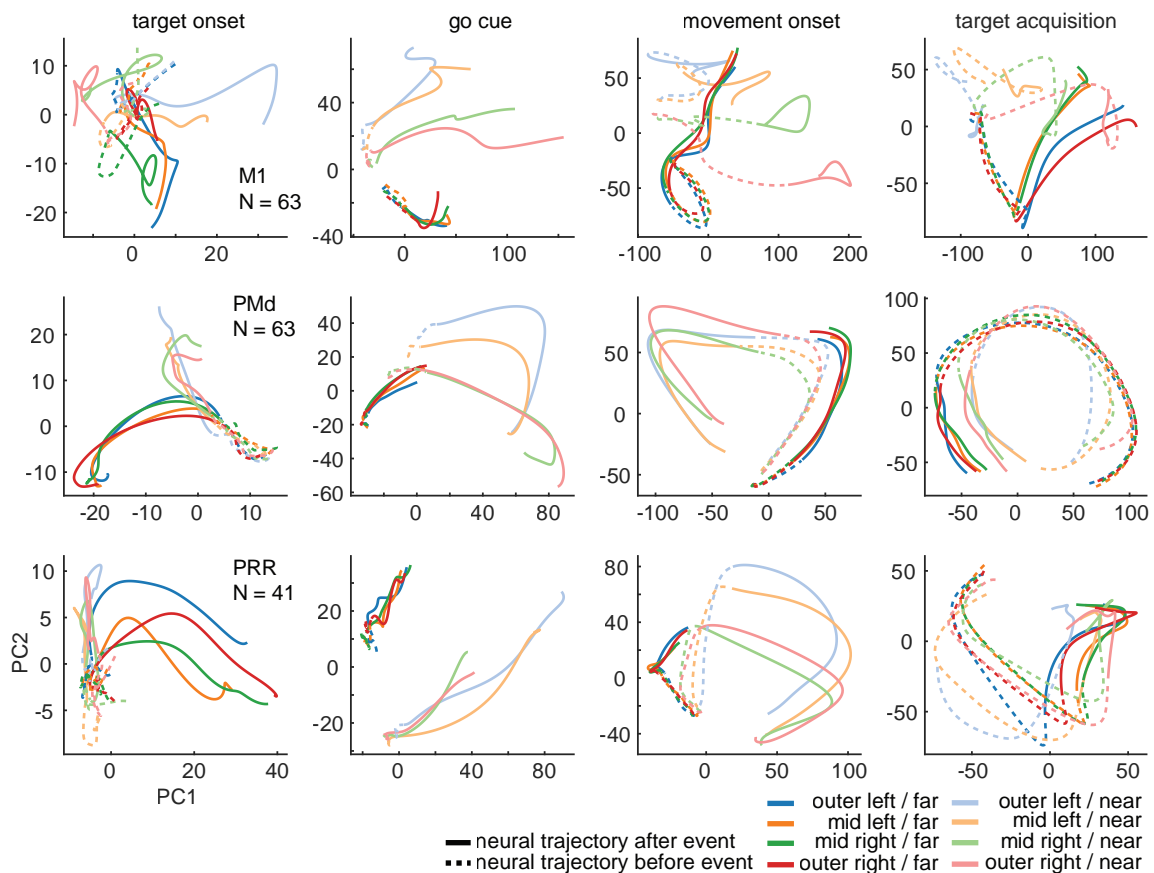


Figure 4.4: First two principle components of the neural trajectories regarding all eight targets. One plot reflects one area (rows) and a time window 500ms before (dashed) and until 500ms after (solid) a respective event (columns). The first column shows how the neural trajectories diverge between near (bright) and far (dark) targets once the monkey gets the information of which target is selected. This more pronounced in PMd and PRR than in M1. Trajectories for near and far targets keep being separated from each other with different curvatures. Exceptions are in PMd and PRR but not M1 around target acquisition (last column). Here, the arm movement towards the target is aligned for near and far targets.

almost all time windows, it is not the case for PMd and PRR just before target acquisition. For this time window, the movement of the left arm towards the target is aligned for near and far targets but body posture and whole-body movement is different. This suggests that PMd and PRR is less involved in whole-body movements or affected by body posture. We need to be careful to draw conclusions out of the first principle components as they only explain around 50% - 70% of the variance. To quantify our observations, we computed the trial- and population-average firing rate and the neural distances (ND) of trial-average neural trajectories for each area towards the eight targets for +/- 500ms around the four events (Figure 4.5).

We analyzed population averaged activity to identify during which stages of the reach and walk-and-reach movements an area is active or suppressed (Figure 4.5A). Specifically, we are interested if population activity reflects body or arm movement. Since low firing units do not contribute much to the overall activity, but would have an impact on the population average, we only used units with an average firing rate during the task higher than 2Hz in the population

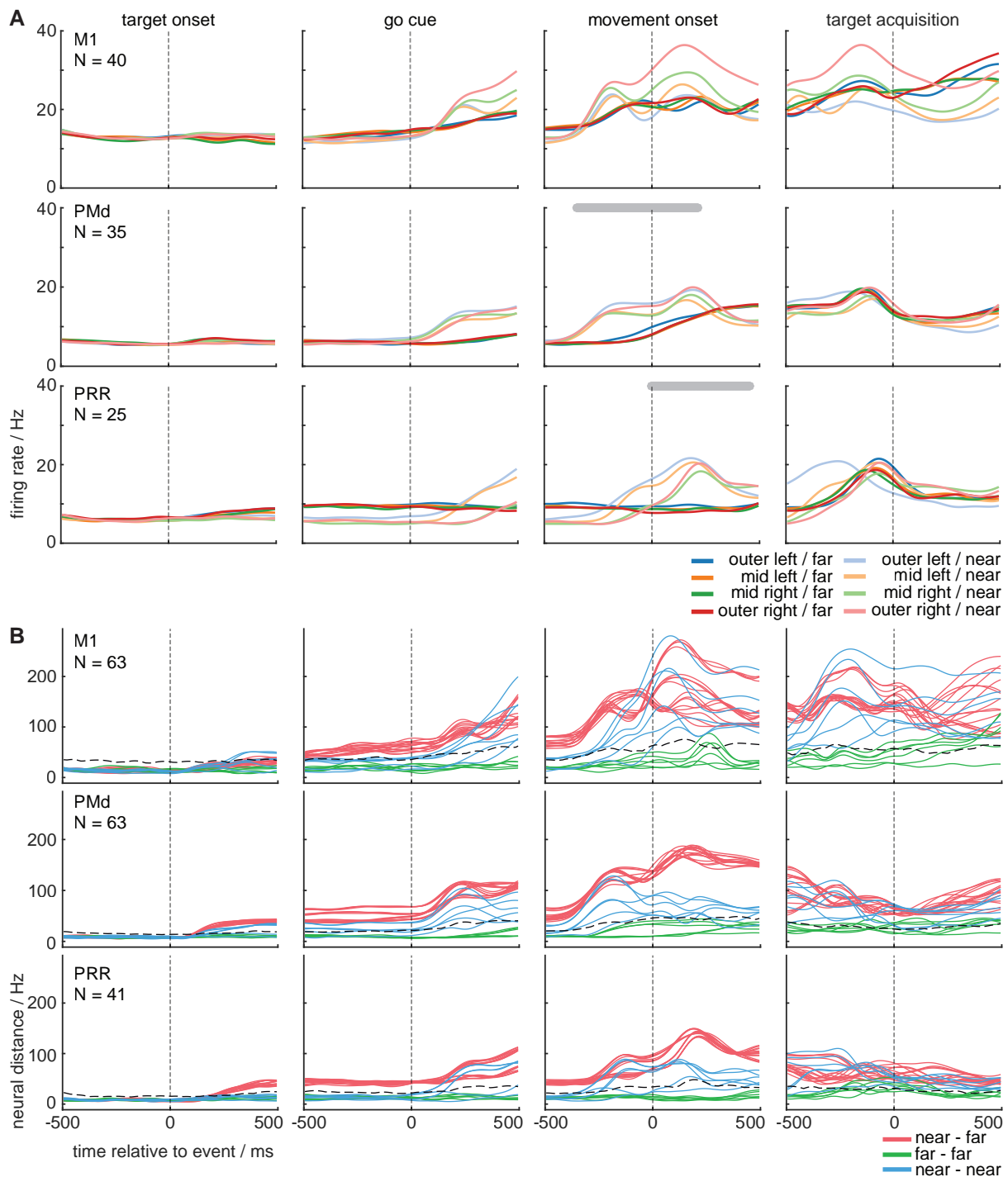


Figure 4.5: Population analysis. Each plot represents the population of one brain area within a time window from 500ms before until 500ms after an event (target onset, go cue, movement onset, target acquisition). A) Averaged spike densities of the population of units above 2Hz average task firing rate. Grey bar indicates phases where the population activity is significantly different between near and far. B) Neural distance (ND) for neural trajectories between all possible target pairs. No unit was excluded for this analysis. Color code indicates whether a pair consists of two near (blue), two far (green) or one near and one far (red) target. Dashed lines show the maximum of the distribution of neural distances gained from a thousand repetitions of permuting the trial - target relationship.

averages. We calculated a cluster-based non-parametric permutation test (Maris & Oostenveld, 2007) to test for differences over time in reach and walk-and-reach movements. The result was Bonferroni corrected for the multiple areas and time windows. We found significant differences between near and far targets in the average population response after movement onset in PRR, and around movement onset in PMd (Figure 4.5A grey bar). After movement onset, the monkey performs an arm movement towards near targets but a whole-body movement towards far targets. Since we did not find this difference before target acquisition when the arm movement toward near and far targets are aligned, this shows that PMd and PRR but not M1 are significantly more active during or shortly before arm movements compared to whole body-movements.

While we already analyzed how many individual units were modulated by target position (Figure 4.3), we did not consider how strong this modulation is nor did we compare this modulation with inter-areal neural variability. To do so, we computed the distance of the trial-average neural trajectories in neural state space for all neurons, not reduced in dimensionality. Neural distance over time is shown in Figure 4.5B and color coded for intra-distance comparisons (near – near target pairs, blue; far – far target pairs, green) and inter-distance comparisons (near – far target pairs, red). A high value for distance means that the activity pattern of the area is different for the two respective targets. This does not necessarily mean that the average activity is different. The dashed line in the figure represents the maximum ND of surrogate data representing condition invariant neural variability. We are mostly interested in the planning phase (after cue onset and before go cue) and the movement phase (after movement onset and before target acquisition). Figure 4.6A shows the average near-far NDs relative to the surrogate maximum during the movement phase. Figure 4.6B shows the proportion of NDs exceeding the surrogate data. Specifically, we wanted to know if 1) Differences between neural activity related to reach and walk-and-reach movements (near-far NDs) can be attributed to whole-body vs arm movements; 2) activity is modulated by near target position during movement planning (near-near NDs), as expected from conventional experiments; 3) such a modulation during movement planning exists towards far targets (far-far NDs).

Most prominent result, and as expected from the analysis of individual unit, is the high difference in activation between near and far targets. In the averaged population activity, such a difference becomes visible after the go cue and around movement onset, in M1 to a lesser extent (and not significantly). The NDs of far versus near targets reveal a similar picture then the analysis of individual units. The NDs between near and far targets increase already with target onset, but less strong in the beginning in M1, and becomes stronger towards the movement phase. In the time after movement start the monkey performs the reach in near conditions, but the goal-directed whole-body movement in far conditions, i.e. comparing near and far in this time window means comparing physically very different movements. In contrast, comparing the activity before target acquisition aligns the actual goal-directed arm movements towards the targets for near and far, i.e. allows comparing rather similar physical movements. In PMd and PRR differences between near and far, visible in average firing (figure 4.5A) and ND

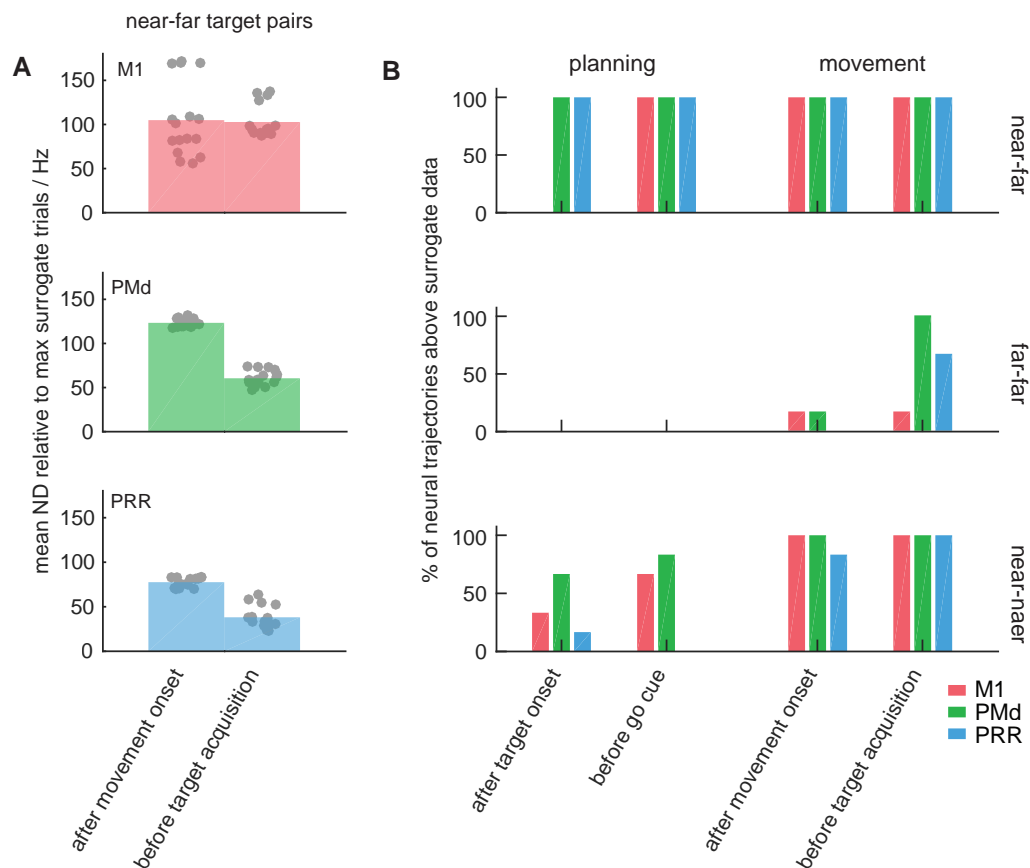


Figure 4.6: Neural distances (ND) relative to surrogate data. The ND is averaged for each 500ms time window before or after an event. A) The plots show time window averaged NDs minus the maximum time window averaged NDs from the surrogate data. Grey points indicate a single neural trajectory in the given time window. Bars show the average of the grey points. B) Ratio neural trajectories exceeding the distribution of surrogate data generated from a thousand permutations of the trial – target relationship. Values show the ratio of neural trajectories with average ND above the maximum of the averaged NDs for the surrogate data.

(figure 4.6A), are clearly smaller when activity is aligned to target acquisition in comparison to movement start.

Neural distances between near targets indicate a slight increase in target selectivity (exceeding the surrogate distribution; dashed line) with target onset in M1 and PMd but not PRR. NDs exceeding surrogate data in the planning phase, after target onset: PRR 1, PMd 4, M1 2; before go cue: PRR 0, PMd 5, M1 4 (Figure 4.6B). With the go cue the distances clearly increase for all areas. Although not visible when we analyzed individual units, the strongest target selectivity in population activities between near targets occurs in M1 during movement. The NDs between far targets revealed clearly lower target selectivity of the activity in all areas. Around movement onset, there is a slight increase in PMd and M1 (1 ND for each area exceeds surrogate data). This selectivity does not increase for M1 towards target acquisition but clearly for PMd (all NDs exceed surrogate data). Notably, PRR does not show any increase in neural population selectivity for far targets relative to baseline until just before the target acquisition (4 NDs exceed surrogate

data). These results show selectivity for near target reach planning in PMd and to a lesser extent in M1 consistent with our findings from individual units. In contrast, PRR does barely show near target selectivity during reach planning. We did not find evidence for far target movement planning. All areas are modulated by near targets during reach execution. For walk-and-reach movement execution, PMd and M1 is weakly modulated in the beginning during the whole-body movement; PMd, PRR and to a lesser extent M1 is modulated during the arm movement.

4.5 Discussion

We recorded single and multi-unit activity from all three cortical areas of the fronto-parietal reach network performing instructed delayed reach and walk-and-reach movements. Two sets of four reach targets were placed near and far from the monkey to investigate if and how the brain areas encode the position of targets immediately within or out of reach during movement planning and execution. Our analysis revealed four findings. First, movements to near targets are already encoded during movement planning in M1, PMd and to a lesser extent in PRR. This modulation increases with the go signal and is particularly strong in M1 during the movement. Such findings are in line with conventional goal-directed reaching experiments using chair-seated animals. Second, the observed modulation between different near targets exceeds the modulation between different far targets in all areas whenever a modulation was observed. Weak modulations between far targets were only present during the arm movement in all areas and even weaker during the whole-body movements. Only PRR activity showed little modulation during movement planning. This suggests that PRR, if at all, is the only area in the fronto-parietal reach network involved in encoding far-located reach goals. Third, neural activity shows strong difference between reach and walk-and-reach movements as soon as the monkey receives the target information. This suggests categorically different neural processes between near and far reach goal encoding already during movement planning. And fourth, PMd and PRR in contrast to M1 show little difference between reach and walk-and-reach movements during reach execution compared to whole-body movement, suggesting a strong involvement in motor control for arm movement independent of whole-body movement.

Modulation in neural activity related to reach targets near and far

Our cage based experimental setup (Reach Cage) is a novel approach for sensorimotor neuroscience (see chapter 3). As the first step, we validated that it is possible in the Reach Cage to study motor goal encoding within the reachable space similar to setups with chair-seated animals (Figure 4.7A). In the classical theory (“tuning hypothesis”) of how the fronto-parietal reach network computes reach kinematics, individual neurons encode reach directions with a cosine tuning (Georgopoulos et al., 1986). It means that a neuron has the strongest firing rate for a certain (preferred) direction and the weakest for the opposite direction. Out of a population of

neurons with different preferred directions, a reach vector can be constructed that resembles the hand movement direction. Using conventional chair-based setups, neurons that follow such a tuning were found in all three areas, PPC (Kalaska et al., 1983), PMd (Crammond & Kalaska, 1994) and M1 (Georgopoulos et al., 1982). During movement planning PRR activity is modulated predominantly in a gaze-centered reference frame while PMd encodes the hand-to-target vector (Andersen & Cui, 2009; Batista et al., 1999; Buneo et al., 2002; Pesaran et al., 2006). In contrast, M1 responds only weakly during movement planning (Crammond & Kalaska, 2000; Kalaska & Crammond, 1992). While hand direction tuning during the movement is stronger in M1 in contrast to PMd and PRR, all areas are modulated during the arm movement. In the present study when comparing only near target modulation (Figure 4.7A), the behavior of the animal resembles the classical studies although we did not impose physical constraints. And indeed, we found neurons to be modulated in all three brain areas during movement execution and during movement planning in PMd, PRR and to a lesser extent in M1 (Figure 4.3B). It shows that we can use the Reach Cage for testing reach-goal encoding like a conventional setup for which monkeys are seated in a primate chair. When we measured neural distances (ND), we obtained a similar picture (Figure 4.6B). The only exception is PRR during the planning phase. While 24% of PRR neurons were modulated during early and 31% during late movement planning, the modulation was not strong enough to show significant NDs of the population activity. Given that PRR is strongly modulated by various sensory inputs (Cohen & Andersen, 2002), it could be that the salience of the target signals are not strong enough to be captured by our ND measure.

Since the Reach Cage is a valid setup to test reach-goal encoding, we can test if the fronto parietal-network also encodes far-located reach-goals, for which a walk-and-reach movement is necessary (Figure 4.7B). Considering our results for the near targets, does the classical tuning hypothesis hold true for far targets during the delay phase? For a tuning relative to external coordinates (cage), we would not expect a difference to the near target tuning. However, we see less modulation of the activity in all three areas. Considering a gaze- or body-centered tuning we would expect less modulation since the far targets span a smaller angle relative to body or gaze. The angle from the starting position between the outer most right and left near targets is roughly around 110 degrees, but the cage only allowed for an angle of around 30 degree between the outermost far targets. Given a perfect cosine tuning of an individual unit, an angle of 30 degree would modulate the activity only about 10%. We did not find any modulation in M1 which is in accordance with the tuning hypothesis and that M1 shows only little planning activity in general. Also, PRR results are in agreement with gaze centered tuning and compared to the near target results. We did not find NDs exceeding the surrogate data which was expected given that this was also the case for near targets. Before the go cue we found 20% of the units in PRR modulated to far targets compared to 36% to near targets. However, results in PMd during the delay phase differ strongly between near and far targets. In contrast to the strong modulation to near targets, we found for near targets no significant NDs and only 9% of the units were modulated. For a better understanding, we need to take the monkey's movement behavior

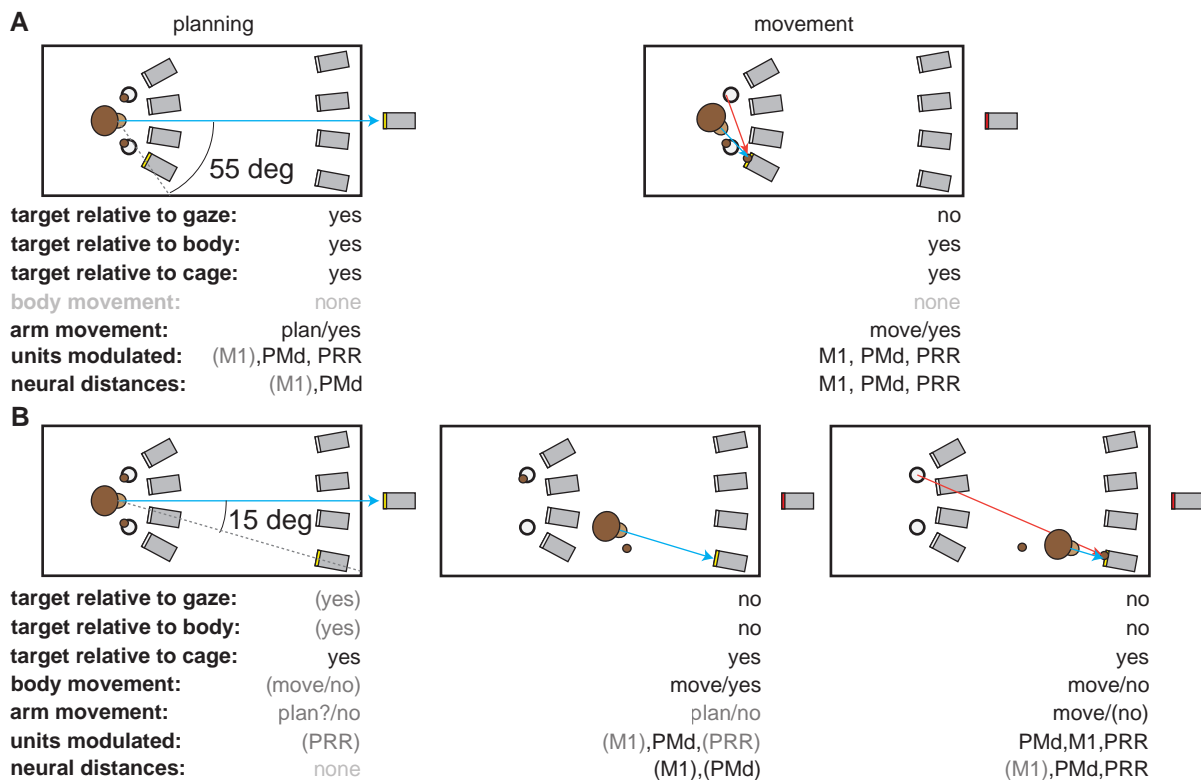


Figure 4.7: Summary of results. The graphics illustrate the monkey's behavior during the task when moving to the outermost right near (top) or far (bottom) target. The blue arrow indicates to gaze direction and the red arrow indicates a movement of the left hand. Below each graphic is shown whether or not target position, whole-body movement, arm movement or recorded neural activity changes dependent on the target selection within the near (top) or far (bottom) set of targets. Brackets indicate weak (expected) modulation. Modulation of target position is explained relative to gaze orientation, body position or in allocentric (cage) coordinates. For the arm and body movement it is indicated if a movement is executed (move), planned (plan). Significant neural modulation found in an area is shown when individual units where modulated (units, see Figure 4.3B) or neural distances fall not within the range of trial-surrogate data (ND, Figure 4.6A).

towards the far targets into account. The movement towards the far targets can be divided in two parts. First, the monkey performs a whole-body movement orienting its body towards the target. Second, the monkey reaches with the left hand towards the target while still moving the body. This means that the orienting movement is mainly performed by the body in the beginning of the movement phase. The arm movement takes place in the second part of the movement phase but should be less modulated between far targets due to the already oriented body. While PMd, in contrast to PRR, is not modulated during movement planning towards far targets, PMd is stronger modulated than PRR during the whole-body movement preceding the arm movement. A reason could be that PMd is involved in the initiation of the movement and therefore, is stronger modulated modulate immediately before the arm movement onset (Kaufman et al., 2016; Mirabella et al., 2011). Not only PMd (Crammond & Kalaska, 1994; di Pellegrino & Wise, 1993) but also PRR predominantly encodes the reach goal and only to a lesser extent the

visual goal (Gail & Andersen, 2006; Gail et al., 2009; Kuang et al., 2016; Westendorff et al., 2010). PRR encodes the second reach goal when performing double reaches (Baldauf et al., 2008). PMd is also known to be involved in encoding movement sequences (Ohbayashi et al., 2016). However, only the encoding of the immediate reach goal was tested. PMd in contrast to PRR might only encode immediate arm movements. As a result, planning related activity in PMd might not be visible before the go cue but during the whole-body movement prior to the arm movement.

Neural activity is related to arm movements

As already mentioned in the previous paragraph, the paradigm presented here allows investigating how goal-directed whole-body movements impacts motor control of goal-directed arm movements. The areas in the fronto-parietal reach network are related to arm movements (Johnson et al., 1996; Kalaska & Crammond, 1992; Kurata, 1991; Wise et al., 1997). However, neurophysiological functional properties related to arm movements were only studied in isolation or in comparison with eye movements (Batista et al., 1999; Cui & Andersen, 2007; Pesaran et al., 2006) or grasping movements (Hao et al., 2014; Rouse & Schieber, 2016; Schaffelhofer et al., 2015). For walk-and-reach movements, the monkey walks towards the far targets and only in the end of the movement phase performs the goal-directed reach towards the target. Directly after movement onset, the monkey performs a reach for the near target but a whole-body movement for the far targets. But aligned to the end-point of the movement, the monkey performs the goal-directed arm movements at the same time with different whole-body movements. In PMd and PRR the activity is remarkably similar between reach and walk-and-reach movements during the phase of the goal-directed arm movement. The population averaged activity reveals peak activity during arm movement for all conditions (Figure 4.5A); neural distances between near and far targets decrease (Figure 4.5B/4.6). This was not the case for M1 indicating that arm area M1 but not PMd and PRR is modulated by goal-directed whole-body movements.

Qualitatively, we could also see in the neural trajectories that PRR and PMd activity is not very different between reach and walk-and-reach movements (Figure 4.4). More recent studies proposed a view that describes the computational processes in the brain related to motor control as a non-linear dynamical system (Churchland et al., 2010; Shenoy et al., 2013). Such a dynamical system would contain a set of attractors each of which describing a stable neuronal activation pattern. Most of the time the brain's activity, described as a point in a high-dimensional space, lies in an attractor. But when the brain responds to changes, for instance during movement or cue integration, the activity will change from one attractor to the next describing a trajectory in the high-dimensional space based on the specific underlying dynamical system. When conditions in the movement task change, the system will either adapt by varying the position of the initial attractor but using the same computational processes for the movement (similar trajectory) or perform a different computation (different trajectory) (Churchland et al., 2010; Sheahan et al.,

2016). Although the immense amount of neurons in the brain span a high-dimensional space, the interesting processes can be usually reduced to a low-dimensional manifold (Gallego et al., 2017). We used the simplest dimensionality reduction technique, principle component analysis, to visualize the two dimensions that capture the most variance of the neural data (Figure 4.4). Except for PRR and PMd during the arm movement, the trajectories look clearly different when comparing between near and far targets. This suggests that PMd and PRR use the same dynamical system for arm motor control during the movement. Changes in posture or whole-body movements alter the initial conditions but not the system itself. To validate this interpretation it would be beneficial to investigate more dimensions since the more complex a behavior is the more likely information is hidden in higher dimensions (Gao & Ganguli, 2015). Also a more advance dimensionality reduction technique would be useful that take the temporal task structure into account such as demixed principle component analysis (Kobak et al., 2016).

For far targets, the monkey already performed a step to place his right foot between the two start buttons. Consequently, we can not fully rule out that differences in activity during the planning phase are related to a change in posture based on this movement and not to motor planning. Such differences are first visible in PRR and PMd but only later and more slowly visible in M1 (Figure 4.5B). All areas in the fronto-parietal reach network receive postural information (Rushworth et al., 1998; Scott & Kalaska, 1997; Scott et al., 1997). However, M1 showed a stronger response to postural modulation than PMd and parietal area 5. In addition, M1 activity differs between near and far targets more strongly during the arm movement than PMd and PRR. It supports the view that especially M1 responds to a change in body posture. Since during the delay phase, differences in neural activity between near and far targets are less in M1 than in PMd and PRR it suggests that the differences in PMd and PRR can not be attributed to a change in body posture.

Conclusion

By using the Reach Cage, a new experimental environment for neurophysiological experiments in physically unconstrained monkeys, we could investigate how goal-directed movements towards targets outside of the reachable space are encoded in the brain. We could revalidate reach-goal encoding in the fronto-parietal reach network obtained from experiments with restraint animals. Furthermore, our results show no, or only little, involvement in goal-directed whole-body movements in agreement with the common view that the fronto-parietal reach network is specific for arm movements. Especially PMd and PRR are only weakly affected by body posture. Finally, not PMd but potentially PRR is involved in encoding far-located motor goals for walk-and-reach movements. PMd might only encode immediate arm movements.

4.6 Acknowledgements

We thank Sina Plümer for help with data collection and technical support, Pierre Morel and Enrico Ferrea for helpful discussions, Klaus Heisig, Leonore Burchardt, Janine Kuntze, Luisa Klotz and Dirk Prüße for technical support.

References

- Andersen, R. A. and Cui, H. (2009). Intention, action planning, and decision making in parietal-frontal circuits. *Neuron*, 63(5):568–583.
- Baldauf, D., Cui, H., and Andersen, R. A. (2008). The posterior parietal cortex encodes in parallel both goals for double-reach sequences. *Journal of Neuroscience*, 28(40):10081–10089.
- Batista, a. P., Buneo, C. a., Snyder, L. H., and Andersen, R. a. (1999). Reach plans in eye-centered coordinates. *Science (New York, N.Y.)*, 285(5425):257–260.
- Berti, A. and Frassinetti, F. (2000). When far becomes near: remapping of space by tool use. *Journal of cognitive neuroscience*, 12(3):415–420.
- Bjoertomt, O., Cowey, A., and Walsh, V. (2002). Spatial neglect in near and far space investigated by repetitive transcranial magnetic stimulation. *Brain: a journal of neurology*, 125(9):2012–22.
- Bonini, L., Maranesi, M., Livi, A., Fogassi, L., and Rizzolatti, G. (2014). Space-dependent representation of objects and other’s action in monkey ventral premotor grasping neurons. *Journal of Neuroscience*, 34(11):4108–4119.
- Botvinick, M. and Cohen, J. (1998). Rubber hands “feel” touch that eyes see. *Nature*, 391(6669):756.
- Brozzoli, C., Cardinali, L., Pavani, F., and Farnè, A. (2010). Action-specific remapping of peripersonal space. *Neuropsychologia*, 48(3):796–802.
- Brozzoli, C., Pavani, F., Urquizar, C., Cardinali, L., and Farnè, A. (2009). Grasping actions remap peripersonal space. *Neuroreport*, 20(10):913–917.
- Buneo, C. A., Jarvis, M. R., Batista, A. P., and Andersen, R. A. (2002). Direct visuomotor transformations for reaching. *Nature*, 416(6881):632–6.
- Caggiano, V., Fogassi, L., Rizzolatti, G., Thier, P., and Casile, A. (2009). Mirror neurons differentially encode the peripersonal and extrapersonal space of monkeys. *Science*, 324(5925):403–406.

- Christopoulos, V., Bonaiuto, J., Kagan, I., and Andersen, R. A. (2015). Inactivation of parietal reach region affects reaching but not saccade choices in internally guided decisions. *Journal of Neuroscience*, 35(33):11719–11728.
- Churchland, M. M., Cunningham, J. P., Kaufman, M. T., Ryu, S. I., and Shenoy, K. V. (2010). Cortical preparatory activity: Representation of movement or first cog in a dynamical machine? *Neuron*, 68(3):387–400.
- Cisek, P. and Kalaska, J. F. (2005). Neural correlates of reaching decisions in dorsal premotor cortex: Specification of multiple direction choices and final selection of action. *Neuron*, 45(5):801–814.
- Coallier, m., Michelet, T., and Kalaska, J. F. (2015). Dorsal premotor cortex: neural correlates of reach target decisions based on a color-location matching rule and conflicting sensory evidence. *Journal of neurophysiology*, page jn.00166.2014.
- Cohen, Y. E. and Andersen, R. a. (2002). A common reference frame for movement plans in the posterior parietal cortex. *Nature reviews. Neuroscience*, 3(7):553–62.
- Colby, C. L. and Goldberg, M. E. (1999). Space and attention in parietal cortex. *Annual Review of Neuroscience*, 22(1):319–349.
- Crammond, D. J. and Kalaska, J. F. (1994). Modulation of preparatory neuronal activity in dorsal premotor cortex due to stimulus-response compatibility. *Journal of Neurophysiology*, 71(3):1281–1284.
- Crammond, D. J. and Kalaska, J. F. (2000). Prior information in motor and premotor cortex: activity during the delay period and effect on pre-movement activity. *Journal of neurophysiology*, 84(2):986–1005.
- Cui, H. and Andersen, R. A. (2007). Posterior parietal cortex encodes autonomously selected motor plans. *Neuron*, 56(3):552–559.
- Dann, B., Michaels, J. A., Schaffelhofer, S., and Scherberger, H. (2016). Uniting functional network topology and oscillations in the fronto-parietal single unit network of behaving primates. *eLife*, 5(AUGUST).
- di Pellegrino, G. and Wise, S. P. (1993). Visuospatial versus visuomotor activity in the premotor and prefrontal cortex of a primate. *The Journal of neuroscience: the official journal of the Society for Neuroscience*, 13(3):1227–43.
- Farnè, A., Serino, A., van der Stoep, N., Spence, C., and Di Luca, M. (2016). Depth: the forgotten dimension. *Multisensory Research*, 29(6–7):1–32.

- Gail, A. and Andersen, R. A. (2006). Neural dynamics in monkey parietal reach region reflect context-specific sensorimotor transformations. *Journal of Neuroscience*, 26(37):9376–9384.
- Gail, A., Klaes, C., and Westendorff, S. (2009). Implementation of spatial transformation rules for goal-directed reaching via gain modulation in monkey parietal and premotor cortex. *Journal of Neuroscience*, 29(30):9490–9499.
- Gallego, J. I., Perich, M. G., Miller, L. E., and Solla, S. A. (2017). Neural manifolds for the control of movement. *Neuron*, invited,(under review):978–984.
- Gao, P. and Ganguli, S. (2015). On simplicity and complexity in the brave new world of large-scale neuroscience. *Current Opinion in Neurobiology*, 32:148–155.
- Georgopoulos, a. P., Kalaska, J. F., Caminiti, R., and Massey, J. T. (1982). On the relations between the direction of two-dimensional arm movements and cell discharge in primate motor cortex. *J.Neurosci.*, 2(11)(11):1527–1537.
- Georgopoulos, A. P., Schwartz, A. B., and Kettner, R. E. (1986). Neuronal population coding of movement direction. *Science*, 233(4771):1416–1419.
- Giglia, G., Pia, L., Folegatti, A., Puma, A., Fierro, B., Cosentino, G., Berti, A., and Brighina, F. (2015). Far space remapping by tool use: A rtms study over the right posterior parietal cortex. *Brain Stimulation*, 8(4):795–800.
- Gilja, V., Chestek, C. A., Nuyujukian, P., Foster, J., and Shenoy, K. V. (2010). Autonomous head-mounted electrophysiology systems for freely behaving primates. *Current Opinion in Neurobiology*, 20(5):676–686.
- Graziano, M. S., Cooke, D. F., and Taylor, C. S. R. (2000). Coding the location of the arm by sight. *Science*, 290(5497):1782–1786.
- Graziano, M. S., Hu, X. T., and Gross, C. G. (1997). Visuospatial properties of ventral premotor cortex. *Journal of neurophysiology*, 77(5):2268–2292.
- Halligan, P. W. and Marshall, J. C. (1991). Left neglect for near but not far space in man. *Nature*, 350(6318):498–500.
- Hao, Y., Zhang, Q., Controzzi, M., Cipriani, C., Li, Y., Li, J., Zhang, S., Wang, Y., Chen, W., Chiara Carrozza, M., and Zheng, X. (2014). Distinct neural patterns enable grasp types decoding in monkey dorsal premotor cortex. *Journal of Neural Engineering*, 11(6):66011.
- Iriki, A., Tanaka, M., and Iwamura, Y. (1996). Coding of modified body schema during tool use by macaque postcentral neurones. *NeuroReport*, 7(14):2325–2330.

- Johnson, P. B., Ferraina, S., Bianchi, L., and Caminiti, R. (1996). Cortical networks for visual reaching: Physiological and anatomical organization of frontal and parietal lobe arm regions. *Cerebral Cortex*, 6(2):102–119.
- Kalaska, J. F., Caminiti, R., and Georgopoulos, A. P. (1983). Cortical mechanisms related to the direction of two-dimensional arm movements: relations in parietal area 5 and comparison with motor cortex. *Experimental Brain Research*, 51(2):247–260.
- Kalaska, J. F. and Crammond, D. J. (1992). Cerebral cortical mechanisms of reaching movements. *Science*, 255(5051):1517–1523.
- Kaufman, M. T., Seely, J. S., Sussillo, D., Ryu, S. I., Shenoy, K. V., and Churchland, M. M. (2016). The largest response component in motor cortex reflects movement timing but not movement type. *eNeuro*, 3(4):ENEURO.0085–16.2016.
- Klaes, C., Westendorff, S., Chakrabarti, S., and Gail, A. (2011). Choosing goals, not rules: Deciding among rule-based action plans. *Neuron*, 70(3):536–548.
- Kobak, D., Brendel, W., Constantinidis, C., Feierstein, C. E., Kepecs, A., Mainen, Z. F., Qi, X. L., Romo, R., Uchida, N., and Machens, C. K. (2016). Demixed principal component analysis of neural population data. *eLife*, 5(APRIL2016):9424–9430.
- Kuang, S., Morel, P., and Gail, A. (2016). Planning movements in visual and physical space in monkey posterior parietal cortex. *Cerebral Cortex*, 26(2):731–747.
- Kurata, K. (1991). Corticocortical inputs to the dorsal and ventral aspects of the premotor cortex of macaque monkeys. *Neuroscience Research*, 12(1):263–280.
- Maris, E. and Oostenveld, R. (2007). Nonparametric statistical testing of eeg- and meg-data. *Journal of Neuroscience Methods*, 164(1):177–190.
- Maynard, E. M., Nordhausen, C. T., and Normann, R. A. (1997). The utah intracortical electrode array: A recording structure for potential brain-computer interfaces. *Electroencephalography and Clinical Neurophysiology*, 102(3):228–239.
- Mirabella, G., Pani, P., and Ferraina, S. (2011). Neural correlates of cognitive control of reaching movements in the dorsal premotor cortex of rhesus monkeys. *Journal of neurophysiology*, 106(3):1454–1466.
- Mountcastle, V. B., Lynch, J. C., Georgopoulos, A., Sakata, H., and Acuna, C. (1975). Posterior parietal association cortex of the monkey: command functions for operations within extrapersonal space. *J Neurophysiol*, 38(April 2016):871–908.

- Musallam, S., Bak, M. J., Troyk, P. R., and Andersen, R. A. (2007). A floating metal microelectrode array for chronic implantation. *Journal of Neuroscience Methods*, 160(1):122–127.
- Musallam, S., Corneil, B. D., Greger, B., Scherberger, H., and Andersen, R. A. (2004). Cognitive control signals for neural prosthetics. *Science*, 305(July):258–262.
- Musial, P. G., Baker, S. N., Gerstein, G. L., King, E. A., and Keating, J. G. (2002). Signal-to-noise ratio improvement in multiple electrode recording. *Journal of Neuroscience Methods*, 115(1):29–43.
- Ohbayashi, X. M., Picard, N., and Strick, P. L. (2016). Inactivation of the dorsal premotor area disrupts internally generated , but not visually guided , sequential movements. *The Journal of Neuroscience*, 36(6):1971–1976.
- Pastor-Bernier, A. and Cisek, P. (2011). Neural correlates of biased competition in premotor cortex. *J Neurosci*, 31(19):7083–7088.
- Pesaran, B., Nelson, M. J., and Andersen, R. A. (2006). Dorsal premotor neurons encode the relative position of the hand, eye, and goal during reach planning. *Neuron*, 51(1):125–134.
- Rajalingham, R., Stacey, R. G., Tsoulfas, G., and Musallam, S. (2014). Modulation of neural activity by reward in medial intraparietal cortex is sensitive to temporal sequence of reward. *Journal of Neurophysiology*, 112(7):1775–1789.
- Rizzolatti, G., Fadiga, L., Fogassi, L., and Gallese, V. (1997). The space around us. *Science*, 277(5323):190–191.
- Rizzolatti, G., Fogassi, L., and Gallese, V. (2002). Motor and cognitive functions of the ventral premotor cortex. *Current Opinion in Neurobiology*, 12(2):149–154.
- Rizzolatti, G., Scandolara, C., Matelli, M., and Gentilucci, M. (1981). Afferent properties of periarculate neurons in macaque monkeys. ii. visual responses. *Behavioural Brain Research*, 2(2):147–163.
- Rouse, A. G. and Schieber, M. H. (2016). Spatiotemporal distribution of location and object effects in primary motor cortex neurons during reach-to-grasp. *Journal of Neuroscience*, 36(41):10640–10653.
- Rushworth, M. F., Johansen-Berg, H., and Young, S. A. (1998). Parietal cortex and spatial-postural transformation during arm movements. *Journal of neurophysiology*, 79(1):478–82.
- Schaffelhofer, S., Agudelo-Toro, A., and Scherberger, H. (2015). Decoding a wide range of hand configurations from macaque motor, premotor, and parietal cortices. *The Journal of neuroscience: the official journal of the Society for Neuroscience*, 35(3):1068–81.

- Schwarz, D. a., Lebedev, M. a., Hanson, T. L., Dimitrov, D. F., Lehew, G., Meloy, J., Rajangam, S., Subramanian, V., Ifft, P. J., Li, Z., Ramakrishnan, A., Tate, A., Zhuang, K. Z., and Nicolelis, M. a. L. (2014). Chronic, wireless recordings of large-scale brain activity in freely moving rhesus monkeys. *Nature methods*, 11(6):670–6.
- Scott, S. and Kalaska, J. (1997). Reaching movements with similar hand paths but different arm orientations. i. activity of individual cells in motor cortex. *Journal of Neurophysiology*, 77(6):826–852.
- Scott, S. H., Sergio, L. E., and Kalaska, J. F. (1997). Reaching movements with similar hand paths but different arm orientations. ii. activity of individual cells indorsal premotor cortex and parietal area 5. *Journal of Neurophysiology*, 78(5):2413–2426.
- Sheahan, H. R., Franklin, D. W., and Wolpert, D. M. (2016). Report motor planning , not execution , separates motor memories. *Neuron*, 92:773–779.
- Shenoy, K. V., Sahani, M., and Churchland, M. M. (2013). Cortical control of arm movements: a dynamical systems perspective. *Annual Review of Neuroscience*, 36(1 SRC-GoogleScholar FG-0):337–359.
- Shokur, S., O’Doherty, J. E., Winans, J. A., Bleuler, H., Lebedev, M. A., and Nicolelis, M. A. L. (2013). Expanding the primate body schema in sensorimotor cortex by virtual touches of an avatar. *Proceedings of the National Academy of Sciences*, 110(37):15121–15126.
- Snyder, L. H., Batista, A. P., and Andersen, R. A. (1997). Coding of intention in the posterior parietal cortex. *Nature*, 386(6621):167–170.
- Stoet, G. and Snyder, L. H. (2004). Single neurons in posterior parietal cortex of monkeys encode cognitive set. *Neuron*, 42(6):1003–1012.
- Thura, D. and Cisek, P. (2014). Deliberation and commitment in the premotor and primary motor cortex during dynamic decision making. *Neuron*, 81(6):1401–1416.
- Vuilleumier, P., Valenza, N., Mayer, E., Reverdin, A., and Landis, T. (1998). Near and far visual space in unilateral neglect. *Annals of Neurology*, 43(3):406–410.
- Westendorff, S., Klaes, C., and Gail, A. (2010). The cortical timeline for deciding on reach motor goals. *Journal of Neuroscience*, 30(15):5426–5436.
- Wise, S. P., Boussaoud, D., Johnson, P. B., and Caminiti, R. (1997). Premotor and parietal cortex: Corticocortical connectivity and combinatorial computations 1. *Annu. Rev. Neurosci*, 20:25–42.

Yin, M., Borton, D. A., Komar, J., Agha, N., Lu, Y., Li, H., Laurens, J., Lang, Y., Li, Q., Bull, C., Larson, L., Rosler, D., Bezard, E., Courtine, G., and Nurmikko, A. V. (2014). Wireless neurosensor for full-spectrum electrophysiology recordings during free behavior. *Neuron*, 84(6):1170–1182.

4.7 Supplementary material

S1 Trial averaged behavior

We judged the movement behavior of the monkey during the task based on trial averaged video images. We placed four cameras around the Reach Cage (Figure 4.8) synchronized to the behavioral task and neural recording. We recorded all six sessions and extracted three time windows for each trial: (1) Target onset – 500ms before and 1500ms after the onset of the target cue. (2) Go cue – 500ms before until 1000ms after the onset of the go cue. (3) Move – 500ms before until 1000/1500ms (near/far) after the release of one of the start buttons. For each session, time window and camera, we average over all trials and then averaged over all sessions again. We did this per target and for all near and all far targets. The resulting 120 videos ([8 targets + near + far] x 3 time windows x 4 cameras) are part of the online version of this manuscript. To easily select the video of interest, we included an html file (SUPPLEMENTARY_VIDEOS.HTML) providing a graphical user interface.

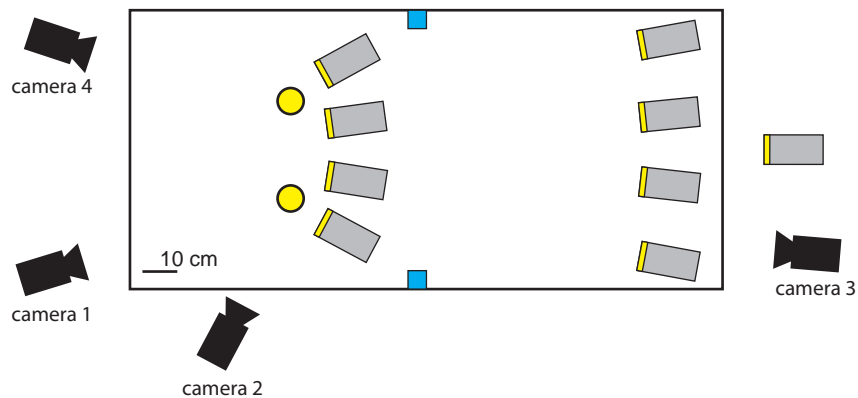


Figure 4.8: Positioning of the four video cameras for behavioral analysis within the schematic top-view of the Reach Cage showing cue, reach targets' and start buttons' placement as in figure 4.1B.

Chapter 5

A cage-based training, cognitive testing and enrichment system optimized for rhesus macaques in neuroscience research

This Manuscript was published (at first online on the 19. February 2016) in *Behavior research methods* 49: 35-45, 2017.

A cage-based training, cognitive testing and enrichment system optimized for rhesus macaques in neuroscience research

A. Calapai¹ · M. Berger¹ · M. Niessing¹ · K. Heisig¹ ·
R. Brockhausen¹ · S. Treue^{1,2,3} · A. Gail^{1,2,3}

Published online: 19 February 2016

© The Author(s) 2016. This article is published with open access at Springerlink.com

Abstract In neurophysiological studies with awake non-human primates (NHP), it is typically necessary to train the animals over a prolonged period of time on a behavioral paradigm before the actual data collection takes place. Rhesus monkeys (*Macaca mulatta*) are the most widely used primate animal models in system neuroscience. Inspired by existing joystick- or touch-screen-based systems designed for a variety of monkey species, we built and successfully employed a stand-alone cage-based training and testing system for rhesus monkeys (eXperimental Behavioral Instrument, XBI). The XBI is mobile and easy to handle by both experts and non-experts; animals can work with only minimal physical restraints, yet the ergonomic design successfully encourages stereotypical postures with a consistent positioning of the head relative to the screen. The XBI allows computer-controlled training of the monkeys with a large variety of behavioral tasks and reward protocols typically used in systems and cognitive neuroscience research.

Keywords Cognitive neuroscience · Non-human primates · Automated testing · Animal housing · Animal welfare · Environmental enrichment · Behavioral management

Electronic supplementary material The online version of this article (doi:10.3758/s13428-016-0707-3) contains supplementary material, which is available to authorized users.

✉ M. Niessing
mniessing@dpz.eu

¹ Cognitive Neuroscience Laboratory, German Primate Center, Kellnerweg 4, 37077 Goettingen, Germany

² Bernstein Center for Computational Neuroscience, Goettingen, Germany

³ Faculty of Biology and Psychology, Goettingen University, Goettingen, Germany

Introduction

In conventional neurophysiological experimental settings, macaque monkeys normally are required to temporarily leave the housing facility to be trained in dedicated experimental settings outside their cage environment. Animals are therefore moved, by means of a *primate chair*, into a dedicated room or area (here referred to as a *setup*) equipped with the apparatuses needed to run the experiment. In the setup the animals are trained to solve behavioral and cognitive tasks, usually by operating levers, sensors, or touch-screens, while their behavior, for example eye and hand movements, is monitored and, once the training has been completed, their brain activity can be recorded. This classic procedure has been widely used for decades to bring animals to the expertise level required for a given experiment in cognitive neuroscience. However, such a procedure limits the scope of research questions in terms of social and motor behavior, limits self-paced engagement of the animal in the behavioral task, and may give rise to animal welfare concerns due to movement constraints during the sessions in the setup. Overcoming these limitations by providing a cage-based training and testing system opens opportunities to investigate a broader range of activities, such as social behavior, by keeping the animal in its housing environment, together with its social group members (for a review see: Drea, 2006; Fagot & Paleressompoulle, 2009), or motor tasks, by removing body movement constraints (McCluskey & Cullen, 2007). From a training perspective, the potentially more self-paced interaction of the animal with the device, rather than an experimentally imposed training schedule, might create a motivational advantage, with a corresponding learning benefit (Andrews & Rosenblum, 1994; Evans et al., 2008; Gazes et al., 2012; Washburn et al., 1989). From an animal welfare perspective, physical constraints and periods of separation from the peer group in the setup should be

refined, reduced, and replaced where possible (3R principle; Russell & Burch, 1959). Even though positive reinforcement training (Fernström et al., 2009; Perlman et al., 2012; Schapiro et al., 2003) is routinely used in neuroscience research to acustom animals to physical movement restraints step-by-step over extended periods, one cannot fully rule out a detrimental effect of movement restraints and setup isolation on well-being. Even for experiments that require physical constraints for scientific reasons, there can be early phases of behavioral training where movement restraints are not yet necessary. Such testing and training therefore could be conducted in the animal's housing environment, perhaps even while maintaining the monkey's social situation.

With the XBI (eXperimental Behavioral Intrument) we developed a cage-based, yet mobile and remotely controllable behavioral testing system for rhesus macaques in research-typical housing environments (for similar devices see Andrews & Rosenblum, 1994; Fagot & Bonté, 2010; Fagot & Paleressompouille, 2009; Gazes et al., 2012; Mandell & Sackett, 2008; Rumbaugh, Hopkins, Washburn, & Savage-Rumbaugh, 1989; Richardson et al., 1990; Truppa et al., 2010; Washburn et al., 1989; Washburn & Rumbaugh, 1992; Weed et al., 1999). To minimize management requirements, the system is very robust and spray-water resistant. For maximal comparability, the XBI mimics conventional neuroscience settings in that it uses a precise fluid reward system. Also, the view of the visual display and physical access to the touch-screen is only minimally constrained, as is desirable for most cognitive neuroscience studies, while maintaining a uniform screen-eye distance. Finally, to allow behavioral assessment beyond the immediate task performance as registered by the touch screen, e.g., analyzing facial expressions of the animal, the XBI includes video surveillance with a full-body frontal view of the animals during task performance.

Here, we provide a technical description of the XBI and preliminary behavioral tests as proof-of-concept, including data on the initial experiences of naïve animals with the XBI. We also provide an account of our experience with the device in the daily routines of an animal housing facility.

Methods

The XBI is designed as a device for training and behavioral testing of rhesus macaques in their housing environment, and can also be used for environmental enrichment. It has been developed with five design requirements in mind. First, the device needs to be cage-mountable to allow easy access for the animals without human interference (Gazes et al., 2012; Richardson et al., 1990; Truppa et al., 2010; Weed et al., 1999) or having to restrain the animals during transportation to the setup. Second, the electronics and other internal parts need to be protected against dirt and spray water typically present in

such environments. Third, the XBI must be robust to resist potential forces applied by the animals. Fourth, operating the device should be easy enough to be handled by different people, including non-scientific personnel. Finally, the XBI's hard- and software should be flexible enough to allow for a wide variety of training procedures and experimental task designs. This includes complex visually instructed cognitive tasks with well-defined stimulus viewing conditions and a high degree of flexibility in how the animal interacts with the device.

To address these needs the XBI's hardware is divided into two parts: the animal Interface (AI) and the control interface (CI) (Fig. 1). In the following, we will describe the main design features and technical specifications. More detailed information on custom-built parts or purchased equipment are available upon request from the corresponding author.

Animal interface (AI)

The AI, used inside the animal facility, is the part of the XBI to which the animal has access (Fig. 2). It consists of mechanical and electronic components. For handling and safety reasons, the mechanical parts are lightweight and, where possible, built from aluminum. The dimensions of the whole device are 106 cm × 93 cm × 30 cm (W × H × D) and it weighs approximately 23 kg. By reducing the size of the outer frame and using lighter panels, we expect to substantially reduce the weight of future versions. The AI can be stored or transported using a custom-built wheeled frame (Fig. 1A), providing comfortable access to the front and rear for cleaning and maintenance. The XBI can be used either with the cart (no lifting required) or by directly attaching it to the animal's enclosure (freeing the cart). For safety reasons all electronics of the AI run on low-voltage (maximum 12 V). Parts close to the animal that have to be powered include the touch-screen as the interaction device, a peristaltic pump for delivering reward, a loud-speaker to provide feedback or instructions, a surveillance camera for remote observation, and a cable connector box to minimize the number of cables between both interfaces. The rest of the XBI electronics reside remotely in the CI.

All animals had access to the AI in their home enclosures. These consisted of a room-sized group compartment and a smaller front compartment, physically separable by a dividing gate. The AI is attached to the front compartment with an aluminum-mounting frame, replacing one side panel of the compartment (Fig. 2B). For nine out of 11 animals the front compartment was connected to the group compartment such that the tested animal could be seated on-sight with peer animals. For two out of 11 animals the arrangement of the front compartment with respect to the group compartment did not allow visual contact.

The middle part of the XBI-AI is shaped as a funnel that narrows to the dimensions of a touch-screen (ELO 1537L),

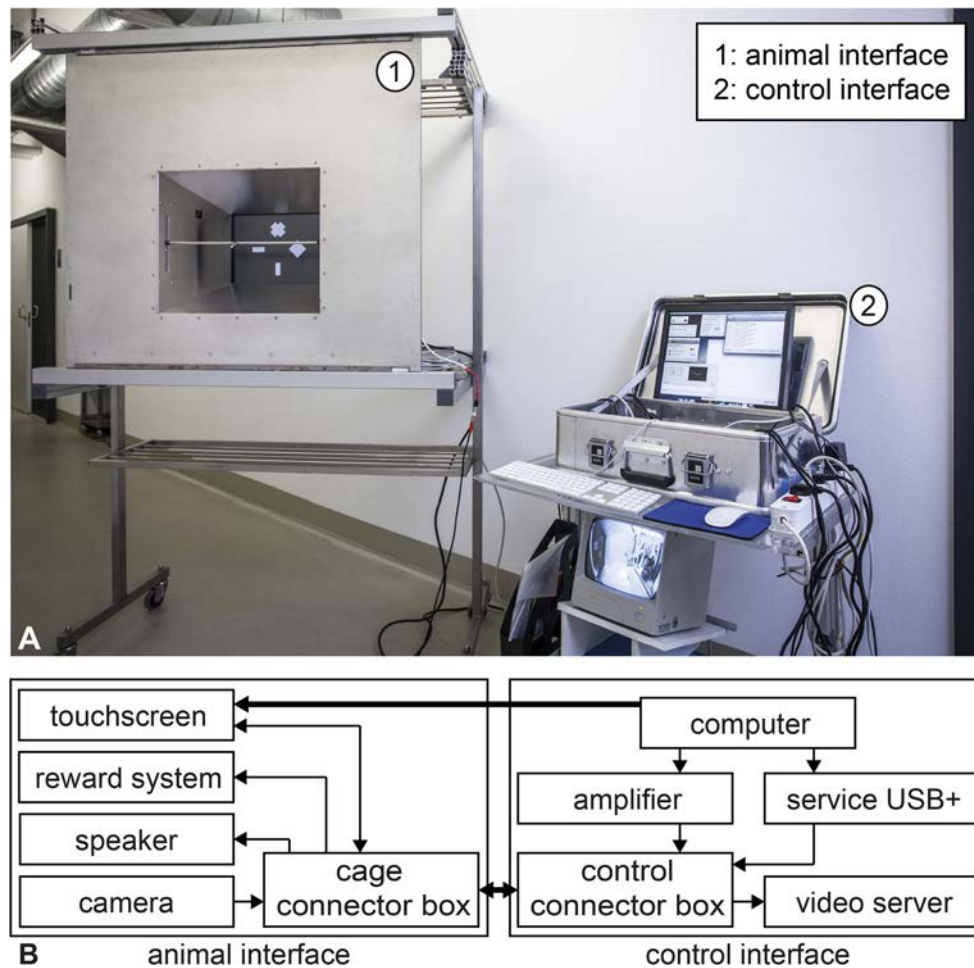


Fig. 1 **A** Image of the XBI. (1) Animal interface (AI) in the wheeled frame. A modified version of this frame is used to mount the AI on the front compartment in cases where it could not be anchored directly. (2) Control interface (CI) on a custom-made cart designed for easy relocation

and accessibility. **B** Schematics of the XBI. Thick arrows represent connections between the two interfaces and thin arrows represent internal connections between elements of the same interface. The direction of an arrow represents the direction of the signal

such that only the 15-in. LCD display is accessible for the animal. The dimensions of the front opening of the funnel are 48.6 cm × 41 cm (W × H) and the distance to the screen is 26.2 cm. This distance was chosen based on prior experience with rhesus macaques interacting with a touch-screen in neurophysiology experiments in our laboratory (Gail et al., 2009; Westendorff et al., 2010). The display is operated at a resolution of 1024 × 768 at 75 Hz. The touch panel in front of the display utilizes ultrasonic waves in combination with piezoelectric transducers for the sensing of the touch signal with a positional accuracy of 2.5 mm or better. The touch-screen is designed to be resistant against mechanical forces. A stainless steel tube with 8-mm inner and 12-mm outer diameter reaches across the funnel, at a fixed distance of 24 cm from the touch-screen. Fluid reward is delivered through a 1-mm opening in a 30-mm spout in the middle of this tube, precisely controlled via a peristaltic pump (see below). The stainless steel tube with the spout can be rotated and adjusted horizontally and vertically in position. In this way it is possible to set it

to comfortable positions for individual monkeys of different size. Given that the animals usually operate the device with the reward tube as close as possible to their mouths (Fig. S1), the eye-to-screen distance is around 28–32 cm, depending on an individual's head orientation and size. The screen size of 30.4 cm horizontal and 22.8 cm vertical provides 54° of visual angle along the horizontal and 42° along the vertical axis.

The AI's backside contains a reward unit consisting of a fluid container (2.5-L plastic bottle), connected to the metal reward tube using flexible PVC tubes with 6-mm inner diameter. These tubes are exchanged after every 2 weeks of use. A peristaltic pump (Verderflex OEM M025 DC) allows electronic control of the reward flow. This reward unit can be placed at either the left or right outer side of the funnel to adapt to different cage structures. The pump delivers 1.8 ml/s of activation time, with a precision of approximately 0.01 ml. The reward was precisely timed and dosed via the experimental control software, which is crucial for cognitive neuroscience testing.

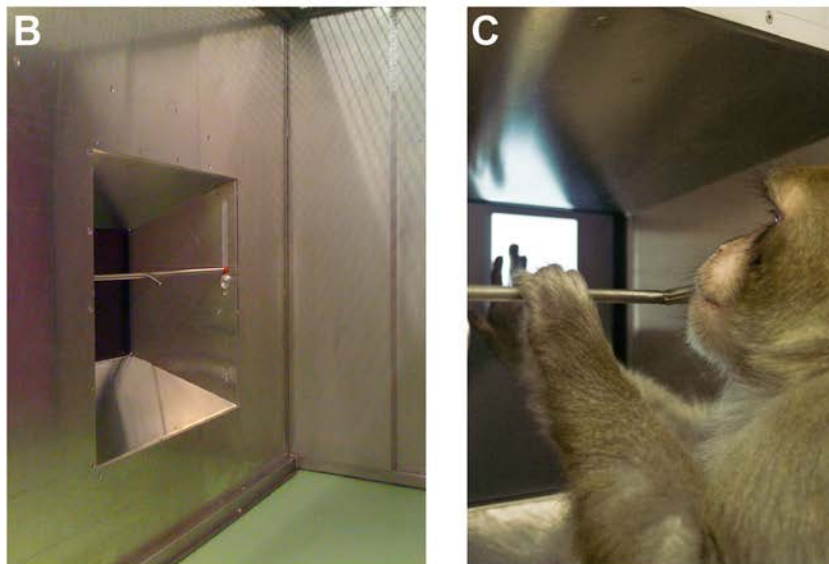
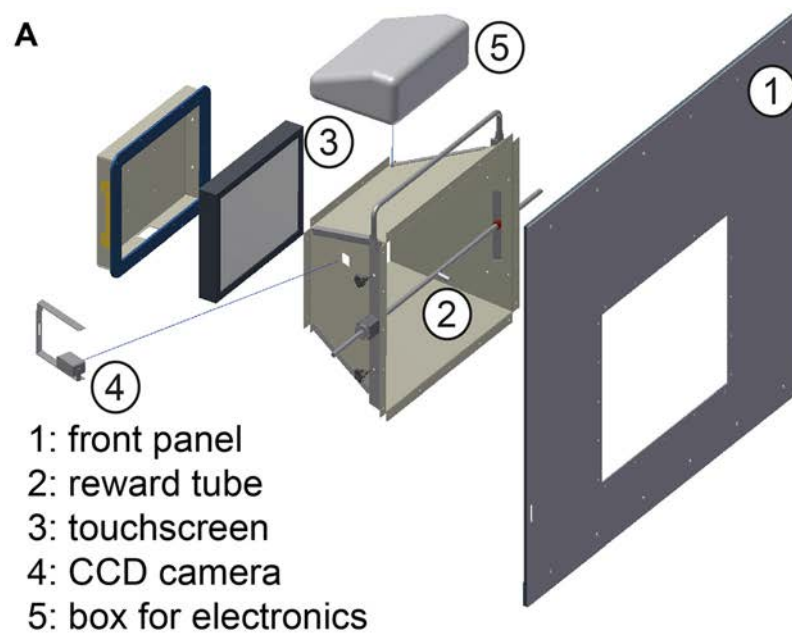


Fig. 2 **A** Exploded-view drawing of the XBI's front, facing the animal. From left to right: the protective frame for the touch-screen, the touch-screen, the funnel, and the reward tube, the mounting frame for cage

anchoring. **B** XBI front from the animals' perspective. **C** One animal working at the XBI, in a trial of the touch-hold-release task

A mono sound transducer (Visaton, SpeaKa 130 mm) is glued on the outside of one of the funnel walls, using the wall as resonator for sound amplification. A compact 160° wide-angle CCD camera (ABUS TV7512) with 480 TV lines (438 kPixel) resolution is attached to a small opening in the metal funnel, protected by a clear polycarbonate window. The wide-angle view enables monitoring of the monkey and of the video screen at the same time.

Except for the VGA video cable, all connections (including power and signal lines) are routed to the CI via a custom-made connector box and a standard parallel D-SUB 25 connector cable (up to 15 m). Thus, only these two cables

have to be routed to the outside of the animal facility. Within the connector cable we used multiple leads for power and ground lines to increase the amount of current that can be delivered through the cable.

The overall maximal nominal power consumption for the AI is 37.6 W (touch-screen 22 W, camera 0.6 W, active peristaltic pump 15 W). With an operating DC voltage of 12 V the XBI draws a maximum nominal current of 3.13 A. In practice we measured a total current of 1.5 A.

The AI is build to be operated for years, even in a dirty and humid work environment such as an animal facility. The front side facing the monkey cage is resistant against feces, urine

and direct water impact during cage cleaning procedures. On the backside of the AI all components are protected against spray water and particles larger than 2.5 mm. According to IEC 60529, the international protection marking level of the whole XBI is IP 33, with a substantially higher protection from the inside of the monkey cage.

Control interface

The CI consists of all the hardware and software needed for controlling the AI. It usually operates from outside the animal facility, weighs 12.2 kg and fits into a transportable box (W: 59 cm, H: 12 cm, D: 38 cm) for easy transport. The CI receives and sends signals from the AI through the VGA and connector cables. A second custom-made connector box distributes all connections from the connector cable to the individual components. The VGA cable as well as the serial RS232 connection from the touch-screen is connected to a computer that controls the XBI (Fig. 1). To control various devices from the computer, we integrated a USB interface (Service USB plus, Böning und Kallenbach). This platform provides multiple analogue and digital GPIOs (General Purpose Inputs/Outputs) which can deliver currents of up to 1.3 A. One of the digital outputs is used for operating the peristaltic pump, while the others have not been used in the context of the experiments described here. In addition, the computer's audio output is connected to a custom-built sound amplifier, which provides the audio signal for the sound transducer. The camera signal is routed to a video server (TRENDnet TV-VS1P) and from the video server to an analogue screen for on-site observation. The video server and the XBI computer are connected to the Local Area Network (LAN). In this way any computer on the LAN can be used for remotely controlling the XBI as well as recording videos and downloading data.

As long as the necessary interfaces are available, hardware requirements for the CI computer to run the XBI do not exceed those of standard desktop or laptop computers. We used VGA and USB connections with a RS232 adapter for the touch-screen in the AI, another USB port for the Service USB plus device, DVI-D for the CI's screen, and the headphone audio out for the audio amplifier. Although LAN connectivity is not necessary for the XBI to operate, it provides useful remote control capability. The video server is not directly connected to the computer but can be accessed via LAN. For the computer we either used an Apple Mac mini (2.5 GHz Intel i5, 8 GB RAM) or an Apple MacBook (2.4 GHz Intel Core 2 Duo, 2 GB RAM). The Mac OS is used since it interfaces optimally with MWorks (<http://mworks-project.org/>). This open-source software is a highly flexible C++-based package for designing and real-time controlling behavioral tasks for neurophysiological and psychophysical experiments. MWorks can be expanded by dedicated software plug-ins to serve a wide range of experimental needs.

Behavioral tasks are coded as XML files. A custom-made XML editor makes programming and modifying task files easy even for users without programming experience. MWorks runs in a client-server structure. The XBI can be run either as a standalone system or be operated via LAN. Data files are generated on the CI-computer that runs the server software.

Animals, grouping and fluid control

Overall, a total of 11 male rhesus monkeys (*Macaca mulatta*) were trained on the XBI within their housing facility. Three animals (Gro, Chi, and Zep) had access to the XBI as a group directly from the group compartment of their home cage. We report their behavioral data as group performance. We confirmed that an off-line analysis of the video footage allows for determining which animal was responsible for each of the XBI interactions. Since performance comparisons between individual animals are not the purpose of this report and since future ID tagging will render manual performance assignment to individuals unnecessary, we did not extend our pilot off-line analysis to the full data set.

The other eight animals had individual access to the XBI from within the smaller front compartment of their home enclosures. These eight animals were physically separated from their social group by a dividing wall separating the front compartment from the group compartment during the XBI sessions. Animals Fla, Alw, Nor, Odo, and Pru were in sight with their social group, while animals Han, Toa, and Zor were in sight only with members of other groups in the housing facility.

Most of the 11 animals had at least 2 h of unlimited access to water and fruits before and after each XBI session (Monday to Friday) and 24 h on all other days (see Table 1 for details). Two animals (Pru and Zor) were trained on the XBI under fluid control, in which the XBI provided the only access to fluid on working days (Monday to Friday). Animal Pru, in the early phases of the training, received plain water as reward. The other animals were rewarded with fruit-flavored sweetened water (active O2, Adelholzener) diluted with plain water at a ratio of 1:3.

Note that monkey Zor, a 12-year-old animal, was tested only during the development phase of the device.

Behavioral paradigms

To date four units of the XBI are in ongoing use and have been tested in various experiments. All experiments complied with institutional guidelines on Animal Care and Use of the German Primate Center and with European (Directive 2010/63/EU) and German national law and regulations, and were approved by regional authorities where necessary. Two experimental paradigms shall serve as examples of the

Table 1 For each of the 11 animals (rows) that took part in the two experiments the table lists the fluid access scheme (before and/or after the XBI session), which, if any, of the social group members was undergoing XBI training, which experiment or experiments were used, and the animals' age at the time of their first encounter with the device

Animal	Fluid access	XBI mates	Experiment	Age (years)
Alw	Before/After	-	AS	4
Chi	Before/After	Gro, Zep	AS	4
Fla	Before/After	-	AS	3
Gro	Before/After	Chi, Zep	AS	4
Han	Before/After	-	AS	3
Nor	Before/After	-	AS	3
Odo	Before/After	-	AS	7
Pru	XBI only, Before/After	Zor	FTS, THR, MS	7
Toa	After	-	AS	3
Zep	Before/After	Chi, Gro	AS	4
Zor	XBI only	Pru	THR	12

AS accommodation study, FTS free-task selection, THR touch-hold-release task, MS delayed match-to-sample

functionality of the system and acceptance by the animals. The first paradigm, the *accommodation study*, probed the ability of naïve animals to autonomously learn how to successfully operate a touch-screen on a basic level with no formal training (e.g., training to human handling). The second experiment, the *free-task selection* tested the XBI as a cognitive testing system and as an enrichment tool.

Accommodation study

Nine animals (age: 4–7 years) participated in the accommodation study (AS). They were naïve with respect to the XBI, and the accommodation study marked their first encounter with the device. Each animal had 90 min of daily access (typically from Monday to Friday) to the XBI over a period of 2 weeks excluding the weekend. None of the animals had previously participated in any type of cognitive training.

In the accommodation study the monkeys had to perform a simple touch task. At the beginning of each trial a steady blue (white for monkey Fla) square target stimulus $20 \times 20 \text{ cm}^2$, was displayed on the screen on a black background. Touching the target for at least 100 ms triggered a fluid reward (successful trial). Touching the background terminated the trial without a reward (unsuccessful trial). Each trial was followed by an inter-trial interval during which the screen remained black. After 1 s without touching the screen the next trial started. This requirement of releasing the touch of the screen prevented the animals from successfully completing a series of tasks by simply keeping a finger (or any other body parts) on the screen. In addition to the delivery of the fluid reward, two different sounds indicated whether a trial was a success or not.

Free-task selection

One animal (Pru, 7 years old) participated in the *Free-Task Selection* (FTS). Note that before entering the free-task selection, the monkey underwent 4 months of positive reinforcement training to enter and exit the primate chair and 12 months of training on the XBI (see below for details).

In the free-task selection, at the beginning of each trial, four symbols were displayed on the screen (see Fig. 3), each one permanently associated with one subtask (Washburn et al., 1991):

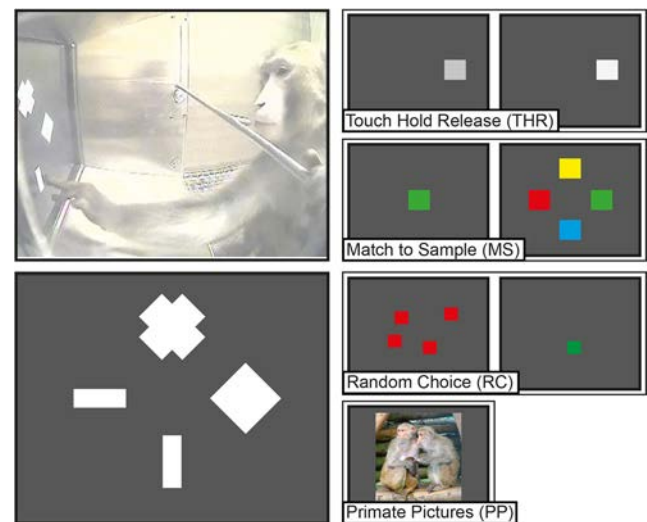


Fig. 3 Left column, top: view of the internal XBI camera while animal Pru chooses which task to execute next. Bottom: representation of the first frame of each trial of the four-choices tasks. Each white symbol is associated with one of the four tasks depicted in the right column, from top to bottom: cross for Touch Hold Release (THR), rhombus for Match to Sample (MS), vertical bar for Random Choice (RC), horizontal bar for Picture Presentation (PP, representative picture)

- *The cross* was associated with a simple *touch-hold-release* (THR) task, an extension of the touch task in the accommodation study. After the animal selected the cross symbol and after a 500-ms delay the four symbols were replaced by a gray square (5×5 cm). The animal had 4,000 ms to reach for the target, which once touched, it brightened. After 500–2,500 ms of maintaining the touch the square dimmed. Now the animal had to release the touch within 500 ms to successfully complete the trial. The position of the stimulus on the screen and the required hold-time were randomized trial-by-trial. For this subtask the average duration of a successful trial was 4.8 s from when the animal selected the cross symbol.
- *The rhombus* was associated with a color-based *delayed match-to-sample* (MS) task. In MS trials the animal had to first touch a colored square (8×8 cm) at the center of the screen and after a randomized delay (1.5–3 s), touch the square with the same color amongst four differently colored squares of the same size displayed left, right, above, and below the screen center. The colors of the squares were randomly assigned trial-by-trial. The animal had to select the target within 4 s for correct performance, otherwise the trial would terminate without a reward. The same outcome would occur if the wrong stimulus was selected. For this subtask, the average length of a successful trial was 2.7 s.
- *The horizontal bar* was associated with a *random choice* (RC) task in which the animal had to touch one of four identical 3×3 cm red squares that were randomly positioned on the screen. Only one randomly determined stimulus would trigger a reward. By setting the amount of reward to four times the reward in the touch-hold-release and match-to-sample tasks the average reward was equated across these task types. For this subtask the average length of a successful trial was 3.6 s.
- *The vertical bar* was associated with a *primate picture* (PP) task in which one out of 20 photographs of non-human primates were shown on the screen for 5 s. After selection, no additional touch was necessary and no fluid reward was given in this task. For this subtask the average length of a trial was 5.6 s.

The animal was trained on the touch-hold-release task for over 6 months while technical aspects of the XBI prototype were under development and the match-to-sample task for 3 months. Once the monkey had reached a consistent performance above 80 % over 10 sessions (2 weeks) in these two tasks he was introduced to the free-task selection task. It included the two known tasks and the two novel tasks each associated with its corresponding symbol (see above). To determine the influence of relative reward amounts on relative choice probabilities, the first 31 sessions (3 months) of the

free-task selection have been collected in two experimental conditions: lower reward RC task (20 sessions) versus higher reward RC task (11 sessions). We statistically verified the influence of relative reward amount on relative choice probabilities by the mean of the Multinomial Logit Model with estimated p-values using pairs cluster bootstrapped t-statistics (Cameron, Gelbach, & Miller, 2008).

Results

The XBI is designed for behavioral training, cognitive testing, and enrichment of physically unrestrained rhesus monkeys in an animal facility. Both of its components (the AI and the CI) are safely useable for the experimenter and the monkeys in this environment. Below, we will describe the usability of the XBI from the experimenter's perspective as well as behavioral example data recorded with the XBI as a proof-of-concept for cognitive testing and environmental enrichment.

Handling by the experimenters

A single person can handle the XBI safely. The use of a wheeled frame for storage and transport allows the XBI to be directly transferred to the sides of a cage avoiding the need to lift the AI. The mesh grid of the cage can be conveniently removed after the XBI has been mounted in front of it.

The XBI can be set up quickly. Given some experience, aligning the device to the cage and preparing a given experiment takes less than 10 min. In this time: the device is mounted to the cage replacing one of the cage's walls, is connected to permanently installed cables for the electronic communication between the two interfaces, the reward system is filled up, and the task and the video recording are initiated. From this point on the system is able to run autonomously, and without supervision, until it is manually stopped. If needed, the touch-screen as well as the cage are briefly cleaned before starting a new XBI session. This takes less than 10 min. To prevent technical malfunction by accumulating dirt the AI is thoroughly cleaned after about five sessions and the plastic tubes for reward delivery are replaced when needed.

The XBI is robust enough to endure repeated mounting and dismounting. In our setting one of the devices was used daily in three different rooms. Despite the substantial amount of mechanical stress of changing the location of the device multiple times per day over many months, malfunctions that delayed the starting procedure or prevented the system from running altogether were very rare. Most of these malfunctions resulted from cables not properly connected or partially damaged by the frequent use. Switching to more resistant cables eliminated such problems. Other technical issues were not observed. Across four separate XBI devices operated for more

than 1 year, only one bent reward tube and one broken peristaltic pump had to be exchanged.

The XBI requires little regular maintenance. The electronic devices attached to the AI are protected against spray water and dirt by their encapsulation. However, water and dirt on the touch surface can interfere with the assessment of behavioral performance by creating false triggers. To reduce dirt accumulation, the floor of the cage in which the XBI was placed was either a mesh or covered with dry wood-chip bedding. Accordingly, regular maintenance is inexpensive in terms of parts and materials. For hygienic reasons, we replaced the silicon tube (1 m) of the reward system after 2 weeks of use.

The XBI is easy to handle. Daily setup routines were performed not only by the experimenters, but also by students and technical assistants. It required only 2–3 sessions under supervision until a person was experienced enough to independently operate the XBI.

The XBI approach is scalable to a larger number of devices. Given the remote control and video surveillance options, we were able to simultaneously control our three XBI devices, even when they were located in different buildings. This allowed one single experimenter to remotely manage the training of several animals.

Monkey interactions

In the following section we will report behavioral data collected to probe (1) the XBI's attractiveness to naïve animals and (2) its suitability for cognitive tests.

Accommodation experiment: Unsupervised training of naïve animals in minimally restrained conditions

With the accommodation experiment we determined that naïve animals learn to operate the XBI without human instruction, supervision, or intervention. The animals were naïve in the sense that while they had received positive reinforcement training for their handling in the housing environment (moving into and out of the front compartment, holding still, etc.), they had never experienced a touch-screen before and never had been part of experimental procedures or computer-controlled training in a cognitive task. During each of the ten sessions of the accommodation experiment, the animal had the opportunity to freely explore the device. Presumably driven by both their curiosity and the odor of the fruit-flavored water at the tip of the reward spout, eight out of nine monkeys approached first the reward tube and subsequently the shiny aluminum frame of the XBI. For eight out of nine animals, the first successful interaction with the touch-screen occurred during the very first 20 min.

During XBI sessions most of the animals were in the front compartment by themselves (with visual contact to their social group, see [Methods](#)), except for three (Chi, Zep, and Gro) that

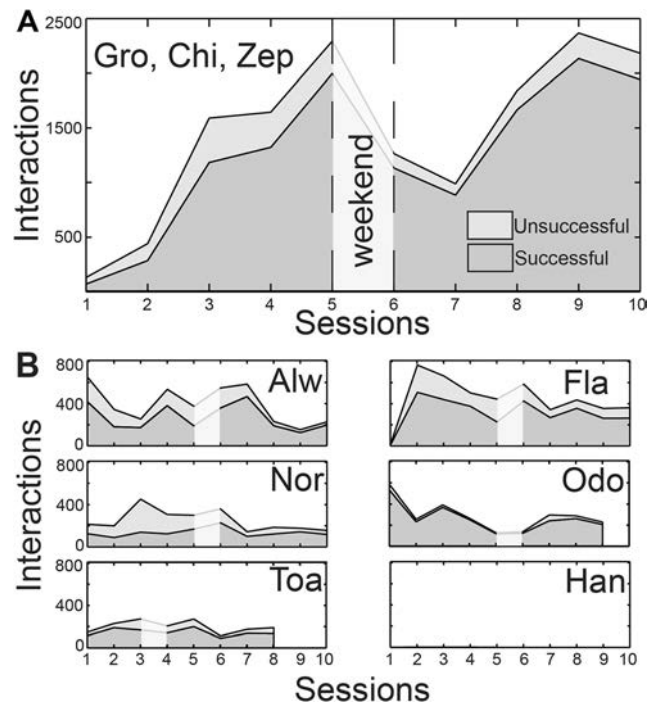


Fig. 4 **A** Number of interactions with the XBI system pooled across the monkeys Zep, Gro, and Chi. Successful trials (dark gray area), unsuccessful trials (light gray area), and total trials (top line) are plotted for up to 10 consecutive working days during the first 2 weeks, interrupted by 2 days off (weekend) between the fifth and sixth sessions. **B** Interactions for monkeys Alw, Fla, Nor, Odo, Toa, and Han. Note that animals Odo and Toa underwent respectively nine sessions (for technical reasons) and eight sessions (for unrelated reasons). Animal Toa started his first week on a Wednesday and the break lasted a whole week instead of a weekend. Animal Han did not interact with the XBI's touchscreen at all during these sessions

had access to the XBI as a group. As shown in Fig. 4A, animals Chi, Zep, and Gro, after gaining some experience with the touch-screen in the first two sessions, substantially increased both their number of interactions with the XBI and the proportion of successful trials in the following days. Although with high variability and different success proportions, animals Alw, Fla, Nor, and Odo showed a substantial interest in the XBI, generating hundreds of successful trials each day and progressively improving their ability to trigger a successful trial (Fig. 4B). Only animal Han showed no interest in the XBI.

Free-task selection experiment

The choice proportions of monkey Pru across the four tasks stabilized within the first two sessions. To determine the influence of relative reward amounts on relative choice probabilities, the reward associated with a successful random choice trial was set to three times the reward associated with the touch-hold-release (THR) and the match-to-sample (MS)

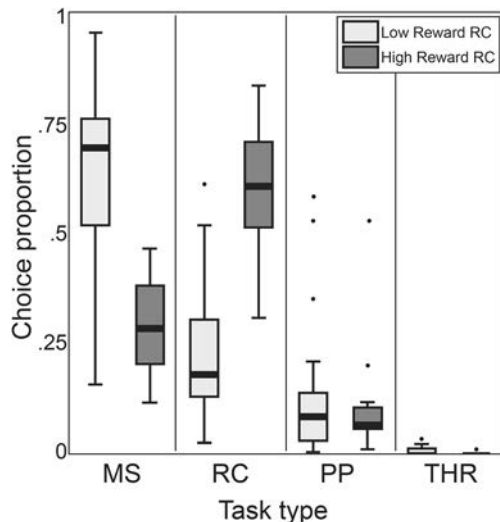


Fig. 5 Box-and-whisker plot of the distribution of choices of task type during the free-task selection, in two conditions for monkey Pru. White boxes represent the experimental condition (20 sessions) in which the reward in the random choice task (RC) was three times the amount of reward in the match-to-sample (MS) and touch-hold-release (THR) tasks. Gray boxes represent the experimental condition (11 sessions) in which the RC reward was increased to four times the amount in the MS and THR tasks. The distribution of the difference between higher reward and lower reward was estimated for each task and compared with the other tasks. To achieve such comparison the data set was repeatedly re-sampled by cluster; a model estimated and inferences were made on the sampling distribution of the pivotal (t) statistic. For each comparison the confidence interval for the significance level was weighted by the number of comparisons (confidence interval's significance level: $1-(0.005/6)$) and the confidence interval for each task comparison was determined (MS to RC 0.0566–0.8195; MS to PP 0.3595–3.9314, MS to THR 0.3760–14.7022; RC to PP 1.2448–24.4346; RC to THR 0.8994–132.1582; PP to THR 0.5127–7.6293). P -values for the six comparisons, corrected with the Bonferroni method for multiple testing, are: MS to RC 0.012; MS to PP 1.00; MS to THR 0.78; RC to PP 0.036; RC to THR 0.60; PP to THR 1.00

tasks (PP did not deliver a fluid reward). For the next 11 sessions it was increased to four times.

We statistically verified the influence of relative reward amount on relative choice probabilities (see [Methods](#) and [Fig. 5](#) legend for details). We found that MS to RC is the only comparison that yields moderate evidences for a statistical difference ($p = 0.012$), while RC to THR comparison shows a trend ($p = 0.036$) and all the other comparisons show no significant influence by the relative reward amount. This suggests that when the RC task was highly rewarded, the animal selected the RC task more often, at the expense of the MS and THR tasks but not the PP task. As can be seen in [Fig. 5](#), the distribution of MS and RC choice proportion are reversed in the two conditions; the distribution of the THR choices, already very low in the low reward condition, approach zero, while the frequency of PP choices is unaffected. This demonstrates that the fluid reward amounts in the XBI can be used to flexibly and precisely change the animal's preferences as needed, for example, in decision-making experiments.

Discussion

We developed the XBI as a cage-based stand-alone device for behavioral training and cognitive testing of rhesus macaques and designed for a seamless integration into conventional neuroscience experiments. We tested the XBI for over a year and found it robust and flexible enough for use in different animal facilities. It is easy to handle such that one non-expert person is able to operate it on a daily basis with short setup times and without the need to remove it during wet cage cleaning procedures. Animals do not have to leave their housing environment and naïve animals learn to interact with the device in an unsupervised fashion, at a self-paced rate within the time window of device access. As a proof of concept, we presented training examples matching neuroscience research questions, e.g., training visually instructed goal-directed movements, but a much broader spectrum of behavioral testing is possible. Despite lacking physical constraints, the animals adopted stereotyped postures, adapted to the ergonomic design of the XBI, creating a well-defined perspective and distance from the visual stimuli and the reach goals on the monitor. The close-up full-body video surveillance embedded in the system allows further behavioral assessments.

Devices similar to the XBI have proved to be highly useful in cognitive assessments of non-human primates (Andrews & Rosenblum, 1994; Fagot & Bonté, 2010; Fagot & Paleressompoulle, 2009; Fagot & Parron, 2010; Gazes et al., 2012; Mandell & Sackett, 2008; Rumbaugh et al., 1989; Richardson et al., 1990; Truppa et al., 2010; Washburn et al., 1989; Weed et al., 1999). In systems and cognitive neuroscience research additional features of such devices are desirable, which we implemented to increase the range of possible uses for the XBI.

First, most existing systems use solid rewards (Andrews & Rosenblum, 1994; Fagot & Bonté, 2010; Gazes et al., 2012; Truppa et al., 2010; Weed et al., 1999), with the exception of Mandell and Sackett (2008). We use fluid rewards for the XBI, since in typical neuroscience behavioral protocols, rewards need to be precisely dosed and timed, e.g., for decision-making studies with fine-grained reward schedules (for example: Klaes et al., 2011; Platt, 2002; Sugrue et al., 2004) and as reinforcers in eye-position contingent, complex visual, and sensorimotor tasks (for example: Gail et al., 2000; Gail & Andersen, 2006; Katzner et al., 2009; Niebergall et al., 2011; Patzwahl & Treue, 2009).

Second, to be suited for a large range of neuroscience questions, the monitor and interactive touch surface should be easily accessible. In most of the touch-screen-based systems using radio-frequency identification (RFID) the monkeys need to reach through ports equipped with antenna coils, to reliably read the RFID tags (Andrews & Rosenblum, 1994; Fagot & Bonté, 2010; Gazes et al., 2012). We do not use view and reach ports to not constrain reaching movements toward

and across the touch-screen and because preliminary technical tests indicate that our design is suitable for hand-specific RFID tagging without such ports. A further advantage of not having ports or physical shielding of the touch-screen is the unobstructed full-body frontal video image of the animal in the XBI, which can be used for various forms of behavioral assessments, e.g., more complex video-based motion tracking, analysis of emotional facial expressions, etc. On the other hand, we want to encourage an ergonomic posture of the animals with a defined viewing distance from the screen. In systems without reach or view ports the screen was placed in the same plane or close to the wall of the cage, allowing the animals more freedom in choice of the posture and screen-eye distance (Gazes et al., 2012; Truppa et al., 2010; Weed et al., 1999). Since many studies in the neurosciences use visually guided tasks, it is critical to provide a controlled visual stimulus, including a well-defined retinal size. We achieved this by positioning the reward tube and touch-screen at opposite ends of a funnel, with the funnel depth adjusted to the arm lengths of rhesus monkeys and the reward tube position optimized for their sitting posture. With the aid of the integrated full-body video recordings, we verified that the animals quickly adopted a desirable and stereotypical posture in front of the screen, with the face in front of the screen and the mouth at the opening of the reward tube (see Supplementary Fig. 1 and supplementary videos). In future, this will presumably allow for an easy integration of video-based eye-tracking and face-recognition systems. Moreover, given the central placement of the reward spout, animals were free to use either hand for interacting with the device (see monkey Nor and Fla in Supplementary Fig. S1 and video).

Third, we designed the XBI to be compact and mobile, including remote control via LAN (Mandell & Sackett, 2008, 2009). This makes individual devices easily transferable between rooms, floors, or even buildings, and adaptable to different enclosures. Using one server we simultaneously operated our three devices in two buildings, switching them amongst six social groups.

Finally, we believe that the spontaneous and continued engagement of the naïve animals that we observed during early exposure to the XBI, despite no restrictions on fluid intake, shows that cage-based devices, beyond showing great potential as an alternative to some conventional setup training for neuroscience research, can also serve as valuable tools for environmental enrichment, in compliance with the 3Rs principle (Evans et al., 2008; Fagot et al., 2014; Richardson et al., 1990; Russell & Burch, 1959; Washburn et al., 1991; Washburn & Rumbaugh, 1992). It is important to note that the XBI does not trigger the same level of interest in all naïve animals (Evans et al., 2008). We are currently expanding these observations in a separate study to address the need for more systematic behavioral profiling of such inter-individual differences.

Acknowledgments A.C. and M.B. are shared first authors. S.T. and A.G. are shared last authors.

This project was supported by the European Commission in the context of the EUPRIM-Net-II consortium (FP7-262443-WP9 to A.G.) and the German Research Foundation in the context of the RU1847 (GA1475-C1 to A.G.). We thank Leonore Burchardt, Valeska Stephan, and Matthias Dörge for help with construction and data collection.

Open Access This article is distributed under the terms of the Creative Commons Attribution 4.0 International License (<http://creativecommons.org/licenses/by/4.0/>), which permits unrestricted use, distribution, and reproduction in any medium, provided you give appropriate credit to the original author(s) and the source, provide a link to the Creative Commons license, and indicate if changes were made.

References

- Andrews, M. W., & Rosenblum, L. A. (1994). Automated recording of individual performance and hand preference during joystick-task acquisition in group-living bonnet macaques (*Macaca radiata*). *Journal of Comparative Psychology*, *108*, 358–362.
- Cameron, A. C., Gelbach, J. B., & Miller, D. L. (2008). Bootstrap-based improvements for inference with clustered errors. *The Review of Economics and Statistics*, *90*(3), 414–427.
- Drea, C. M. (2006). Studying primate learning in group contexts: Tests of social foraging, response to novelty, and cooperative problem-solving. *Methods*, *38*, 162–177.
- Evans, T. A., Beran, M. J., Chan, B., Klein, E. D., & Menzel, C. R. (2008). An efficient computerized testing method for the capuchin monkey (*Cebus apella*): Adaptation of the LRC-CTS to a socially housed nonhuman primate species. *Behavior Research Methods*, *40*(2), 590–596.
- Fagot, J., & Bonté, E. (2010). Automated testing of cognitive performance in monkeys: Use of a battery of computerized test systems by a troop of semi-free-ranging baboons (*Papio papio*). *Behavior Research Methods*, *42*(2), 507–516. doi:10.3758/BRM.42.2.507
- Fagot, J., Gullstrand, J., Kemp, C., Defilles, C., & Mekouache, M. (2014). Effects of freely accessible computerized test systems on the spontaneous behaviors and stress level of Guinea baboons (*Papio papio*). *American Journal of Primatology*, *76*, 56–64.
- Fagot, J., & Paleressompouille, D. (2009). Automatic testing of cognitive performance in baboons maintained in social groups. *Behavior Research Methods*, *41*(2), 396–404. doi:10.3758/BRM.41.2.396
- Fagot, J., & Parron, C. (2010). Relational matching in baboons (*Papio papio*) with reduced grouping requirements. *Journal of Experimental Psychology: Animal Behavior Processes*, *36*(2), 184–193. doi:10.1037/a0017169
- Fernström, A. L., Fredlund, H., Spångberg, M., & Westlund, K. (2009). Positive reinforcement training in rhesus macaques—training progress as a result of training frequency. *American Journal of Primatology*, *71*(5), 373–379. doi:10.1002/ajp.20659
- Gail, A., & Andersen, R. A. (2006). Neural dynamics in monkey parietal reach region reflect context-specific sensorimotor transformations. *Journal of Neuroscience*, *26*(37), 9376–9384.
- Gail, A., Brinksmeier, H. J., & Eckhorn, R. (2000). Contour decouples gamma activity across texture representation in monkey striate cortex. *Cerebral Cortex*, *10*(9), 840–850.
- Gail, A., Klaes, C., & Westendorff, S. (2009). Implementation of spatial transformation rules for goal-directed reaching via gain modulation in monkey parietal and premotor cortex. *Journal of Neuroscience*, *29*(30), 9490–9499. doi:10.1523/JNEUROSCI.1095-09.2009

- Gazes, R. P., Brown, E. K., Basile, B. M., & Hampton, R. R. (2012). Automated cognitive testing of monkeys in social groups yields results comparable to individual laboratory-based testing. *Animal Cognition*, *16*, 445–458.
- Katzner, S., Busse, L., & Treue, S. (2009). Attention to the color of a moving stimulus modulates motion-processing in macaque area MT: Evidence for a unified attentional system. *Frontiers in Systems Neuroscience*, *3*(12), 11–18.
- Klaes, C., Westendorff, S., Chakrabarti, S., & Gail, A. (2011). Choosing goals, not rules: Deciding among rule-based action plans. *Neuron*, *70*(3), 536–548.
- Mandell, D. J., & Sackett, G. P. (2008). A computer touch screen system and training procedure for use with primate infants: Results from pigtail monkeys (*Macaca nemestrina*). *Developmental Psychobiology*, *50*(2), 160–170. doi:10.1002/dev.20251
- Mandell, D. J., & Sackett, G. P. (2009). Comparability of developmental cognitive assessments between standard and computer testing methods. *Developmental Psychobiology*, *51*(1), 1–13. doi:10.1002/dev.20329
- McCluskey, M. K., & Cullen, K. E. (2007). Eye, head, and body coordination during large gaze shifts in rhesus monkeys: Movement kinematics and the influence of posture. *Journal of Neurophysiology*, *97*(4), 2976–2991. doi:10.1152/jn.00822.2006
- Niebergall, R., Khayat, P. S., Treue, S., & Martinez-Trujillo, J. (2011). Multifocal attention filters out distracter stimuli within and beyond receptive field boundaries of primate MT neurons. *Neuron*, *72*, 1067–1079.
- Patzwahl, D., & Treue, S. (2009). Combining spatial and feature-based attention within the receptive field of MT neurons. *Vision Research*, *49*, 1188–1193.
- Perlman, J. E., Bloomsmith, M. A., Whittaker, M. A., McMillan, J. L., Minier, D. E., & McCowan, B. (2012). Implementing positive reinforcement animal training programs at primate laboratories. *Applied Animal Behaviour Science*, *137*(3–4), 114–126. doi:10.1016/j.applanim.2011.11.003
- Platt, M. L. (2002). Caudate clues to rewarding cues. *Neuron*, *33*, 316–318.
- Richardson, W. K., Washburn, D. A., Hopkins, W. D., Savage-Rumbaugh, E. S., & Rumbaugh, D. M. (1990). The NASA/LRC computerized test system. *Behavior Research Methods, Instruments, & Computers*, *22*(2), 127–131.
- Rumbaugh, D. M., Hopkins, W. D., Washburn, D. A., & Savage-Rumbaugh, E. S. (1989). Lana chimpanzee learns to count by “NUMATH”: A summary of a videotaped experimental report. *Psychological Record*, *39*(4), 459–470.
- Russell, W. M. S., & Burch, R. L. (1959). *The principles of humane experimental technique*. Methuen, London. ISBN 0900767782.
- Schapiro, S. J., Bloomsmith, M. A., & Laule, G. E. (2003). Positive reinforcement training as a technique to alter nonhuman primate behavior: Quantitative assessments of effectiveness. *Journal of Applied Animal Welfare Science: JAAWS*, *6*(3), 175–187. doi:10.1207/S15327604JAWS0603_03
- Sugrue, L. P., Corrado, G. S., & Newsome, W. T. (2004). Matching behavior and the representation of value in the parietal cortex. *Science*, *304*(5678), 1782–1787.
- Truppa, V., Garofoli, D., Castorina, G., Piano Mortari, E., Natale, F., & Visalberghi, E. (2010). Identity concept learning in matching-to-sample tasks by tufted capuchin monkeys (*Cebus apella*). *Animal Cognition*, *13*(6), 835–848. doi:10.1007/s10071-010-0332-y
- Washburn, D. A., Hopkins, W. D., & Rumbaugh, D. M. (1989). Video-task assessment of learning and memory in macaques (*Macaca mulatta*): Effects of stimulus movement on performance. *Journal of Experimental Psychology: Animal Behavior Processes*, *15*(4), 393–400.
- Washburn, D. A., Hopkins, W. D., & Rumbaugh, D. M. (1991). Perceived control in rhesus monkeys (*Macaca mulatta*): Enhanced video-task performance. *Journal of Experimental Psychology: Animal Behavior Processes*, *17*(2), 123–129.
- Washburn, D. A., & Rumbaugh, D. M. (1992). Testing primates with joystick-based automated apparatus: Lessons from the language research center’s computerized test system. *Behavior Research Methods, Instruments, & Computers*, *24*(2), 157–164. doi:10.3758/BF03203490
- Weed, M. R., Taffe, M. A., Pollis, I., Roberts, A. C., Robbins, T. W., Koob, G. F., ... Gold, L. H. (1999). Performance norms for a rhesus monkey neuropsychological testing battery: Acquisition and long-term performance. *Cognitive Brain Research*, *25*;8(3), 185–201.
- Westendorff, S., Klaes, C., & Gail, A. (2010). The cortical timeline for deciding on reach motor goals. *Journal of Neuroscience*, *30*(15), 5426–5436. doi:10.1523/JNEUROSCI.4628-09.2010


Chapter 6

Standardized automated training of rhesus monkeys for neuroscience research in their housing environment

This Manuscript was published on the 1. March 2018 in *Journal of Physiology* 119: 796-807, 2018.

INNOVATIVE METHODOLOGY | *Higher Neural Functions and Behavior*

Standardized automated training of rhesus monkeys for neuroscience research in their housing environment

 M. Berger,^{1,2*} A. Calapai,^{1,3*} V. Stephan,¹ M. Niessing,¹ L. Burchardt,¹ A. Gail,^{1,2,3,4*} and S. Treue^{1,2,3,4*}

¹Cognitive Neuroscience Laboratory, German Primate Center–Leibniz-Institute for Primate Research, Goettingen, Germany;

²Faculty of Biology and Psychology, University of Goettingen, Goettingen, Germany; ³Leibniz-ScienceCampus Primate Cognition, Goettingen, Germany; and ⁴Bernstein Center for Computational Neuroscience, Goettingen, Germany

Submitted 18 August 2017; accepted in final form 7 November 2017

Berger M, Calapai A, Stephan V, Niessing M, Burchardt L, Gail A, Treue S. Standardized automated training of rhesus monkeys for neuroscience research in their housing environment. *J Neurophysiol* 119: 796–807, 2018. First published November 15, 2017; doi:10.1152/jn.00614.2017.—Teaching nonhuman primates the complex cognitive behavioral tasks that are central to cognitive neuroscience research is an essential and challenging endeavor. It is crucial for the scientific success that the animals learn to interpret the often complex task rules and reliably and enduringly act accordingly. To achieve consistent behavior and comparable learning histories across animals, it is desirable to standardize training protocols. Automating the training can significantly reduce the time invested by the person training the animal. In addition, self-paced training schedules with individualized learning speeds based on automatic updating of task conditions could enhance the animals' motivation and welfare. We developed a training paradigm for across-task unsupervised training (AUT) of successively more complex cognitive tasks to be administered through a stand-alone housing-based system optimized for rhesus monkeys in neuroscience research settings (Calapai A, Berger M, Niessing M, Heisig K, Brockhausen R, Treue S, Gail A. *Behav Res Methods* 5: 1–11, 2016). The AUT revealed interindividual differences in long-term learning progress between animals, helping to characterize learning personalities, and commonalities, helping to identify easier and more difficult learning steps in the training protocol. Our results demonstrate that 1) rhesus monkeys stay engaged with the AUT over months despite access to water and food outside the experimental sessions but with lower numbers of interaction compared with conventional fluid-controlled training; 2) with unsupervised training across sessions and task levels, rhesus monkeys can learn tasks of sufficient complexity for state-of-the-art cognitive neuroscience in their housing environment; and 3) AUT learning progress is primarily determined by the number of interactions with the system rather than the mere exposure time.

NEW & NOTEWORTHY We demonstrate that highly structured training of behavioral tasks, as used in neuroscience research, can be achieved in an unsupervised fashion over many sessions and task difficulties in a monkey housing environment. Employing a pre-defined training strategy allows for an observer-independent comparison of learning between animals and of training approaches. We

believe that self-paced standardized training can be utilized for pre-training and animal selection and can contribute to animal welfare in a neuroscience research environment.

animal welfare; automated training; cognitive training; environmental enrichment; 3R

INTRODUCTION

Cognitive neuroscience research with nonhuman primates (NHPs) often requires extensive animal teaching using positive reinforcement training. Animals have to learn to accurately operate devices such as a touchscreen, a joystick, a lever, or a button, interpret sensory cues, and react according to the behavioral paradigm. Training an animal from naive to expert in a cognitive task can last many months, with its success depending on the animal's motivation and cognitive abilities but also the training strategy chosen based on the trainer's experience and intuition.

Standardizing training protocols for cognitive tasks should help in improving the quality of experimental data. It avoids variability in training history that could otherwise lead to variability in cognitive strategy. The more precise an animal's cognitive behavior is shaped by the design of the cognitive task and its training, the better it can be understood by the experimenter, and the lower is the risk of confounding interpretations of the behavioral and neurophysiological data collected for understanding the neural basis of cognitive behavior. Especially with multiple animals having to be trained on the same task, it is crucial that the same cognitive strategies are instructed to achieve comparability of behavioral and neural results between animals. However, the trainer's choice of training strategy or even the trainers themselves might differ between animals, potentially leading to mismatching task-solving behavior of the animals and making their comparison difficult.

Standardizing training of cognitive tasks does not imply that each animal after a certain training time is confronted with exactly the same task demands according to a fixed protocol. Instead, task demands and their progression should depend on the individual performance. We propose to standardize only the rules according to which animals progress through the

* M. Berger and A. Calapai, and A. Gail and S. Treue contributed equally to this work.

Address for reprint requests and other correspondence: M. Berger, Cognitive Neuroscience Laboratory, German Primate Center–Leibniz-Institute for Primate Research, Kellnerweg 4, 37077 Goettingen, Germany (e-mail: mberger@dpz.eu).

predefined learning steps of a new task. This approach aims at ensuring an optimal learning rate for the individual animal by maintaining an intermediate performance level, avoiding both the frustration of too many errors and the decline of the learning rate when the task becomes too easy. Within a specific project, the predefined learning steps should be the same for all participating animals, but they will obviously have to differ between projects. The standardized rules of progression through successive training steps can nevertheless be applied to a variety of projects.

Standardizing the training of cognitive tasks is particularly promising in combination with an automated unsupervised approach, since this minimizes the “human factor.” Additionally, automated and unsupervised training substantially reduces the trainer’s work load, while additionally allowing the animal a self-paced training schedule (Miller et al. 2015; Tulip et al. 2017). The training period for complex cognitive neuroscience projects can often last over several months, such that automatization creates a major potential for time savings. Also, with the need for human interaction, the training schedule is typically determined by the experimenter and not by the animal (Prescott et al. 2010). Automated unsupervised training in the home enclosure allows animals to choose time and duration of their training. Such choice provides the animal with more control over its environment, potentially enhancing animal welfare (Westlund 2014).

Automated and unsupervised training can be used in the animals’ home enclosures and serve as environmental enrichment (Clark 2017). Environmental enrichment is an important factor in maintaining the welfare of NHPs, but monkeys can quickly lose interest in unchanging enrichment toys, by becoming habituated (Murphy et al. 2003). Maintaining an animal’s interest requires variations and novelty in the environment and the involvement of primary reinforcers, such as food or fluid rewards, variety, or novelty (Tarou and Bashaw 2007). Cognitive training by an automated protocol, which dynamically adjusts the difficulty of a rewarded task to the animal’s current skill level as suggested here, might increase the animal’s motivation to continuously interact with the device. Thus such an automated training device marks a cognitively challenging interaction tool that could serve as cognitive enrichment to positively impact animals’ welfare (Bennett et al. 2016; Clark 2017; Newberry 1995).

In our study, we aimed at introducing standardization and automation of training to standard tasks used in sensorimotor neuroscience in NHP and toward fully unsupervised training with self-adaptive selection of the task and of task difficulty. The idea was, as proof of concept, to instruct naive animals toward proficient performance in a memory-guided center-out reach task in an unsupervised fashion across all gradual training steps within and across sessions. With the standardization and automation and the use of a larger number of animals we aimed at two goals. First, we wanted to characterize interindividual differences in learning behavior based on performance differences between animals, e.g., to identify fast and slow learners. Second, we wanted to characterize task demand over the course of training based on commonalities in performance among animals, e.g., to identify challenging training steps for later training optimization.

For this, we developed and implemented an across-task unsupervised training protocol (AUT), particularly suited to

run cognitive task training on touchscreen-based kiosk systems in the animals home enclosure, like our previously designed XBI (Calapai et al. 2016). Inspired by other successful housing-based testing systems (Andrews and Rosenblum 1994; Bennett et al. 2016; Fagot and Bonté 2010; Gazes et al. 2013; Kangas and Bergman 2012; Richardson et al. 1990; Washburn et al. 1989; Washburn and Rumbaugh 1992), standardized training procedures developed for studying learning of certain cognitive skills in isolation (Baxter and Gaffan 2007; Crofts et al. 1999; Fagot and Paleressompoulle 2009; Fagot and Parron 2010; Hutsell and Banks 2015; Kangas et al. 2016; Mandell and Sackett 2008; Nagahara et al. 2010; Shnitko et al. 2017; Truppa et al. 2010; Washburn and Rumbaugh 1991; Weed et al. 1999), and successful approaches to automated training approaches for rodents (Duan et al. 2015), we developed a computerized training algorithm, with which we trained eight rhesus monkeys from very basic touchscreen interactions to the memory-guided reach task. We show that the AUT 1) standardizes training of animals in tasks typical for NHP cognitive neuroscience research, 2) keeps animals engaged over several months of training in their home enclosure without fluid restriction, and 3) allows for animal characterization and training optimization based on learning performance. As an example, we show that the animals’ numbers of interactions with the training device better explain the variability of training progress across monkeys than does their time spent with the training device.

MATERIALS AND METHODS

All animal procedures of this study were approved by the responsible regional government office [Niedersaechsisches Landesamt fuer Verbraucherschutz und Lebensmittelsicherheit (LAVES), Permit No. 33.9-42502-04-13/1100]. The animals were group housed with other macaque monkeys in facilities of the German Primate Center in Goettingen, Germany, in accordance with all applicable German and European regulations. The facilities provide the animals with an enriched environment (including a multitude of toys and wooden structures and natural as well as artificial light, exceeding the size requirements of the European regulations, including access to outdoor space).

The German Primate Center has several staff veterinarians that regularly monitor and examine the animals and consult on procedures. Throughout the study the animals were monitored by the veterinarians, the animal facility staff, and the laboratory’s scientists, all highly experienced and knowledgeable in working with NHPs. This study did not involve any invasive procedures, and the animals were subsequently used in other studies.

Animals. A total of eight male rhesus monkeys (*Macaca mulatta*, age: 4–7 yr) had 90 min of daily individual access (hereafter referred to as “session”) to the XBI, a housing-based and computerized interactive system (Calapai et al. 2016), from Monday to Friday with free access to water for at least 2 h before and for at least 2 h after every session [with variable delays (up to a maximum of 4 h) until water accessibility] and 24 h during both days of the weekend (with one exception: during training days animal Toa did not receive fluid before the session but after). During sessions, the participating animal was kept in a smaller (~1 or 1.8 m³) housing compartment, in auditory and visual contact with the members of its social group and of other groups in the same animal facility. All eight animals were accustomed to the XBI with at least 8 days of prior access and showed interest in repeatedly interacting with it, as described in a previous study (Calapai et al. 2016). We excluded a ninth animal, which had been part of the previous study, since it had not interacted with the XBI in this

previous study. None of the animals received specific prior training toward the behavioral tasks introduced in the current study. All animals received fruit-flavored sweetened water (Active O2 Orange; Adelhöfer Alpenquellen) diluted with plain water as reward for correct performance on the XBI.

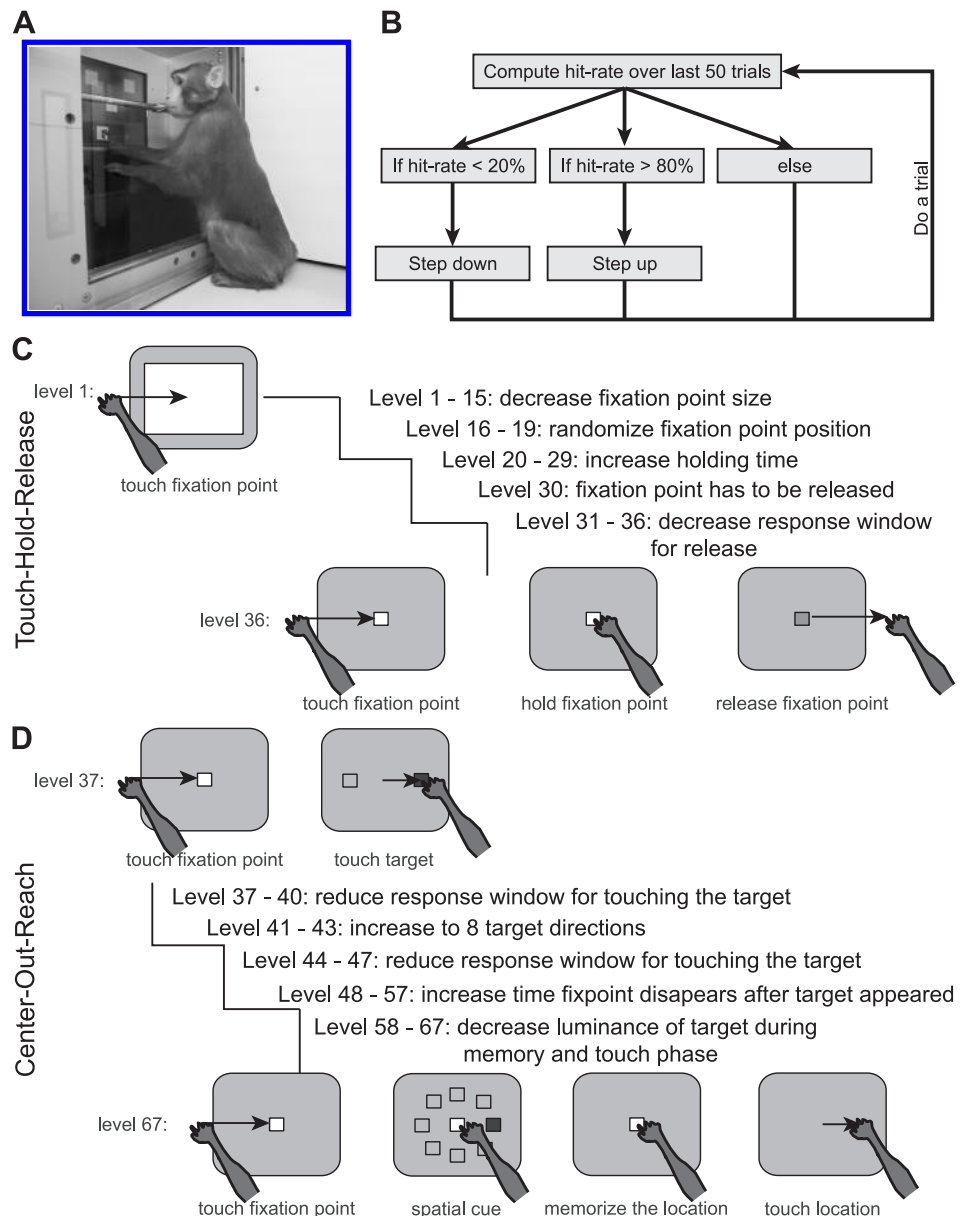
AUT protocol. All training procedures were performed on the XBI, a touchscreen-based training and testing device for rhesus monkeys, optimized for use in an animal facility (Fig. 1A) and for cognitive behavioral experiments in neuroscience (Calapai et al. 2016). Animals have access to a 15-in. touchscreen (ELO 1537L; 1,024 × 768 resolution, 75-Hz refresh, 2.5-mm touch accuracy) mounted in an aluminum frame, which replaces one wire-mesh wall panel of the housing compartment. We used three devices to simultaneously test animals belonging to three groups and housed in two different facilities.

To automate training, the AUT adjusts the complexity of the task gradually. Animals start with a very easy task and then are introduced to more and more challenging task levels and new tasks at a speed that is determined by the individual animal's performance. Within each training level, individual stimulus parameters might vary randomly

but only if these changes do not affect the practical and conceptual difficulty of the task. For example, within a training level the position of a reach target on the screen might vary randomly (if the animal has learned or is supposed to learn to generalize the target's position), but the spatial and temporal precision of the requested behavioral response (reach accuracy) does not vary. Moving to the next level will increase the task difficulty. For example, the reach target might decrease in size, thereby requiring higher reach accuracy, without changing other parameters of the task.

In the AUT, a simple staircase algorithm uses the animal's performance to determine when the current training level is incremented or decremented (Fig. 1B). If during a given experimental session the proportion of correctly executed trials over the previous 50 trials on the current level exceeds 80%, the training level is incremented (increasing the task difficulty). If performance is less than 20%, the training level is decremented (decreasing the difficulty). If performance is between 20 and 80%, the algorithm keeps drawing the trials from the current level (the difficulty stays the same while individual performance-irrelevant task parameters might vary). After every level change, the performance counter is reset and the staircase level

Fig. 1. Across-task unsupervised training (AUT) protocol. **A:** photo of a monkey working on the housing-based touch-screen device (XBI). The device shown here is an updated version of the XBI used in this study. An image of the XBI placed inside a housing facility is shown in Fig. 1A. **B:** staircase algorithm to determine the trial-by-trial training level based on the performance in the preceding 50 trials. **C:** automated touch-hold-release (THR) training protocol. Over a total of 36 different task levels the animals learn to touch a small blue square on the screen (fixation point), keep their hand on the square as long as it is visible, and release the screen within a certain response time window once the square disappears. **D:** automated memory-guided center-out-reach (COR) training protocol; following the THR training. Over a total of 30 task levels, the animals learn to touch and hold a small blue square in the middle of the screen (fixation point), remember the location of a flashing white square (target) in one out of 8 possible peripheral locations, wait for a certain instructed-delay period, release the fixation point within a certain period of time (response window) after the fixation stimulus disappears, and reach to the remembered (now invisible) target location.



remains unchanged for the next 50 trials. The performance is recalculated after each trial.

Note that, because the animal's performance is computed based on the last 50 trials at the current level, the animal needs to perform at least 50 successive trials at a level before the training can reach the next level. This means that the AUT in this configuration is not optimized for fastest possible learning progression. Note also that the initial design of the series of training levels is based on a priori assumptions of the difficulty of each level and of the transitions to the next level, based on our experience with conventional training of rhesus monkeys on these and comparable tasks (Gail and Andersen 2006; Klaes et al. 2011; Niebergall et al. 2011; Patzwahl and Treue 2009; Westendorff et al. 2010). We purposefully aimed for a mixture of easy and more challenging steps to reveal expected performance differences between animals. Importantly, we maintained the same initial parameters of all training levels and transitions across our animals in the current study to ensure comparability. When using the device outside the study for everyday training, testing, or enrichment, we routinely adapt parameters to optimize training progress or usability.

Since we did not adapt the AUT parameters, a training step in our predefined protocol might turn out insurmountable for an animal. Therefore, we defined two criteria for ending an animal's training if no training progress was observed for a prolonged amount of time (stagnation): 1) after reaching level n , the animal did not reach the next level ($n + 1$) within 25 sessions (days of training) and performed less than 1,250 trials across those 25 sessions (i.e., less than an average of 50 trials per session); 2) after reaching level n , the animal did not reach the next level ($n + 1$) within 35 sessions, independent of daily number of trials. If one of the two stagnation criteria was met, the training was ended for the animal.

We used MATLAB (MathWorks) and the graphics toolbox *gramm* (Morel 2016) for data analysis and visualization.

Touch, hold, and release task. The touch, hold, and release (THR) task is a basic task for goal-directed reaching toward visual targets on a touchscreen. To complete the 36 levels of the THR training staircase, the animal needs to learn to reach for a blue square on the screen, maintaining his touch until the square dims, and release the square within a reaction time window to receive the reward (Fig. 1C). This is achieved by 1) progressively reducing the stimulus size and hence the required reach accuracy from a width of 13–3 cm in levels 1–16; 2) randomizing the target position on the screen, first only along the horizontal, then only along the vertical axis, and finally along both axes within a square of 12-cm side length in levels 17–19; 3) increasing the required hold time from 150 ms to random times between 700 and 1,500 ms in levels 20–29; and 4) rewarding the hold and timely release rather than just the long-enough hold (level 30), and finally by gradually decreasing the reaction time window for releasing the stimulus from 1,000 to 500 ms in levels 31–36.

All eight animals participated in the training of the THR task. One of the eight animals (Fla) was removed from the study during this first phase of the experiment since the animal was needed for a different project. We still included this animal's data in the analysis, since our quantification of the results does not depend on reaching the final level.

We started the analysis of the THR task for each monkey with the session where the animal reached level 2 for the first time and ended with the session where it reached level 36 for the first time. This is because level 1 was used to habituate the animals to the device (Calapai et al. 2016), and the step from levels 36 to 37 was not automated but instead initiated by the experimenter, since it marked the transition between two training modules (see below).

Memory-guided center-out reach task. The memory-guided center-out reach (COR) task (Fig. 1D) is widely used in sensorimotor neuroscience for goal-directed motor planning based on spatial working memory content (Kuang et al. 2016; Snyder et al. 1997; Wise and Mauritz 1985). The 31 levels (levels 37–67) of the COR training

staircase are designed for animals that have learned the THR task. In the COR training, the animal has to learn to reach for the same blue screen-centered square as in the THR task, additionally remember the position of another stimulus (cue) briefly flashed at one of eight discrete peripheral locations uniformly distributed over eight positions along an invisible circle surrounding the central square, and finally reach for the memorized cue location as soon as the central stimulus disappears.

For the first COR training level (step 37), no working memory is required. The monkey has to hold the central stimulus for 500 ms and then touch the cue within a 5,000-ms reaction time window. The cue appears either left or right of the central fixation stimulus at the same time when the hand-fixation stimulus disappears ("go" cue). The AUT protocol then guides the monkeys toward the final COR task design by 1) reducing the reaction time window from 5,000 to 3,000 ms in steps 37–40; 2) randomizing the position of the cue (up/down, 4 cardinal directions relative to fixation, all 8 directions) in steps 41–43; 3) shortening the reaction time window further from 2,500 to 800 ms in steps 44–47; 4) delaying the go cue from 100 to 1,300 ms after appearance of the peripheral cue in steps 48–57 (instructed-delay reach); and finally 5) reducing the cue luminance from 50% to invisibility during the instructed delay and movement time in steps 58–67. Once the cue becomes invisible after initial presentation, the instructed reach direction has to be memorized for proper reach goal selection (memory-guided reach).

Five animals that had completed the THR training (staying on level 36 for at least 2 wk and reaching a within-level performance of 80% at least once) were available and participated in the AUT of the COR task.

Memory-guided center-out pro-anti-reach task. Additional to the main experimental design, in which we used standardized training for a larger group of animals, we also wanted to explore the power of the AUT for training a more challenging task. The pro-anti-reach (PAR) task is an extension of the COR task in which proper selection of the reach goal is contingent upon choosing the correct visual-to-motor transformation rule instructed by a colored context cue (Crammond and Kalaska 1994; Gail and Andersen 2006). The color of the peripheral cue instructs the animal either to perform a direct (pro) reach (magenta cue) or to reach the opposite location of the cue, i.e., to perform an anti-reach (cyan cue). For training of the PAR task, we adapted the staircase such that not all animals in this third training phase experienced the exact same protocol. Therefore, only anecdotal results will be reported. We consider them noteworthy, since the PAR task represents an advanced level of task difficulty relevant for cognitive neuroscience, particular the analysis of context-dependent goal-directed behavior (Gail and Andersen 2006; Klaes et al. 2011; Westendorff et al. 2010). Three of the four animals that had completed the final level of the COR task (Chi, Gro, and Zep) participated in the PAR task. We used a small subset of animals only, since for the other animal this advanced task was not relevant for its later use in neuroscience projects.

RESULTS

The aim of this study was to test the suitability of standardized and automated protocols for training rhesus monkeys. Table 1 shows an overview of the overall performance of all monkeys that took part in this study for the THR and COR task training. Five out of seven animals completed the full THR training staircase, requiring between 13 and 120 sessions and between 4,680 and 11,778 trials (correct and error trials) to progress through the 36 THR task training levels. While the number of trials needed partially scales with the number of sessions needed, the amount of trials and of sessions was not directly related. Animals Odo and Toa stagnated at levels 26 and 30, respectively in the THR task. Animal Odo successfully

Table 1. Overview of participating animals

Monkey	Touch-Hold-Release		Center-Out-Reach		Final Level
	Trials	Sessions	Trials	Sessions	
Alw	5,052	20	14,184	71	67
Chi	11,778	33	20,272	57	67
Gro	5,787	23	24,511	126	67
Zep	4,680	13	18,639	59	67
Nor	8,148	120	28,391	160	63
Toa	8,424	83			30
Fla	8,961	46			30*
Odo	4,254	64			26

The table shows the number of trials/session the animals performed in each task. “Final Level” denotes the maximally reached level, where touch-hold-release (THR) covers levels 1–36 and center-out-reach (COR) levels 37–66. “Trials” denotes the total number of trials (successful or not) needed to reach the highest achieved level within the training for this task, and “Sessions” denotes the corresponding number of training sessions. Animals Alw, Chi, Gro, and Zep finished both tasks; Nor finished THR but not COR; and Odo, Toa, and Fla did not finish THR and thus did not participate in COR. *Animal Fla was taken out of the experiment for reasons unrelated to the current study.

accomplished to touch the target stimulus but not to hold for a prolonged period of time. The training was ended when animal Odo performed 25 sessions with <50 trials on average after reaching level 26 (criterion 1). Animal Toa accomplished holding the stimulus but did not learn to release it in response to its dimming. The training was stopped when animal Toa did not reach level 31 within 35 sessions after reaching level 30 (criterion 2).

Four out of five animals mastered the final level of the COR task. Again, the numbers of sessions and trials needed varied substantially (57–126 sessions, 14,184–24,511 trials) even if considering only the successful animals. Given that the training was standardized across animals, this large variability in number of sessions and trials needed to learn the task must reflect an interindividual variability of the learning progress, which we will analyze below. Animal Nor, stagnating at level 63 in the COR task, learned to wait for the reach instruction before reaching to the target (instructed-delay task) but did not learn to memorize the target position. Animal Nor did not reach level 31 within 35 sessions after reaching level 30 (criterion 2).

Three out of the four animals that had been successful in the COR task were included in the PAR task staircase training. For two of the animals, we modified the staircase in response to performance difficulties that both animals encountered at the same level of the PAR staircase (see below for a discussion of this deviation from our otherwise strict adherence to the initial staircase parameters). Since the stagnation added extra sessions to the training, the PAR learning is not fully comparable across animals anymore and thus not included in Table 1 and the corresponding analysis.

Note that the first and last steps of the THR task (level 1 and 36) are excluded from all analyses because level 1 was identical to the task used to initially accustom the animals to the XBI (Calapai et al. 2016) and the transition to COR (level 36 and 37) was not automated. Excluding these two levels ensures that our analysis only includes automated level transitions.

Motivated by the observed variability in training progress, we analyzed the learning progress across and within animals for the THR and COR training protocols for two different purposes. First, we used the performance data from the AUT to

quantify interindividual differences between animals and to test whether time spent in training or experience with the task better explains the average training progress of animals. Second, we used the performance data to characterize different phases of the training protocols in terms of their difficulty for the animals.

Performance in THR and COR task. Over the course of 2 yr, we collected data from 874 training sessions (13 sessions excluded due to technical malfunctions). The daily number of interactions with the XBI differed substantially between and within animals, as did the within-animal spread. Figure 2 plots the number of interactions per session (1 session per working day) for each animal. The median number of interactions varied from 43 trials (Odo) to 380 trials (Chi). The difference between the 25th and 75th within-animal percentile varied from 78 trials (Odo) to 259 trials (Zep). While the amount of interactions per session of an animal partly varied over the course of the study, none of the animals stopped interacting completely with the device. A more detailed illustration of the average amount of interactions as function of session number can be found in the APPENDIX (see Fig. A2).

All animals had been habituated to the XBI before study begin (Calapai et al. 2016), so that they knew that a successful interaction with the touchscreen would cause flavored water to be dispensed. The progress for stepwise learning of the two new tasks (THR and COR) is shown in Fig. 3 for each animal. In general, the achieved level of difficulty increased monotonically for all animals, with slower speed of progression at higher training levels in both tasks. When plotted as a function of session number (a proxy for exposure time; Fig. 3, right), the achieved level of difficulty after a certain time differed between animals up to a factor of 2–3. When the same performance data were analyzed as a function of number of trials performed in each training protocol (a proxy for task experience; Fig. 3, left), the spread between animals was reduced. This suggests that learning progress does not depend on the time of exposure to the task but rather the experience gained through individual interactions with the task.

To test for the effect of exposure time vs. task experience on the learning progress we determined the level demand, i.e., how long it takes an animal to accomplish each training level. We computed the level demand both as the time (in minutes, including time within and between trials) and the number of

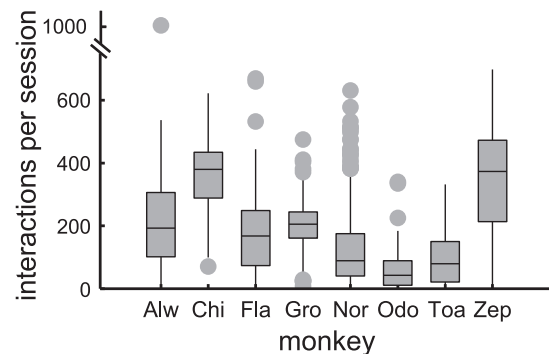


Fig. 2. Performance of individual animals. Number of touchscreen interactions per session for each monkey during the THR and COR tasks. The boxplot indicates median (middle line) and 25th to 75th percentile (box). The whiskers correspond to $q_{75} + 1.5(q_{75} - q_{25})$ and $q_{25} - 1.5(q_{75} - q_{25})$, where q_{25} and q_{75} are the 25th and 75th percentiles. Data points exceeding this range are plotted individually.

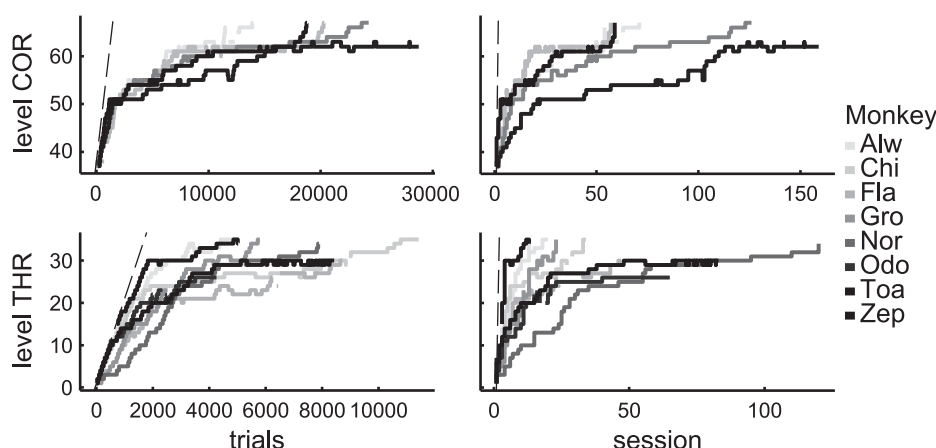


Fig. 3. Learning progress. Training progress of individual animals over time during the THR (*bottom*) and the COR training (*top*). Training progress is plotted against number of trials (*left*) and sessions (*right*) conducted on the XBI. The dashed lines represent the fastest theoretically possible training progress, which was 1 level per 50 trials (*left*) and maximum of 33 levels per 90 min session (*right*), given the minimal mandatory trial-to-trial delay of 3.3 s.

trials needed by each animal for reaching a certain level for the first time, after they reached the preceding level for the first time (Fig. 4, *inset*). By comparing the average level demands across levels (Fig. 4), we can identify individual levels or phases of the training for which the animals needed more time or attempts. As an example, between levels 58 and 67, the luminance of the touch target decreased stepwise until it reached threshold visibility. Around level 62, the touch target was not visible anymore for the animals so that they needed to memorize the visual cue shown at the beginning of the trial to know the correct touch position (memory-guided reach). Since most of the animals spent more trials on this level compared with the average of the other levels, we can infer an elevated difficulty for this level. In this way, the AUT approach can be used to evaluate a given training strategy and identify the difficulty of each training step within this strategy.

Some animals needed longer than others to complete a staircase or certain levels of it. To quantify the interindividual variability, we determined the difference in this variability if demand is quantified via time exposed to the XBI or the number of trials. For each level, we thus computed the coefficient of variation across animals of the time demand in minutes CV_{time} and trial demand CV_{trial} : $CV = \sigma/\mu$, where σ is the standard deviation and μ is the mean. Figure 5 shows the distributions of CV_{time} and CV_{trial} . On average CV_{time} was 1.15 and higher than CV_{trial} , which was 0.84 (Wilcoxon signed rank test, $P < 0.001$). This indicates that experience with the task rather than time spent on the task is a better predictor for the learning progress.

PAR task. The idea behind the PAR task staircase, which was run only with few animals and was not as strictly pre-

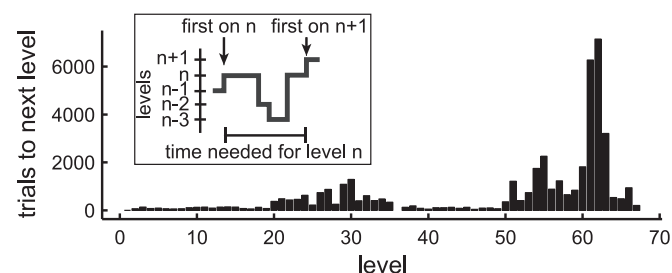


Fig. 4. Level demand. Average amount of trials animals needed to complete each training level (level demand). The horizontal axis indicates all levels within the THR task (1–35) and COR task (37–67). The inset shows how to compute the level demand.

defined as the other training protocols, was to provide a proof-of-concept that the animals could also be trained on more advanced rule-based cognitive tasks with our standardized algorithm-based training protocol. In contrast to COR, the visual cue in PAR is presented in either of two colors instructing to touch the location of the cue (as in COR) or opposite to it starting from the position in the middle of the screen (see MATERIALS AND METHODS). In our experience, such rule-based tasks can pose some challenges even when taught to rhesus monkeys by experienced trainers.

After two animals stagnated at the same training level (dimming of an auxiliary target stimulus at the anti-position to render it invisible), we modified this training level (by delaying the disappearance of the salient auxiliary stimulus until after reach onset but before reach termination). Using this modified approach, both animals succeeded in learning the memory-guided anti-reaches, although one of the two animals did not generalize the anti-rule to all reach directions. The third animal that arrived at this level later did not manage to pass the level, despite the modified strategy. One of the first animals, monkey Chi, learned the final level of the PAR task and performed it with a success rate of 71%.

DISCUSSION

Eight rhesus monkeys were trained on a visually instructed reach task with increasing complexity on a touchscreen device within their housing environment using an across-task unsupervised training (AUT) protocol (Fig. A1). Within our rigid

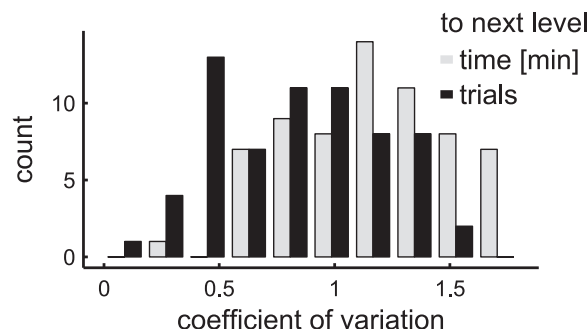


Fig. 5. Interindividual variability of level demand. Distributions of the coefficient of variation (CV) of the time animals needed to reach a level after they reached the previous level for the first time. CVs were computed for number of trials (dark) or time in minutes (light).

training schedule, stagnation criteria, and the free access to fluid, five of the eight animals succeeded in learning a simple touchscreen interaction task [touch-hold-release (THR)] and continued training in a standard task for sensorimotor research, the memory-guided center-out reach (COR). Four of these five animals were able to complete this training staircase and three of them continued to an extension of the COR, the pro-anti-reach task (PAR), the last level of which was reached and completed by one animal only. By comparing the learning behavior between animals, we found that the learning progress was better predicted by the amount of trials rather than by the time spent training. Additionally, the unsupervised nature of the training progress allowed us to identify easy as well as difficult steps of the tasks, which in turn helped in the evaluation of the effectiveness of our training approach. Finally, all animals continued to use the device over several months despite fluid and food intake not being restricted outside the training sessions, suggesting that the AUT of cognitive tasks is a valuable tool for environmental enrichment (Clark 2017).

Unbiased behavioral training and assessment of learning performance. In cognitive neuroscience research with NHPs, monkeys are often required to solve complex cognitive tasks, for which the learning process requires extensive training. Some factors that influence training duration are task difficulty, physical and cognitive effort, motivation level of the animal, reward attractiveness, group rank, and training strategy. The latter is set by the trainer and hence is influenced by the trainer's subjective decisions on which task level to offer to the animal on daily basis. Also, despite mostly automated experimental control software being in place, well-intended direct interactions such as seemingly minor adjustments of task parameters based on a subjective estimate of the animal's performance will interfere with the learning process. In the worst case, this could lead to undesired behaviors. At the least, it leads to idiosyncratic training protocols for individual animals, which makes performance comparisons between animals difficult to impossible. In the AUT, the training strategy is still set by the trainer but predefined and can be applied to each animal in the same manner. Compared with more traditional types of training in NHP neuroscience, the AUT procedure ensures that differences observed when comparing learning progress do not reflect a trainer or experimenter bias since all the animals underwent exactly the same routine.

Moreover, a direct and unbiased comparison of the learning behavior shown by different animals in the same learning protocol is essential for quantifying the spectrum of cognitive skills within a group of animals (Andrews and Rosenblum 1994; Evans et al. 2008; Fagot and Paleressompoulle 2009; Harlow 1949; Hutsell and Banks 2015; Kangas et al. 2016; Truppa et al. 2010; Washburn and Rumbaugh 1992; Weed et al. 1999) or between species (Amici et al. 2010; Crofts et al. 1999; Herrmann et al. 2007; Rogge et al. 2013; Schmitt et al. 2012) or identifying animals particularly suited for specific research projects (Capitanio et al. 2006).

Given that our approach removes trainer effects from the list of factors potentially influencing learning progress, this should enable a closer look at other factors. For example, we used the same reward for all animals, which is likely more attractive for some animals than for others, and we did not systematically investigate the influence of the social rank of our animals.

Interindividual variability in learning. When designing AUT staircases, we aimed for a steady increase in difficulty at a moderate speed to minimize the risk of insurmountable conceptual changes of task rules. To ensure identical conditions across animals we maintained a rigid training schedule and unchanged stagnation criteria. Under these conditions one animal (Nor) did not complete the COR task before the stagnation criteria were reached and two (Odo and Toa) did not complete the preceding THR task. Interestingly, these three animals performed on average the least number of interactions per day on the device (Fig. 1), suggesting that interaction behavior with the device could be a quantitative predictor of long-term performance. To look at this more closely, we investigated which interaction dimension, trials performed or time spent practicing, would best predict the animals' learning, by looking at the variability across the learning curves. We found the variability to be lower when progress was measured across number of interactions (or trials) rather than absolute time spent on the device. This result suggests that the number of trials performed is a better predictor of the training progress of a given animal, than the amount of time the animal spends practicing a given task. Note, we do not think that the low number of interactions in the poorly performing animals was due to excessive task demand, since below-average interaction was noticeable from early during the training when the task was still rather trivial (Fig. A2).

The observed correlation between number of interactions with the XBI and learning progress has twofold implications. First, maximizing the number of interactions per session by creating additional incentives for conducting the task should lead to a gain in learning progress. This will be discussed further when comparing conventional training approaches below. Second, the variability in housing-based training performance might be used to preselect animals for research projects requiring complex and demanding tasks (either cognitive and/or physical). While any form of performance-based animal preselection obviously prohibits scientific conclusion on the general cognitive capacities of the species as such in comparative studies, in other fields such as cognitive neuroscience it might still be justified to select those individuals, which reach a certain experimental level faster than others for reasons of practicality and animal welfare.

Optimizing training protocols. By measuring the number of trials different animals needed on average to master a certain level, we learned about the inherent difficulty of that level. This measure can be used to evaluate the training approach implemented by the predefined set of levels. For instance, the first 20 steps of the THR task seem to be very easy for all the animals, since most animals performed at or close to the maximum possible speed of progression (dashed line in Fig. 3). Thus, by skipping several of those early levels, it might be possible to speed up the training. On the other hand, level 30, having the highest amount of trials across all animals in the THR task, seems to be the most difficult. In fact, it is the level where two animals dropped out due to lack of learning progress.

Beyond the study presented here, it would be useful to expand our automated approach to reduce the risk of animals stagnating. To optimize the training strategy toward a constant moderate task difficulty over the whole training, easy levels could be omitted and difficult levels could be broken down or adjusted. This avoids unnecessary idling at trivial levels and at

the same time keeping the risk of stagnation low. Expanding the adaptivity of our staircase by also iteratively changing the parameters of the staircase steps based on the recent history of the individual animal's progress would thus boost the effectiveness of the unsupervised approach.

The above approach is advisable if the goal is to guide as many animals as possible toward successful completion of the final task level without investing unnecessary training time and without frustrating the animal with excessive cognitive demands. If, on the other hand, the goal is to emphasize interindividual performance differences and titrate the lower and upper end of the performance spectrum, one would purposefully use a broad spectrum of level demands, including moderate and more advanced training levels, to reveal the highest variability across animals. The task levels then should be easy enough for most animals to succeed but too difficult for all to master them trivially. By fanning out the performance across animals, interindividual differences become particularly apparent and one can identify the best performers.

Using such training approach with a large spectrum of task difficulties would be useful in cases of larger variability of cognitive abilities, such as in interspecies comparisons (Amici et al. 2010; Herrmann et al. 2007; Rogge et al. 2013; Schmitt et al. 2012).

By employing such a multifaceted training procedure, it will be possible to identify the relative difficulty related to certain aspects of the task. The pattern in Fig. 4 could mark a species- or animal-specific learning profile useful for characterization of cognitive skills and thereby serve as a cognitive fingerprint. For example, as seen in Fig. 4, the animals needed more trials to accomplish levels 58–67 (waiting for the cue to respond) than levels 48–57 (memorizing the target location). This could indicate that rhesus monkeys find it easier to learn withholding an action for a few hundred milliseconds than to learn memorizing a certain spatial position for the same time. Quantifying the learning progress, especially by means of AUT, could in turn help mitigating confounds related to the human administration of the tasks, typical for studies employing test batteries (Herrmann et al. 2007). Although beyond the scope of the present study, we believe that the approach so far discussed might help dissociating the social components of primate cognition, an important challenge in the field of primate cognition (Schmitt et al. 2012; Seed and Tomasello 2010).

Environmental enrichment. Recently, a study proposed housing-based training as a valuable tool for environmental enrichment of captive NHPs (Bennett et al. 2016). Our automated and standardized approach to cognitive training resembles some of the key features of what make a good environmental enrichment tool (Clark 2017; Murphy et al. 2003).

Environmental enrichment ideally expands the possibilities for species-specific behavior (Newberry 1995). A useful enrichment tool thus triggers the interest of animals and keeps them engaged for an extended period of time. While monkeys explore new devices for a short period due to curiosity, primary reinforcers, such as food, seem to prolong the interest of an animal into a certain activity. However, even with primary reinforcers, a within-session reduction in the number of interactions has to be expected due to habituation (McSweeney et al. 1991). We observed that across sessions only one of the animals stopped working on the task (Fig. A2), even though they were not subject to fluid or caloric control schedules. Only

animal Odo stagnated in training due to a low interaction rate (criterion 1), but note that this animal performed dozens of previous sessions with substantially higher interaction rates with the device. Our experiment was not built to test the habituation hypothesis. Yet, our results suggest that a dynamic device that changes gradually but constantly is less likely to lead to habituation and hence might be particularly suited as enrichment tool as it keeps the animal engaged for an extended period of time (Tarou and Bashaw 2007). It should be noted, although, that in the current phase of the project the animals were in a compartment connected to, but separated from, their group-housing compartment for the training. There, the environment was less varied than in their housing compartment during the rest of the day. The lack of other opportunities might have triggered some of the interactions with the device. On the other hand, occasional access to other objects or peers in the adjacent compartment did not seem to have a negative effect on the motivation to interact with the device.

Comparison to standardized learning tasks used in behavioral and cognitive studies. Standardized cage-based cognitive testing is well established in behavioral and cognitive research (Washburn et al. 1989; Richardson et al. 1990; Washburn and Rumbaugh 1992; Andrews and Rosenblum 1994; Fagot and Bonté 2010; Kangas and Bergman 2012; Gazes et al. 2013; Bennett et al. 2016). In this research, learning progress has been systematically quantified with experimental paradigms measuring the success rate or the number of trials needed to reach a criterion (Washburn and Rumbaugh 1991; Crofts et al. 1999; Weed et al. 1999; Baxter and Gaffan 2007; Mandell and Sackett 2008; Fagot and Paleressompoulle 2009; Fagot and Parron 2010; Nagahara et al. 2010; Truppa et al. 2010; Hutsell and Banks 2015; Kangas et al. 2016; Shnitko et al. 2017). For studies of complex behavior, there is the need to learn a combination of cognitive and motor skills. For example in the PAR task subjects have to 1) learn how to precisely handle a touch screen, 2) react only upon cue appearance, 3) memorize sets of spatial locations, and 4) understand and integrate contextual information from multiple cues. It is an important challenge to quantify the step-by-step learning in such paradigms. The AUT employs a series of small increments in task difficulty matched to the animal's own learning pace in an unsupervised across-session manner, allowing quantification of the learning performance of each level. This strategy might be especially useful when training animals to a new type of task that is not yet well characterized.

Across NHP tasks with various movement requirements, such as saccades (Yao et al. 2016), button presses (Niebergall et al. 2011), touchscreen interactions (Klaes et al. 2011), three-dimensional joystick (Morel et al. 2015), or large hand/arm movements (personal observation), we observe a decline of the number of interactions as a function of the physical effort involved. Both tasks in the present study involved touching a stimulus on the screen for up to more than a second without an arm rest, a considerable effort when repeated many hundred times within one session. Nonetheless, 7 out of 8 animals performed on average more than 100 trials per session, over many months and despite no food or fluid restriction.

Automated housing-based training vs. conventional laboratory-based training. Our approach allowed us to train animals without fluid or caloric control schedules and without time-consuming supervision by an experimenter. Four out of seven

animals learned a full memory-guided COR task, a standard task in cognitive neuroscience. However, compared with standard training approaches, this is a low success rate given the type of task. Also, there are several additional disadvantages in comparison to conventional neuroscience training where the animal sits in a primate chair. First, even the four best animals, which finished the COR task, still needed on average 77.3 sessions and 19,285 trials to learn the COR task, not considering THR training before. Five animals, which we trained conventionally, i.e., with fluid control, learned the almost identical task on average in 16.8 sessions and 8,488 trials (Gail and Andersen 2006; Klaes et al. 2011) (see APPENDIX). This means that fluid control schedules for increasing the perceived value of fluid rewards decreased the total training period on average by a factor of 4.6, a reduction in overall training duration of 2–3 mo. This suggests that the stagnation in training due to a low interaction rate of one of our animals (Odo) with the device might have been prevented by using fluid control or a different reward regime. Second, most cognitive neuroscience tasks require devices other or additional to a touchscreen, such as eye tracking, joysticks, or three-dimensional vision. Especially scientific or technical constraints that mandate steady head position or body posture are much harder if not impossible to implement in a housing-based training device. Third, training within the housing environment introduces additional distracting stimuli, which cannot be controlled for, such as various noise sources, personnel entering the room, and other monkeys in view. Fourth, the conventional training is already performed inside the experimental setup, which the monkey needs to be accustomed to before invasive experimental procedures start. It is not clear yet how well monkeys will generalize a complex task from the housing-based to a laboratory-based setting, but the recent study of Tulip et al. (2017) suggests that a knowledge transfer is likely at least for simple button-press tasks.

Finally, a well-experienced trainer should be able to adapt a training protocol to an individual animal in a way that is beneficial for a fast training progress. Part of the reported difference in the speed of learning between our AUT approach and the conventional training could be explained by the fact that our automated algorithm was not optimized for speed and animals spent an unnecessarily long time on easy task levels. It was not the primary aim of our study to develop the fastest and most efficient training strategy. We designed the AUT to serve as a new approach to train animals to various, more or less complex tasks in their own housing environment. Therefore, various features could be easily implemented in the AUT if learning needs to be accelerated. For example, 1) in cage-based training within the housing environment, the exposure time to the training device could be considerably prolonged (Fagot and Paleressompouille 2009); 2) to increase the animal's motivation to perform more trials per session, food or fluid intake could be controlled (Evans et al. 2008); and 3) the training algorithm could be improved by taking into account the individual animal's recent learning history. On the other hand, deviating from a predefined training protocol bears the risk of introducing variable learning histories, potentially confounding later results of cognitive testing and neurophysiological recordings. An attractive “best-of-both-worlds” approach could be, for example, to combine the automated approach with fluid control schedules and to optimize the algorithm for learning speed,

while not giving up on the standardization of the training across animals. Similarly, cage-based training using AUT, employed for pretraining to the cognitive task, could be combined with the laboratory-based setting to accustom the animal to the experimental environment and for the final training.

Conclusion

Our study shows that housing-based unsupervised training is suitable to aid animal training for cognitive neuroscience research, despite slower training progress compared with traditional setup-based approaches. Using our XBI device (Catalpai et al. 2016), we demonstrate that it is possible to teach rhesus monkeys demanding behavioral paradigms used in cognitive neuroscience research by employing an across-task unsupervised training protocol. Such an approach can be used even in housing settings without setups for neuroscience training and research. By providing an animal more choice in when and how much it engages in the training, it gains an increased level of control over its environment, which benefits welfare. Providing training opportunities in the familiar housing environment might also be beneficial for practicing difficult training steps accelerating the setup-based training. Furthermore, our AUT, which increases in difficulty according to the animal's abilities, keeps the animal engaged with the device over extended periods. This supports the usability of the XBI as an enrichment tool for animals in their home cage.

APPENDIX

Comparison with conventionally trained animals. To get an intuition on how automated training matches conventional training in a neurophysiology setup, we compared the COR training progress of the XBI animals with five animals trained with the conventional approach (Gail and Andersen 2006; Klaes et al. 2011). The latter animals were seated in a primate chair in front of a touchscreen in the experimental setup separated from their home environment. All of



Fig. A1. XBI inside a housing environment. The XBI replaces a wall of a single cage compartment (back, displays a task not used in this study). An opening connects those compartments to the housing cage of the social group (right). During a training session, the animal was isolated in the compartment with the XBI attached.

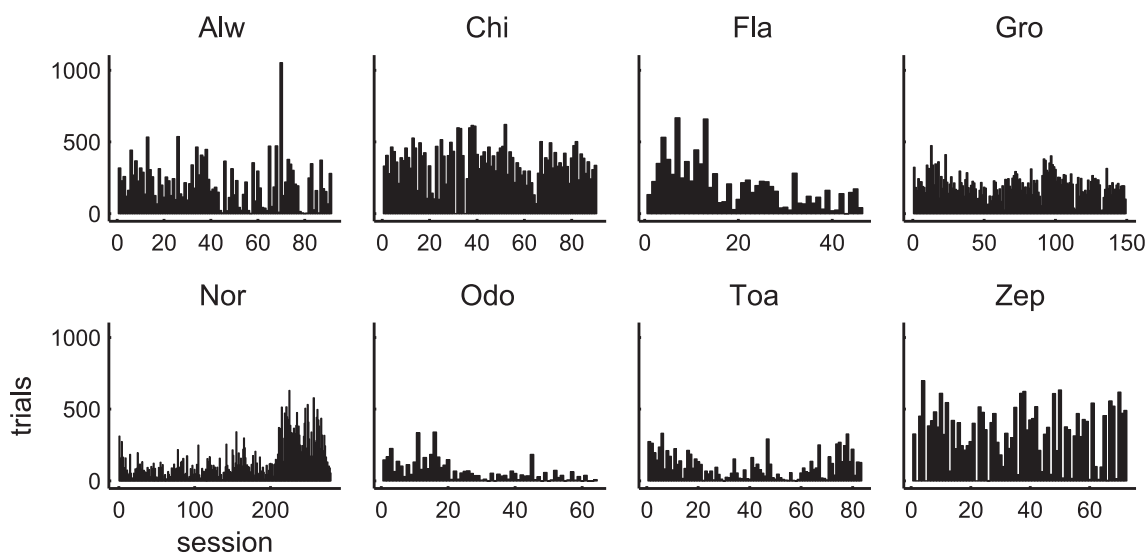


Fig. A2. Individual performance over the course of the study. Number of trials per session all animals performed on the XBI over the course of the study.

them received the majority of their fluids during working days through training contingent upon performance. The duration of a given session was determined by the assessment of the experimenter of the animal's motivational state, i.e., the sessions were ended when the animal indicated no further interest in continuing the training for this day. To reduce variability introduced by different trainers, we included only animals trained under the guidance of the same experienced trainer (author A. Gail). Note that the conventionally trained animals, different to the XBI animals, were not trained on the THR task before, but all animals were familiar with the general setting and the fact that touching the touchscreen can trigger a reward. Although all XBI animals learned COR after THR, the COR task was designed in a way that it could also be trained to naive animals. Furthermore, we designed the automated COR training that it resembles the conventional training strategies.

The conventional training strategies, although slightly varied across animals, always followed three main training steps: 1) direct reach, accurately touching a visual stimulus in the center of the screen (fixation point) to then touch a second visual stimulus in the periphery (target) (corresponding to levels 37–47 of the COR); 2) delayed reach, holding the fixation point until its disappearance before touching the target, i.e., fixation and target stimulus overlap in time (corresponding to levels 48–57 of COR); memory reach, memorizing the target's location and reaching for it after it had disappeared (corresponding to levels 58–67).

Here, we report the total number of sessions (Fig. A3, left) and number of trials (Fig. A3, right) each animal needed to succeed in a

given phase. With the automated XBI training reported in the main text, animals learned COR in 77.5 sessions and 19,348 trials on average. In conventional training including fluid control, animals learned COR on average in 16.8 sessions and 8,488 trials. It means that animals trained on the XBI needed 2.3 times more trials to learn COR than animals in the conventional setup and 4.6 times more training sessions.

Certainly one reason for the slower progression in the XBI training was the fixed training strategy predefined in automated training, which was not designed to optimize training speed but to be easy enough to potentially lead the most animals through the training. In conventional training, trainers had the opportunity to adapt to the individual animal's performance more flexibly than the staircase algorithm does. This could explain why XBI animals needed more trials than conventionally trained animals to achieve the same task level. It also suggests that the difference could likely be reduced by more advanced staircase algorithms optimized for fast adaptation.

Another reason certainly was that animals in conventional training, even though in a very early phase of training and not used to longer training sessions yet, performed on average 505 trials per session while animals in automated training performed 250 trials per session. This difference cannot be attributed to a suboptimal staircase algorithm. Factors contributing to this difference likely are 1) the increased incentive of the reward due to water control; 2) more focused animals in the conventional setup due to a less distracting environment; and 3) the fact that XBI sessions lasted always 90 min while in

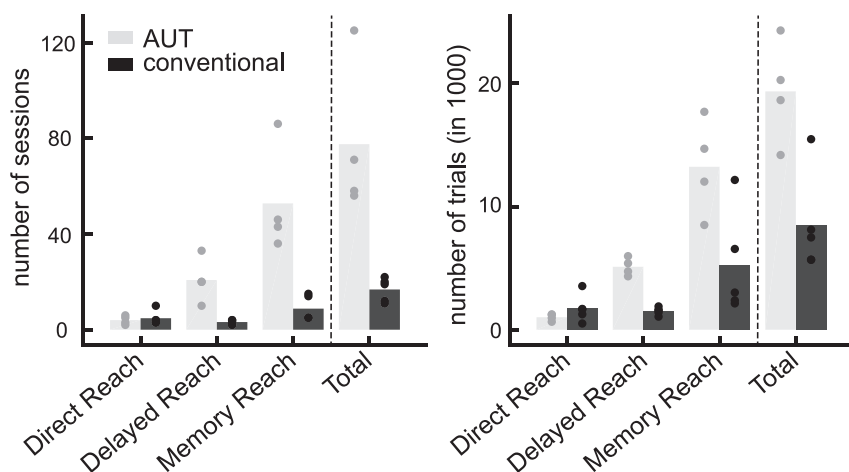


Fig. A3. Comparison with conventional training. Number of sessions (left) and number of trials (right) performed in COR training by animals trained with AUT (light) or conventionally (dark). COR training can be divided in three phases: direct reach (levels 37–47), delayed reach (levels 48–57), and memory reach (levels 58–67). Only animals that learned COR were considered. Dots indicate individual animals. Bars represent the mean values over the animals.

conventional training the duration of session was determined by the experimenter judging the animal's motivation to carry on or not with the session.

Given that training strategies and conditions varied substantially, the results from a comparison between these approaches deserve some clarifications. First, in the conventional approach animals did not experience the perfectly same training. Even though at least the supervising trainer (not necessarily the executing trainer) was the same person, the training approaches likely varied due to skill improvements or different personal bonds of the trainers with the animals. Second, animals in the automated training were already trained to THR and only those animals that succeeded in THR and COR were added to the comparison, whereas no criterion was applied to preselect conventionally trained animals. In this sense, the observed difference in learning speed is a conservative estimate and true differences could be even larger.

In conclusion, our comparison of the two approaches has to be taken with some care, since not all relevant parameter could be matched retrospectively. It is only meant to give an intuition on how the same training level can be reached either with the aid of an automated algorithm in an unsupervised fashion or with conventional training, with each of them having their own benefits and disadvantages.

ACKNOWLEDGMENTS

We thank Cheng Xue, Pinar Yurt, Laura Molina, Peter Neumann, Christin Schwarz, and Baltasar Rüdhardt for help with data collection.

GRANTS

This project was supported by the European Commission (ec.europa.eu/research/fp7) in the context of the EUPRIM-Net-II consortium (FP7-262443-WP9 to A. Gail) and the German Research Foundation (www.dfg.de) in the context of the RU1847 (GA1475-C1 to A. Gail and S. Treue).

The funders had no role in study design, data collection and analysis, decision to publish, or preparation of the manuscript.

DISCLOSURES

No conflicts of interest, financial or otherwise, are declared by the authors.

AUTHOR CONTRIBUTIONS

M.B., A.C., V.S., M.N., L.B., A.G., and S.T. conceived and designed research; M.B., A.C., V.S., M.N., and L.B. performed experiments; M.B. analyzed data; M.B., A.C., V.S., M.N., A.G., and S.T. interpreted results of experiments; M.B. prepared figures; M.B. and A.C. drafted manuscript; A.G. and S.T. edited and revised manuscript; M.B., A.C., V.S., M.N., L.B., A.G., and S.T. approved final version of manuscript.

REFERENCES

- Amici F, Aureli F, Call J.** Monkeys and apes: are their cognitive skills really so different? *Am J Phys Anthropol* 143: 188–197, 2010. doi:[10.1002/ajpa.21305](https://doi.org/10.1002/ajpa.21305).
- Andrews MW, Rosenblum LA.** Automated recording of individual performance and hand preference during joystick-task acquisition in group-living bonnet macaques (*Macaca radiata*). *J Comp Psychol* 108: 358–362, 1994. doi:[10.1037/0735-7036.108.4.358](https://doi.org/10.1037/0735-7036.108.4.358).
- Baxter MG, Gaffan D.** Asymmetry of attentional set in rhesus monkeys learning colour and shape discriminations. *Q J Exp Psychol (Hove)* 60: 1–8, 2007. doi:[10.1080/17470210600971485](https://doi.org/10.1080/17470210600971485).
- Bennett AJ, Perkins CM, Tenpas PD, Reinebach AL, Pierre PJ.** Moving evidence into practice: cost analysis and assessment of macaques' sustained behavioral engagement with videogames and foraging devices. *Am J Primatol* 78: 1250–1264, 2016. doi:[10.1002/ajp.22579](https://doi.org/10.1002/ajp.22579).
- Calapai A, Berger M, Niessing M, Heisig K, Brockhausen R, Treue S, Gail A.** A cage-based training, cognitive testing and enrichment system optimized for rhesus macaques in neuroscience research. *Behav Res Methods* 5: 1–11, 2016. doi:[10.3758/s13428-016-0707-3](https://doi.org/10.3758/s13428-016-0707-3).
- Capitanio JP, Kyes RC, Fairbanks LA.** Considerations in the selection and conditioning of Old World monkeys for laboratory research: animals from domestic sources. *ILAR J* 47: 294–306, 2006. doi:[10.1093/ilar.47.4.294](https://doi.org/10.1093/ilar.47.4.294).
- Clark FE.** Cognitive enrichment and welfare: current approaches and future directions. *Anim Behav Cogn* 4: 52–71, 2017. doi:[10.12966/abc.05.02.2017](https://doi.org/10.12966/abc.05.02.2017).
- Crammond DJ, Kalaska JF.** Modulation of preparatory neuronal activity in dorsal premotor cortex due to stimulus-response compatibility. *J Neurophysiol* 71: 1281–1284, 1994. doi:[10.1152/jn.1994.71.3.1281](https://doi.org/10.1152/jn.1994.71.3.1281).
- Crofts HS, Muggleton NG, Bowditch AP, Pearce PC, Nutt DJ, Scott EA.** Home cage presentation of complex discrimination tasks to marmosets and rhesus monkeys. *Lab Anim* 33: 207–214, 1999. doi:[10.1258/002367799780578174](https://doi.org/10.1258/002367799780578174).
- Duan CA, Erlich JC, Brody CD.** Requirement of prefrontal and midbrain regions for rapid executive control of behavior in the rat. *Neuron* 86: 1491–1503, 2015. doi:[10.1016/j.neuron.2015.05.042](https://doi.org/10.1016/j.neuron.2015.05.042).
- Evans TA, Beran MJ, Chan B, Klein ED, Menzel CR.** An efficient computerized testing method for the capuchin monkey (*Cebus apella*): adaptation of the LRC-CTS to a socially housed nonhuman primate species. *Behav Res Methods* 40: 590–596, 2008. doi:[10.3758/BRM.40.2.590](https://doi.org/10.3758/BRM.40.2.590).
- Fagot J, Bonté E.** Automated testing of cognitive performance in monkeys: use of a battery of computerized test systems by a troop of semi-free-ranging baboons (*Papio papio*). *Behav Res Methods* 42: 507–516, 2010. doi:[10.3758/BRM.42.2.507](https://doi.org/10.3758/BRM.42.2.507).
- Fagot J, Paleressompouille D.** Automatic testing of cognitive performance in baboons maintained in social groups. *Behav Res Methods* 41: 396–404, 2009. doi:[10.3758/BRM.41.2.396](https://doi.org/10.3758/BRM.41.2.396).
- Fagot J, Parron C.** Relational matching in baboons (*Papio papio*) with reduced grouping requirements. *J Exp Psychol Anim Behav Process* 36: 184–193, 2010. doi:[10.1037/a0017169](https://doi.org/10.1037/a0017169).
- Gail A, Andersen RA.** Neural dynamics in monkey parietal reach region reflect context-specific sensorimotor transformations. *J Neurosci* 26: 9376–9384, 2006. doi:[10.1523/JNEUROSCI.1570-06.2006](https://doi.org/10.1523/JNEUROSCI.1570-06.2006).
- Gazes RP, Brown EK, Basile BM, Hampton RR.** Automated cognitive testing of monkeys in social groups yields results comparable to individual laboratory-based testing. *Anim Cogn* 16: 445–458, 2013. doi:[10.1007/s10071-012-0585-8](https://doi.org/10.1007/s10071-012-0585-8).
- Harlow HF.** The formation of learning sets. *Psychol Rev* 56: 51–65, 1949. doi:[10.1037/h0062474](https://doi.org/10.1037/h0062474).
- Herrmann E, Call J, Hernandez-Lloreda MV, Hare B, Tomasello M.** Humans have evolved specialized skills of social cognition: the cultural intelligence hypothesis. *Science* 317: 1360–1366, 2007. doi:[10.1126/science.1146282](https://doi.org/10.1126/science.1146282).
- Hutsell BA, Banks ML.** Effects of environmental and pharmacological manipulations on a novel delayed nonmatching-to-sample “working memory” procedure in unrestrained rhesus monkeys. *J Neurosci Methods* 251: 62–71, 2015. doi:[10.1016/j.jneumeth.2015.05.009](https://doi.org/10.1016/j.jneumeth.2015.05.009).
- Kangas BD, Bergman J.** A novel touch-sensitive apparatus for behavioral studies in unrestrained squirrel monkeys. *J Neurosci Methods* 209: 331–336, 2012. doi:[10.1016/j.jneumeth.2012.06.028](https://doi.org/10.1016/j.jneumeth.2012.06.028).
- Kangas BD, Bergman J, Coyle JT.** Touchscreen assays of learning, response inhibition, and motivation in the marmoset (*Callithrix jacchus*). *Anim Cogn* 19: 673–677, 2016. doi:[10.1007/s10071-016-0959-4](https://doi.org/10.1007/s10071-016-0959-4).
- Klaes C, Westendorff S, Chakrabarti S, Gail A.** Choosing goals, not rules: deciding among rule-based action plans. *Neuron* 70: 536–548, 2011. doi:[10.1016/j.neuron.2011.02.053](https://doi.org/10.1016/j.neuron.2011.02.053).
- Kuang S, Morel P, Gail A.** Planning movements in visual and physical space in monkey posterior parietal cortex. *Cereb Cortex* 26: 731–747, 2016. doi:[10.1093/cercor/bhu312](https://doi.org/10.1093/cercor/bhu312).
- Mandell DJ, Sackett GP.** A computer touch screen system and training procedure for use with primate infants: results from pigtail monkeys (*Macaca nemestrina*). *Dev Psychobiol* 50: 160–170, 2008. doi:[10.1002/dev.20251](https://doi.org/10.1002/dev.20251).
- McSweeney FK, Hatfield J, Allen TM.** Within-session responding as a function of post-session feedings. *Behav Processes* 22: 177–186, 1991. doi:[10.1016/0376-6357\(91\)90092-E](https://doi.org/10.1016/0376-6357(91)90092-E).
- Miller B, Lim AN, Heidbreder AF, Black KJ.** An automated motion detection and reward system for animal training. *Cureus* 7: e397, 2015. doi:[10.7759/cureus.397](https://doi.org/10.7759/cureus.397).
- Morel P.** *Gramm: Grammar of Graphics Plotting for Matlab* (Online). <https://zenodo.org/record/59786#.WnnAsq6nGUK>. Zenodo. [2016].
- Morel P, Ferrea E, Taghizadeh-Sarshouri B, Audí JM, Ruff R, Hoffmann KP, Lewis S, Russold M, Dietl H, Abu-Saleh L, Schroeder D, Krautschneider W, Meiners T, Gail A.** Long-term decoding of movement force and

- direction with a wireless myoelectric implant. *J Neural Eng* 13: 016002, 2016. doi:10.1088/1741-2560/13/1/016002.
- Murphy ES, McSweeney FK, Smith RG, McComas JJ.** Dynamic changes in reinforcer effectiveness: theoretical, methodological, and practical implications for applied research. *J Appl Behav Anal* 36: 421–438, 2003. doi:10.1901/jaba.2003.36-421.
- Nagahara AH, Bernot T, Tuszyński MH.** Age-related cognitive deficits in rhesus monkeys mirror human deficits on an automated test battery. *Neurobiol Aging* 31: 1020–1031, 2010. doi:10.1016/j.neurobiolaging.2008.07.007.
- Newberry RC.** Environmental enrichment: increasing the biological relevance of captive environments. *Appl Anim Behav Sci* 44: 229–243, 1995. doi:10.1016/0168-1591(95)00616-Z.
- Niebergall R, Khayat PS, Treue S, Martinez-Trujillo JC.** Multifocal attention filters targets from distracters within and beyond primate MT neurons' receptive field boundaries. *Neuron* 72: 1067–1079, 2011. doi:10.1016/j.neuron.2011.10.013.
- Patzwahl DR, Treue S.** Combining spatial and feature-based attention within the receptive field of MT neurons. *Vision Res* 49: 1188–1193, 2009. doi:10.1016/j.visres.2009.04.003.
- Prescott MJ, Brown VJ, Flecknell PA, Gaffan D, Garrod K, Lemon RN, Parker AJ, Ryder K, Schultz W, Scott L, Watson J, Whitfield L.** Refinement of the use of food and fluid control as motivational tools for macaques used in behavioural neuroscience research: report of a Working Group of the NC3Rs. *J Neurosci Methods* 193: 167–188, 2010. doi:10.1016/j.jneumeth.2010.09.003.
- Richardson WK, Washburn DA, Hopkins WD, Savage-Rumbaugh ES, Rumbaugh DM.** The NASA/LRC computerized test system. *Behav Res Methods Instrum Comput* 22: 127–131, 1990. doi:10.3758/BF03203132.
- Rogge J, Sherenco K, Malling R, Thiele E, Lambeth S, Schapiro S, Williams L.** A comparison of positive reinforcement training techniques in owl and squirrel monkeys: time required to train to reliability. *J Appl Anim Welf Sci* 16: 211–220, 2013. doi:10.1080/10888705.2013.798223.
- Schmitt V, Pankau B, Fischer J.** Old world monkeys compare to apes in the primate cognition test battery. *PLoS One* 7: e32024, 2012. doi:10.1371/journal.pone.0032024.
- Seed A, Tomasello M.** Primate cognition. *Top Cogn Sci* 2: 407–419, 2010. doi:10.1111/j.1756-8765.2010.01099.x.
- Shnitko TA, Allen DC, Gonzales SW, Walter NA, Grant KA.** Ranking cognitive flexibility in a group setting of rhesus monkeys with a set-shifting procedure. *Front Behav Neurosci* 11: 55, 2017. doi:10.3389/fnbeh.2017.00055.
- Snyder LH, Batista AP, Andersen RA.** Coding of intention in the posterior parietal cortex. *Nature* 386: 167–170, 1997. doi:10.1038/386167a0.
- Tarou LR, Bashaw MJ.** Maximizing the effectiveness of environmental enrichment: Suggestions from the experimental analysis of behavior. *Appl Anim Behav Sci* 102: 189–204, 2007. doi:10.1016/j.applanim.2006.05.026.
- Truppa V, Garofoli D, Castorina G, Piano Mortari E, Natale F, Visalberghi E.** Identity concept learning in matching-to-sample tasks by tufted capuchin monkeys (*Cebus apella*). *Anim Cogn* 13: 835–848, 2010. doi:10.1007/s10071-010-0332-y.
- Tulip J, Zimmermann JB, Farningham D, Jackson A, Jennifer T, Jonas ZB, David F, Andrew J.** An automated system for positive reinforcement training of group-housed macaque monkeys at breeding and research facilities. *J Neurosci Methods* 285: 6–18, 2017. doi:10.1016/j.jneumeth.2017.04.015.
- Washburn DA, Hopkins WD, Rumbaugh DM.** Video-task assessment of learning and memory in macaques (*Macaca mulatta*): effects of stimulus movement on performance. *J Exp Psychol Anim Behav Process* 15: 393–400, 1989. doi:10.1037/0097-7403.15.4.393.
- Washburn DA, Rumbaugh DM.** Rhesus monkey (*Macaca mulatta*) complex learning skills reassessed. *Int J Primatol* 12: 377–388, 1991. doi:10.1007/BF02547618.
- Washburn DA, Rumbaugh DM.** Testing primates with joystick-based automated apparatus: lessons from the Language Research Center's Computerized Test System. *Behav Res Methods Instrum Comput* 24: 157–164, 1992. doi:10.3758/BF03203490.
- Weed MR, Taffe MA, Polis I, Roberts AC, Robbins TW, Koob GF, Bloom FE, Gold LH.** Performance norms for a rhesus monkey neuropsychological testing battery: acquisition and long-term performance. *Brain Res Cogn Brain Res* 8: 185–201, 1999. doi:10.1016/S0926-6410(99)00020-8.
- Westendorff S, Klaes C, Gail A.** The cortical timeline for deciding on reach motor goals. *J Neurosci* 30: 5426–5436, 2010. doi:10.1523/JNEUROSCI.4628-09.2010.
- Westlund K.** Training is enrichment—and beyond. *Appl Anim Behav Sci* 152: 1–6, 2014. doi:10.1016/j.applanim.2013.12.009.
- Wise SP, Mauritz KH.** Set-related neuronal activity in the premotor cortex of rhesus monkeys: effects of changes in motor set. *Proc R Soc London B Biol Sci* 223: 331–354, 1985.
- Yao T, Treue S, Krishna BS.** An attention-sensitive memory trace in macaque MT following saccadic eye movements. *PLoS Biol* 14: e1002390, 2016. doi:10.1371/journal.pbio.1002390.

Part III

General discussion

Chapter 7

General discussion

The general aim of this thesis was to expand the workspace in sensorimotor neuroscience studies by removing physical constraints. This allows for studying movement types that have never before been investigated before such as goal-directed walk-and-reach movements, and can increase animal welfare when working with non-human primates. The five manuscripts in this thesis presented the following findings:

First, the peripersonal space around the hand (peri-hand space) extends towards reach targets even beyond the reach when performing goal-directed walk-and-reach movements. Second, we presented an experimental environment (Reach Cage) that allows for sensorimotor neuroscience in large workspaces with physically unconstrained non-human primates. Third, in the Reach Cage we could replicate results from experiments with monkeys restrained in a primate chair showing that the fronto-parietal reach network in the macaque's brain encodes near-located motor goals of reach movements. In addition, the dorsal premotor cortex (PMd) and the parietal reach region (PRR) are mainly modulated by arm movements, even when performing walk-and-reach movements towards far-located targets. Fourth, we presented a touchscreen-based cage-mountable system (XBI) that allows for cognitive training and testing of macaques in their housing environment. And fifth, using the XBI it is possible to incorporate a fully unsupervised training routine for tasks used in cognitive neuroscience, providing valid comparisons among animals' learning ability and the freedom for the monkeys to choose their own working schedule.

Parietal and frontal cortical areas were found to play a key role in motor control of arm, hand, eye and defensive movements (see reviews Graziano & Cooke, 2006; Johnson et al., 1996; Rizzolatti & Luppino, 2001; Snyder et al., 2000). Homologues in the human brain were also identified by using functional magnetic resonance imaging (Connolly et al., 2003; Corbetta et al., 1998; Gertz et al., 2017). But goal-directed whole-body movements have never been studied before since in conventional experiments monkeys are seated in a primate chair or humans are lying inside an MRI scanner. With the Reach Cage, this is now possible. We studied walk-and-reach movements, i.e. whole-body movements with an arm movement towards a reach target. We decided to test the fronto-parietal network related to arm movements. And since we

showed in a human psychophysics study that the peri-hand space extends towards reach goals for walk-and-reach movements, we hypothesized that areas related to reach movements also encode far-located motor goals during planning of walk-and-reach movements. Since the primary motor cortex (M1) is less involved in motor planning (Crammond & Kalaska, 2000; Kalaska & Crammond, 1992), this question focused mainly on PMd and PRR. Our results suggest that PRR is involved in motor goal encoding early after receiving the target information but PMd only shortly before the onset of the arm movement. However, in both cases the modulation towards far targets was clearly weaker than to near targets. This could be due to a different encoding of the space near and far from the body in contrast to our hypothesis. However, at least three other factors in the current implementation of the task in the Reach Cage could be responsible for the weaker modulation of far targets during movement planning. First, due to the dimensions of the physical reach goals and the cage itself, the angular distance relative to the monkeys starting position is smaller between far than between near targets. Thus, we expect less modulation in the neural activity for a spatial encoding relative to body or gaze. This confound could be avoided by implementing the setup in a larger cage environment. The monkey interaction device we developed to implement the behavioral task (*MaCaQuE*) is not restricted to a certain spatial configuration. It means that the space is only restricted by the size of the cage. Second, we do not control eye movements. While position of the visual cue that indicates the “go” signal encourages the animal to not change the gaze relative to the target position, we can not be certain of the animals’ eye position. A change in eye-position relative to the target would reduce neuronal activity based on a gaze-centered encoding. We could avoid such undesired eye movements by training the animal to fixate a certain point. To do so, an eye tracking system needs to be implemented such as a scleral search coil or a non-invasive optical method (see Kimmel et al., 2012, for a comparison of the two approaches). Third, the monkey orients its body towards the far targets leading to similar arm movements relative to the body for different walk-and-reach movements. Since the areas we investigated are considered to be involved in arm movements (Johnson et al., 1996), which is supported by our results, modulation in motor planning towards different targets might be mainly related to differences in joint kinematics of the reaching arm. To test walk-and-reach movements towards far targets for which the arm instead of the whole-body moves towards the target, the monkey could be trained to move in a straight line in front the far targets and then perform a reach. For this training, it would be necessary to know the body position of the monkey. We already showed that 3D real-time motion capture of colored objects is possible in the Reach Cage. It could be used to track the colored protection cap mounted on the animals’ head to protect the wireless recording equipment.

While the monkey performs a goal-directed whole-body movement towards the far targets, our results do not suggest the fronto-parietal reach network is involved in encoding whole-body movements. The question remains, which fronto-parietal network does encode goal-directed whole-body movements? A study with optic flow stimuli that resemble visual motion induced by walking suggests that the ventral intraparietal area (VIP) encodes heading direction (Zhang et al.,

2004). In addition, VIP together with the caudal part of the ventral premotor cortex (PMv) is considered to play a major role in peripersonal space encoding (Cléry et al., 2015; Graziano & Cooke, 2006). Studies of the VIP-PMv network involving walk-and-reach movements would be necessary to test if this network is modulated by the whole-body movement towards the target rather than the arm movement.

It would be beneficial to investigate neural processing underlying free behavior. For instance, conventional studies using structured tasks showed that the primary motor cortex is modulated by various parameters of reaching movements, for example direction (Georgopoulos et al., 1982), speed (Moran & Schwartz, 1999) and posture (Scott & Kalaska, 1997). The tasks are designed to restrict behavioral variations to the movement parameter of interest. It allows to test if the activity of a certain brain area is “tuned” to the movement parameter, but there is a risk of overinterpretation. In one study, researchers tracked free arm movements in 3D space of a chair-seated untrained animal while recording from primary motor cortex (Aflalo & Graziano, 2007). They tested how much variance of the neuronal activity could be explained by different tuning models. Interestingly, a model based on directional tuning could explain 8% of the variance, but the same model explained 42% of the variance when applied on a subset of movements that resemble a center-out-reach task. With the Reach Cage, the workspace for the behavioral task extends to a whole cage, allowing for more complex behavior such as walking. But we still restrict the behavior to a subset of arm and whole-body movements by applying a behavioral task. Otherwise, we would not be able to identify the monkey’s behavior properly, to distinguish between movement planning and execution or to obtain enough repetitions of a certain behavior allowing for statistical analysis. If we want to interpret free movement behavior, we are facing at least three challenges: 1) The movement behavior must be known at any given time for appropriate interpretations; 2) Neural activity related to motor planning needs to be separated from neural activity that directly produces a motor output; 3) Analysis methods can not rely on repetitions of behavior. Recent studies provided methods to approach each of the three challenges. One study presented a markerless motion capture system capable of identifying complex posture and full-body movements in three dimensional space of a monkey (Nakamura et al., 2016). This system can capture complex body and limb movements very accurately at high speeds but is only tested in a small cage with no other objects that could potentially occlude parts of the body. The issue of separating activity related to execution from preparation was addressed by studies investigating motor and premotor activity. The researchers could identify the components in the activity that do not lead to a motor output, the null space (Kaufman et al., 2014). In a more recent study, the same group could differentiate between motor output and null-space activity related to mid-movement visuo-motor perturbations (Stavisky et al., 2016). Before the actual experiment, the researchers identified the null-space of the recorded activity in the individual animal by a simple reaching task without perturbation. If it is possible to identify the null space for all movements, i.e. also lower limb and whole-body movements, it might be possible to separate components related to a motor output from other components in free behavior. Finally,

another study proposed an approach based on a neural-network model that identifies the behavior related components in premotor and primary motor cortical activity of a single trial (Pandarinath et al., 2017). Once the neural network model is learned, their algorithm ‘de-noises’ the neural activity of a single trial and provides a meaningful signal. Although not tested yet, such an algorithm could provide a way to interpret single movements of a freely behaving animal. In the future, combining such developments might allow for meaningful conclusions from neural data recorded wirelessly in freely moving monkeys. This approach would lead to new hypotheses that can be more specifically tested in an experimental environment such as the Reach Cage.

Within the Reach Cage, we do not constrain the monkey physically and do not have the full control over all sensory parameters. Yet, we could revalidate findings of the fronto-parietal reach network from conventional experiments such as its involvement in spatial coding of near reach targets during movement planning (Crammond & Kalaska, 2000; Kalaska & Crammond, 1992; Snyder et al., 1997, 1998; Wise & Mauritz, 1985) and execution (Caminiti et al., 1990; Georgopoulos et al., 1982; Kalaska et al., 1983). Using the XBI, we even have been developed an experimental setup for sensorimotor neuroscience that can be used within the housing environment of the animals. In combination with wireless neural recording (Fernandez-Leon et al., 2015; Gilja et al., 2010; Schwarz et al., 2014; Yin et al., 2014), it is consequently possible to perform neuroscientific experiments without the need for the animals to leave their housing environment. Further developments in wireless neural recordings have focused on fully implantable devices (Agha et al., 2013; Borton et al., 2013; Montgomery et al., 2015; Su et al., 2016) for which it would not be necessary anymore to get animals out of the cage for implant care. Furthermore, cognitive training and testing devices, similar to the XBI, are used in the field of behavioral biology even inside large groups of socially housed non-human primates using radio-frequency identification for automatic identification of individuals (Fagot & Bonté, 2010; Gazes et al., 2013). All those developments lead to experimental environments under more natural conditions and to a reduction in direct human interventions. Consequently, there is a clear benefit for animal welfare as monkeys can get more control over the environment by choosing their own working schedule (Westlund, 2014). Given that training benefits welfare of captive animals (Westlund, 2014), it is desirable to expose monkeys to automatic devices with automatized training algorithm, as proposed in this thesis. Experimental and training environments within the housing setting, for which monkeys do not have to be separated from their peers, can thus be seen as cognitive enrichment (Clark, 2017).

It is important to note, however, that neuroscience will not fully transition to such enriched experimental environments any time soon. First, wireless neural technology usually requires chronically implanted electrodes which can not be replaced once implanted. This is a disadvantage to conventional head-mounted microdrives which place electrodes on a new position every session (Mountcastle et al., 1975). Semi-chronic systems exist that allow to reposition the electrodes but leave them inside the brain once the microdrive is detached (Ferrea et al., 2017; Gray et al., 2007). One more recent system achieved to combined movable electrodes, microdrive

and wireless transmitter in one headstage (Schwarz et al., 2014). The second, more notable, disadvantage of enriched experimental environments remains the loss of control over behavioral and environmental variables. We could show that it is possible to study certain neuroscience questions regarding motor and sensorimotor neuroscience in less constraining environments and argued that refined behavioral observation methods, such as motion capture, will reduce the need for constraints on behavior even more. But many studies in cognitive neuroscience will likely remain dependent on highly controlled and constraining setups. In visual neuroscience, for instance, eye movements or additional visual inputs have a strong influence on neural activity in visual areas.

7.1 Conclusion

This thesis presented new cage-based experimental environments, Reach Cage and XBI, for sensorimotor neuroscience to study physically unconstrained behavior of non-human primates. The Reach Cage in combination with wireless electrophysiology allowed for studying encoding of near- and far-located motor goals in the macaque fronto-parietal reach network. It was highlighted that results from conventional highly constraining environments, involving monkeys to sit in a primate chair, could be replicated without those physical constraints. Furthermore, goal-directed whole-body movements to far-located targets could be studied for the first time validating the classical view that the fronto-parietal reach network is mainly involved in the control of arm movements. Accompanying these results, it could be shown that the extent of the peripersonal space around the hand in humans expands towards motor-goals even when located far away for which walking is necessary. Finally, the XBIs allows for cage-based unsupervised training of non-human primates to conventional sensorimotor task. The work described here, highlights the welfare benefits of cage-based training and cognitive testing especially when the monkeys can choose their own working pace and are trained within their housing environment.

References

- Aflalo, T., Kellis, S., Klaes, C., Lee, B., Shi, Y., Pejsa, K., Shanfield, K., Hayes-Jackson, S., Aisen, M., Heck, C., Liu, C., and Andersen, R. (2015). Decoding motor imagery from the posterior parietal cortex of a tetraplegic human. *Science*, 348(6237):906–910.
- Aflalo, T. N. and Graziano, M. S. A. (2007). Relationship between unconstrained arm movements and single-neuron firing in the macaque motor cortex. *J Neurosci*, 27(11):2760–80.
- Agha, N. S., Komar, J., Yin, M., Borton, D. A., and Nurmikko, A. (2013). A fully wireless platform for correlating behavior and neural data from an implanted, neural recording device: Demonstration in a freely moving swine model. *International IEEE/EMBS Conference on Neural Engineering, NER*, page 989–992.
- Andersen, R. A., Asanuma, C., Essick, G., and Siegel, R. M. (1990). Corticocortical connections of anatomically and physiologically defined subdivisions within the inferior parietal lobule. *Journal of Comparative Neurology*, 296(1):65–113.
- Andersen, R. A. and Buneo, C. A. (2002). Intentional maps in posterior parietal cortex. *Annual review of neuroscience*, 25(1):189–220.
- Andersen, R. A. and Cui, H. (2009). Intention, action planning, and decision making in parietal-frontal circuits. *Neuron*, 63(5):568–583.
- Andrews, M. W. and Rosenblum, L. A. (1994). Automated recording of individual performance and hand preference during joystick-task acquisition in group-living bonnet macaques (*macaca radiata*). *Journal of Comparative Psychology*, 108(4):358–362.
- Ballesta, S., Reymond, G., Pozzobon, M., and Duhamel, J. R. (2014). A real-time 3d video tracking system for monitoring primate groups. *Journal of Neuroscience Methods*, 234:147–152.
- Batista, a. P., Buneo, C. a., Snyder, L. H., and Andersen, R. a. (1999). Reach plans in eye-centered coordinates. *Science (New York, N.Y.)*, 285(5425):257–260.
- Bennett, A. J., Perkins, C. M., Tenpas, P. D., Reinebach, A. L., and Pierre, P. J. (2016). Moving evidence into practice: Cost analysis and assessment of macaques’ sustained behavioral engagement with videogames and foraging devices. *American Journal of Primatology*, 78(12):1250–1264.
- Berger, M., Calapai, A., Stephan, V., Niessing, M., Burchardt, L., Gail, A., and Treue, S. (2017). Standardized automated training of rhesus monkeys for neuroscience research in their housing environment. *Journal of Neurophysiology*, 119:796–807.
- Berger, M. and Gail, A. (2018). The reach cage environment for wireless neural recordings during structured goal-directed behavior of unrestrained monkeys. *bioRxiv*.

- Berti, A. and Frassinetti, F. (2000). When far becomes near: remapping of space by tool use. *Journal of cognitive neuroscience*, 12(3):415–420.
- Bhattacharyya, R., Musallam, S., and Andersen, R. A. (2009). Parietal reach region encodes reach depth using retinal disparity and vergence angle signals. *Journal of Neurophysiology*, 102(2):805–816.
- Bjoertomt, O., Cowey, A., and Walsh, V. (2002). Spatial neglect in near and far space investigated by repetitive transcranial magnetic stimulation. *Brain*, 125(9):2012–22.
- Blanke, O., Slater, M., and Serino, A. (2015). Behavioral, neural, and computational principles of bodily self-consciousness. *Neuron*, 88(1):145–166.
- Bonini, L., Maranesi, M., Livi, A., Fogassi, L., and Rizzolatti, G. (2014). Space-dependent representation of objects and other’s action in monkey ventral premotor grasping neurons. *Journal of Neuroscience*, 34(11):4108–4119.
- Borton, D. a., Yin, M., Aceros, J., and Nurmikko, A. (2013). An implantable wireless neural interface for recording cortical circuit dynamics in moving primates. *Journal of neural engineering*, 10(2):26010.
- Botvinick, M. and Cohen, J. (1998). Rubber hands “feel” touch that eyes see. *Nature*, 391(6669):756.
- Brozzoli, C., Cardinali, L., Pavani, F., and Farnè, A. (2010). Action-specific remapping of peripersonal space. *Neuropsychologia*, 48(3):796–802.
- Brozzoli, C., Ehrsson, H. H., and Farnè, A. (2014). Multisensory representation of the space near the hand: from perception to action and interindividual interactions. *The Neuroscientist*, 20(2):122–35.
- Brozzoli, C., Makin, T. R., Cardinali, L., Holmes, N. P., and Farnè, A. (2011). Peripersonal Space: A Multisensory Interface for Body–Object Interactions. In Murray, M. and Wallace MT, editors, *The Neural Bases of Multisensory Processes*, page 449–466.
- Brozzoli, C., Pavani, F., Urquizar, C., Cardinali, L., and Farnè, A. (2009). Grasping actions remap peripersonal space. *Neuroreport*, 20(10):913–917.
- Caggiano, V., Fogassi, L., Rizzolatti, G., Thier, P., and Casile, A. (2009). Mirror neurons differentially encode the peripersonal and extrapersonal space of monkeys. *Science*, 324(5925):403–406.
- Calapai, A., Berger, M., Niessing, M., Heisig, K., Brockhausen, R., Treue, S., and Gail, A. (2017). A cage-based training, cognitive testing and enrichment system optimized for rhesus macaques in neuroscience research. *Behavior research methods*, 49(1):35–45.
- Caminiti, R., Ferraina, S., and Johnson, P. B. (1996). The sources of visual information to the primate frontal lobe: A novel role for the superior parietal lobule. *Cereb Cortex*, 6:319–328.
- Caminiti, R., Johnson, P. B., and Urbano, A. (1990). Making arm movements within different parts of space: dynamic aspects in the primate motor cortex. *The Journal of neuroscience*, 10(July):2039–2058.

- Capogrosso, M., Milekovic, T., Borton, D., Wagner, F., Moraud, E. M., Mignardot, J.-B., Buse, N., Gandar, J., Barraud, Q., Xing, D., Rey, E., Duis, S., Jianzhong, Y., Ko, W. K. D., Li, Q., Detemple, P., Denison, T., Micera, S., Bezaud, E., Bloch, J., and Courtine, G. (2016). A brain–spine interface alleviating gait deficits after spinal cord injury in primates. *Nature*, 539(7628):284–288.
- Clark, F. E. (2017). Cognitive enrichment and welfare : Current approaches and future directions. *Animal Behavior and Cognition*, 4(1):52–71.
- Cléry, J., Guipponi, O., Wardak, C., and Ben Hamed, S. (2015). Neuronal bases of peripersonal and extrapersonal spaces, their plasticity and their dynamics: Knowns and unknowns. *Neuropsychologia*, 70:313–326.
- Cohen, Y. E. and Andersen, R. a. (2002). A common reference frame for movement plans in the posterior parietal cortex. *Nature reviews. Neuroscience*, 3(7):553–62.
- Colby, C. L. (1998). Action-oriented spatial reference frames in cortex. *Neuron*, 20(1):15–24.
- Colby, C. L. and Duhamel, J. R. (1991). Heterogeneity of extrastriate visual areas and multiple parietal areas in the macaque monkey. *Neuropsychologia*, 29(6):517–537.
- Colby, C. L. and Goldberg, M. E. (1999). Space and attention in parietal cortex. *Annual Review of Neuroscience*, 22(1):319–349.
- Collinger, J. L., Wodlinger, B., Downey, J. E., Wang, W., Tyler-Kabara, E. C., Weber, D. J., McMorland, A. J. C., Velliste, M., Boninger, M. L., and Schwartz, A. B. (2013). High-performance neuroprosthetic control by an individual with tetraplegia. *The Lancet*, 381(9866):557–564.
- Connolly, J. D., Andersen, R. A., and Goodale, M. A. (2003). Fmri evidence for a “parietal reach region” in the human brain. *Experimental Brain Research*, 153(2):140–145.
- Corbetta, M., Akbudak, E., Conturo, T. E., Snyder, A. Z., Ollinger, J. M., Drury, H. A., Linenweber, M. R., Petersen, S. E., Raichle, M. E., Van Essen, D. C., and Shulman, G. L. (1998). A common network of functional areas for attention and eye movements. *Neuron*, 21(4):761–773.
- Crammond, D. J. and Kalaska, J. F. (1989). Neuronal activity in primate parietal cortex area 5 varies with intended movement direction during an instructed-delay period. *Experimental Brain Research*, 76(2):458–462.
- Crammond, D. J. and Kalaska, J. F. (1994). Modulation of preparatory neuronal activity in dorsal premotor cortex due to stimulus-response compatibility. *Journal of Neurophysiology*, 71(3):1281–1284.
- Crammond, D. J. and Kalaska, J. F. (1996). Differential relation of discharge in primary motor cortex and premotor cortex to movements versus actively maintained postures during a reaching task. *Experimental Brain Research*, 108(1):45–61.
- Crammond, D. J. and Kalaska, J. F. (2000). Prior information in motor and premotor cortex: activity during the delay period and effect on pre-movement activity. *Journal of neurophysiology*, 84(2):986–1005.
- Crawford, J. D., Henriques, D. Y., and Medendorp, W. P. (2011). Three-dimensional transformations for goal-directed action. *Annual Review of Neuroscience*, 34(1):309–331.

- D Foster, J., Nuyujukian, P., Freifeld, O., Gao, H., Walker, R., I Ryu, S., H Meng, T., Murmann, B., J Black, M., and V Shenoy, K. (2014). A freely-moving monkey treadmill model. *Journal of neural engineering*, 11(4):46020.
- Desmurget, M., Reilly, K. T., Richard, N., Szathmari, A., Mottolese, C., and Sirigu, A. (2009). Movement intention after parietal cortex stimulation in humans. *Science (New York, N.Y.)*, 324(811):811–813.
- Dum, R. P. and Strick, P. L. (2002). Motor areas in the frontal lobe of the primate. *Physiology and Behavior*, 77(4–5):677–682.
- Evarts, E. (1969). Activity of pyramidal tract neurons during postural fixation. *Journal of Neurophysiology*, 32(3):375–385.
- Evarts, E. V. (1968). Relation of pyramidal tract activity to force exerted during voluntary movement. *Journal of neurophysiology*, 31(1):14–27.
- Fagot, J. and Bonté, E. (2010). Automated testing of cognitive performance in monkeys: use of a battery of computerized test systems by a troop of semi-free-ranging baboons (*papio papio*). *Behavior research methods*, 42(2):507–16.
- Fan, D., Rich, D., Holtzman, T., Ruther, P., Dalley, J. W., Lopez, A., Rossi, M. A., Barter, J. W., Salas-Meza, D., Herwik, S., Holzhammer, T., Morizio, J., and Yin, H. H. (2011). A wireless multi-channel recording system for freely behaving mice and rats. *PLoS ONE*, 6(7):e22033.
- Felleman, D. J. and Van Essen, D. C. (1991). Distributed hierarchical processing in the primate cerebral cortex. *Cerebral Cortex*, 1(1):1–47.
- Fernandez-Leon, J. a., Parajuli, A., Franklin, R., Sorenson, M., Felleman, D. J., Hansen, B. J., Hu, M., and Dragoi, V. (2015). A wireless transmission neural interface system for unconstrained non-human primates. *Journal of neural engineering*, 12(5):56005.
- Ferraina, S., Battaglia-Mayer, A., Genovesio, A., Archambault, P., and Caminiti, R. (2009). Parietal encoding of action in depth. *Neuropsychologia*, 47(6):1409–1420.
- Ferrea, E., Suriya-Arunroj, L., Hoehl, D., Thomas, U., and Gail, A. (2017). Implantable computer-controlled adaptive multi-electrode positioning system (amep). *in preparation*.
- Fogassi, L., Gallese, V., Fadiga, L., Luppino, G., Matelli, M., and Rizzolatti, G. (1996). Coding of peripersonal space in inferior premotor cortex (area f4). *Journal of neurophysiology*, 76(1):141–57.
- Fulton, J. F. (1938). *Physiology of the Nervous System*. Oxford University Press, Inc.
- Gazes, R. P., Brown, E. K., Basile, B. M., and Hampton, R. R. (2013). Automated cognitive testing of monkeys in social groups yields results comparable to individual laboratory-based testing. *Animal Cognition*, 16(3):445–458.
- Georgopoulos, a. P., Kalaska, J. F., Caminiti, R., and Massey, J. T. (1982). On the relations between the direction of two-dimensional arm movements and cell discharge in primate motor cortex. *J.Neurosci.*, 2(11)(11):1527–1537.
- Georgopoulos, A. P., Schwartz, A. B., and Kettner, R. E. (1986). Neuronal population coding of movement direction. *Science*, 233(4771):1416–1419.

- Gertz, H., Lingnau, A., and Fiehler, K. (2017). Decoding movement goals from the fronto-parietal reach network. *Frontiers in Human Neuroscience*, 11:84.
- Giglia, G., Pia, L., Folegatti, A., Puma, A., Fierro, B., Cosentino, G., Berti, A., and Brighina, F. (2015). Far space remapping by tool use: A rtms study over the right posterior parietal cortex. *Brain Stimulation*, 8(4):795–800.
- Gilja, V., Chestek, C. A., Nuyujukian, P., Foster, J., and Shenoy, K. V. (2010). Autonomous head-mounted electrophysiology systems for freely behaving primates. *Current Opinion in Neurobiology*, 20(5):676–686.
- Goodale, M. A. and Milner, A. D. (1992). Separate visual pathways for perception and action. *Trends in Neurosciences*, 15(I):20–25.
- Gray, C. M., Goodell, B., and Lear, A. (2007). Multichannel micromanipulator and chamber system for recording multineuronal activity in alert, non-human primates. *Journal of neurophysiology*, 98(1):527–536.
- Graziano, M. (2006). The organization of behavioral repertoire in motor cortex. *Annual Review of Neuroscience*, 29:105–34.
- Graziano, M. S., Cooke, D. F., and Taylor, C. S. R. (2000). Coding the location of the arm by sight. *Science*, 290(5497):1782–1786.
- Graziano, M. S. and Gross, C. G. (1994). The representation of extrapersonal space: A possible role for bimodal, visual-tactile neurons. *The cognitive neurosciences*, page 1021–1034.
- Graziano, M. S. A. and Cooke, D. F. (2006). Parieto-frontal interactions, personal space, and defensive behavior. *Neuropsychologia*, 44(13):2621–2635.
- Grohrock, P., Häusler, U., and Jürgens, U. (1997). Dual-channel telemetry system for recording vocalization-correlated neuronal activity in freely moving squirrel monkeys. *Journal of Neuroscience Methods*, 76(1):7–13.
- Hage, S. R. and Jurgens, U. (2006). On the role of the pontine brainstem in vocal pattern generation: A telemetric single-unit recording study in the squirrel monkey. *Journal of Neuroscience*, 26(26):7105–7115.
- Halligan, P. W. and Marshall, J. C. (1991). Left neglect for near but not far space in man. *Nature*, 350(6318):498–500.
- Holmes, N. P. (2012). Does tool use extend peripersonal space? a review and re-analysis. *Experimental Brain Research*, 218(2):273–282.
- Iriki, A., Tanaka, M., and Iwamura, Y. (1996). Coding of modified body schema during tool use by macaque postcentral neurones. *NeuroReport*, 7(14):2325–2330.
- Johnson, P. B., Ferraina, S., Bianchi, L., and Caminiti, R. (1996). Cortical networks for visual reaching: Physiological and anatomical organization of frontal and parietal lobe arm regions. *Cerebral Cortex*, 6(2):102–119.
- Jürgens, U. and Hage, S. R. (2006). Telemetric recording of neuronal activity. *Methods*, 38(3):195–201.

- Kalaska, J. F., Caminiti, R., and Georgopoulos, A. P. (1983). Cortical mechanisms related to the direction of two-dimensional arm movements: relations in parietal area 5 and comparison with motor cortex. *Experimental Brain Research*, 51(2):247–260.
- Kalaska, J. F. and Crammond, D. J. (1992). Cerebral cortical mechanisms of reaching movements. *Science*, 255(5051):1517–1523.
- Kangas, B. D. and Bergman, J. (2012). A novel touch-sensitive apparatus for behavioral studies in unrestrained squirrel monkeys. *Journal of Neuroscience Methods*, 209(2):331–336.
- Kaufman, M. T., Churchland, M. M., Ryu, S. I., and Shenoy, K. V. (2014). Cortical activity in the null space: permitting preparation without movement. *Nature neuroscience*, 17(3):440–8.
- Kaufman, M. T., Seely, J. S., Sussillo, D., Ryu, S. I., Shenoy, K. V., and Churchland, M. M. (2016). The largest response component in motor cortex reflects movement timing but not movement type. *eNeuro*, 3(4):ENEURO.0085–16.2016.
- Kimmel, D. L., Mammo, D., and Newsome, W. T. (2012). Tracking the eye non-invasively: simultaneous comparison of the scleral search coil and optical tracking techniques in the macaque monkey. *Front Behav Neurosci*, 6:49.
- Krakauer, J. W., Ghazanfar, A. A., Gomez-Marin, A., MacIver, M. A., and Poeppel, D. (2017). Neuroscience needs behavior: Correcting a reductionist bias. *Neuron*, 93(3):480–490.
- Kurata, K. (1991). Corticocortical inputs to the dorsal and ventral aspects of the premotor cortex of macaque monkeys. *Neuroscience Research*, 12(1):263–280.
- Li, K. and Malhotra, P. A. (2015). Spatial neglect. *Practical neurology*, 15(5):333–9.
- Ludvig, N., Tang, H. M., Gohil, B. C., and Botero, J. M. (2004). Detecting location-specific neuronal firing rate increases in the hippocampus of freely-moving monkeys. *Brain Research*, 1014(1–2):97–109.
- Maravita, A. and Iriki, A. (2004). Tools for the body (schema). *Trends in Cognitive Sciences*, 8(2):79–86.
- Maravita, A., Spence, C., and Driver, J. (2003). Multisensory integration and the body schema: Close to hand and within reach. *Current Biology*, 13(13):R531–R539.
- Maravita, A., Spence, C., Kennett, S., and Driver, J. (2002). Tool-use changes multimodal spatial interactions between vision and touch in normal humans. *Cognition*, 83(2).
- Marconi, B., Genovesio, A., Battaglia-Mayer, A., Ferraina, S., Squatrito, S., Molinari, M., Lacquaniti, F., and Caminiti, R. (2001). Eye-hand coordination during reaching. i. anatomical relationships between parietal and frontal cortex. *Cerebral Cortex*, 11(6):513–527.
- Maynard, E. M., Nordhausen, C. T., and Normann, R. A. (1997). The utah intracortical electrode array: A recording structure for potential brain-computer interfaces. *Electroencephalography and Clinical Neurophysiology*, 102(3):228–239.
- Miller, E. K. and Cohen, J. D. (2001). An integrative theory of prefrontal cortex function. *Annual Review of Neuroscience*, 24(1):167–202.
- Mirabella, G., Pani, P., and Ferraina, S. (2011). Neural correlates of cognitive control of reaching movements in the dorsal premotor cortex of rhesus monkeys. *Journal of neurophysiology*, 106(3):1454–1466.

- Miranda, H., Gilja, V., Chestek, C. A., Shenoy, K. V., and Meng, T. H. (2010). Hermesd: A high-rate long-range wireless transmission system for simultaneous multichannel neural recording applications. *IEEE Transactions on Biomedical Circuits and Systems*, 4(3):181–191.
- Mishkin, M. and Ungerleider, L. G. (1982). Contribution of striate inputs to the visuospatial functions of parieto-preoccipital cortex in monkeys. *Behavioural Brain Research*, 6(1):57–77.
- Montgomery, K. L., Yeh, A. J., Ho, J. S., Tsao, V., Mohan Iyer, S., Grosenick, L., Ferenczi, E. A., Tanabe, Y., Deisseroth, K., Delp, S. L., and Poon, A. S. Y. (2015). Wirelessly powered, fully internal optogenetics for brain, spinal and peripheral circuits in mice. *Nature Methods*, 12(10):969–974.
- Moran, D. W. and Schwartz, A. B. (1999). Motor cortical representation of speed and direction during reaching. *J. Neurophysiol.*, 82(5):2676–2692.
- Mountcastle, V. B., Lynch, J. C., Georgopoulos, A., Sakata, H., and Acuna, C. (1975). Posterior parietal association cortex of the monkey: command functions for operations within extrapersonal space. *J Neurophysiol*, 38(April 2016):871–908.
- Musallam, S., Bak, M. J., Troyk, P. R., and Andersen, R. A. (2007). A floating metal microelectrode array for chronic implantation. *Journal of Neuroscience Methods*, 160(1):122–127.
- Nakamura, T., Matsumoto, J., Nishimaru, H., Bretas, R. V., Takamura, Y., Hori, E., Ono, T., and Nishijo, H. (2016). A markerless 3d computerized motion capture system incorporating a skeleton model for monkeys. *PLOS ONE*, 11(11):e0166154.
- Ohbayashi, X. M., Picard, N., and Strick, P. L. (2016). Inactivation of the dorsal premotor area disrupts internally generated, but not visually guided, sequential movements. *The Journal of Neuroscience*, 36(6):1971–1976.
- Pandarathna, C., O’Shea, D., Collins, J., Jozefowicz, R., Stavisky, S. D., Kao, J. C., Trautmann, E. M., Kaufman, M. T., Ryu, S. I., Hochberg, L. R., Henderson, J. M., Shenoy, K. V., Abbott, L. F., and Sussillo, D. (2017). Inferring single-trial neural population dynamics using sequential auto-encoders. *bioRxiv*.
- Pandya, D. N. and Kuypers, H. G. J. M. (1969). Cortico-cortical connections in the rhesus monkey. *Brain research*, 13(1):13–36.
- Pavani, F., Spence, C., and Driver, J. (2000). Visual capture of touch : Out-of-the-body experiences with rubber gloves. *Psychological Science*, 11(5):353–359.
- Pesaran, B., Nelson, M. J., and Andersen, R. A. (2006). Dorsal premotor neurons encode the relative position of the hand, eye, and goal during reach planning. *Neuron*, 51(1):125–134.
- Prescott, M. J., Brown, V. J., Flecknell, P. A., Gaffan, D., Garrod, K., Lemon, R. N., Parker, A. J., Ryder, K., Schultz, W., Scott, L., Watson, J., and Whitfield, L. (2010). Refinement of the use of food and fluid control as motivational tools for macaques used in behavioural neuroscience research: Report of a working group of the nc3rs. *Journal of Neuroscience Methods*, 193(2):167–188.
- Rajangam, S., Tseng, P.-H., Yin, A., Lehew, G., Schwarz, D., Lebedev, M. A., and Nicolelis, M. A. L. (2016). Wireless cortical brain-machine interface for whole-body navigation in primates. *Scientific Reports*, 6:22170.

- Richardson, W. K., Washburn, D. a., Hopkins, W. D., Savage-Rumbaugh, E. S., and Rumbaugh, D. M. (1990). The nasa/lrc computerized test system. *Behavior research methods*, 22(2):127–131.
- Rizzolatti, G., Fadiga, L., Fogassi, L., and Gallese, V. (1997). The space around us. *Science*, 277(5323):190–191.
- Rizzolatti, G. and Luppino, G. (2001). The cortical motor system. *Neuron*, 31(6):889–901.
- Rizzolatti, G., Scandolara, C., Matelli, M., and Gentilucci, M. (1981). Afferent properties of periarculate neurons in macaque monkeys. ii. visual responses. *Behavioural Brain Research*, 2(2):147–163.
- Rouse, A. G. and Schieber, M. H. (2016). Spatiotemporal distribution of location and object effects in primary motor cortex neurons during reach-to-grasp. *Journal of Neuroscience*, 36(41):10640–10653.
- Roy, S. and Wang, X. (2012). Wireless multi-channel single unit recording in freely moving and vocalizing primates. *Journal of Neuroscience Methods*, 203(1):28–40.
- Sakagami, M., Pan, X., and Uttl, B. (2006). Behavioral inhibition and prefrontal cortex in decision-making. *Neural Networks*, 19(8):1255–1265.
- Schwartz, a. B., Kettner, R. E., and Georgopoulos, A. P. (1988). Primate motor cortex and free arm movements to visual targets in three-dimensional space. i. relations between single cell discharge and direction of movement. *J.Neurosci.*, 8(August):2913–2927.
- Schwartz, A. B., Taylor, D. M., and Tillery, S. I. H. (2001). Extraction algorithms for cortical control of arm prosthetics. *Current Opinion in Neurobiology*, 11(6):701–707.
- Schwarz, D. a., Lebedev, M. a., Hanson, T. L., Dimitrov, D. F., Lehew, G., Meloy, J., Rajangam, S., Subramanian, V., Ifft, P. J., Li, Z., Ramakrishnan, A., Tate, A., Zhuang, K. Z., and Nicolelis, M. a. L. (2014). Chronic, wireless recordings of large-scale brain activity in freely moving rhesus monkeys. *Nature methods*, 11(6):670–6.
- Scott, S. and Kalaska, J. (1997). Reaching movements with similar hand paths but different arm orientations. i. activity of individual cells in motor cortex. *Journal of Neurophysiology*, 77(6):826–852.
- Snyder, L. H., Batista, A. P., and Andersen, R. A. (1997). Coding of intention in the posterior parietal cortex. *Nature*, 386(6621):167–170.
- Snyder, L. H., Batista, a. P., and Andersen, R. a. (1998). Change in motor plan, without a change in the spatial locus of attention, modulates activity in posterior parietal cortex. *Journal of neurophysiology*, 79(5):2814–9.
- Snyder, L. H., Batista, A. P., and Andersen, R. A. (2000). Intention-related activity in the posterior parietal cortex: A review. *Vision Research*, 40(10–12):1433–1441.
- Spence, C., Pavani, F., and Driver, J. (2004a). Spatial constraints on visual-tactile cross-modal distractor congruency effects. *Cognitive, affective & behavioral neuroscience*, 4(2):148–169.
- Spence, C., Pavani, F., Maravita, A., and Holmes, N. (2004b). Multisensory contributions to the 3-d representation of visuotactile peripersonal space in humans: Evidence from the crossmodal congruency task. *Journal of Physiology Paris*, 98(1–3 SPEC. ISS.):171–189.

- Stavisky, S. D., Kao, J. C., Ryu, S. I., and Shenoy, K. V. (2016). Motor cortical visuomotor feedback activity is initially isolated from downstream targets in output-null neural state space dimensions. *Neuron*, page 1–14.
- Su, Y., Routhu, S., Moon, K., Lee, S. Q., Youm, W., and Ozturk, Y. (2016). A wireless 32-channel implantable bidirectional brain machine interface. *Sensors*, 16(10):1–19.
- Sun, N. L., Lei, Y. L., Kim, B. H., Ryou, J. W., Ma, Y. Y., and Wilson, F. A. W. (2006). Neurophysiological recordings in freely moving monkeys. *Methods*, 38(3):202–209.
- Takahashi, K., Best, M. D., Huh, N., Brown, K. A., Tobaa, A. A., and Hatsopoulos, N. G. (2017). Encoding of both reaching and grasping kinematics in dorsal and ventral premotor cortices. *The Journal of Neuroscience*, page 1537–16.
- Velliste, M., Perel, S., Spalding, M. C., Whitford, a. S., and Schwartz, a. B. (2008). Cortical control of a robotic arm for self-feeding. *Nature*, 453(June):1098–1101.
- Vuilleumier, P., Valenza, N., Mayer, E., Reverdin, A., and Landis, T. (1998). Near and far visual space in unilateral neglect. *Annals of Neurology*, 43(3):406–410.
- Washburn, D. a., Hopkins, W. D., and Rumbaugh, D. M. (1989). Video-task assessment of learning and memory in macaques (*macaca mulatta*): effects of stimulus movement on performance. *Journal of experimental psychology. Animal behavior processes*, 15(4):393–400.
- Washburn, D. a. and Rumbaugh, D. M. (1992). Testing primates with joystick-based automated apparatus: lessons from the language research center’s computerized test system. *Behavior research methods*, 24(2):157–164.
- Westlund, K. (2014). Training is enrichment—and beyond. *Applied Animal Behaviour Science*, 152:1–6.
- Wise, S. P., Boussaoud, D., Johnson, P. B., and Caminiti, R. (1997). Premotor and parietal cortex: Corticocortical connectivity and combinatorial computations 1. *Annu. Rev. Neurosci.*, 20:25–42.
- Wise, S. P. and Mauritz, K. H. (1985). Set-related neuronal activity in the premotor cortex of rhesus monkeys: effects of changes in motor set. *Proceedings of the Royal Society of London. Series B, Biological sciences*, 223(1232):331–354.
- Wodlinger, B., Downey, J. E., Tyler-Kabara, E. C., Schwartz, a. B., Boninger, M. L., and Collinger, J. L. (2014). 10 dimensional anthropomorphic arm control in a human brain-machine interface: Difficulties, solutions, and limitations. *J Neural Eng*, In Press(1):16011.
- Yin, M., Borton, D. A., Komar, J., Agha, N., Lu, Y., Li, H., Laurens, J., Lang, Y., Li, Q., Bull, C., Larson, L., Rosler, D., Bezard, E., Courtine, G., and Nurmikko, A. V. (2014). Wireless neurosensor for full-spectrum electrophysiology recordings during free behavior. *Neuron*, 84(6):1170–1182.
- Zhang, T., Heuer, H. W., and Britten, K. H. (2004). Parietal area vip neuronal responses to heading stimuli are encoded in head-centered coordinates. *Neuron*, 42(6):993–1001.

Declaration

I hereby declare that except where specific reference is made to the work of others, the contents of this dissertation are original and have not been submitted in whole or in part for consideration for any other degree or qualification in this, or any other university. This dissertation is my own work and contains nothing which is the outcome of work done in collaboration with others, except as specified in the text and Acknowledgements.

Michael Berger
Göttingen, 2018

Michael Berger

Curriculum Vitae

✉ michael.berger.l4u@gmail.com

Education

- 11/2012 - **PhD Systems Neuroscience**, *Georg-August University*, Göttingen.
- 10/2017 Employed: *Sensorimotor Group, German Primate Center*, Göttingen;
Analysis of high-bandwidth neural and behavioral data (machine learning and conventional statistics);
Studied goal-directed arm and body movements and developed corresponding microcontroller-based experimental environments (design, hardware and software);
Studied how goal-directed behavior shapes multi-sensory perception (psychophysics);
Grade: "summa cum laude" (highest grade: "summa cum laude")
- 10/2006 - **Diplom Physics (equivalent to M.Sc.)**, *Ruhr-Universität*, Bochum.
- 05/2012 Major: Computational Neuroscience
Minors: 1) Neurophysiology, 2) Medical Engineering
Thesis: Developed a neural network model for visual motion detection
Grade: "sehr gut" (highest grade: "sehr gut")

Professional Experience

- 10/2017 - **Postdoctoral Researcher**, *German Primate Center*, Göttingen.
today Continuing the research from my graduate studies partly for developing a brain-machine-interface for smart home applications
- 06/2015 - **Editor**, *GGNB-Times*, Göttingen.
- 08/2018 Editorial work and leading an international group of graduate students;
From 10/2016 to 11/2017, **editor-in-chief**
- 06/2012 - **Research Assistant**, *Institute for Neural Computation*, Bochum.
- 10/2012 Adapted motion detection model from Diplom-thesis for an autonomous robotics platform
- 01/2009 - **Teaching Assistant**, *Ruhr-Universität*, Bochum.
- 06/2012 Supervised physics tutorial courses and basic laboratory courses for non-physics students
Developed and supervised projects for the laboratory course for physics students
- 06/2006 - **Internship in R&D**, *Elmos Semiconductor AG*, Dortmund.
- 07/2006 Developed and implemented a tester for triaxial cables

Skills

- Programming Matlab, C++, Arduino, R, Python, Processing, PHP, HTML/CSS
- Software 3D-CAD (Autodesk Inventor), PCB design (Autodesk Eagle)
- Languages German (native), English (fluent), Spanish (basic)

Awards

- 2018 chosen as a young scientist for the *68th Lindau Nobel Laureate Meeting*
- 2018 *Society for the Neural Control of Movement* Scholarship Award

Extracurricular Activities

- 2016 - today Science communication with *Pro-Test Deutschland e.V.*
2017 - today Organizer of *March for Science Göttingen*
2015 - 2017 Organizer of the PhD-colloquium of the *German Primate Center*
2016 Amateur stage actor at *Theater im OP*
2014 - 2016 Fencing coach at the university sports program

Scientific Contributions

Peer-Reviewed Publications

- Journal Article **Berger M***, Calapai A*, Stephan V, Niessing M, Burchardt L, Gail A+, Treue S+. (2017). Standardized automated training of rhesus monkeys for neuroscience research in their housing environment. *J. Neurophys.*, 119(3), 796-807.
- Journal Article Calapai A*, **Berger M***, Niessing M, Heisig K, Brockhausen R, Treue S+, Gail A+. (2017). A cage-based training, cognitive testing and enrichment system optimized for rhesus macaques in neuroscience research. *Behav. Res. Methods*, 49(1):35-45.

Conference Proceedings and Editorials

- Editorial Mazurek KA, **Berger M**, Bollu T, Chowdhury RH, Elangovan N, Kuling IA, Sohn MH. (2018) Highlights from the 28th Annual Meeting of the Society for the Neural Control of Movement. *J. Neurophys.* (in press)
- Conference Proceeding **Berger M**, Faubel C, Norman J, Hock H, Schöner G. (2012). The counter-change model of motion perception: an account based on dynamic field theory. *Artificial Neural Networks and Machine Learning-ICANN 2012*, 579-586.

Preprints and in progress Publications

- Preprint **Berger M**, Gail A. (2018). The Reach Cage environment for wireless neural recordings during structured goal-directed behavior of unrestrained monkeys. bioRxiv, 305334.
- in progress **Berger M**, Neumann P, Gail A. Peri-hand space expands beyond reach in the context of walk-and-reach movements
- in progress **Berger M**, Gail A. Neural encoding of far-located reach goals in motor, premotor, and parietal cortex in a physically unconstrained monkey performing a walk-and-reach task

Conference Oral Presentations

- 2018 **Berger M**, Gail A. The contribution of the fronto-parietal reach network to walk-and-reach movements performed by a physically unconstrained rhesus monkey. *Society for the Neural Control of Movement 28th Annual Meeting*
- 2017 **Berger M**, Gail A. Neural encoding of far-located reach goals in motor, premotor, and parietal cortex in a physically unconstrained monkey performing a walk-and-reach task. *Society for Neuroscience Annual Meeting 2017*
- 2017 **Berger M**, Gail A. The Reach Cage - an experimental environment for wireless neural recordings during structured behavior of physically unconstrained monkeys. *Society for Neuroscience Annual Meeting 2017 Satellite Symposium* (invited)